Université du Québec
à Rimouski

Optimisation opérationnelle, écologique et énergétique des groupes électrogènes diesel

Thèse présentée

dans le cadre du programme de doctorat en ingénierie

en vue de l'obtention du grade de Philosophiæ doctor

PAR

© Mohamad Issa

Janvier 2020

Composition du jury :

Dr. Jean Brousseau, président du jury, Université du Québec à Rimouski

Dr. Adrian Ilinca, directeur de recherche, Université du Québec à Rimouski

Dr. Hussein Ibrahim, codirecteur de recherche, Institut Technologique de Maintenance Industrielle (ITMI)

Dr. Mohamad Yasser Hayyani, membre du jury, Université du Québec à Rimouski

Dr. Miloud Rezquallah, examinateur externe, École Technologie Supérieure (ETS)

Dépôt initial le 30 Octobre 2019 Dépôt final le 24 Janvier 2020

بسم الله الرحمن الرحيم

(وَقُلْ رَبِّ زِدْنِي عِلْماً)

صدق الله العلي العظيم

سورة طه: من الآية114

À mes chers parents

إلى من كلله الله بالهيبة والوقار ... إلى من علمني العطاء بدون انتظار ... إلى من أحمل اسمه بكل افتخار ... أرجو من الله أن يمد في عمرك لترى ثماراً قد حان قطافها بعد طول انتظار وستبقى كلماتك نجوما أهتدي بها اليوم وفي الغد والى الأبد (والدي العزيز)

إلى من كان دعائها سر نجاحي وحنانها بلسم جراحي إلى أغلى الحبايب... إلى من بها أكبر وعليها أعتمد ... إلى شمعة متقدة تنير ظلمة حياتي... إلى من بوجودها أكتسب قوة ومحبة لا حدود لها إلى من عرفت معها معنى الحياة (أمي الحبيبة)

À ma femme Sandie, pour la patience et le soutien dont elle a fait preuve pendant toute la durée de cette thèse

À mes petits bijoux
Adam et Noah

À mes chers sœurs et frère

Je dédie cette thèse

REMERCIEMENTS

Le travail de cette thèse a été effectué au sein du Laboratoire de Recherche en Énergie Éolienne (LREE) à l'université du Québec à Rimouski (UQAR) qu'ainsi au Laboratoire International des Matériaux Antigivre (LIMA) à l'Université du Québec à Chicoutimi et au Centre de Recherche d'Innovation Maritime à l'Institut Maritime du Québec à Rimouski qu'ainsi au sein de l'entreprise Genset-Synchro à Lévis.

Ce travail n'aurait pu être mené à bien sans le soutien de nombreuses personnes à qui je souhaite témoigner ma reconnaissance de m'avoir accompagné durant cette période et que je désire remercier pour leur soutien et d'être activement intervenues dans le déroulement de ces travaux de thèse. Je tiens à m'excuser d'avance auprès de celles que j'aurais omis de citer.

J'adresse mes vifs remerciements à mon directeur Adrian ILINCA, professeur à l'UQAR et directeur du LREE, pour m'avoir accepté pour le doctorat, pour sa direction attentive et sa disponibilité malgré ses diverses occupations, son appui scientifique et pour la confiance qu'il a placée en moi en me donnant cette opportunité de travailler sur un sujet innovant et d'actualité.

J'exprime également ma reconnaissance à mon co-directeur Hussein IBRAHIM, directeur de l'Institut Technologique de Maintenance Industrielle à Sept-Îles, pour son encadrement et son soutien tout au long de ce travail ainsi que pour les discussions enrichissantes, ses remarques constructives et ses grands conseils concernant la réalisation des bancs d'essais et les différentes méthodologies proposées. Nonobstant, sa relecture finale méticuleuse de chacun des chapitres m'a sans aucun doute permis de préciser mon propos. Hussein, vous êtes un frère.

Parfois, des passages pour certaines personnes restent gravés dans le mémoire pour toujours. Une admiration et un remerciement tout particulier pour monsieur Jean FISET, Directeur et Propriétaire de l'entreprise Genset-Synchro ainsi qu'à madame Geneviève GIRARD, directrice des opérations pour leur soutien financier des deux bancs d'essais réalisés à Lévis,

pour leurs profondes implications dans la recherche et le développement et surtout pour m'avoir ouvert les portes de l'entreprise sans aucune limite.

Il est difficile de mener à bien un travail aussi dense qu'une thèse sans un ensemble de personnes n'apparaissant généralement pas dans les documents officiels. J'adresse un merci très chaleureux à monsieur Jean PERRON, professeur à l'UQAC et aux techniciens du LIMA, toujours modestes, Martin TRUCHON et Carol MERCIER pour leur travail extraordinaire et leur disponibilité. Sans eux, nous n'avons pas pu valider les tests de suralimentation. Merci énormément pour votre énorme contribution à ce projet.

Merci également à monsieur Sylvain LAFRANCE, directeur d'Innovation Maritime et pour son équipe de recherche pour l'étroite collaboration sur les différents sujets et tests réalisés et pour les bons moments passés ensembles.

J'adresse mes remerciements aussi à l'ensemble du département des Mathématiques, Informatiques et Génie de l'UQAR pour leurs contributions à la mise en service un bureau et les outils informatiques nécessaires.

Je tiens à remercier mes collègues de recherche à l'UQAR surtout Richard Lepage, Philippe BEAULAC et Fahed MARTINI. Pendant nos séjours en mois de Mai 2019 à Chicoutimi, dans le cadre de notre mission scientifique à LIMA, vous m'avez fait tellement rire que j'ai oublié complétement la fatigue accumulée tout au long de ces quatre dernières années.

La famille doit aussi endosser sa part de responsabilité dans l'accomplissement de ces travaux et à qui je dédie cette thèse. Je ne peux pas passer sous silence le soutien permanent de toute ma famille, mes parents au Liban, qui attendent la fin de mon doctorat depuis le commencement mais qui n'ont cessé de me soutenir et de m'encourager tout au long du chemin. Merci à mon père qui a été mon premier professeur. Merci à ma mère, qui m'a toujours poussée et encouragée à poursuivre mes objectifs. Merci à l'autre moitié de moi, mon frère Majd et mes sœurs Amal et Assil. Vous avez toujours cru en moi, Merci 1000 fois.

Je ne saurais terminer ces remerciements sans évoquer mon épouse Sandie pour sa patience, sa compréhension ainsi que son soutien moral, sentimental tout au long de mon doctorat surtout la dernière année. Sandie, ma moitié douce, mon cœur qui bat dans cette vie, je m'excuse pour tout ce que tu avais enduré et subi à cause de mon doctorat et merci d'avoir passé par mon chemin.

Pour mes deux petits trésors, mes fils Adam et Noah. J'adresse mes excuses pour toutes les journées et les soirées que j'ai dû passer loin de vous à cause de mon doctorat. Adam et Noah, mon âme, quand vous grandirez, vous comprendrez que tout ce que j'ai fait n'était que pour assurer vos bonheurs et garantir une bonne vie de qualité pour vous.

Enfin, que toutes les personnes qui ont contribué à l'élaboration de ce projet, trouvent ici l'expression de ma profonde gratitude.

Mohamad ISSA

RÉSUMÉ

Les générateurs diesel (GD) modernes deviennent de plus en plus complexes, et aussi sévèrement soumis à des normes internationales constamment mises à jour en termes de consommation et du respect de l'environnement. Le moindre défaut dans leurs moteurs peut engendrer une dégradation de ses performances ainsi qu'une augmentation de ses consommations et de ses émissions polluantes.

Les GD sont la principale source d'énergie électrique qui alimente la plupart des régions éloignées et isolées dans le monde. Malheureusement, ces générateurs diesel posent encore d'énormes défis techniques, financiers et environnementaux.

Au Canada, la majorité de la population bénéficie de l'électricité fiable, garantie et à prix abordable. Toutefois, sa production dans les communautés éloignées s'avère problématique du fait qu'ils ne sont pas connectés aux réseaux électriques nationaux. Dans ces communautés, disséminées dans tout le pays, vivent à peu près 211,000 personnes dont la plupart sont des populations autochtones (première nation, inuit et métis). Incontestablement, les GD figurent au premier rang parmi les fournisseurs. Plus précisément, 72% des communautés éloignées privilégient l'utilisation des générateurs à combustion fossile, plus particulièrement le diesel afin de s'auto-suffire en énergie électrique.

En dépit de nombreux avantages qu'ils possèdent (fiabilité et stabilité), les GD présentent plusieurs inconvénients et leur usage pose de sérieux problèmes environnementaux, sociaux, économiques et techniques. En effet, dans un contexte de production d'électricité en régions éloignées, l'utilisation de GD, seuls ou en hybridation avec des sources d'énergies renouvelables fait face à des problématiques techniques bien connues. L'instabilité électrique qui caractérise souvent les réseaux isolés, qui est due au caractère fluctuant des ressources renouvelables et aux variations de la charge, induit un fonctionnement des GD en régime dynamique transitoire et/ou à faibles charges. De plus, un fonctionnement prolongé des GD à faibles niveaux de charges favorise la condensation des résidus de combustion sur les parois de cylindres de moteurs des GD ce qui, au bout d'un certain temps, augmente la friction,

diminue leur rendement et accroît leur consommation en carburant et assure une usure prématurée.

D'autre part, l'organisation maritime internationale (OMI) a adoptée des règles relatives aux polluants atmosphériques provenant des navires notamment des moteurs de propulsion et des GD, ainsi que des mesures obligatoires relatives au rendement énergétique ayant pour objectif de réduire les émissions de gaz à effet de serre (GES) d'au moins 50% d'ici 2050 par rapport à 2008. Des nouveaux plafonds mondiaux de la teneur en soufre du fuel-oil utilisé ainsi des limites d'émission pour les oxydes d'azotes (NOx) ont été récemment adopté poussant ainsi les manufacturiers à optimiser leurs moteurs et groupes électrogènes diesel par des technologies basées sur des solutions de prétraitement, traitement-internes et de post-traitement. Une réduction progressive des émissions a été adoptée et la création de zones de contrôle des émissions dans des zones maritimes désignées ont vu le jour.

Cette thèse présente une analyse et une comparaison détaillées des différentes technologies et solutions permettant l'optimisation des performances opérationnelles, écologiques et énergétiques des GD d'un part, et les techniques les plus adaptables aux GD sans apporter de modifications majeures à l'architecture de leurs moteurs afin d'optimiser leurs performances et réduire leurs consommations de carburant, d'autre part. Elle expose également le fonctionnement des GD en sous-performances et la détection des indices de dégradation du rendement basée sur les analyses de gaz d'échappement. Elle expose de plus, une nouvelle technologie électrique brevetée au Canada, aux États-Unis et en Australie connue sous le nom de Genset-Synchro et qui n'a jamais fait l'objet d'une application commerciale ou d'un projet pilote.

D'autre part, les résultats expérimentaux obtenus dans cette thèse concernant la suralimentation d'un moteur diesel, ont démontré le grand potentiel du système hybride éolien-diesel-stockage d'air comprimé pour des applications à petite et à moyenne échelle surtout pour les communautés isolées et qui sont situées dans des régions possédant une

ressource éolienne suffisante pour une exploitation commerciale. L'utilisation du jumelage éolien-diesel avec stockage d'air comprimé dans ces réseaux pourrait donc réduire les déficits d'exploitation.

Finalement, pour le cas de l'industrie de transport maritime, un système de lavage de gaz a été choisi pour l'étude. De plus, une étude techno-économique a été réalisée sur les différentes technologies permettant l'optimisation écologique et énergétique des groupes électrogènes diesel marins et qui sont forcés à rencontrer les exigences relatives au contrôle des émissions des navires et la réglementation sur l'efficacité énergétique adoptés par l'OMI depuis 2015.

Des simulations numériques, mathématiques, des bancs d'essais avec des tests pratiques et des analyses techno-économiques des systèmes sont de ce fait étudiés pour des applications d'électrification autonomes (hors réseau).

Le contenu de la thèse est présenté sous forme de huit articles originaux publiés dans des journaux scientifiques avec comité de lecture. Chacun de ces articles fait, au moment de sa soumission, l'objet de l'état de l'avancement de l'étude, selon la méthodologie détaillée dans le chapitre I.

Mots clés : [Groupes électrogènes diesel, Optimisation, Performance, Faible charge, site isolé, Marpol Annexe VI, Alternateur Genset-Synchro, Système hybride éolien-diesel SHEDAC, Scrubber]

ABSTRACT

Modern diesel generators are becoming more and more complex, and subject to strict international standards that are constantly updated in terms of consumption and respect for the environment. The slightest defect in their engines can lead to a deterioration in their performance as well as an increase in their consumption and pollutant emissions.

Diesel generators (DGs) are the main source of electrical energy that supplies most remote and isolated areas of the world. Unfortunately, these diesel generators still pose enormous technical, financial and environmental challenges.

In Canada, most of the population benefits from reliable, guaranteed and affordable electricity. However, its production in remote communities is problematic because they are not connected to the national electricity grids. Approximately 211,000 people live in these communities, spread across the country, most of whom are Aboriginal (First Nation, Inuit and Métis). There is no doubt that diesel generators are the leading supplier. More specifically, 72% of remote communities favor the use of fossil fuel generators, particularly diesel, to self-sufficient in electrical energy.

Despite their many advantages (reliability and stability), DGs have several disadvantages and their use poses serious environmental, social, economic and technical problems. Indeed, in a context of electricity production in remote regions, the use of DG, alone or in hybridization with renewable energy sources, faces well-known technical problems. The electrical instability that often characterizes isolated networks, which is due to the fluctuating nature of renewable resources and load variations, induces the operation of DGs in a transient dynamic regime and/or at low loads. In addition, prolonged operation of low load DGs promotes the condensation of combustion residues on the walls of DG engine cylinders, which, over time, increases friction, reduces their efficiency and increases fuel consumption and ensures premature wear.

On the other hand, the International Maritime Organization (IMO) has adopted rules on air pollutants from ships, including propulsion engines and DGs, as well as mandatory energy

efficiency measures aimed at reducing greenhouse gas (GHG) emissions by at least 50% by 2050 compared to 2008. New global caps on the Sulphur content of fuel oil used and emission limits for nitrogen oxides (NOx) have recently been adopted, pushing manufacturers to optimize their diesel engines and generators with technologies based on pre-treatment, internal treatment and post-treatment solutions. A gradual reduction of emissions has been adopted and the creation of emission control areas in designated marine areas has been initiated.

This thesis presents a detailed analysis and comparison of the different technologies and solutions allowing the optimization of the operational, ecological and energy performance of DGs on the one hand, and the techniques most adaptable to DGs without making major modifications to the architecture of their engines in order to optimize their performance and reduce their fuel consumption, on the other hand. It also discusses the operation of underperforming DGs, and the detection of performance degradation indices based on exhaust gas analyses. It also features a new electrical technology patented in Canada, the United States and Australia known as Genset-Synchro that has never been commercially applied or piloted before.

On the other hand, the experimental results obtained in this thesis concerning the supercharging of a diesel engine, have demonstrated the great potential of the hybrid wind-diesel-compressed air storage system for small and medium scale applications, especially for communities that are located in regions with sufficient wind resources for commercial operation. The use of wind/diesel twinning with compressed air storage in these networks could therefore reduce operating deficits.

Finally, in the case of the shipping industry, a gas washing system (closed-loop scrubber) was chosen for the study. In addition, a techno-economic study was carried out on the various technologies that allow the ecological and energy optimization of marine diesel generators and that are forced to meet the ship emission control requirements and the ship energy efficiency regulations adopted by the IMO and coming into force in 2015.

Numerical and mathematical simulations, test benches with practical tests and techno-economic analyses of the systems are therefore studied for autonomous (off-grid) electrification applications.

The content of the thesis is presented in the form of eight original articles published in peer-reviewed scientific journals. Each of these articles is, at the time of its submission, the subject of the study's progress report, according to the methodology detailed in Chapter I.

Keywords: [Diesel generator sets, Optimization, Performance, Low charge, isolated site, Marpol Annex VI, Genset-Synchro alternator, SHEDAC-wind diesel hybrid system, Scrubber]

TABLE DES MATIÈRES

REMERCIEMENTS ix
RÉSUMÉ xii
ABSTRACT xv
TABLE DES MATIÈRES xviii
LISTE DES FIGURES xx
LISTE DES TABLEAUX xxii
LISTE DES ABBRÉVIATIONS, DES SIGLES ET DES ACRONYMES xxiii
CHAPITRE I – PROBLÉMATIQUES DES GED 1
I.1 Introduction 1
I.2 Problématique 3
I.3 Origine de dégradation des performances des GED 9
I.4 Les causes environnementales 12
I.5 État de l'art et analyse des travaux d'antériorité 19
I.6 Motivations et objectifs 33
I.7 Méthodologie 34
I.8 Originalité de la thèse 36
I.9 Structure de la thèse 37
CHAPITRE II – Article 1 40
CHAPITRE III – Rapport technique sur la détection des sous-performances 67
CHAPITRE IV – Article 2 87
CHAPITRE V – Article 3 113
CHAPITRE VI – Article 4 125
CHAPITRE VII – Article 5 133
CHAPITRE VIII – Article 6 145
CHAPITRE IX – Article 7 163
CHAPITRE X – Article 8 173
CHAPITRE XI – Conclusions et perspectives 200
XI.1 – Conclusions 200

XI.2 – **Perspectives** 204
RÉFÉRENCES 206
ANNEXE I – Plan du circuit de contrôle de l'alternateur Genset-Synchro 215
ANNEXE II – Code de programmation – Main C 216
ANNEXE III – Analyseur de post combustion (Testo 350 V.2) 222
ANNEXE IV – Caractéristiques des garnissages structurées 223
ANNEXE V – Caractéristiques du banc d'essai de la suralimentation 225
ANNEXE VI – Formules mathématiques utilisées 226
ANNEXE VII – Les réactions chimiques (Scrubber) 227

LISTE DES FIGURES

Figure 1 : Stockage et transport du carburant diesel dans les communautés isolées canadiennes 4

Figure 2 : Vieux réservoirs de stockage du carburant avec une capacité insuffisante dans une communauté isolée canadienne 5

Figure 3 : Distance qu'un litre de carburant peut faire parcourir à une tonne de marchandises au Canada, dans la région des grands Lacs et de la voie maritime du Saint-Laurent 7

Figure 4 : Illustration de la zone de navigation restreinte entre le port de Baie-Comeau et le port de Montréal-distance à parcourir est de 338 miles nautiques 8

Figure 5 : Impact du changement brusque de la charge sur la performance du moteur diesel 11

Figure 6 : Influence des différents paramètres sur le démarrage à froid 14

Figure 7 : Illustration du circuit du Blow-by 15

Figure 8 : Illustration du gel du circuit Blow-by 16

Figure 9 :L'émulsion du circuit de Blow-by 17

Figure 10 : Illustration des différentes solutions et technologies pour optimiser les GED 19

Figure 11 : (à gauche)-Impact de l'utilisation du Méthanol dans les GED sur le taux d'oxyde d'azote Vs l'utilisation du diesel seul, une réduction moyenne de 8% est constatée; (à droite) – Comparaison de la consommation du carburant lorsque le GED fonctionne complétement au diesel (D) et avec le méthanol (D+M), une réduction en moyenne de 2,5% est enregistrée 20

Figure 12 : Principe d'opération du système d'injection Eau-Diesel dans les blocs moteurs diesel. 22

Figure 13 : Principe de fonctionnement de la technologie de recirculation des gaz d'échappement (RGE) 23

Figure 14 : Principe d'opération d'un système de balayage monté sur un moteur de propulsion diesel marin à vitesse moyenne 23

Figure 15 : Intégration d'une RCS sur un moteur de propulsion de navire catégorie 3. 25

Figure 16 : Génératrice diesel d'une puissance de 125kW équipée par une TVC (Source : CVTcorp) 26

Figure 17 : Centrale de cogénération typique 29

Figure 18 : Principe d'une mesure différentielle 69

Figure 19 : Illustration de l'analyseur des gaz utilisé (modèle Testo 350 V.2).....70

Figure 20 : Illustration du branchement de la sonde de l'analyseur de combustion des gaz d'échappement. 71

Figure 21 : Illustration simplifié du banc d'essai utilisé.....72

Figure 22 : Courbe de tendance pour la consommation du carburant par rapport à la charge appliquée. 74

Figure 23 : Illustration de la moyenne du taux de SO_2 en fonction de la charge appliquée 76

Figure 24 : Variation en pourcentage du taux de CO_2 enregistré en fonction de la charge appliquée.....78

Figure 25 : Variation en ppm du taux d'oxyde d'azote en fonction de la charge.....79

Figure 26 : L'étendue du taux d'O_2 en fonction de la charge appliquée 81

Figure 27 : Étendue du taux de monoxyde de carbone en fonction de la charge 82

Figure 28 : Variation de la température des gaz d'échappement en fonction de la charge appliquée.....84

Figure 29 : Variation du taux de soufre dans les gaz d'échappement en fonction de la charge appliquée 85

LISTE DES TABLEAUX

Tableau 1 :Niveaux de charges en pourcentages de la puissance nominale 9

Tableau 2 : Description des différents phénomènes survenant après le fonctionnement d'un GED sous faible charge 10

Tableau 3 : Variation de la puissance d'un moteur Caterpillar en fonction de la température et de l'altitude 18

Tableau 4 : Spécifications techniques de la génératrice utilisée pour les tests. (Source : Caterpillar).....68

Tableau 5 : Liste des capteurs reliés au système d'acquisition de données (l'OP5) 69

Tableau 6 : Précision et temps de réponse de l'analyseur utilisé (Source : Testo.com).....71

Tableau 7 : Description du protocole utilisé pour les trois tests.....73

Tableau 8 : Investigation sur la consommation du carburant en fonction de la charge.....74

Tableau 9 : Taux du SO_2 enregistré en fonction de la charge appliquée.....76

Tableau 10 : Taux du CO_2 enregistré en fonction de la charge appliquée.....77

Tableau 11 : Taux de NO_x enregistré en fonction de la charge 79

Tableau 12 : Taux d'O_2 enregistrée en fonction de la charge appliquée 80

Tableau 13 : Taux du CO enregistrée en fonction de la charge appliquée 82

Tableau 14 : Température des gaz d'échappement enregistrée en fonction de la charge.....83

Tableau 15 : Taux du soufre enregistré dans les gaz d'échappement en fonction de la charge appliquée 85

LISTE DES ABRÉVIATIONS, DES SIGLES ET DES ACRONYMES

APAE	Air Power Assist Engine
BC	Black Carbon
BSS	Battery Storage System
CAES	Compressed Air Energy Storage
CO	Monoxyde de carbone
CO_2	Dioxyde de carbone
CVT	Continuous Variable Transmission
D	Diesel
DE	Diesel Engine
DFIG	Dual Fed Induction Generator
DG	Diesel Generator
D+M	Diesel + Methanol
DMCC	Diesel/Methanol Compound Combustion
DPF	Diesel Particulate Filter
DPG	Diesel Power Generator
DSP	Digital Signal Processor
DWI	Direct Water Injection
ECA	Emission Control Area
ECM	Engine Control Module

EGR Exhaust Gas Recirculation

EIVC Early Intake Valve Closing

EPA Environmental Protection Agency

GHG Greenhouse Gas

GPIO General Purpose Input/Output

GW Gigawatt

HAM Humid Air Moisturised

HC Hydrocarbons

HFO Heavy Fuel Oil

Hz Hertz

IGBT Integrated Gate Bipolar Transistor

IMO International Maritime Organization

KW Kilowatt

LCC Life Cycle Cost

LNG Liquefied Natural Gas

MARPOL Marine Pollution

MEA Monoethanolamine

MDO Marine Diesel Oil

MW Megawatt

NaOH Sodium Hydroxide

NOx Oxides of Nitrogen

PM Particulate Matter

PWM Pulse Width Modulation

QEP Quadrature Encoder Pulse

SAT Scavenging Air Temperature

SHEDAC Système Hybride Éolien-Diesel avec Air Comprimé

SCR Selective Catalytic Reduction

SO_x Sulphur Oxides

SPWM Sine Pulse Width Modulation

THD Total Harmonic Distortion

TBPRD Time-Base Period Register

VSDE Variable Speed Diesel Engine

ZCE-AN Zone de contrôle des émissions en Amérique du Nord

CHAPITRE I

PROBLÉMATIQUES DES GROUPES ÉLECTROGÈNES DIESEL

I.1 INTRODUCTION

Un groupe électrogène est un dispositif autonome capable de produire de l'électricité. La plupart des groupes sont constitués d'un moteur thermique qui actionne un alternateur. Les groupes électrogènes sont disponibles dans une large gamme de puissances. La plupart des petites unités (quelques centaines de Watt) fonctionnent à l'essence alors que les plus grandes (MW) utilisent le diesel ou le gaz naturel. Des manufacturiers européens tel que l'entreprise finlandaise Wärtsilä et l'entreprise allemande MAN Energy Solutions, proposent des génératrices fonctionnant au bicarburant (diesel/gaz naturel) afin de réduire l'impact écologique des centrales thermiques.

Cependant, les groupes électrogènes diesel (GED) sont la principale source d'énergie électrique qui alimente la plupart des régions éloignées et isolées dans le monde. Malheureusement, ces générateurs diesel posent encore d'énormes défis techniques, financiers et environnementaux [1].

Au Canada, la majorité de la population bénéficie de l'électricité fiable, garantie et à prix abordable. Toutefois, sa production dans les communautés éloignées s'avère problématique du fait qu'ils ne sont pas connectés aux réseaux électriques nationaux. Dans ces communautés, disséminées dans tout le pays, vivent à peu près 211,000 personnes dont la plupart sont des populations autochtones (première nation, inuit et métis) [2]. Incontestablement, les générateurs diesel figurent au premier rang parmi les fournisseurs. Plus précisément, 72% des communautés éloignées privilégient l'utilisation des générateurs à combustion fossile, plus particulièrement le diesel afin de s'autosuffire en énergie électrique.

En dépit de nombreux avantages qu'ils possèdent (fiabilité et stabilité), les générateurs diesel présentent plusieurs inconvénients et leur usage pose de sérieux problèmes environnementaux, sociaux, économiques et techniques. En effet, dans un contexte de production d'électricité en régions éloignées, l'utilisation de GED, seuls ou en hybridation avec des sources d'énergies renouvelables fait face à des problématiques techniques bien connues. L'instabilité électrique qui caractérise souvent les réseaux isolés, qui est due au caractère fluctuant des ressources renouvelables et aux variations de la charge, induit un fonctionnement des GED en régime dynamique transitoire et/ou à faibles charges. De plus, un fonctionnement prolongé des GED à faibles niveaux de charges favorise la condensation des résidus de combustion sur les parois de cylindres de moteurs des GED ce qui, au bout d'un certain temps, augmente la friction, diminue leur rendement et accroît leur consommation en carburant et assure une usure prématurée [3].

Dans ce contexte, les GED sont sévèrement soumis à des normes internationales constamment mises à jour en termes de consommation et du respect de l'environnement. À cause de la complexité conceptuelle et opérationnelle des moteurs diesel, il n'est toujours pas facile d'avoir des données réelles ou d'émuler la dégradation de leurs performances énergétiques et opérationnelles.

D'autre part, l'organisation maritime internationale (OMI) a adopté des règles relatives aux polluants atmosphériques provenant des navires notamment des moteurs de propulsion et des GED, ainsi que des mesures obligatoires relatives au rendement énergétique ayant pour objectif de réduire les émissions de gaz à effet de serre (GES) d'au moins 50% d'ici 2050 par rapport à 2008 [4]. Des nouveaux plafonds mondiaux de la teneur en soufre du fuel-oil utilisé ainsi que des limites d'émission pour les oxydes d'azotes (NOx) ont été récemment adopté poussant ainsi les manufacturiers à optimiser leurs GED par des technologies basées sur des solutions de prétraitement, traitement-interne et de post-traitement [5]. Une réduction progressive des émissions a été adoptée et la création de zones de contrôle des émissions (ZCE) dans des zones maritimes désignées ont vu le jour.

I.2 PROBLÉMATIQUE

De nombreuses difficultés font obstacle au processus de la production d'électricité dans les communautés isolées canadiennes. Elles relèvent de différents ordres : technique, économique, environnementale et social alors que l'obstacle principal dans l'industrie du transport maritime réside aux niveaux environnemental et technique. Ci-dessous un aperçu.

I.2.1 Les défis techniques dans les sites isolés canadiens

Le rapport des Ressources Naturelles de Canada en 2015 indique que la plus grande partie des générateurs diesel dans les régions nordiques isolées de Canada ont déjà atténué leur durée de vie [6]. De plus, les GED vieillissant, nécessitent des professionnels concernés par les tâches de maintenance en visite permanente et ceci n'est pas facilement disponible dans les sites isolés. Dans certaines communautés, les générateurs diesel sont surdimensionnés de sorte à répondre à la demande de pointe qui peut être cinq fois plus grande que la charge électrique moyenne. Ces générateurs fonctionnent la plupart du temps à des charges partielles au-delà de leurs capacités, ce qui cause le glaçage des cylindres ; la perte d'adhérence de l'huile entre le cylindre et les segments, engendre une perte d'étanchéité, puis un encrassement s'amplifiant rapidement et finalement, une usure des pièces [7]. Ce phénomène réduit l'efficacité énergétique et augmente la consommation de carburant. De plus, le coût de maintenance est très élevé lorsque le moteur fonctionne régulièrement dans une telle marge de puissance [8].

L'accès aux carburants est un problème pour la majorité des communautés éloignées qui comptent sur la production d'électricité à moteur diesel. En effet, de nombreuses communautés sont situées à de longues distances des centres de population et donc inaccessibles. Si certaines régions éloignées pourraient être fréquentées par les routes normales de circulation au cours des quatre saisons, d'autres ne sont accessibles en hiver que par voie maritime ou aérienne (Figure 1).

Figure 1 : Stockage et transport du carburant diesel dans les communautés isolées canadiennes *(Source : Nunavikrotors)*

I.2.2 Les défis économiques dans les sites isolés canadiens

La production d'électricité par les générateurs diesel parait très coûteuse en comparaison avec les autres sources de production électrique. Par exemple, cette production atteint 300 GWh par année au Québec avec un coût de 50 cents / kWh dans certaines régions, alors que le prix de vente dans le reste du Québec est de 6 cents / KWh [8]. Ce coût élevé de la production électrique par les générateurs diesel est dû :

- Aux coûts de transport du carburant diesel : Ils sont généralement élevés, en particulier pour les communautés sans accès routier. Le carburant diesel doit être transporté sur des longues routes d'hiver ou transporté par avion ce qui entraîne des coûts de transport très élevés. Le prix de l'électricité est donc beaucoup plus élevé dans les régions isolées que dans le reste du pays. (1,14 $ /kWh au Nunavut contre 0,12 $ / kWh pour la moyenne canadienne).

- Aux prix volatiles du carburant diesel (Mazout) : Imprévisibles et sujets à augmentation, ces prix sont fortement liés au coût du pétrole brut qui subit toujours des fluctuations et probablement va continuer de fluctuer à l'avenir, en fonction de l'offre et de la demande globales. Ainsi les coûts d'électricité dans les régions éloignées peuvent changer brusquement et soudainement ; le carburant n'y est transporté qu'une ou deux fois par an. Une telle pratique expose conséquemment ces communautés à un risque financier important suite aux contrats d'achat du carburant. De plus, le stockage de gros volumes de

diesel pour de longues périodes augmente également les coûts, surtout que les installations requises sont chères et nécessitent une maintenance permanente.

I.2.3 Les défis environnementaux dans les sites isolés canadiens

La génération électrique par les groupes diesel dans les communautés isolées peut avoir de graves dommages et risques environnementaux. En effet, les générateurs diesel sont néfastes pour l'environnement et émettent de grandes quantités des gaz à effet de serre (GES) (environ 800 tonnes de CO2 par GWh d'électricité générée) ainsi que les oxydes d'azote, le dioxyde de soufre et des émissions de particules, qui ont tous un impact sur la qualité de l'air et sur la santé humaine. Cet effet aussi est particulièrement problématique dans les communautés où les générateurs diesel sont situés à proximité des lieux de résidence des habitants. Des émissions supplémentaires très toxiques sont également générées lorsque le carburant est transporté pour des longues distances ou stocké localement en grande quantité pour assurer un approvisionnement sécurisé (Figure 2). Dans les deux cas, les risques de déversements et de fuites augmentent causant d'une part la contamination du sol et des eaux souterraines et provoquant d'autre part des accidents sur les routes ce qui nécessite urgemment des interventions de remédiation souvent difficiles et coûteuses.

Figure 2 : Vieux réservoirs de stockage du carburant avec une capacité insuffisante dans une communauté isolée canadienne [9].

I.2.4 Les défis sociaux dans les sites isolés canadiens

Le diesel est importé de loin et ne crée à peu près aucun emploi dans les communautés. De plus, au cours des années, et pour plusieurs raisons, la demande électrique dans certaines communautés a augmenté pour atteindre des niveaux proches de la limite de la capacité de production installée. Ceci devient un facteur limitant qui restreint la croissance du service électrique ainsi que le développement économique [10]. Pour éviter la surcharge, les nouveaux bâtiments et maisons sont dans l'impossibilité de se connecter au réseau électrique ; il en résulte nécessairement des restrictions au droit de la construction de nouveaux logements, une limitation de la croissance et du développement économique de la communauté ainsi que la perte des opportunités en matière d'investissements. Ces restrictions affectent l'infrastructure publique et les autres activités économiques comme les magasins, les écoles, les services de santé et les autres commerces et services qui seront contraints de faire face à des pannes d'électricité [11].

I.2.5 Les défis environnementaux dans l'industrie du transport maritime

Près de 80% des marchandises de la planète sont transportées par bateau . Lorsqu'il s'agit de déplacer de grandes quantités de marchandises, le transport maritime est le mode du transport le plus éco énergétique [13]. Comme tous les autres modes de transport qui brûlent des combustibles hydrocarbonés pour produire de l'énergie, les navires génèrent une pollution atmosphérique qui nuit à la qualité de l'air, affecte la santé humaine et contribue aux effets à grande échelle du changement climatique.

Bien que les navires émettent moins de gaz à effet de serre (GES) que les autres modes de transport par tonne-kilomètre de marchandises transportées (Figure 3), ils ont tout de même contribué à hauteur de 2,2 % aux émissions mondiales de CO2 en 2012 et à l'accélération des fontes des glaces de mer de l'Arctique [12]. Alors que le défi principal de l'industrie maritime reste au niveau environnemental, le type du carburant utilisé pour les moteurs de propulsion et pour l'électrification à bord des navires est la cause principale derrière cette pollution. En effet, les armateurs utilisent du carburant lourd (Heavy fuel oïl-HFO) qui est très riche en soufre et qui a un impact majeur sur les émissions émis par les navires. Ceci pourra s'expliquer

par le fait que le prix d'une tonne de HFO est trois fois moins cher que le prix d'une tonne de diesel propre. Pour les armateurs, c'est une question d'économie de millions de dollars par année.

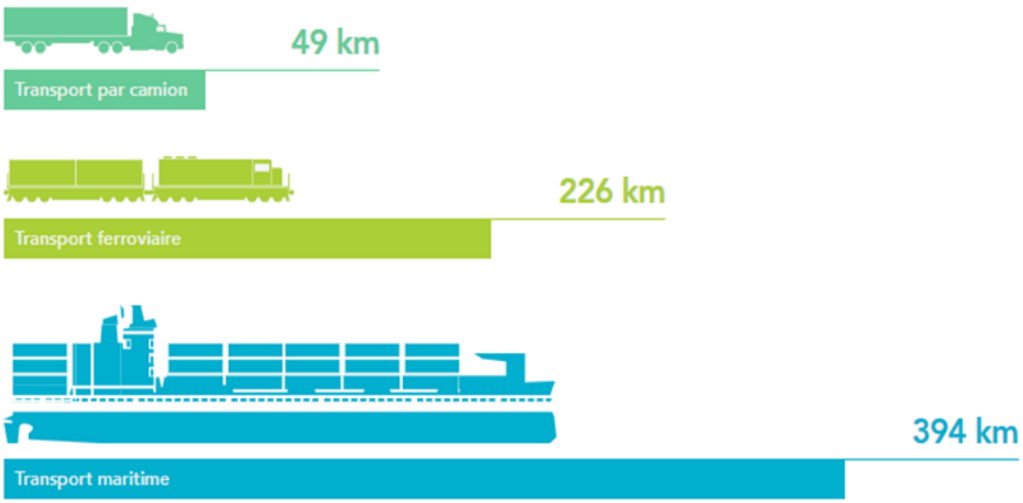

Figure 3 : Distance qu'un litre de carburant peut faire parcourir à une tonne de marchandises au Canada, dans la région des grands Lacs et de la voie maritime du Saint-Laurent [14].

Dans les années à venir, le trafic maritime mondial devrait se développer, car les échanges commerciaux s'intensifient. Si aucune mesure supplémentaire n'est prise pour limiter les émissions de GES des navires, celles-ci pourraient augmenter de 20 à 120 % d'ici 2050, selon la conjoncture [15].

I.2.6 Les défis opérationnels dans l'industrie du transport maritime

Comme tous les défis techniques rencontrés dans les communautés isolées, les navires marchands eux aussi sont sujets à faire fonctionner leurs GED sous une faible charge lorsqu'ils naviguent dans des zones restreintes. Ces zones restreintes sont définies comme des chenaux étroits. Il s'agit de démarrer une deuxième génératrice et la mettre en mode stand-by sous une très faible charge ou souvent à vide tout au long du passage dans ces zones afin d'éviter les abordages en mer en cas où la génératrice principale tombe en panne. Pour un navire faisant le lien entre le port de Baie-Comeau et celui de Montréal (distance de 338 miles nautiques, un aller, (Figure 4) à une vitesse de 15 nœuds nécessite 23 heures de navigation). Ceci

force le GED à opérer pendant 23 heures sous des conditions de sous-performances accélérant ainsi sa Prématuration.

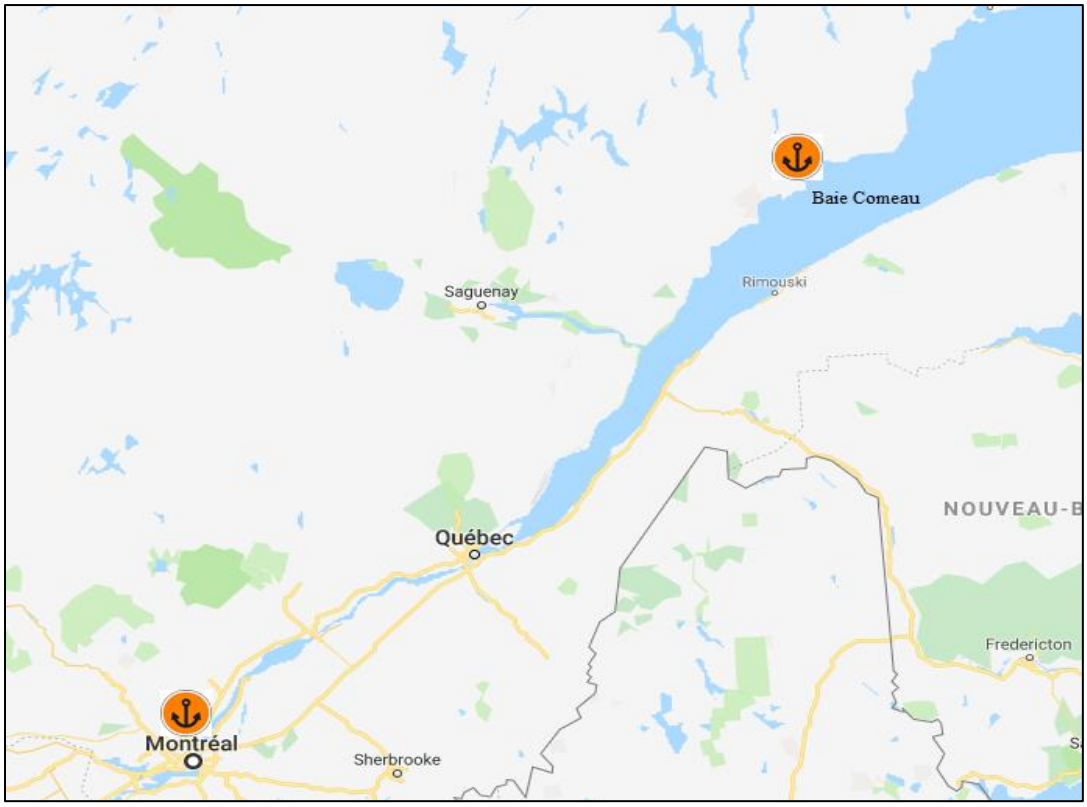

Figure 4 : Illustration de la zone de navigation restreinte entre le port de Baie-Comeau et le port de Montréal-distance à parcourir est de 338 miles nautiques *(Source :Sea-distances.org)*

C'est dans ce contexte que s'inscrit notre thèse de doctorat dont l'objectif consiste à faire la recherche, l'étude, la comparaison et l'analyse des différentes techniques et solutions permettant l'optimisation globale des performances énergétiques, opérationnelles et écologiques des GED sans apporter des modifications majeures à l'architecture principale de leurs moteurs afin d'optimiser leurs performances énergétiques et réduire leurs consommations de carburant. Des simulations numériques, des tests pratiques et des analyses techno-économiques des systèmes d'optimisation seront de ce fait étudiés pour des applications d'électrification autonomes.

I.3 ORIGINE DE DÉGRADATION DE PERFORMANCE DES GED

De nombreuses causes environnementales et opérationnelles sont à l'origine de dégradation de performances des GED, engendrant ainsi leur vieillissement rapide ou même leur endommagement. Dans une première étape, nous parcourons et expliquons les différents phénomènes mécaniques et naturels qui sont à l'origine de la détérioration des performances du GED, alors que dans une deuxième étape, nous présentons et comparons les différentes techniques et solutions pour assurer l'optimisation des moteurs diesel et les GED.

I.3.1 Les causes opérationnelles – fonctionnement sous une faible charge

Selon les expertes (Ingénieurs et techniciens) de Caterpillar, le taux au-dessous duquel un GED commence à fonctionner à faible charge est de 30 % de sa puissance maximale tandis que d'autres études réalisées par DNV-GL limitent ce seuil à 40 % [16]. Cependant, il est considéré que le GED fonctionne à une charge extrêmement basse quand cette dernière est inférieure à 25 % de la puissance maximale du GED (PMGED). D'un autre côté, la zone de fonctionnement normal et adéquat (recommandé) d'un GED correspond à la plage de charges variant de 40 — 80 % de la PMGED. Les définitions de l'ensemble des plages de charge sont présentées dans le Tableau 1 .

Tableau 1 :Niveaux de charges en pourcentages de la puissance nominale [16].

Pourcentage de la puissance	Niveau de la charge
0-25%	Très faible charge
25-40%	Faible charge
40-80%	Charge régulière
80-90%	Charge élevée
90-100%	Charge très élevée

Un fonctionnement prolongé des GED à faibles charges favorise la condensation des résidus de combustion sur les parois de cylindres ce qui, au bout d'un certain temps, augmente la friction, diminue le rendement du moteur et augmente la consommation de carburant par kilowattheure produit. D'autre part, faire fonctionner le GED à de

faibles charges est le facteur majeur de vieillissement et d'usure du système de la combustion. Cela se traduit par l'apparition de plusieurs phénomènes notamment le glaçage, le polissage du cylindre ainsi que l'encrassage « anglais : wetstacking » [17]. Le Tableau 2 décrit les différents phénomènes survenant après le fonctionnement d'un GED sous faible charge.

Tableau 2 : Description des différents phénomènes survenant après le fonctionnement d'un GED sous faible charge [17].

	Glaçage des cylindres	**Polissage des cylindres**	**L'encrassage des cylindres**
Définition	Phénomène chimique, créant sur les pistons et les chemises, un revêtement présentant une certaine coloration.	Phénomène physique qui se traduit par une formation d'une zone ayant l'apparence de miroir sur la surface intérieure du cylindre	C'est un phénomène qui décrit un moteur diesel qui gouttait une substance épaisse et sombre dans ses tuyaux d'échappement due à la présence des résidus imbrulés de carburant dans le système d'échappement
Signes d'apparition	• Une consommation accrue d'huile • Fumée du moteur • Perte de puissance	• Une consommation accrue d'huile • Perte de puissance	Liquide noir rassemblant à l'huile du moteur qui coule du turbocompresseur ou du pot d'échappement. Liquide humide ou sombre autour de la partie droite du moteur au niveau du collecteur d'échappement
Causes	• Jeux important à froid • Huile fortement additive (intervalle de vidange allongée) et fluide (réduction de la consommation) • Condition d'utilisation en sous-régime à faible charge	La friction mécanique locale, probablement due à des dépôts de carbone autour des segments engendrés par une mauvaise combustion originaire d'un fonctionnement du moteur à faible charge.	Le Fonctionnement prolongé du moteur à faible charge, empêche la température d'atteindre sa valeur nécessaire pour une combustion complète de la totalité du carburant injecté.
Effets	Coût : l'apparition excessive de ces phénomènes réduit de plusieurs années la durée de vie restante du moteur et ses composantes principales. Ces phénomènes augmentent la consommation du carburant. Pollution : émission des fumées Puissance : réduction de la puissance maximale produite par le moteur par rapport à sa puissance nominale. Maintenance : un moteur qui connait ces problèmes nécessite de travaux d'entretien plus fréquents en comparaison à un moteur fonctionnant à des charges adéquates.		

I.3.2 Fonctionnement d'un GED sous des charges transitoires

Le fonctionnement des GED à des régimes transitoires et à faibles charges est à l'origine de la détérioration de leurs performances ainsi que leurs conditions de fonctionnement. Les GED, en général, sont capables d'éprouver une grande variété de conditions d'exploitation qui peuvent être qualifiées comme des modes opératoires transitoires. L'opération à des régimes transitoires d'un GED faisant partie d'un système hybride éolien-diesel, est due principalement à des variations brusques de la charge ou de la production des sources d'énergie renouvelables (éolien ou le solaire photovoltaïque). L'impact du changement de la charge sur un GED est illustré dans la Figure 5 . Les étapes importantes du changement de la charge sont affichées en caractères gras.

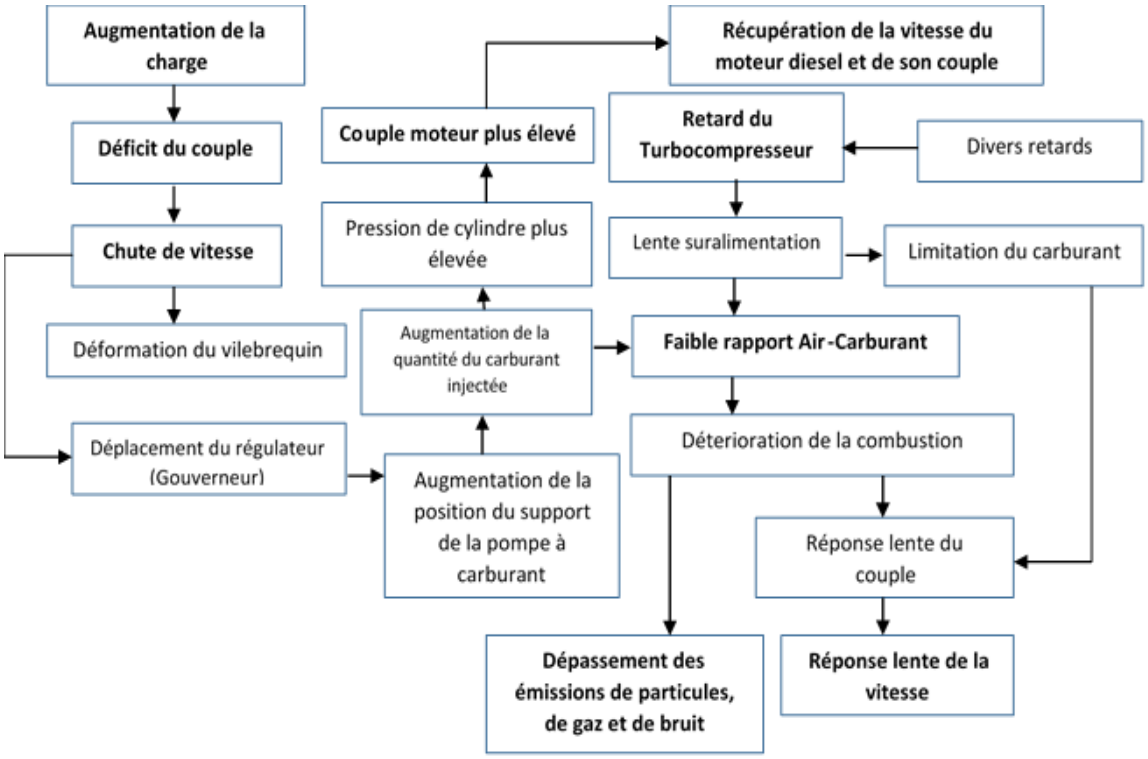

Figure 5 : Impact du changement brusque de la charge sur la performance du moteur diesel [17].

L'impact de l'augmentation de la charge sur le fonctionnement du GED, illustrée dans la Figure 5, peut être décrit comme suit : dans un premier temps, le couple moteur et la charge sont égaux et le rapport air/fuel est relativement élevé. Lorsque la charge

augmente, le moteur subit une perte nette de couple parce que le couple moteur ne peut pas répondre instantanément à la variation accrue de la charge. La perte de couple provoque une baisse de la vitesse du moteur et le gouverneur augmente la quantité de carburant pour pouvoir ajuster la vitesse. En conséquence, le rapport air/fuel diminue en raison du débit massique d'air insuffisant, ce qui est dû à un délai de réponse du turbocompresseur. Le retard du turbocompresseur peut être expliqué par le fait que l'augmentation de la puissance des gaz d'échappement n'est pas capable d'augmenter la puissance instantanée de la turbine due à l'inertie du turbocompresseur. Pendant cette courte période de retard, le moteur tourne comme un moteur à aspiration naturelle et le rapport air/fuel peut atteindre des valeurs beaucoup plus faibles. Ces faibles valeurs peuvent conduire à des émissions de fumée intolérables et la formation de suie. Un faible rapport air/fuel augmente la température dans la chambre de combustion, ce qui peut entraîner la formation de NOx en grandes quantités. Des contraintes mécaniques sous la forme de décélération sont appliquées au vilebrequin (cas où le couple de charge est supérieur au couple moteur). La valeur la plus élevée de décélération est atteinte dans les premiers cycles où la différence de couples entre le moteur et la charge est à son maximum.

I.4 LES CAUSES ENVIRONNEMENTALES

La puissance du moteur est principalement limitée par des contraintes structurelles et thermiques. Ces contraintes comprennent la pression maximale du cylindre pendant la phase de combustion, la vitesse du turbocompresseur et la température des gaz d'échappement. Cependant, ces contraintes doivent prendre en considération les limites de certains facteurs environnementaux, ayant un impact sur les performances de la partie moteur et de la partie génératrice, et par conséquent sur l'ensemble du GED. Parmi ces facteurs, se trouvent notamment l'altitude, la température, l'atmosphère corrosive, l'humidité et la poussière [18]. L'altitude et la température ambiante où des limites maximales de ces variables doivent être imposées en fonction des conditions météorologiques et de sites où les GED sont installés. En effet, lorsqu'un moteur dépasse l'altitude maximale ou la température ambiante, une baisse des performances du moteur peut être remarquée.

I.4.1 La température

Des températures extrêmement hautes ou basses ont un impact négatif sur les performances du GED. Par exemple, lorsque la température de l'air d'admission est supérieure à 40 °C (104 °F), la puissance produite par un GED aura la tendance à diminuer. D'autre part, l'air entrant aux cylindres du moteur à faible température pourra contribuer à l'augmentation de la puissance produite due à la densité relativement élevée de l'air froid. Cependant, deux autres phénomènes en lien avec la faible température de l'air et le fonctionnement du GED peuvent aussi être observés : le démarrage à froid et la formation de gels et d'émulsions dans le système de récupération des gaz du carter moteur (*en anglais : Blow –by circuit*).

I.4.2 Démarrage à froid du GED

Le démarrage d'un GED est considéré à froid tant que le moteur et les fluides n'ont pas atteint la température de fonctionnement normal. À des températures inférieures à 60 °C, un changement au niveau du temps d'injection et la quantité de carburant injecté est requis afin d'optimiser la stabilité de la combustion et réduire les émissions au cours de la phase d'échauffement du moteur. Les températures inférieures à 0 °C nécessitent des changements plus radicaux surtout au niveau du type d'huile utilisé (huile moins visqueuse est plus adapté à des conditions froides). La qualité de démarrage se dégradera fortement en fonction de la température ambiante allant jusqu'au point où un démarrage du moteur n'est plus possible [19].

La phase de démarrage à froid et d'échauffement du moteur dépend des caractéristiques du moteur comme le taux de compression, la taille de la batterie et son état de charge, le démarreur et l'équipement auxiliaire, le système d'injection et les auxiliaires de démarrage à froid. Les caractéristiques du carburant, du système d'air, de l'huile du moteur et de la transmission ont toutes, aussi, une influence sur le démarrage à froid et de la phase d'échauffement du moteur. La Figure 6 montre les paramètres du moteur les plus importants qui influencent la qualité de démarrage à froid et la relation entre ces paramètres.

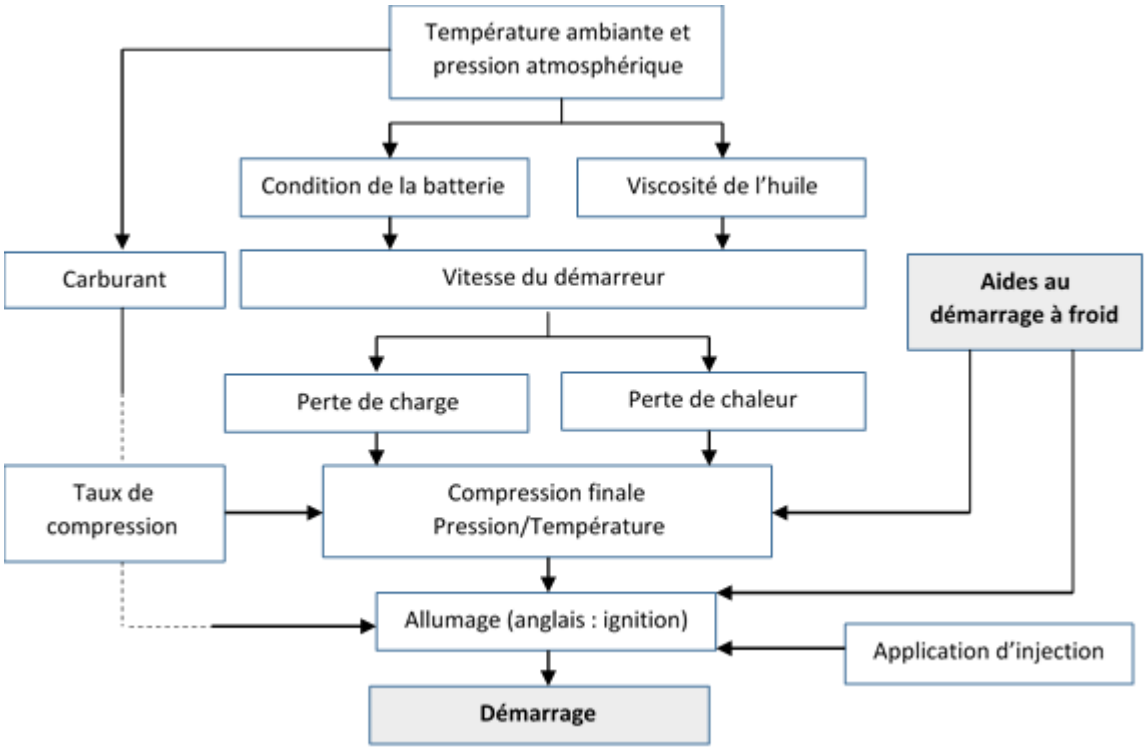

Figure 6 : Influence des différents paramètres sur le démarrage à froid [19].

D'autres parts, les basses températures diminuent la capacité de la batterie et augmentent à la fois la friction du moteur et la viscosité de l'huile. Cela conduit à une demande de couple élevée du moteur, et cela, à une faible vitesse de rotation. Ainsi, la puissance produite par un moteur diesel qui opère sous des températures extrêmes et/ou dans des sites se caractérisant par des conditions d'altitude non optimales ne suffit pas pour accroître la vitesse du moteur jusqu'à un niveau supérieur à celle qui correspond au fonctionnement à des faibles régimes. Ceci se traduit, en conséquence, par une augmentation du temps de démarrage [20].

Il est important de mentionner que pendant le démarrage et le fonctionnement au ralenti, les pertes de chaleur sont importantes, ce qui provoque une température de fin de compression et un pic de pression réduits. D'autres conséquences de ce type de fonctionnement se traduisent par une augmentation de délais de l'injection de carburant (délai physique) et aussi de la combustion (délai chimique). La combinaison de ces conséquences peut mener à une détérioration de la vitesse de l'auto-inflammation et à un

dysfonctionnement total du moteur diesel. De plus, un taux de compression faible tel qu'utilisé dans les GED modernes pourra augmenter ces effets [21].

I.4.3 Formation de gels et d'émulsions dans le système de récupération des gaz du carter moteur (circuit de Blow-by)

La Figure 7 représente le schéma simplifié d'un cylindre dans un moteur diesel. Dans la partie supérieure, on distingue la chambre de combustion qui est séparée du carter basse pression (circuit de lubrification) par les pistons. Lors d'un cycle moteur, à cause du défaut des segments d'étanchéité, la pression qui règne dans la chambre de combustion entraîne une fuite de gaz vers le bas moteur. On l'appelle « gaz de carter » ou « gaz de Blow-by ».

Comme l'exigent les règlements, le gaz du Blow-by ne doit pas être rejeté dans l'atmosphère à cause du risque de pollution [22]. Ainsi, le gaz est recyclé vers le circuit d'admission à travers des conduites et d'un système de décantation appelés circuit de Blow-by.

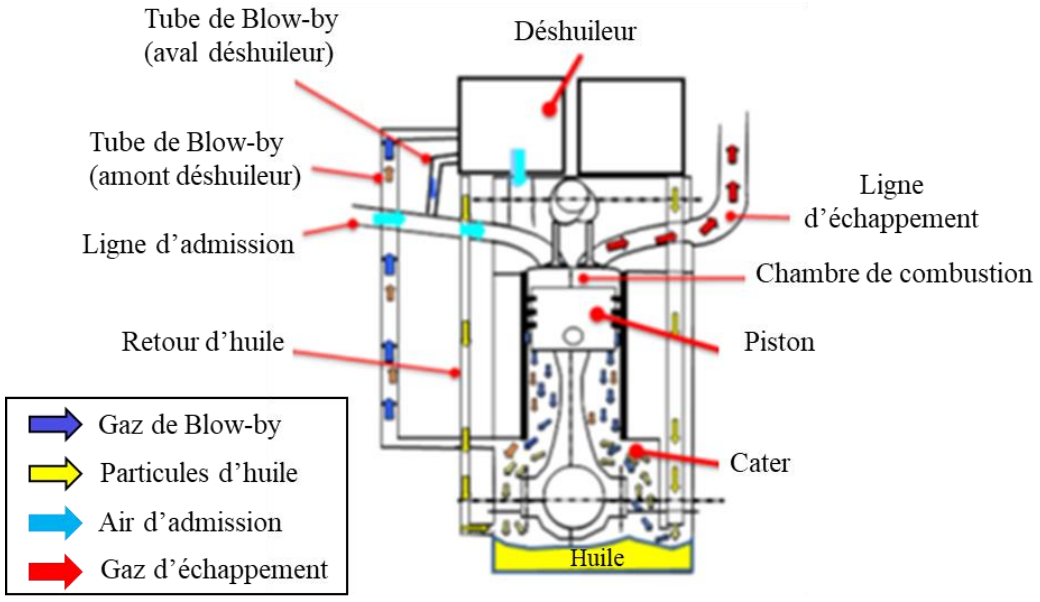

Figure 7 : Illustration du circuit du Blow-by [22]

Dans les pays froids, comme le Canada, la faible température ambiante (en dessous de 0°C) peut durer plusieurs mois ce qui résulte en l'apparition des phénomènes de gel et l'émulsion

de Blow-by. Le phénomène est accentué par le comportement client dans les régions concernées entre autres, l'emplacement du GED à ciel ouvert dans des conditions climatiques froides, et le fonctionnement durant une courte durée et à faible charge où le moteur n'aura pas suffisamment du temps pour se chauffer.

I.4.4 GEL de Blow-by

Dans de conditions de faibles températures extérieures, les parois des tubes du circuit de Blow-by se refroidissent et leur température descend en dessous de la température de condensation du gaz de Blow-by (en dessous de 0 °C), ce qui entraîne la condensation et la solidification d'une partie de la vapeur d'eau contenue dans le gaz. La condensation ou le gel de l'eau peuvent se présenter sous diverses formes. Dans certains endroits du tube, il peut être sous forme de givre poreux tapissant la paroi ou sous forme de glaçons compacts, mélangés ou non avec de l'huile, Figure 8 [22].

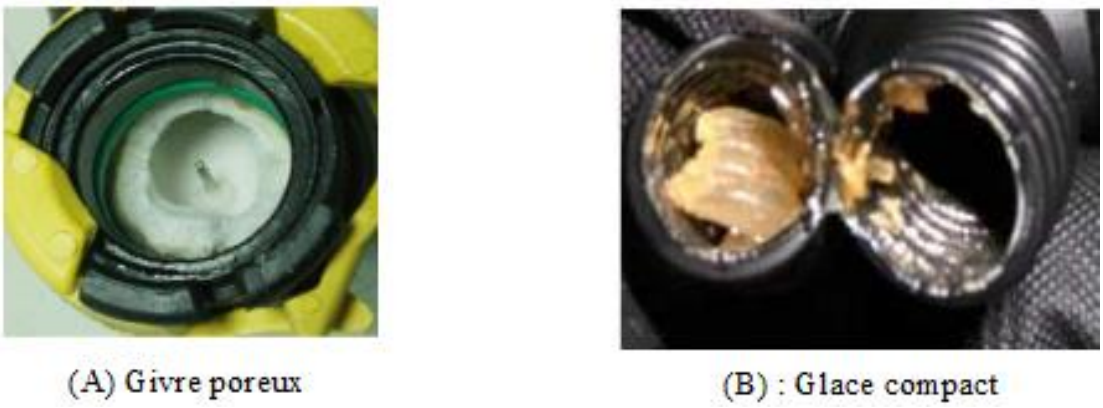

Figure 8 : Illustration du gel du circuit Blow-by [22].

La présence simultanée d'eau liquide et de gouttelettes d'huile dans le circuit de Blow-by entraine la formation d'une émulsion qui est un mélange intime d'eau et d'huile appelée communément « mayonnaise ». C'est l'émulsion de Blow-by. La Figure 9 montre l'émulsion du circuit Blow-by.

Le gel et l'émulsion de Blow-by peuvent engendrer des problèmes non négligeables sur le fonctionnement du moteur.

Figure 9 :L’émulsion du circuit de Blow-by [22].

En s’accumulant aux divers endroits du circuit de Blow-by, le gel ou l’émulsion peuvent conduire à une obturation du circuit de Blow-by entrainant la montée en pression du carter suivi de l’éjection de l’huile (vidange). À terme, cela peut conduire à une perte du moteur voire un incendie si l’huile est éjectée sur une partie chaude du moteur.

I.4.5 L’humidité

La condensation résultant de l’humidité présente un problème pour tous les GED à moins qu’ils ne soient totalement dans un espace clos. La montée de la température et la circulation de l’air de refroidissement du moteur avec une charge d’opération suffisante et régulière peuvent empêcher cette condensation. Des appareils de chauffage peuvent être utilisés pour élever la température à 5 °C au-dessus de la température ambiante pour éviter la condensation dans les zones à haute humidité.

I.4.6 Atmosphère corrosive

Le sel et autre élément corrosif peuvent causer des dégâts à l’isolation des enroulements, conduisant ainsi à l’endommagement des GED. La protection contre ces éléments peut être prise en considération lors du processus de fabrication par l’ajout d’autres couches de revêtements d’isolation au niveau sur les enroulements.

I.4.7 Accumulation de la poussière

Les poussières abrasives aspirées à travers le ventilateur de refroidissement peuvent être très dommageables pour un GED. Parmi ces poussières on retrouve, la poussière de fer, la poussière de carbone, sable, le graphite en poudre, la poussière de coke, la fibre de bois, et la poussière de carrière. Lorsque ces particules étrangères s'infiltrent dans le moteur, elles agissent comme du papier de verre qui frotte avec l'isolation. Ces abrasifs peuvent causer un court-circuit dans le GED. Une accumulation de ces matériaux dans les crevasses du système d'isolation agira en tant qu'isolant ou comme attracteur d'humidité. Les filtres qui s'adaptent sur l'unité d'ouvertures d'admission d'air ou l'ouverture de ventilation peuvent empêcher ces problèmes. Lors de l'utilisation des filtres, il est important qu'ils soient régulièrement changés de manière à ne pas entraver le flux d'air. L'utilisation d'un filtre d'air pourra provoquer, à son tour, la diminution de puissance produite à cause de l'élévation de la température résultante de la baisse du débit d'air de refroidissement.

I.4.8 L'altitude

Les groupes diesel opérant à une altitude supérieure à 1000 mètres (3281 pieds) nécessitent une réduction de l'élévation de la température de 1 % pour chaque 100 mètres au-dessus de 1000 m. Le Tableau 3 montre un exemple de dégradation de la puissance produite en fonction de l'altitude et la température de l'air.

Tableau 3 : Variation de la puissance d'un moteur Caterpillar en fonction de la température et de l'altitude [23].

Température ambiante d'opération	50°F	68°F	86°F	104°F	122°F	Normale
Altitude	2,876 hp	2,876 hp	2,876 hp	2,876 hp	2,876 hp	2,876 hp
0 pieds	2,876 hp	2,876 hp	2,876 hp	2,876 hp	2,876 hp	2,876 hp
984 pieds	2,876 hp	2,876 hp	2,876 hp	2,876 hp	2,876 hp	2,876 hp
1,640 pieds	2,876 hp	2,876 hp	2,876 hp	2,876 hp	2,876 hp	2,876 hp
3,281 pieds	2,876 hp	2,876 hp	2,876 hp	2,876 hp	2,808 hp	2,876 hp
4,921 pieds	2,876 hp	2,876 hp	2,816 hp	2,726 hp	2,642 hp	2,876 hp
6,562 pieds	2,835 hp	2,737 hp	2,647 hp	2,563 hp	2,484 hp	2,876 hp
8,202 pieds	2,663 hp	2,572 hp	2,488 hp	2,407 hp	2,333 hp	2,876 hp
9,843 pieds	2,500 hp	2,415 hp	2,335 hp	2,261 hp	2,190 hp	2,876 hp
10,499 pieds	2,473 hp	2,353 hp	2,277 hp	2,203 hp	2,135 hp	2,876 hp

I.5 ÉTAT DE L'ART ET ANALYSE DES TRAVAUX D'ANTÉRIORITÉ

Afin de bien synthétiser les travaux de recherche touchant l'optimisation des GED, nous avons classifié les différentes techniques en fonction des solutions existantes et à venir. Nous avons distingué 5 catégories selon leur nature électrique, mécanique, prétraitement, traitement-interne et post-traitement [24-26]. La Figure 10 montre les différentes classes des technologies et les solutions possibles pour optimiser les GED.

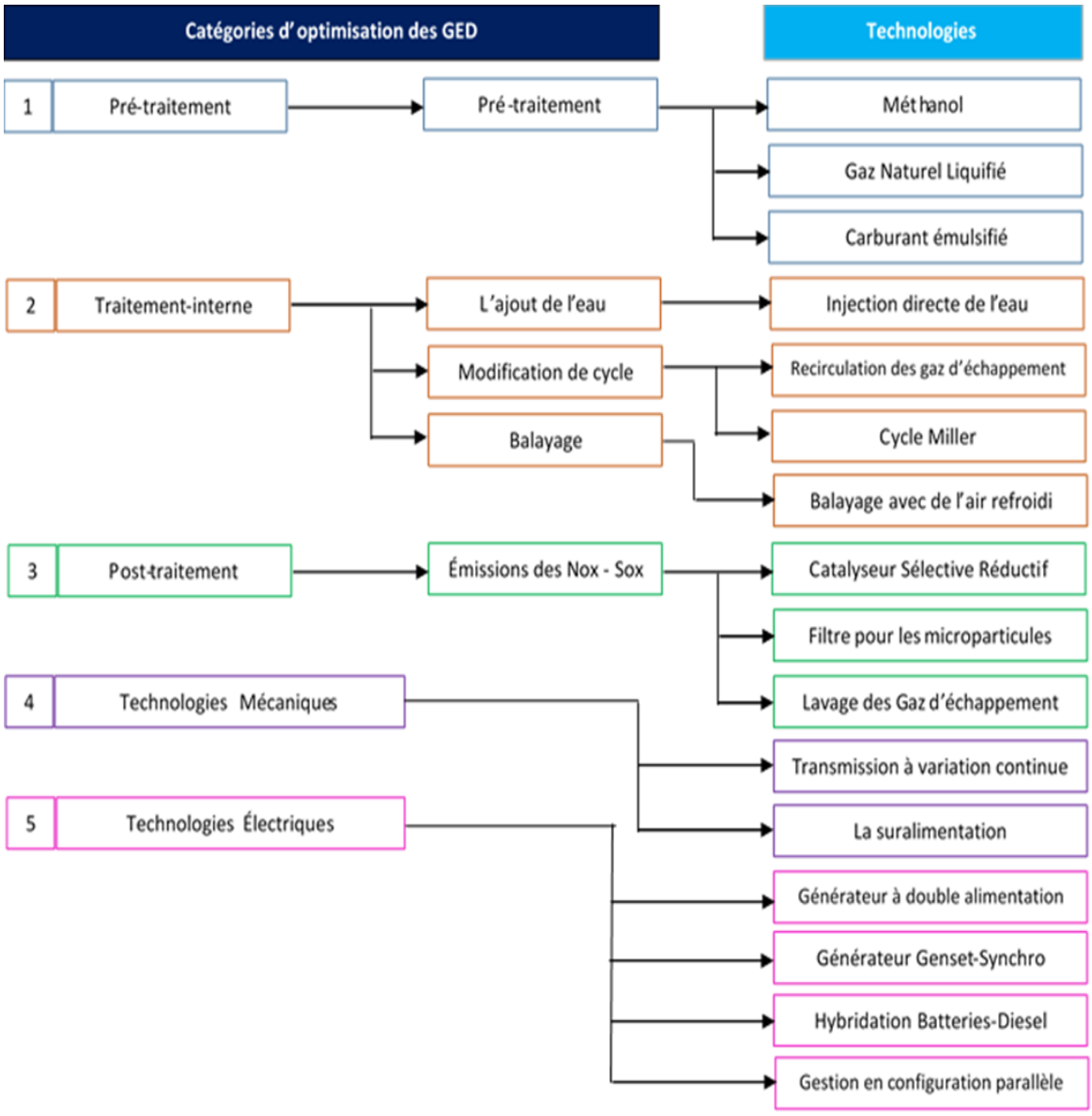

Figure 10 : Illustration des différentes solutions et technologies pour optimiser les GED

I.5.1 Optimisation des GED par les solutions de Prétraitement

La méthodologie de prétraitement est basée sur l'utilisation de combustibles de substitution tel que le méthanol et le gaz naturel liquéfié qui se caractérisent par leurs faibles teneurs en soufre, permettant une réduction des émissions de dioxyde de soufre (SOx), d'oxyde d'azote (NOx) et des matières particulaires (PM). Toutefois, le méthanol présente des défis pour ses adaptations sur les GED rendant leur allumage automatique difficile en raison de la faible teneur en indice de cétane [24]. L'attraction la plus récente dans l'optimisation des GED provient de la combinaison d'une combustion diesel/méthanol proposée par Wang W. et al. [25] à la fin des années 90. Le GED fonctionnera au diesel seul au démarrage et lorsqu'il est soumis sous une faible charge ≤40%, tandis qu'à charge moyenne et élevé, le GED fonctionnera sur un mélange Air/Méthanol uniforme réduisant ainsi les émissions du NOx et de PM. La Figure 11 illustre l'impact de la combinaison d'une combustion Diesel/Méthanol sur les émissions NOx et sur la consommation spécifique du carburant diesel [25].

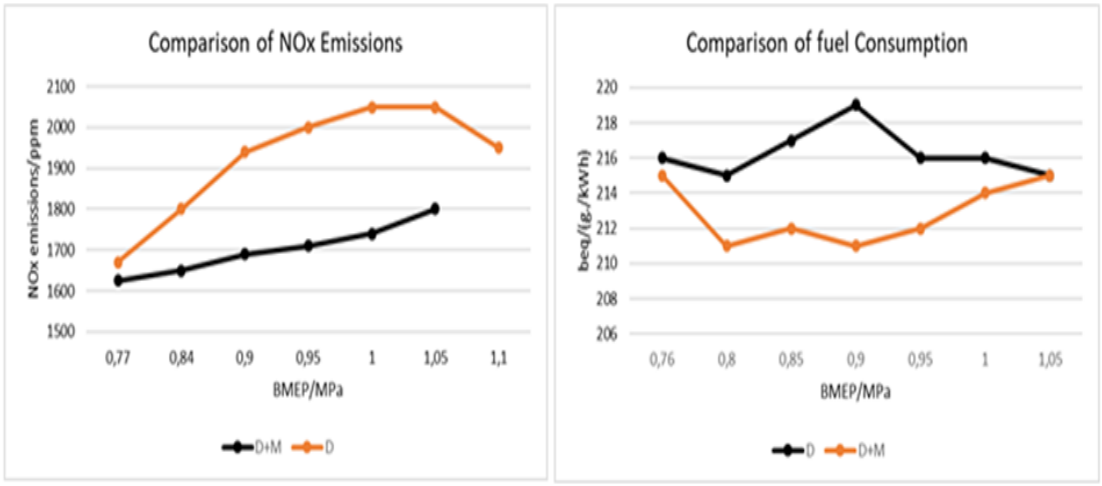

Figure 11 : (à gauche)-Impact de l'utilisation du Méthanol dans les GED sur le taux d'oxyde d'azote Vs l'utilisation du diesel seul, une réduction moyenne de 8% est constatée; (à droite) – Comparaison de la consommation du carburant lorsque le GED fonctionne complètement au diesel (D) et avec le méthanol (D+M), une réduction en moyenne de 2,5% est enregistrée [25].

Malgré ses avantages, le méthanol augmente le risque de corrosion et il est hautement inflammable. Ses réservoirs de stockage doivent être suffisamment mises à niveau et protéger [26]. D'autre part, le gaz naturel liquéfié (GNL) semble être une option attrayante, prometteuse et techniquement adaptée pour satisfaire à la réglementation sur la pollution atmosphérique [27]. Il a l'avantage de réduire de 98%, 86%, 11% et 96% respectivement les émissions de SOx, NOx, CO2 et du PM par rapport à l'utilisation d'un carburant lourd tel fut le cas dans les navires marchands et les centrales électriques [27] ; [28]. De plus, le GNL offre un avantage important par rapport à l'utilisation du fioul lourd en termes de coût, soit environ de 31% par année [28] ; [29]. Malgré ses avantages, le défi du GNL réside d'une part, dans ses installations coûteuses et d'autre part, dans ses réservoirs qui sont 4 fois plus grands que les réservoirs du diesel ou du fioul lourd [27-29].

Pour conclure la catégorie du prétraitement, l'émulsion eau-gazole (Carburant émulsifié) qui a été proposé par le professeur B. Hopkinson, consiste à mélanger deux liquides entièrement non miscibles offrant l'avantage d'une meilleure atomisation et d'une meilleure distribution du carburant résultant en une combustion complète [30] ; [31]. Cette technique offre la possibilité de réduire davantage le taux du NOx par 30% et les PM par 80%, En revanche elle favorise la corrosion des composants du moteur de la génératrice et augmente la consommation du carburant par 3% pour assurer une même puissance avec l'utilisation du diesel seul [30-32].

I.5.2 Optimisation des GED par les solutions de traitement-interne

D'une manière générale, le traitement-interne consiste en une modification directe du bloc moteur de la génératrice diesel [27]. Les modifications internes d'un moteur – ajout d'eau, recyclage des gaz d'échappement, modification du temps de croisement des soupapes ou du temps d'ouverture de la soupape d'admission (Cycle Miller) – peuvent permettre de supprimer presque complètement ou une grande partie les émissions de NOx [33-36]. De plus, l'optimisation des GED par traitement-interne permet de rencontrer les normes minimales d'efficacité

énergétique pour les bateaux neufs adoptées par l'Organisation Maritime Internationale (OMI) en 2015.

L'injection directe de l'eau utilise un injecteur composé de deux parties (voir Figure 12), l'une pour pulvériser l'eau et l'autre pour injecter le diesel [33]. Durant la phase d'injection du diesel, l'eau déminéralisée est injectée à haute pression dans la chambre de combustion permettant une réduction des températures de combustion et des émissions de NOx jusqu'à 60%. L'avantage de cette technologie réside dans le fait qu'elle ne nécessite pas d'espace supplémentaire et qu'elle peut être intégrée sur des GED à vitesse moyenne. Toutefois, cette technologie peut entraîner une augmentation du taux de consommation de carburant d'environ de 2% [27] ; [33].

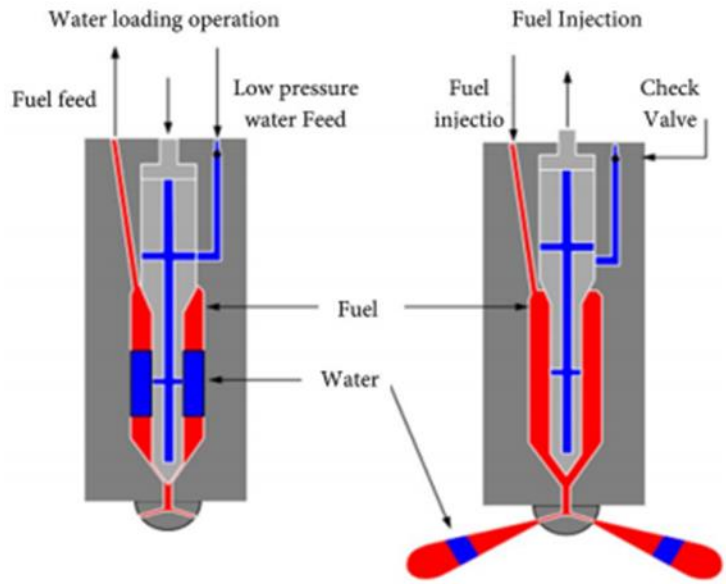

Figure 12 : Principe d'opération du système d'injection Eau-Diesel dans les blocs moteurs diesel [33].

D'autre part, la recirculation des gaz d'échappement permet de réduire la température de combustion et d'obtenir une faible teneur en NOx, Figure 13 . Cette technique est considérée comme la principale solution permettant de réduire les émissions du NOx émis par les GED de 40% [27] ; [34]. Toutefois, cette technique ne peut pas être employée lorsque le GED est soumis à une grande charge 75% ~ 90% car elle cause une baisse dans le rendement du moteur et une chute dans sa puissance de sortie (crête).

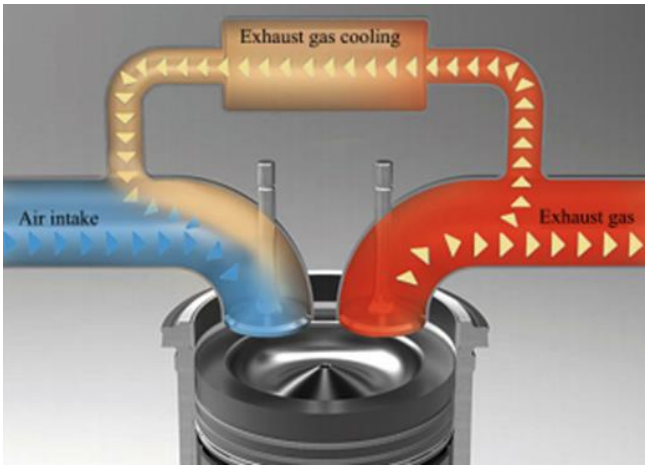

Figure 13 : Principe de fonctionnement de la technologie de recirculation des gaz d'échappement (RGE) [34].

Une autre technique permettant l'optimisation des GED par un traitement-interne est basée sur la technique de balayage [35]. Elle consiste à pousser la charge de gaz d'échappement hors du cylindre et à aspirer un courant d'air frais ou un mélange air-carburant pour le cycle suivant. Pour les applications maritimes, voir Figure 14, de l'eau de mer est injectée dans l'air du turbocompresseur à haute température pour le refroidir et le saturer. L'humidification de l'air est contrôlée en maintenant la température de l'air de récupération entre 60ºC et 70ºC. Elle permet une diminution dans les émissions du NOx de 60% à 65% [36].

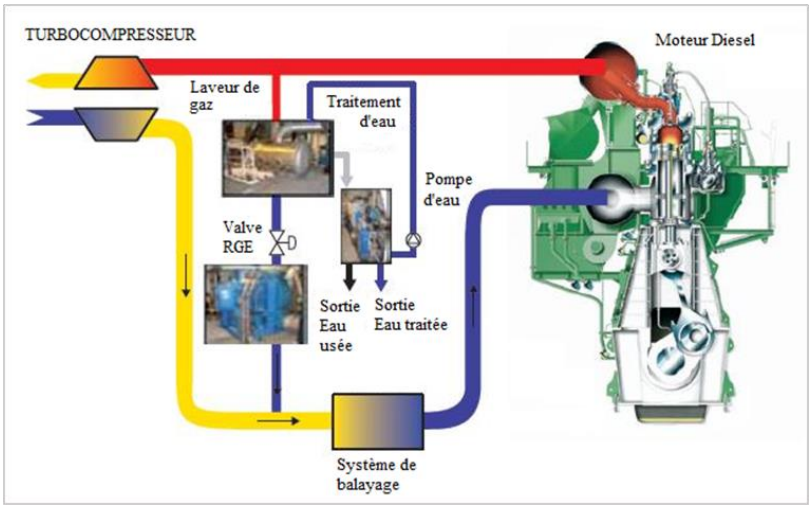

Figure 14 : Principe d'opération d'un système de balayage monté sur un moteur de propulsion diesel marin à vitesse moyenne [36].

Pour conclure cette catégorie, la modification du temps d'ouverture de la soupape d'admission connu sous le nom du cycle de Miller qui a été proposé par R.H. Miller en 1947, consiste à fermer la vanne d'admission d'avance pour obtenir un refroidissement interne afin de réduire le travail du cycle de compression [37]. L'avantage de cette technique réside dans l'amélioration de l'efficacité du moteur diesel d'une part, et dans la réduction du NOx par 40-60%, de l'autre part [27] ; [37]. Toutefois, une maintenance prévisionnelle est fortement recommandée [37-39].

I.5.3 Optimisation des GED par les solutions de post-traitement

L'optimisation des GED ainsi que les moteurs diesel (MD) par les techniques de post-traitement consiste à amener des modifications à la sortie des gaz d'échappement. Son avantage réside dans le fait qu'aucune modification sur le bloc moteur est nécessaire et la majorité des travaux sont réalisés sur le tuyau d'échappement ou à la sortie de la cheminée du navire ou de la centrale électrique. Le post-traitement regroupe trois principales technologies : (i) l'utilisation de la réduction catalytique sélective (RCS) ; (ii) les épurateurs des gaz d'échappement et (iii) les filtres des matières particulaires [40-43].

La RCS permet de traiter les gaz d'échappement avant leur rejet dans l'atmosphère, et de réduire ainsi les émissions de NOx de 95% [27] ; [44]. Toutefois, l'adaptation d'une RCS dans une centrale électrique existante ou sur un navire peut présenter certains défis pour l'entreposage de son urée et de l'espace requise pour son installation [44], Figure 15.

D'autre part, les épurateurs (anglais : Scrubbers) mélangent les gaz d'échappement avec de la soude caustique ou de l'eau, ce qui permet d'éliminer jusqu'à 99 % des SOx et 98 % des matières particulaires du carburant à forte teneur en soufre. Une étude récente a révélé qu'à l'échelle internationale 983 navires se sont équipés d'épurateurs ou en ont commandé [46]. Par contre, ils sont confrontés à la corrosion, à l'augmentation de la consommation du carburant du moteur diesel et à une maintenance continuelle [27] ; [44] ; [46].

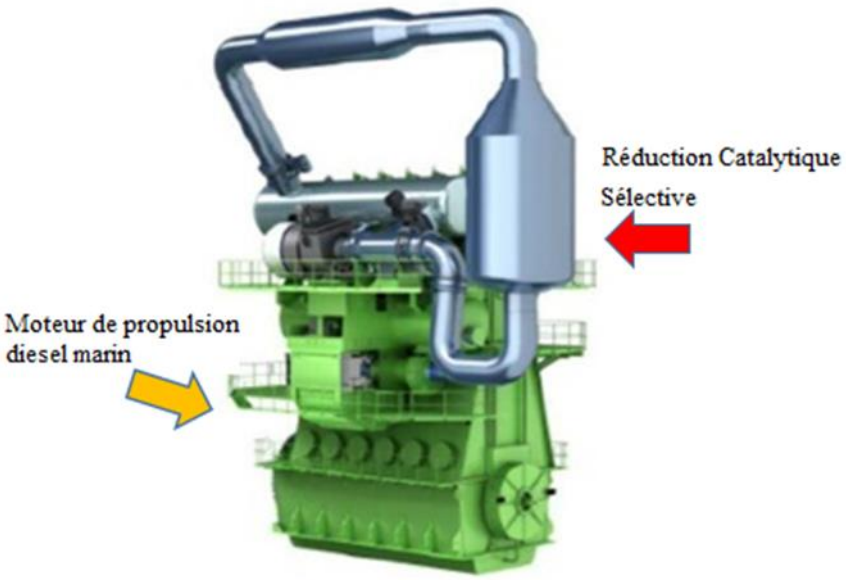

Figure 15 : Intégration d'une RCS sur un moteur de propulsion de navire catégorie 3 [45].

Pour conclure cette catégorie, les filtres des matières particulaires utilisés sur les GED et les moteurs diesel marins se caractérisent par leurs simples installations et dans la réduction des émissions du carbone suie (anglais : Black Carbon) par 99%. Toutefois, il crée une contre-pression (back-pressure) dans le moteur impliquant une surconsommation de carburant de 4% [47].

I.5.4 Optimisation des GED par des technologies mécaniques

L'optimisation des GED par des technologies mécaniques pour les sites isolés regroupe deux technologies principales : (i) l'utilisation de la transmission à variation continue ; et (ii) la suralimentation qui consiste à l'hybridation des GED. Cependant, d'autres technologies mécaniques font partie d'une optimisation pour les GED et qui sont utilisés largement à bord des navires marchands et dans des grandes centrales thermiques. Il s'agit de la cogénération ainsi que des laveurs des gaz (scrubbers). Cependant, ces deux dernières s'avèrent compliquées pour les sites isolés en termes des coûts de maintenance et d'opération. Ci-dessous, une aperçue de leurs principes de fonctionnement, avantages et inconvénients.

I.5.4.1 Optimisation des GED à l'aide de la transmission à variation continue

Inventé par Hans Marshall, ingénieur chez Fendt dans les années 60/70, ce type de transmission vise à éliminer les changements de rapport mécaniques dans les tracteurs agricoles afin de pouvoir parcourir la plage de vitesse complète (de 0.02 km/h à 60 km/h) sans rupture de couple transmis [48]. Un avantage de la transmission à variation continue (TVC) est bien évidemment de pouvoir adapter la vitesse de travail de façon indépendante du régime moteur, ce qui permet en conséquence de réduire la consommation du carburant d'environ de 15%. L'entreprise Québécoise CVT Corp. (www.cvtcorp.com) a intégré une TVC dans un GED afin d'optimiser la consommation du carburant et diminuer les GES. Ce projet a été réalisé en septembre 2013 avec ALASKA ENERGY AUTHORITHY pour la centrale électrique de Puvurnaq, sur un groupe électrogène de 125KW offrant une réduction importante allant jusqu'à 25% en consommation du carburant pour un prix de 125 000$U.S [49]. La Figure 16 illustre le prototype utilisé à la centrale électrique de Puvurnaq.

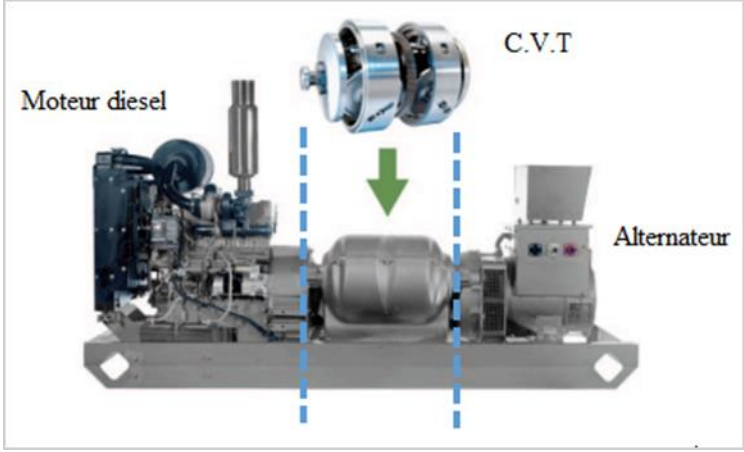

Figure 16 : Génératrice diesel d'une puissance de 125kW équipée par une TVC (Source : CVTcorp)

Malgré une économie importante en termes de carburant et de GES, la TVC semble avoir des limites de fonctionnement au-delà d'une certaine puissance. L'entreprise CVTcorp affiche sur son site internet (www.cvtcorp.com) que la puissance maximale de la génératrice pour laquelle la transmission peut s'intégrer ne doit pas excéder 150KW. Ceci pourra s'expliquer dans les travaux menés et expliqués par [50] et [51], que les limites d'une CVT sont dues à des pertes

de couples à cause de l'utilisation des courroies métalliques et aux frictions entre la poulie et la courroie entrainant des usures importantes.

I.5.4.2 Optimisation des GED à l'aide de la suralimentation pneumatique

La suralimentation est un procédé qui consiste, par une compression préalable, à élever la masse volumique de l'air à l'admission des moteurs pour en augmenter leur puissance spécifique (puissance par unité de cylindrée) [52]. En effet, ce procédé permet d'atteindre, avec une même cylindrée, des puissances supérieures à la puissance d'un moteur non suralimenté avec des augmentations de masse et de volume de l'ordre de 10% [53]. Basbous [54] raffine les travaux de [52] qui sont, eux-mêmes, en partie appuyés sur son propre mémoire qui détaille le modèle d'un hybride pneumatique diesel. Ces efforts de recherche portent sur l'identification d'une configuration optimale pour la restitution de l'énergie stockée en injectant directement l'air comprimé dans le moteur. L'idée est reprise, tout récemment, par [55] qui y incorporent un système de récupération de chaleur. L'hypothèse avancée est qu'il existe deux voies de production du couple dans le moteur diesel, soit : la voie du carburant et la voie pneumatique. Les modèles présentés sont appuyés sur une vérification expérimentale avec une génératrice hybridée de 5kW, [52] ainsi que des simulations récentes à l'échelle de 50kW [55]. Des travaux antérieurs avaient aussi démontré l'augmentation d'efficacité liée à la suralimentation pneumatique [56]. Des réductions de consommation de 32% et 34% [57] sont rapportées dans des simulations avec des cycles variés. L'hybridation pneumatique des moteurs à combustion interne est donc envisagée par d'autres équipes et constitue un domaine d'étude actif en soi.

Kang et al. [58] proposent un concept différent, l'Air Power Assist (APA), qui consiste à souffler l'air comprimé à l'entrée de la turbine du turbocompresseur. Malheureusement, ce concept requiert un entraînement hydraulique des soupapes avec une séquence d'opération très éloignée de ce qu'il est possible de mettre en œuvre avec un moteur diesel traditionnel. Dans la même lignée que le APA, une série de simulations visant l'optimisation du calage des soupapes en mode pneumatique démontrent des efficacités de restitution qui atteignent 48% dans des cycles

automobiles avec freinage régénératif, Trajkovic et al. [60]. On remarque finalement que les travaux portant sur des moteurs hybrides pneumatiques sont clairement partagés en deux catégories : • avec modification à la culasse du moteur, notamment par l'ajout de soupapes, par le recours au séquençage variable des soupapes ou encore par la modification importante de la séquence et la durée de leur mouvement [55-57]; • sans modification particulière au moteur [52-54] ; [58] et [60].

La relative petitesse du marché que représente l'approvisionnement des sites isolés ne permet probablement pas la rentabilisation de la production de générateurs diesel dont l'architecture est grandement modifiée. Pour cette raison, l'idée de proposer un système hybride fonctionnant sans modification spécifique à la culasse du moteur revêt un intérêt notable et est favorisée dans cette thèse face aux autres approches jugées plus complexes et plus coûteuses.

I.5.4.3 Optimisation des GED à l'aide de la cogénération

La cogénération permet aussi l'optimisation des groupes électrogènes diesel. C'est le cas du projet qui a été développé par la firme de génie-conseil canadienne BBA pour la centrale électrique de la mine d'or de Meadowbank dans le Nord canadien en 2016. La centrale consiste en 6 génératrices diesels de 4,4MW/unité afin de répondre aux besoins énergétiques du site. L'intégration de la cogénération à cette centrale a permis une réduction de consommation annuelle de diesel de deux millions de litres (soit l'équivalence de 6%) et une diminution des GES de 5500 tonnes par année [61]. La Figure 17 illustre le principe de la cogénération.

Malgré une économie intéressante, l'utilisation de la cogénération ne présente pas que des avantages. Elle induit également de nombreux obstacles à franchir [62]. La chaleur est par exemple une source d'énergie dont le transport est difficile sur des distances importantes. Des pertes inévitables d'énergie surviennent. Quant à son stockage, il engendre des frais élevés. D'autre part, le mécanisme de la cogénération ne permet pas de modifier aisément la quantité d'électricité et de chaleur produite. Conséquence : impossible de s'adapter à la consommation de ces deux énergies. Enfin, la rentabilité de la cogénération est dépendante du prix des combustibles si elle utilise du pétrole ou du

gaz. Une vision à long terme est difficile à établir lorsqu'il s'agit d'évaluer les coûts plusieurs années plus tard.

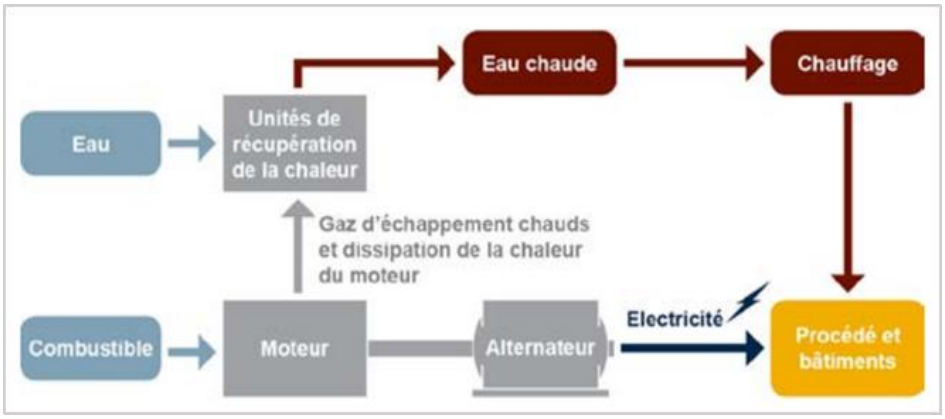

Figure 17 : Centrale de cogénération typique [61].

I.5.4.4 Optimisation des GED à l'aide des épurateurs de gaz *(anglais : Scrubber)*

Un système de lavage de gaz est composé de plusieurs éléments destiné principalement à éliminer les particules des gaz émises par les échappements des moteurs thermiques tels que le dioxyde de carbone et le souffre. Ces systèmes présentent une solution importante pour le marché maritime canadienne et s'inscrivent dans le sillage des engagements du Canada en tant que signataire de la convention MARPOL régissant les normes relatives aux émissions de soufre à l'égard de tout bâtiment navigant dans la Zone nord-américaine de contrôle des émissions (ZCE-AN) dont font partie les 13,000 km de la zone côtière maritime du Québec [62]. Les 3 systèmes d'épuration de gaz actuellement déployés dans le domaine maritime et industriel sont les laveurs humides en boucle ouverte à l'eau de mer (pour les centrales à bord de l'eau), ou en boucle fermée à l'eau douce et les laveurs à sec. [63]. À puissance égale, les laveurs humides sont 2 fois plus compacts plaidant en leur faveur pour réaménager les bâtiments existants [64]. Cependant, la perte de charge est un facteur déterminant de leur dimensionnement qui dépend du type d'internes et des débits des fluides. Un laveur mal dimensionné génère une pression de refoulement élevée contraignant le moteur à opérer hors des limites enjointes par la norme sur les émissions des NOx. Pour prévenir tout reflux, l'installation d'un ventilateur en aval du laveur permet de maintenir une pression négative, mais

imposerait une surconsommation de puissance et une perte d'efficacité du navire jusqu'à ~3% [64]. Aussi, plus le tonnage du navire est important plus la conception d'un laveur embarqué devient-elle ardue : un bâtiment mu par un moteur de 32 MW nécessiterait une colonne de lavage de 10 m de haut pour laquelle la perte de charge maximale doit être limitée à 100 Pa/m pour éviter d'installer un organe de succion (ABS). Force est de constater que les laveurs SOx proposés par les équipementiers spécialisés en marinisation répliquent en majorité les procédés onshore. Si la technologie Venturi [65-67] offre une aire inter faciale élevée grâce au haut degré d'atomisation du liquide de lavage, elle reste pénalisée par une perte de charge élevée et un temps de contact court empêchant des efficacités d'enlèvement aussi poussées que dans une colonne à garnissage, > 99.9% [68]. Les solutions alternatives au laveur Venturi ne sont guère meilleures. La colonne à bulles à buse immergée de Marine Exhaust Solutions Inc. a peu de flexibilité sur le débit de gaz qui est subordonné à la puissance du moteur. Ce mode de dispersion est inapte à générer des bulles aussi fines qu'un Venturi, tandis qu'opter pour un temps de séjour plus long et donc une colonne plus grande va à l'encontre des exigences de compacité sur les navires. Enfin, le laveur à garnissage en vrac d'Alfa Laval Aalborg est particulièrement intéressant puisque l'aire inter faciale gaz-liquide nécessaire à l'abattement des SOx provient non pas d'une brumisation du liquide, gourmande en énergie à l'instar des systèmes Venturi, mais plutôt du ruissellement de films liquides sur le garnissage [68].

I.5.5 Optimisation des GED par des technologies électriques

Les technologies électriques telles que l'application de l'alternateur Genset-Synchro à un moteur diesel a permis de réaliser des économies significatives en carburant et une réduction des GES [69-72]. Son avantage principal réside dans le fait qu'elle pourra être appliquer dans les sites isolés sur la génératrice existante sans recours à la modification du bloc moteur diesel. Dans les travaux menés dans [69-71], l'alternateur Genset-Synchro assure une économie allant jusqu'à 15% lorsque la charge appliquée ≤40% et une réduction moyenne de 7% pour les émissions polluantes. Malgré son avantage, la présence des balais dans l'alternateur nécessite une maintenance

fréquentielle et sa puissance maximale est limitée à 85% due à l'alimentation du moteur de compensation entrainant le stator [69-72].

D'autre part, l'utilisation de l'alternateur à double alimentation connu sous le nom de DFIG (anglais : Dual Fed Induction Generator), ont permis de réduire les convertisseurs de puissance de 70% [72-75]. Ces types des machines peuvent assurer une diminution de consommation en carburant une fois appliquée à un moteur diesel d'ordre 20% lorsque des faibles charges sont appliquées (charge <40%) et autour de 10% pour des grandes charges [76]. Son principe est simple : : l'introduction du convertisseur de puissance entre le stator et le réseau dans une machine conventionnelle donne lieu à un découplage entre la fréquence du réseau électrique et la vitesse de rotation de la machine ce qui permet de fonctionner à vitesse variable. Toutefois, ce convertisseur doit être dimensionné pour faire transiter la totalité de la puissance générée par la machine. Il doit donc être correctement refroidi et représente un encombrement non négligeable surtout dans le cas où il se trouve dans la nacelle d'une éolienne ou dans une place restreinte telle que la salle des machines dans un navire. De plus, c'est un générateur de perturbations harmoniques importantes et la présence de balais au rotor demande un travail de maintenance plus important [77].

Toutefois, et dans le même contexte d'optimisation, l'utilisation de plusieurs petites unités de GED dont la puissance de sortie combinée est égale à une seule unité, permettra d'atteindre des économies en carburant jusqu'à 26% [78]. L'avantage principale de cette approche est qu'il permet une multiple puissance de sortie en raison de ses multiples combinaisons possibles, permettant d'éviter que le GED fonctionne en sous-performance lorsqu'il est soumis sous une faible charge.

Finalement, pour conclure cette revue de littérature, l'hybridation des génératrices diesel avec un système de stockage de batteries a fait l'objet de plusieurs chercheurs et différentes applications notamment pour les micro-réseaux autonomes [79]. Il a été démontré dans des études antérieures [79], [80] que les systèmes hybrides Diesel-Batteries assurent une économie en carburant allant jusqu'à 5%. Cependant, pour des applications autonomes dans le nord du Québec, la température ambiante doit être prise

en considération pour éviter que l'efficacité et le rendement des batteries ne soient pas négligés et des systèmes de filtration s'avèrent nécessaires pour assurer une bonne qualité de signal.

Une analyse critique de ces travaux de recherches antérieurs conduit à la conclusion que les solutions basées sur le prétraitement et traitement-interne ne sont pas idéales pour les régions éloignées. En effet, le prétraitement nécessite l'extension des nouvelles installations pour le stockage des gaz naturels liquéfiés (4 fois plus de réservoirs par rapport au diesel) d'une part, et parce que la majorité des GED et des centrales électriques existantes dans les régions isolées ne sont pas équipés par la nouvelle génération des GED qui leur permettent de fonctionner en bicarburant d'autre part. En revanche, des solutions de post-traitement tel que l'utilisation des filtres des microparticules semblent le plus simple à les intégrer pour ces régions, alors que l'utilisation d'un système de RCS ou d'un laveur à gaz est plus complexe et nécessite beaucoup d'investissement et de maintenance.

Cependant, les solutions de prétraitement sont plus intéressantes pour des applications dans le secteur du transport maritime surtout pour la nouvelle génération des navires qui doivent être lancés après l'adoption de l'annexe VI de la MARPOL (Maritime Pollution) par l'IMO en Avril 2018. Ceci pourra s'expliquer par le fait que les réservoirs du stockage du gaz naturel ainsi que les types des GED et des moteurs à installer seront prévus à l'avance, voir au moment même de la définition du cahier de charge. Pour ce qui est des laveurs de gaz, c'est une solution très intéressante pour les navires déjà existant et à venir. Il faut noter ici, que le lavage de gaz d'échappement est la seule technique aujourd'hui qui permet aux armateurs de rencontrer les exigences de la prévention de la pollution de l'air par les navires en continuant à utiliser le HFO comme carburant principal. De ce fait, le système de lavage de gaz a été sélectionné parmi les autres technologies comme une solution potentielle pour assurer une optimisation écologique dans le secteur du transport maritime. À cet effet, deux bancs d'essais ont été réalisé pour explorer davantage le rendement d'un tel système.

D'autre part, les technologies électriques telles que l'utilisation de l'alternateur Genset-Synchro semble être le plus intéressant pour des sites isolés du fait qu'il pourra être adapté sur les génératrices existantes d'une part, et parce qu'il nécessite aucune modification sur l'architecture du moteur diesel d'autre part. De plus, c'est une technologie qui a démontré

dans les travaux [69-72] une optimisation écologique et énergétique sur le GED en question. Pour ces raisons, l'alternateur Genset-Synchro sera étudié en profondeur dans cette thèse due à sa simplicité d'adaptation dans les réseaux autonomes.

Quant aux concepts de la transmission à variation continue, elle satisfait les critères d'optimisation, cependant elle est limitée en puissance, ce qui limite son champ d'utilisation dans des centrales électriques et ainsi son efficacité globale.

Enfin, la suralimentation des moteurs diesel entrainant des alternateurs tel qu'elle est exploitée et proposer par H. Ibrahim et T. Basbous [81-83], satisfait les critères d'adaptabilité pour des applications autonomes et sera valider sur un banc d'essai réel avec des recommandations pour un système de contrôle optimal.

I.6 MOTIVATIONS ET OBJECTIFS

L'intérêt que nous portons sur l'optimisation des GED trouve son origine dans notre volonté de prolonger les études manufacturières afin d'aboutir à une meilleure performance des systèmes en question. Ainsi située dans la postériorité de ces recherches, la thèse a pour objectif principal d'identifier, de comparer et d'analyser des solutions permettant d'assurer une optimisation globale (opérationnelle, énergétique et écologique) des GED dans des sites isolés et à bord des navires sans apporter des modifications majeures à l'architecture de leurs blocs moteurs.

Signalons particulièrement que notre recherche découle de la constatation de deux lacunes. En premier lieu, la plupart des GED situés dans des communautés éloignées sont continuellement mis en marche sous faible charge causant un faible rendement, une détérioration accélérée du bloc moteur et une augmentation des dépenses notamment où le prix du carburant est très élevé dans ces régions. En deuxième lieu, la plupart des systèmes hybrides proposés nécessitent l'apport de modifications majeures sur l'architecture des GED, modifications que les producteurs d'électricité dans les communautés isolées et les armateurs, ne sont pas toujours prêts à faire, surtout que des telles interventions peuvent entrainer la perte de la garantie du bloc moteur émis par les manufacturiers et plus particulièrement, dans l'industrie du transport maritime. Ajoutons que la finalité de ce

travail de recherche rejoint le désir de proposer un système performant, économique, rendant ainsi son applicabilité crédible au niveau opérationnel, énergétique et écologique.

Afin de pouvoir valoriser l'intérêt de ce projet, cet objectif principal peut être divisé en quatre sous-objectifs:

1) Explorer toutes les techniques possibles pour optimiser les GED et les moteurs diesel marins et retenir celle qui assure le meilleur compromis entre la complexité des changements qu'il faut apporter à un moteur diesel ou à un GED existant d'une part, et l'économie de carburant atteignable grâce à cette technique d'autre part;

2) Valider par des essais pratiques lorsque c'est possible le concept choisi et déterminer les performances techniques (bilan énergétique), économiques (coût du revient du kWh) et environnementale du système sélectionné;

3) Concevoir, développer et simuler un système de contrôle si nécessaire pour assurer l'asservissement et la commande du concept choisi dans des conditions réalistes et caractéristiques d'un site isolé ou d'un navire;

4) Valider par des essais expérimentaux le système sélectionné afin de vérifier ses performances et déterminer les contraintes qui limitent son fonctionnement.

I.7 MÉTHODOLOGIE

La méthodologie suivie pour atteindre l'objectif principal est tributaire de la réalisation des activités suivantes :

Activité 1 : Conduire une analyse comparative des différentes architectures, solutions et technologies (électrique, mécanique, prétraitement, traitement-interne, post traitement, etc.) concernant l'optimisation des groupes électrogènes diesel actuellement en usage. En effet, afin de pouvoir comparer les performances des différentes technologies ou architectures dans les catégories choisies, une liste des

critères sera analysée comme par exemple le coût, la puissance spécifique, la contribution à la réduction de la consommation du carburant et l'émission de GES de chaque technologie. Cette analyse mène à déterminer l'indice de performance de chaque technologie en fonction de la nature d'application du projet et à valider le choix de la technologie ou de l'architecture la plus adéquate ou la plus rentable pour une application cible.

Activité 2 : Une étude expérimentale basée sur l'analyse des gaz d'échappement permettant de prédire et de détecter le fonctionnement en sous-performance des GED afin d'être en mesure d'appliquer des solutions correctives et adéquates.

Activité 3 : Conduire une analyse techno-économique des systèmes d'optimisation pour l'industrie du transport maritime basée sur l'application des solutions de prétraitement, traitement-interne et post-traitement, afin de déterminer les paramètres critiques et/ou optimaux de conception de ces systèmes (avantages et contraintes de leurs applications sur des navires existants et à venir).

Activité 4 : Conduire une investigation pratique et une analyse approfondie sur le rendement des systèmes de lavage de gaz en boucle fermée pour des applications de transport maritime en eau-douce (tel que le Saint-Laurent et les Grands Lacs) utilisant une solution aqueuse d'amine pour le captage du CO_2 et l'abat du SO_x. Nous analysons le taux d'abattement et du captage, la rencontre des exigences des normes établies par l'OMI ainsi que les avantages et les inconvénients du système.

Activité 5 : Instrumenter et valider par des essais expérimentaux la consommation du carburant et les émissions des GES des concepts électriques et mécaniques choisis lorsqu'ils sont appliqués sur un groupe électrogène diesel afin de déterminer l'impact environnemental et la rentabilité des systèmes proposés à petite et moyenne échelle. Nous analysons aussi les avantages et les inconvénients des systèmes en déterminant les paramètres critiques et/ou optimaux de conception et leurs impacts sur le moteur

thermique (combustion des huiles, température, rendement et émission des gaz) et sur les distorsions harmoniques en tension et en courant de l'alternateur.

Activité 6 : Valider expérimentalement le modèle SHEDAC développé et évaluer son impact sur la consommation du carburant d'une part, et sur les émissions d'échappement d'autre part.

Activité 7 : Proposer un système de contrôle pour le concept de Genset-Synchro et valider expérimentalement le modèle développé pour déterminer ses performances et ses limites d'application.

Activité 8 : Élaborer des recommandations pour une étude de validation expérimentale des résultats théoriques obtenus.

I.8 ORIGINALITÉ DE LA THÈSE

La nouveauté de la thèse réside dans l'idée proposée pour optimiser les groupes électrogènes diesel utilisés dans l'électrification des sites isolés (village nordique, mines, tours de télécommunication, base militaire, etc.) et autonomes tels que les navires marchands. En effet, le système Genset-Synchro représente un concept très innovateur. Ce système tel que proposé dans ce projet, n'a jamais fait l'objet d'une application commerciale ou d'un projet pilote et aucun système automatisé n'a été développé pour gérer automatiquement la vitesse statorique de la génératrice lorsque la charge varie. De plus, nous avons pu mener des tests réels dans un site isolé sous des températures hivernales à des fins de validations.

Une originalité de cette thèse apparaît aussi dans l'investigation sur la détection des sous-performances lorsqu'un GED fonctionne sous une faible charge. Les tests menés chez innovation maritime sur un GED de 250kW n'ont jamais été largement exploité sur un banc d'essai réel comme nous l'avons réalisé. De nouveaux indices opérationnels ont été signalés pour la première fois et le développement d'une carte de détection automatique pour prévenir un fonctionnement en sous-performance à base de réseau de neurones s'avère

aujourd'hui réaliste. De plus, l'investigation pratique sur les laveurs des gaz comme solution pour réduire les empreintes écologiques des navires ainsi que la validation pratique menée au sein de laboratoire de LIMA à l'UQAC concernant la suralimentation des moteurs diesel et de l'efficacité énergétique qu'elle pourra apporter au système hybride-éolien-diesel d'une part, et les recommandations techniques sur la limite de la suralimentation d'autre part, ajoute de la valeur à cette thèse de doctorat.

I.9 STRUCTURE DE LA THÈSE

La présente thèse est produite « par articles ». Les différents articles soumis ou publiés dans des journaux scientifiques avec comité de lecture suivent les objectifs et la méthodologie décrits dans le chapitre I.

Le **chapitre II présente le premier article** intitulé « A Review and Comparison on Recent Optimization Methodologies for Diesel Engines and Diesel Power Generators » et q**ui est le fruit de l'activité 1** de la méthodologie. Il expose une évaluation du potentiel et des limites du gain en carburant et des émissions des GES pour les différentes technologies et solutions étudiées et les compares entre elles-mêmes afin de déterminer l'indice de performance de chaque technologie en fonction de la nature d'application du projet.

Le **chapitre III présente un rapport technique** basé sur une étude expérimentale sur l'analyse des gaz d'échappement d'un GED de 250kW et **qui est le fruit de l'activité 2** de la méthodologie. Il expose une investigation approfondie sur la détection des indices de fonctionnement en sous-performance basé plus précisément sur l'analyse du taux de dioxyde de soufre (SO_2), de dioxyde de carbone (CO_2), d'oxyde d'azote (NO_x), de monoxyde de Carbone (CO), du dioxygène (O_2) et de la température des gaz d'échappement. Ce travail couvre l'optimisation opérationnelle des GED en général et ouvre la porte à l'élaboration d'un algorithme de détection et de correction de dégradation du rendement des centrales électriques autonomes.

Le chapitre IV présente le deuxième article intitulé « A Review and Economic Analysis of Different Emission Reduction Techniques for Marine Diesel Engines » et **qui est le fruit de l'activité 3 de la méthodologie**. Il expose la norme adoptée par l'OMI (MARPOL-annexe VI : réglementation relative à la prévention de la pollution atmosphérique par les

navires) ainsi les différentes techniques basées sur le prétraitement, traitement-interne et post-traitement. Une étude techno-économique par le fait est réalisée afin d'évaluer les coûts d'investissement pour un retrofit d'un part, les avantages et les inconvénients de chacune des techniques d'autre part.

Le chapitre V présente le troisième article intitulé « Marinization of a Two-Stage Mixed Structured Packing Scrubber for SO_x Abatement and CO_2 capture » et **qui est le fruit de l'activité 4 de la méthodologie**. Il présente en premier temps les différents types d'épurateurs de gaz utilisés dans le domaine de transport maritime et par la suite les résultats obtenus à partir d'une validation expérimentale, voir le taux d'abattement du dioxyde de soufre et le taux de captage du CO_2 en utilisant des solutions d'amines pour un système à boucle fermée destiné pour des navires naviguant dans des eaux douces.

Le chapitre VI présente le quatrième article intitulé « Modeling and Optimization of the Energy Production Based on Eo-Synchro Application » et **qui est le fruit de l'activité 5 de la méthodologie**. Il expose la conception et le principe du fonctionnement de la nouvelle technologie électrique d'Eo-Synchro connue aussi sous le nom de Genset-Synchro d'un part, ainsi que les résultats obtenus en termes de consommation de carburant lorsqu'elle est appliquée à un GED de 80kW.

Le chapitre VII présente le cinquième article intitulé « Optimizing the Performance of a 500kW Diesel Generator : Impact of the Eo-Synchro concept on Fuel Consumption and Greenhouse Gases » et **qui est le fruit de l'activité 5 de la méthodologie**. Cet article n'est que la suite de l'article précédent dans laquelle sont présentées la consommation du carburant, le taux de GES et les harmonies en courant en tension sur une génératrice diesel de 500kW. Le but principal de ce travail, est d'évaluer si les résultats obtenus en termes de gain en carburant sur un GED de 80kW (petite échelle) tiennent toujours pour un GED de 500kW (moyenne échelle). De plus, une analyse approfondie sur l'impact de la technologie de Genset-Synchro sur les émissions des GES sont présentés et discutés.

Le chapitre VIII présente le sixième article intitulé « Eco-Friendly Selection of Diesel Generator Based on Genset-Synchro Technology for Off-Grid Remote Area Application in the North of Quebec » **et qui est le fruit de l'activité 5.** Dans ce travail, une génératrice

diesel d'ordre de 600kW dotée de la technologie Genset-Synchro a été testé dans le Grand Nord du Québec dans un site isolé sous des températures hivernales atteignant les -30ºC. Ce travail même s'il ressemble à l'article précédent, a été réalisé et soumis à ce journal pour deux raisons :

1) Démontrer que l'application du concept Genset-Synchro peut assurer des gains significatifs en carburant et en GES sous des températures hivernales extrêmement froides;
2) Tester les performances du concept sous des conditions réelles et étudier ses limites d'application.

Le chapitre IX présente le septième article intitulé « Integrated a Variable Frequency Drive for a Diesel-Generating Set Using the Genset-Synchro Concept » **et qui est le fruit de l'activité 7 dans la méthodologie**. Il porte sur la modélisation et le développement d'un circuit de contrôle pour entraîner le moteur de compensation qui assure la rotation du stator de la génératrice Genset-Synchro ainsi que les résultats des tests obtenus sur une génératrice de 500kW.

Le chapitre X présente le huitième et dernier article de cette thèse intitulé « Supercharging of Diesel Engine with Compressed Air : Experimental Investigation on Greenhouse Gases and Performance for a Hybrid Wind-Diesel System » **et qui est le fruit de l'activité 6 dans la méthodologie**. Il décrit le banc d'essais conçu et réalisé à l'université du Québec à Chicoutimi (UQAC) et confirme expérimentalement le potentiel de la suralimentation supplémentaire du moteur diesel par l'air comprimé stocké et ceci pour différents niveaux de charge électrique. L'article présente aussi l'impact de la suralimentation sur les GES et la limite de la suralimentation.

Le chapitre XI termine avec les grandes conclusions et recommandations qu'il est possible de tirer de ce travail et la thèse s'achève par la bibliographie et la section des annexes.

CHAPITRE II

ARTICLE 1

A Review and Comparison on Recent Optimization Methodologies for Diesel Engines and Diesel Power Generators

Publié dans Journal of Power and Energy Engineering, 2019

Volume 7:31-56 / ISSN: 2327-5901

Résumé

Cet article présente **une revue de littérature des technologies existantes** disponibles pour optimiser le rendement énergétique des moteurs et des génératrices diesel afin de réduire le coût de l'électricité, d'accroître le rendement des groupes électrogènes et de réduire leur consommation de carburant et leurs émissions de gaz à effet de serre (GES).

Les méthodes d'optimisation proposées reposent sur l'application des technologies de prétraitement, traitement-interne et de post-traitement pour les moteurs diesel d'un part, et sur l'application des technologies mécaniques et électriques pour les groupes électrogènes diesel (GED) d'autre part.

L'article **compare par la suite les différentes technologies et présente les avantages et les inconvénients** de chacune d'entre elles. Le travail démontre que les techniques basées sur le traitement-interne apportées au moteur diesel pour réduire l'oxyde d'azote (NO_x) sont parvenues largement à maturité et sont présentes dans la plupart des nouveaux moteurs et GED. Quant aux exigences en matière d'émissions de dioxyde de soufre (SO_x), l'intégration des systèmes d'épuration des gaz de postcombustion (anglais :Scrubber) est

la plus efficace avec un taux de réduction de 98%, permettant ainsi aux centrales électriques et aux navires de continuer à utiliser du fuel-oil lourd.

Cependant, les prix élevés du carburant et les fluctuations du prix du pétrole ainsi que les préoccupations relatives aux émissions, ont accru l'importance accordée à utiliser le gaz naturel liquéfié (GNL) comme carburant principal. Il a été démontré que l'utilisation du GNL est une solution technologiquement réalisable puisque les constructeurs ont conçu et développé une large gamme des moteurs fonctionnant au GNL.

Le travail démontre aussi que l'utilisation de plusieurs petites génératrices (N-génératrices) au lieu d'une simple génératrice de grande taille, révèle une économie de carburant et d'émission des GES d'ordre 26%. D'autre part, l'utilisation des GED variables tel que l'application des alternateurs de Genset-Synchro et des alternateurs à double alimentation, permet de réaliser des économies en carburant et en GES allant de 15% à 20% mais sont soumis à des limites en puissance (cas de Genset-Synchro) et de vitesse (pour l'alternateur à double alimentation).

Quant à la technique de suralimentation à air comprimé, il a été démontré que les systèmes hybrides éolien-diesel avec stockage d'énergie sous forme d'air comprimé (SHEDAC), sont les plus avantageux pour des applications autonomes avec une bonne ressource éolienne.

Cette revue nous a permis de mieux comprendre les enjeux et d'aborder les différents aspects économiques et environnementaux qui nous ont motivés d'aller de l'avant dans ce projet. Pour ces raisons, trois concepts étudiés dans cet article ont été sélectionné pour les étudier en profondeur. Il s'agit d'un système d'épuration des gaz de post combustion, de l'alternateur de Genset-Synchro et de la suralimentation à l'aide de l'air comprimé. Le choix est fait en fonction des modifications à apporter aux GED existants d'un part, et aux économies réalisés en termes de carburant et des GES d'autre part.

Scientific Research Publishing

Journal of Power and Energy Engineering, 2019, 7, 31-56
http://www.scirp.org/journal/jpee
ISSN Online: 2327-5901
ISSN Print: 2327-588X

A Review and Comparison on Recent Optimization Methodologies for Diesel Engines and Diesel Power Generators

Mohamad Issa[1*], Hussein Ibrahim[2], Richard Lepage[1], Adrian Ilinca[1]

[1]Laboratory of Wind Energy Research, Université du Québec à Rimouski, Rimouski, Canada
[2]Technological Institute of Industrial Maintenance, Sept-Iles, Canada
Email: *missa@imq.qc.ca, Hussein.Ibrahim@itmi.ca, Richard_lepage01@uqar.ca, Adrian_ilinca@uqar.ca

How to cite this paper: Issa, M., Ibrahim, H., Lepage, R. and Ilinca, A. (2019) A Review and Comparison on Recent Optimization Methodologies for Diesel Engines and Diesel Power Generators. *Journal of Power and Energy Engineering*, **7**, 31-56.
https://doi.org/10.4236/jpee.2019.76003

Received: May 12, 2019
Accepted: June 23, 2019
Published: June 26, 2019

Abstract

The electrical instability that frequently distinguishes the isolated networks and depends on diesel generators to supply their energy requirements leads to an operation of the diesel generator in a transient dynamic condition and/or at low loads. In addition, extended operation of the diesel generator at partial load develops the condensation of combustion residues on the engine cylinder walls, which, after a certain time, increases friction, reduces the efficiency of the equipment and increases its fuel consumption. On the other hand, recent regulatory changes have led to ever more stringent and evolving emission standards. Among these, the International Maritime Organization (IMO) and the Environmental Protection Agency (EPA) have implemented emission standards in order to reduce exhaust gas emitted by marine diesel engines. To phase lower emission engines as soon as possible, a Tier system was adopted. This paper presents a literature review of existing technologies available to optimize the energy performance of diesel engines and diesel generators in order to reduce the cost of electricity, to increase the diesel engine efficiency and to decrease their fuel consumption and greenhouse gases (GHG) emissions. The proposed optimization methodologies are based on the application of Pre-treatment, Internal treatment and Post-treatment technologies for diesel engines and on the application of mechanical and electrical technologies for diesel power generators (DPGs). The list of references given at the end of the paper should offer aids for students and researchers working in this field.

Keywords

Diesel Engine, Diesel Generator, Greenhouse Gas, Tier System, Energy Efficiency, MARPOL Annex VI, Isolated Communities, Off-Grid

1. Introduction

Statistics Canada reported in 2016 that 113,604 people live in the north [1] and rely on diesel generators (DGs) to meet their electricity requirements. In addition, mining facilities, telecommunications infrastructure (cellular, microwave, optical, etc.) and islands such as Anticosti and Iles-de-la-Madeleine are not connected to the main grids and depend on diesel fuel, which is relatively inefficient, expensive and responsible for emission of large amounts of greenhouse gas emissions [2]. Furthermore, in the context of electricity production in these remote areas, the use of DG's alone or in hybridization with renewable energy sources, faces many technical problems. Indeed, the electrical instability that often characterizes the isolated networks, due to the fluctuating character of renewable resources and the high variability in the load profile, lead to an operation of the diesel generator in a transient dynamic condition and/or at low loads. In addition, extended operation of the DG at low levels of charge develops the condensation of combustion residues on the engine cylinder walls, which, after a certain time, increases friction, reduces the efficiency of the equipment and increases its fuel consumption. One way to solve this problem and to eliminate these deposits is to operate the engine at a higher speed until the operating temperature is attained. According to [3], using DPGs with weak operating factors increases wear and fuel consumption. This results in the appearance of several phenomena, including icing, polishing and wet stacking. For these reasons, DPG's supplying autonomous networks are not optimal and should be improved:

- **In terms of energy**: the majority of DGs are oversized and it is recognized that the use of diesel generators under low load factors is very harmful to them in terms of wear and causes high fuel consumption. This is mainly due to an inadequate viscosity of the lubricating oil due to a lack of thermal energy released by engine combustion [4]. This lack of viscosity degrades the lubrication quality of the camshaft bearings and the crankshaft of the engine. The consequence of this wear is directly related to the fuel consumption, which increases during the nominal load. In general, prolonged operation of the DGs under light loads, favors the condensation of the combustion residues on the cylinder walls, which, at the end of a certain time, increases the friction, decreases the efficiency of the engine and increases fuel consumption per kilowatt-hour produced. The objective at this level is therefore to maintain the generator utilization factor greater than 30%.
- **Economically**: DGs, while relatively cheap to purchase, are generally expensive to operate and maintain, particularly at the partial load, because of the high price of fuel delivered to isolated sites [5]. Thus, since the price of diesel fuel is very dependent on the mode of transport used, it is the transport difficulties and the particularities of delivery, which make this cost vary and further increase the cost of exploitation of the diesel generators. For example, the cost of the kWh produced in the localities accessible only by air is gener-

ally higher than that produced in those accessible by boat or by land. In Quebec, the average cost of generating electricity from diesel in the last decades was more than 40/kWh in stand-alone grids, while the average price of electricity sales was established, as in the aggregate Quebec, at about 6/kWh [6].

- **In terms of the environment:** in addition to being non-optimal and expensive, the operation of DGs in autonomous networks has significant environmental impacts [7] [8]. It contaminates local air and soil (old and rusty generators) and contributes greatly to the emission of GHGs. In total, the GHG emissions resulting from the use of generators are estimated at 140,000 tons per year for the subscribers of the Canadian and Quebec independent networks. This quantity of emissions is equivalent to the quantity of GHG emitted by 35,000 cars during a year [9]. The fact that the exploitation of these DGs is not optimal and very expensive, it was necessary to find solutions to reduce operating deficits by favoring alternatives based on different techniques such as mechanical, electrical and ecological solutions.

On the other hand, even though pollution from ship's exhaust gases represents only 3% to 4% of global pollution, the IMO and EPA have adopted strict new standards in order to reduce pollutant emissions including nitrous oxides (NO_x) and Sulphur oxides (SO_X) from marine diesel engines. The new reform to the maritime pollution (MARPOL) annex VI convention adopted in 1997 includes the establishment of emission control areas (ECAs) to scale down emissions in specified sea zones with a gradual reduction in emissions of NO_X, SO_X and particulate matter (PM) [10]. Since then, several measures have been taken into consideration. A tier system has been adopted to reduce NO_X levels, while SO_X will be reduced from current 3, 50% to 0, 50% beginning from 1 January 2020 and PM has been reduced to 0, 10% since January 2015. In particular, the fundamental strategy NO_X limitations for diesel engines (DE's) are tiered as indicated in Figure 1, while Table 1 summarizes the regulatory requirements to reduce ship emissions of Sulphur oxides for ship categories 1, 2 and 3 [11].

The structure of the present article is as follows. Section 2 presents the state of art of DE's optimization using Pre-treatment, Internal-Treatment and Post-treatment technologies, while DPGs optimization relies on mechanical and electrical technologies. Section 3 analyzes the advantages and disadvantages of these technologies (benefits and limitations), while Section 4 provides a preliminary conclusion of our study and a perspective for future work.

2. State of Art

In this section, we present the different technologies and solutions available to optimize the efficiency of DEs and DPGs and reduce their emissions of greenhouse gases (GHGs). Figure 2 shows the global diagram of available technologies for DE optimization while Figure 3 shows the recent methodologies applied for DPG optimization using electrical and mechanical technologies.

Table 1. Low sulphur phase-in dates [11].

Starting year (January 1st)	Category 3 Ships				Category 1 & 2 Ships
	Oceans	Emission Control Areas	EU Ports	California Coastal	
2010	4.5%	1.0%	0.1%	0.5%*	0.05%
2012	3.5%	1.0%	0.1%	0.1%	0.0015%
2015	3.5%	0.1%	0.1%	0.1%	0.0015%
2020-(2025)**	0.5%	0.1%	0.1%	0.1%	0.0015%

0, 5%*: Marine Gas Oil, or 0, 1% Marine Diesel Oil. (2025)**: Implementation of Oceans limit at 0, 5% sulphur.

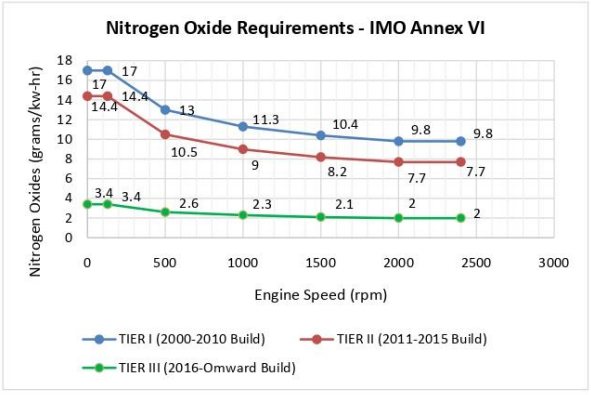

Figure 1. IMO Annex VI TIER nitrous oxides requirements [11].

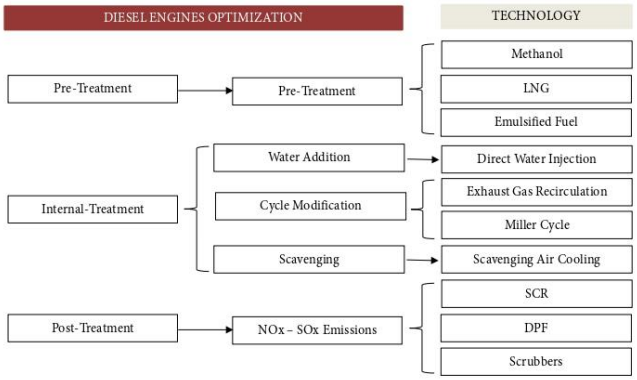

Figure 2. Optimization of the DE using pre-treatment, internal-treatment and post-treatment solutions.

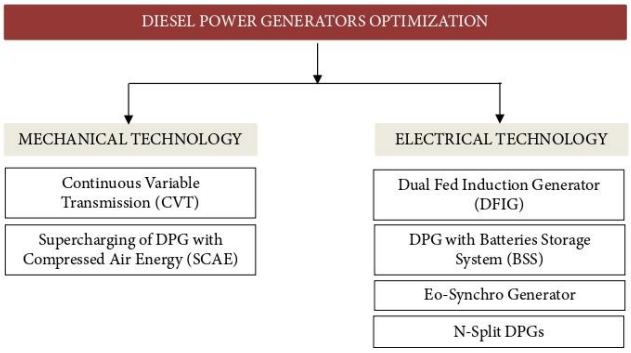

Figure 3. Optimization of the DPG mechanical and electrical technologies.

DE's optimization can be achieved using one of the three methods mentioned in **Figure 2**, such as pre-treatment, internal-treatment or post-treatment technologies. However, most of these technologies do not have a significant impact on fuel consumption reduction but are very effective in reducing SO_X, NO_X and PM by over of 80%. On the other hand, mechanical and electrical technologies applied to DPG's have a significant impact on fuel consumption and GHG's reduction. Some of these technologies can be considered for remote areas, while others are technically restricted. Below, the literature review of state-of-the-art technologies of DE's and DPG's optimization.

2.1. Diesel Engine Optimization Using Pre-Treatment Solutions

Pre-treatment methodology is based on the use of substitute fuel such as methanol and liquified natural gas(LNG), which are characterized by their low Sulphur content, allowing a reduction of SO_x, NO_X and PM emissions. In addition, methanol was a major research topic in the 80s and 90s for transportation application [12] and because of its availability, production and application in fuel cell cars [13] [14] [15] [16]. However, methanol presents challenges for its adaptation on DE's making auto ignition hard due to the low methanol cetane number [17]. Emissions from DE with different fuel were compared and analyzed by Wang *et al.* and have shown reduction of NO_x and PM but an increase in carbon monoxide (CO) and Hydrocarbon (HC) emissions from the methanol-fueled engines. The most recent attraction is the combination of diesel and methanol, which Wang W. *et al.* [17] proposed a diesel/methanol compound combustion (DMCC). By using a DMCC, engine will operate on diesel alone at engine start and light loads to provide a cold starting capacity and prevent the production of aldehydes, while at medium and high loads; the engine operates on a uniform air/methanol mixture to reduce NO_x and PM emissions. **Figure 4** shows the impact of DMCC on NO_X emissions and on the specific fuel consumption [17].

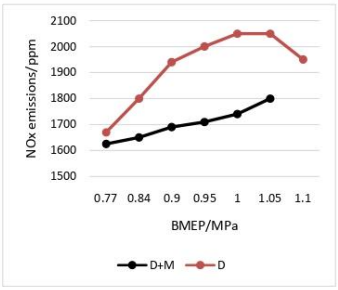

(a)

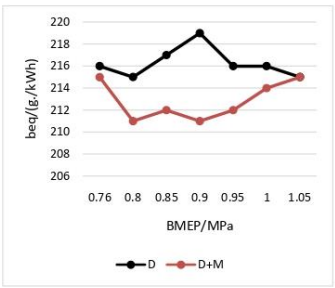

(b)

Figure 4. In (a), comparison of NO_x emissions D for diesel turbocharged engine and D + M for MDCC; In (b), comparison of equivalent fuel consumption [17].

According to **Figure 4**, there is approximately 8% reduction in NOx and 2.8% of fuel consumption when operating with MDCC. Despite its advantages, methanol increases the corrosion risk, which must be sufficiently upgraded to fuel tanks. On the other hand, LNG seems to be an attractive, promising and technically suitable option to satisfy with the regulations on air pollution [17]. LNG has the advantage of reducing SO_x, NO_x, CO_2 and PM compared to the use of a heavy fuel oil (HFO) by 98%, 86%, 11% and 96% respectively [18], **Figure 5**.

Moreover, LNG offers an important benefit over the current HFO in terms of the cost by about 31% per year [18]. A previous study assessed by Wärtsilä in order to evaluate the advantages of changing from HFO fueled engine equipped with a Sea scrubber to LNG fueled engine [19] has shown additional savings from the annual machinery cost (maintenance, oil lubricating, scrubber and SCR with annual capital) by an amount of 500$/kW. Despite these advantages, the LNG's challenge lies in its expensive installations on the one hand and is the higher sizes of its tanks which are 4 times greater than the marine diesel oil tanks [20] on the other hand.

While the use of methanol and LNG appears to increase over the next couple of years in ECAs, emulsified fuel, which was proposed by Professor B. Hopkin-

son, consists in mixing two entirely immiscible liquids offering the advantage for a better atomization and a better distribution of the fuel resulting in a complete combustion [21] [22]. Emulsified fuel has the advantage of reducing NO_x and PM emissions by an amount of 30% and 80% respectively [23] [24].

However, it also motives corrosion of engine components and the short common of oil-water separation phenomenon [25]. Furthermore, emulsified fuel increases the fuel consumption by 2% - 3% to achieve a same output, **Figure 6**.

2.2. Diesel Engine Optimization Using Internal-Treatment

Generally speaking, Internal-treatment consists of a direct modification in the diesel engine. This is done by the DE manufacturers and may require modifications in the injectors design such as the use of direct water injection (DWI) and/or engine cycle such as the use of Miller cycle, exhaust gas recirculation (EGR) and/or combustion chamber such as the use of scavenge air temperature. All these technologies have a positive impact on the reduction of NO_X and PM and can further achieve the standards set out in Annex VI of the MARPOL convention.

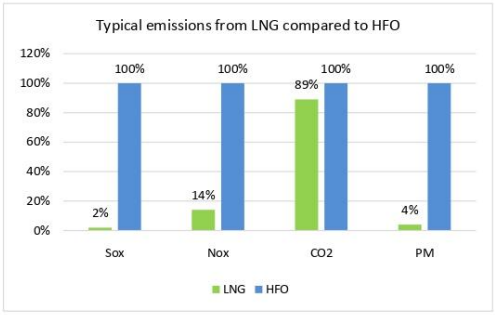

Figure 5. Relative gas emissions for LNG and HFO [18].

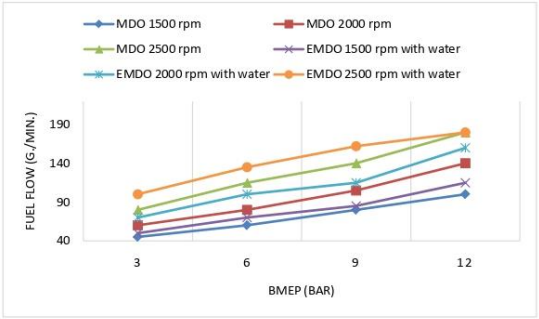

Figure 6. Comparison of fuel consumption with marine diesel oil and emulsified fuel according to rpm tested on a four-stroke-turbo-charged direct injection DE [25].

DWI technology uses an injector composed of two parts, one to spray water and the other to inject fuel oil [26], **Figure 7**. During the fuel injection phase, the water-fuel density 0.4 - 0.7 high pressure water is injected into the combustion chamber and the mixture of water and combustion gas is completed, allowing a reduction of combustion temperatures and NO_X emissions by up to 60% [27]. Another advantage of using this technology appears in the fact that it does not require an extra space or additional cost and can be integrated for a medium speed marine diesel engine. However, this technology can bring to lightly more fuel consumption rate by 2% approximately.

Nevertheless, Miller cycle, which was initially proposed by R. H. Miller in 1947, consist to use the Early Intake Valve Closing (EIVC) to achieve internal cooling before compression in order to reduce the compression cycle work [28].

The Miller cycle is considered as a cold cycle and allows a lower NO_X emission up to 40% - 60% and increase the efficiency of the engine [29]. Furthermore, Miller cycle can be used on four stroke marine diesel engine to complete low scavenge air temperature [30], **Figure 8**. By reducing the scavenge air temperature, combustion temperatures and NO_X are reduced. According to [31], for each 3˚C reduction, nitrogen oxide decreases approximatively by 1 percent.

Moreover, internal engine technology such as Exhaust Gas Recirculation (EGR) results in combustion temperature reduction and small NO_X composition. It is considered as the principal technology to reduce NO_X from DE. **Figure 9** illustrates the schematic diagram of EGR technology [32]. The resulting combination of exhaust gas with the fresh air has a low volume calorific value, which reduces the combustion chamber temperatures, and allows NO_x less formation by 40 percent and more.

It should also be noted that other technologies such as Humid Air Moisturizer (HAM) could reduce nitrogen oxides formation by up to 65%. The HAM technology reposes of a moisturizer, circulating pump, heat exchanger and can require a treatment system to control the mineral content of the water [33].

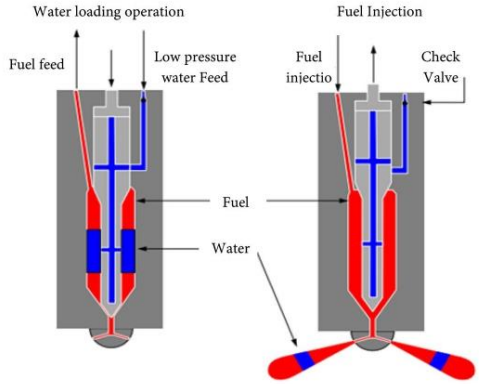

Figure 7. Operation of a classical fuel-water injection system [26].

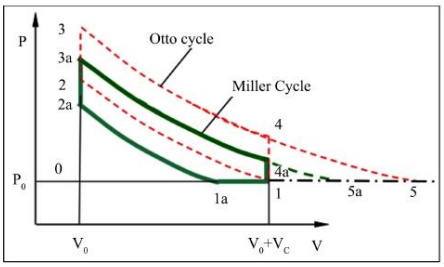

Figure 8. A comparison between Otto cycle and Miller cycle diagram [30].

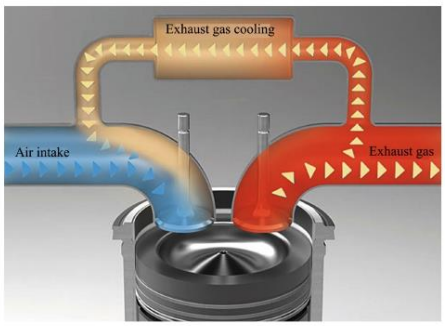

Figure 9. Schematic diagram of EGR [32].

2.3. Diesel Engine Optimization Using Post-Treatment

During 1994 and 2006, exhaust gas emissions regulations for heavy-duty DE's adopted by the EPA aimed attention on reducing NO_X emissions. During this period, NO_X emission requirements declined from 5 g/bhp-hr to 2.4 g/bhp-hr [34]. Consequently, most manufacturers of DE's have adopted the post-treatment technologies to meet NO_X emissions limit. While NO_x abatement relies on post-treatment technologies and/or Internal-treatment such as the EGR and Miller cycle, there is no consequence on Sulphur oxides emissions by bringing measures within the DE [35]. Currently, there is one way to minimize the NO_x emissions by applying after-treatment technology such as the selective catalytic reduction (SCR), diesel particulate filter (DPF), scrubbers or using low Sulphur content fuel such as LNG, methanol and light marine fuel oil (LMFO). However, SCR has an advantage in its adaptation and does not require a modification of the engine architecture but can be subject to space restrictions. Moreover, SCR offers the largest reduction of nitrogen oxide up to 90 percent on DE's. The functioning principle is that the waste exhaust gas is combined with ammonia (NH_3) or urea before passing over a special catalyst layer at a high temperature between 300˚C - 400˚C, reducing the NO_x to N_2 and water (H_2O) [36], **Figure 10**.

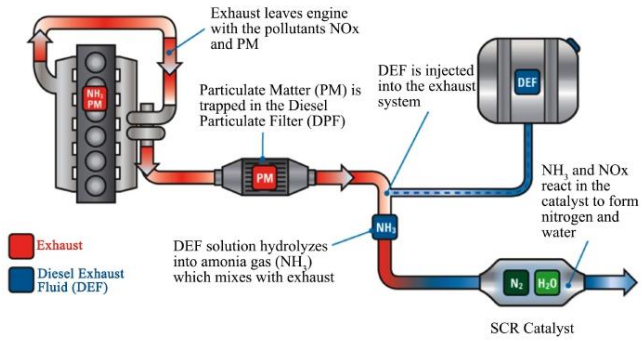

Figure 10. Illustration of the SCR system [36].

For optimal operation, engine load should be higher than 40% and exhaust gas temperature between 270˚C and 400˚C, **Figure 11**. If the temperature is below of 270˚C, ammonium sulphates can form and destroy the catalyst. If temperature exceeds 400˚C, ammonia burns rather than reacting with nitrogen oxides [37] [38].

While SCR offers up to 90% of efficiency for NO_X reduction, a diesel particulate filter (DPF) is used in order to reduce the particulate matter (PM) by an amount of 80% approximately [39]. However, the captured particles will result in an increasing backpressure on the engine allowing an increase in fuel consumption. For this reason, it is therefore important to remove the captured particles using a so-called regeneration technique.

On the other hand, wet or dry-scrubbers are considered the most suitable solutions in order to reduce the SO_x, NO_X, and PM from exhaust of heavy-duty DE's. They are very effective systems, removing up to 99% and 60% abatement of SO_X and NO_X according to [40] [41] but they are very expensive to install and maintain [42]. **Table 2** shows the performance of the Ecospec $CSNO_x$ scrubber developed for marine diesel engines industry that removes Sulphur dioxide, nitrogen dioxide and carbon dioxide all in one process, in a single system [43], while **Figure 12** and **Figure 13**, show a schematic of wet and dry scrubbers [44].

$CSNO_x$ scrubber relies on the patented Ultra Low Frequency (ULF) wave treatment of water to remove the gases. Unlike conventional systems, the system does not require purely fresh water and a cooler to support the chemical process.

Despite their advantages, Scrubbers require frequent maintenance, and can suffer from very severe corrosion [44].

2.4. Diesel Power Generator Optimization Using Mechanical and Electrical Technologies

It is known that running a fixed speed DPG at a light load is harmful to the environment, consumes more fuel and leads to wet stacking phenomena [45]. To overcome this challenge, variable speed diesel engine (VSDE) offers the possibil-

ity to adapt the speed of shaft rotation according to the applied load and allows fuel consumption to be reduced and combustion temperature to be improved. VSDE can be achieved by adopting one of two approaches, with mechanical or electrical technologies. The mechanical solution includes the integration of a continuous variable transmission (CVT), while electrical solution involves the replacement of the synchronous alternator by Eo-synchro alternator or by dual fed induction generator (DFIG) which is applied widely in wind turbine projects.

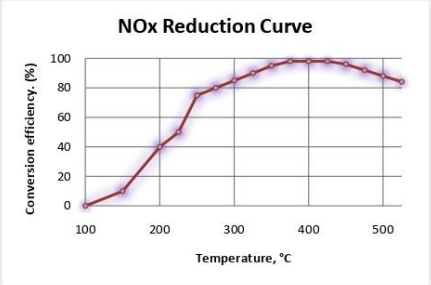

Figure 11. NO_X reduction performance using SCR [38].

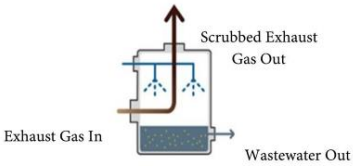

Figure 12. A schematic of wet-scrubber system. Absorbent solution is diffused over the exhaust flue gases allowing the abatement of SO_x and NO_x [44].

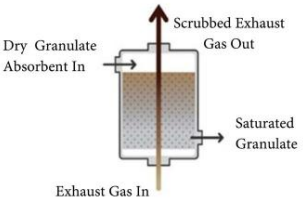

Figure 13. A schematic of dry-scrubber system. The flue gases are passed over granulate absorbent packing bed allowing the abatement of the $SO_x$and NO_x [44].

Table 2. Performance of the $CSNO_x$ scrubber system [43].

	SO_x Removal	NO_x Removal	CO_2 Removal
$CSNO_x$	99%	66%	77%

Mechanically talking, The CVT can adjust the working speed independently of the engine speed, which in turn reduces fuel consumption and GHG's [46]. The Quebec Company CVT Corp. has incorporated a continuously variable transmission in a 125 kW DPG set in order to optimize fuel consumption and reduce GHG emissions for the Puvurnaq power station in Alaska [47], **Figure 14**. Tests have shown a significant saving in terms of fuel and GHG's by an amount of 25%. However, CVT Corp discloses on its website that the maximum power of the generator for which the transmission can be integrated, must not exceed 150 kW. This can be explained in the work carried out by [46] [47] [48] that the limits of a CVT are due to losses of couples due to the use of metal belts, **Figure 15**, and friction between the pulley and the belt resulting in significant wear [48].

In addition, it is normally obligated to be replaced when a CVT fails. This is because individual components can be very expensive or because the specific defective component can be difficult to locate or impossible. For this reasons, electrical solutions seem more advantageous within off-grid applications.

Optimization of DPG's can also be achieved through several methodologies such as the use of compressed air produced by renewable energies to supercharge the DE [49] [50] [51] [52] [53]. Results and tests demonstrated the viability of the supercharge approach by compressed air energy and its storage (CAES) [54], which enabled a significant reduction on fuel consumption and GHG by 25%. Another simpler approach, the air power assist engine (APAE), **Figure 16**, was proposed and tested by [55]. It consists of connecting the air storage tank to the exhaust collector and the use of 3-way valve to change the flow between the turbine and the air storage tank. The APAE shows a fuel consumption reduction up to 15% and generate a positive power by using the compressed air energy.

In addition, pneumatic overfeeding showed an increase in engine efficiency and up to 34% reduction in fuel consumption were reported in simulations with various cycles in the work of [49]-[55]. **Figure 17** shows the fuel consumption reduction with different air intake pressure tested on a 5kW hybrid pneumatic-diesel generator [49].

On the other hand, electrical technology such as application of Genset-Synchro alternator to a diesel engine has shown a significant fuel saving in [56] [57] [58]. The Genset-Synchro alternator is a power unit control system with a highly original approach for power generation based on an innovative alternator design [58], **Figure 18**. Modifications to the structure holding the stator windings are the leading principle behind the Genset-Synchro alternator where this structure now rotates freely in reference to the rotor and frame [56] [57]. An auxiliary motor, driven by a dedicated automatic controller, dictates the desired position, speed or acceleration of the stator structure. This concept ensures regular wave quality regardless of speed variations of the rotor. No energy goes through power electronic equipment as in conventional technologies [56] [57]

[58].

However, with the Genset-Synchro concept, it becomes possible to control the synchronous speed of a 3-phase alternator by controlling the mechanical speed of the stator (control of stator speed only). A significant fuel saving up to 12% can be achieved at low loads (less than 40%) and up to 5% at high loads (85%), Figure 19 [57]. However, the presence of rotor brushes requires more maintenance work and the maximum power delivered by the generator is limited to 85% due to the compensator motor and electronic drive, which are powered by the same output of the generator.

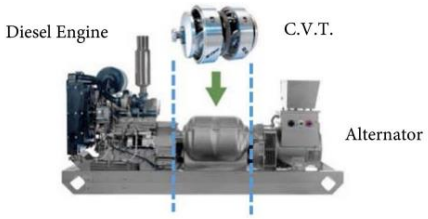

Figure 14. A 125 KW diesel generator equipped with a CVT [47].

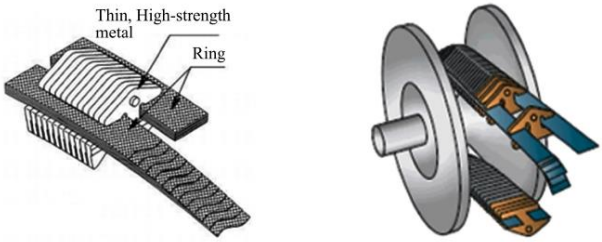

Figure 15. Metal belt design layout [48].

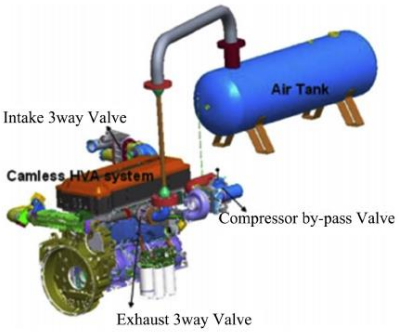

Figure 16. The air power assist engine (APAE) as proposed by Hyungsuk *et al.* [55].

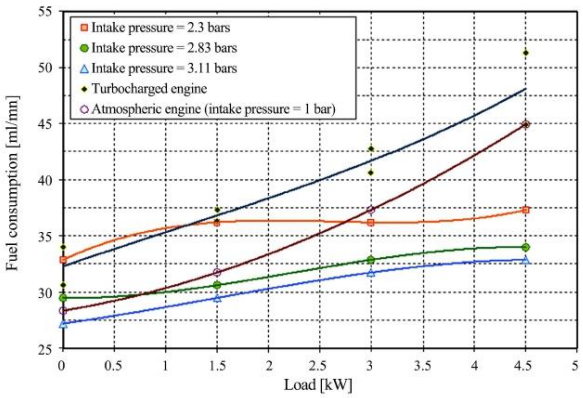

Figure 17. Comparison on fuel consumption reduction with different air intake pressure [49].

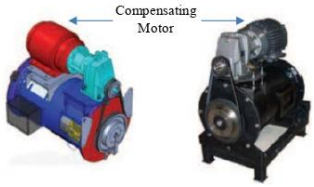

Figure 18. The concept and prototype of an 80 kW Genset-Synchro alternator [58].

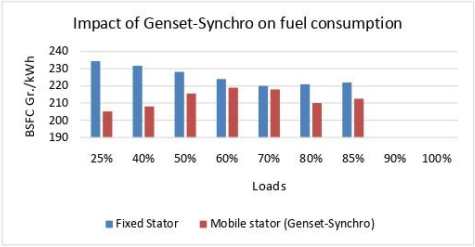

Figure 19. Impact of the Genset-Synchro alternator on fuel consumption applied to a 500 kW DPG [57].

Furthermore, application of DFIG in a DPG can achieve a reduction of fuel consumption and GHG's by up to 20% [59]. Another advantage lies in the use of lower power converters range of 20% of power delivered by stator at synchronous speed [60]. DFIG is built from slip-ring induction generator (SIG) and power electronic converter (PEC) placed between the stator and rotor slip rings [59] [60], **Figure 20**.

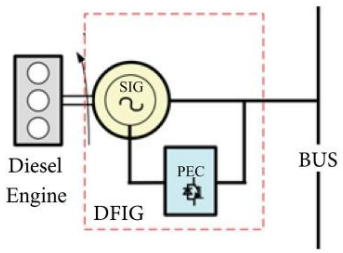

Figure 20. DFIG applied on DPG for energy saving [59].

Despite their advantages, the DFIGs present important harmonic disturbances [59] and require more maintenance due the presence of rotor brushes [59] [60] [61].

DPG optimization can also include the management of electricity generated to minimize losses to the greatest extent possible. This can be done according to two approaches such as the use of n-split DPG's or by using DPG's with storage batteries. In the first approach, it consists of using several smaller units of DPG's whose combined power output is equal to a single DPG, which would otherwise have been used [62]. The big advantage is that it permits multiple power output levels due to the multiple possible combinations of small DPG's thus avoiding the engine to operate under a partial load. **Figure 21** illustrates a typical arrangement of the n-split DPGs [62].

According to the research conducted by Ayodele T.R. *et al.* [62] and which consist the use 3-split DPG's instead of a large sized DPG has shown an improved performance for life cycle cost (LCC), net dump energy, net CO_2 emission and net fuel consumption, **Figure 22**.

According to **Figure 22(a)** and **Figure 22(b)**, there is a reduction by 26% in LCC and a 26.5% on fuel consumption when compared to the single DPG. Moreover, **Figure 22(c)** and **Figure 22(d)** reveal that the CO_2 emissions and the net dump energy of the 3-split DPG's acquired over the period of 9 years, were 27% and 85% lower versus the use of one single large sized DPG.

Finally, and to complete this literature review, application of DPG with batteries storage systems (BSS) has been the subject of researchers for different applications such as stand-alone Microgrid [63]-[68]. **Figure 23** illustrates a typical plan of stand-alone Microgrid. The system contains one local and one general battery storage. The general battery storage should supply the Microgrid for long periods of time in case of emergency situations while the local battery storage is to supply the necessary power conversion parameters for short periods of time [64]. DPG'S and BSS can be combined at any time and the length of their duration work depends on the amount of fuel and batteries discharge. According to [65], realization and application of this methodology in control system allows a fuel consumption reduction for 2% - 5% at acceleration intervals.

Last but not least, different strategies could be investigated in the future to improve the global optimization of the DPG, such as combination of two or three technologies in order to increase efficiency of the DE and to reduce the GHG.

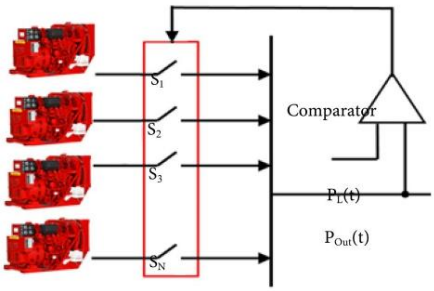

Figure 21. Control of the n-split DPGs model [62].

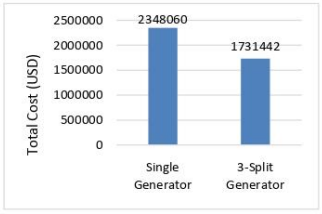

(a)

(b)

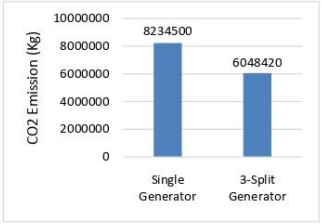

(c)

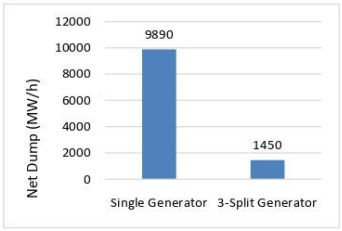

(d)

Figure 22. Comparison of the performance indices between 3-split DPG's versus a single large sized DPG [62]. (a) System LCC; (b) Fuel usage; (c) CO_2 emission; (d) System dump energy.

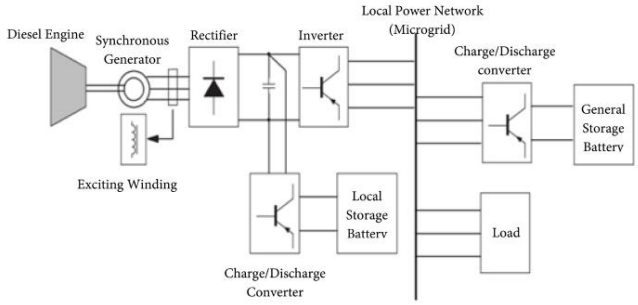

Figure 23. Typical configuration of a stand-alone Microgrid with DPG and BSS [65].

3. Analysis of the Benefits and Limitations of the Proposed Technologies

Each of the above-mentioned techniques has its advantages and disadvantages. To do this, we have created for each of the methodologies applied, a table summarizing the benefits and limitations of the technologies discussed in Section 2. Table 3 covers optimization solutions for DE's using Pre-treatment solutions while Table 4 covers optimization solutions for DE's using Internal and Post-treatment technologies. Finally, Table 5 covers optimization solutions applied for DPG's using electrical and mechanical technologies.

However, in order to be able to evaluate the various solutions proposed and to identify the most efficient techniques according to the application, a list of criteria can be considered by the operator such as:

- Adaptability to the diesel engine: the chosen system must be able to adapt to the engines already in place in the isolated sites or ships without having to change the internal architecture of the engines. The selected technique must be applicable over a wide range of engine and DG models.
- Efficiency of the technology: the chosen system must have a good performance. This criterion is strongly related to the amount of fuel saved and/or

the reduction of GHG.

- Cost: The costs should be as low as possible. In fact, the capital invested is the most important decision factor for the buyer.
- Simplicity of the design: This criterion is essential for maintenance and service. The simplicity of the design improves the maintainability and reduces the operating costs.

Table 3. Benefits and limitations of the selected technologies for DE'S applying pre-treatment solutions

Technology	Benefits	Limitations	References
Emulsified Fuel	• Allows significant NO_x reduction by an amount of 80%	• Increase the fuel consumption by 3% to achieve the same Output	[21]-[27] [68] [69] [70]
Methanol	• Renewable resource • Biodegradable • Allows NO_x reduction by an amount of 60% and fuel consumption by 2% - 3%	• Corrosive • Toxic • Burns with non-luminous flame • Cost	[12] [13] [14] [15] [16]
LNG	• Has environmental benefits through an average reduction of SO_X, NO_X, CO_2 and PM	• Highly flammable • Requires huge investments for storage and installation	[18] [19] [20]

Table 4. Benefits and limitations of the selected technologies for DE's applying internal-treatment and post-treatment solutions.

Technology	Benefits	Limitations	References
Direct Water Injection (DWI)	• Potential reduction of NO_x by an amount of 60% • Can be applied for medium speed marine diesel engine	• Increase the fuel consumption by 2% to achieve the same output	[24] [26] [27]
Exhaust Gas Recirculation (EGR)	• Low operating cost • Allows significant NOx reduction by an amount of 30%	• Cannot be employed at high loads because it will reduce the peak power output • Increase the creation of PM • Drop in engine efficiency	[32]
Miller Cycle	• Increase the efficiency of the DE • Allows potential reduction of NOx by an amount of 40% - 60%	• High cost engine • Requires more maintenance	[28] [29] [30]
Scavenge Air Temperature	• Reduce the number and size of exhaust ports • Allows a potential reduction of NO_x by an amount of 60%	• Cylinder head complex • Requires periodical maintenance	[33]
Selective Catalytic Reduction (SCR)	• Potential reduction of NO_x by an amount of 95% • Relatively simple installation	• May suffer from erosion • High efficiency turbocharger is required to overcome the pressure drop • Require space for urea storage and a good surface for installation	[36] [37] [38]

Continued

Diesel Particulate Filter (DPF)	• Simple installation • Reduces PM pollutant by 95% and Black Carbon (BC) emissions by an amount of 99%	• Allows a backpressure in the engine involving additional fuel consumption by an amount of 4% • Requires regeneration techniques to remove the captured particles	[39]
Open-Loop Wet Scrubber	• Potential reduction of SOX by an amount of 98% • Potential reduction of PM by 60% • Allows the possibility to continue to use the cheaper bunker fuel instead of low sulphur fuel	• Subject to corrosion (seawater) • Requires regular maintenance • Requires additional electric power source • Increase fuel consumption • High cost	[40] [41] [42] [44]
Closed-Loop Wet Scrubber	• Potential reduction of SOX by an amount of 98% and PM by 60% • Allows the possibility to continue to use the cheaper bunker fuel instead of low sulphur fuel	• Requires storage space to hold wastewater and hazardous chemical solutions • High consumption of fresh water • High cost	[40] [41] [42] [44]

Table 5. Benefits and limitations of the selected technologies for DPG's optimization using electrical and mechanical technologies.

Technology	Benefits	Limitations	References
Doubly Fed-Induction Generator (DFIG)	• Potential reduction of fuel consumption and GHG's by an amount of 15% - 20% • Requires a low power converter	• Generates important harmonic disturbances • Very sensitive to grid faults • Requires more maintenance due to the presence of rotor brushes	[61] [62]
Genset-Synchro Generator	• Potential reduction of fuel consumption and GHG's by an amount of 8% - 12% • Can be adapted or integrated on existing DPG and/or Wind turbine generator • Possibility to maintain voltage and frequency constant at the output of the generator by controlling only the stator speed	• Maximum generator power is limited to 85% - 90% due to the presence of the compensating motor • Requires more maintenance due to the presence of rotor brushes • Harmonics level are higher by an amount of 3% compared to a standard Genset	[56] [57] [58]
N-Split DPG	• Potential reduction of fuel consumption and GHG by an amount of 25%	• Requires a large space for installation • Requires more maintenance • High capital costs for purchase and for installation	[62]
DPG with BSS	• Reduction of fuel consumption and GHG by an amount of 5% • Ideal for twining and Hybridization systems such as Solar-Diesel-BSS and Wind-Diesel-BSS	• Batteries management and cost • Requires electronic converters • Not suitable for cold areas	[64] [65] [66] [67] [68]

Continued

Supercharging DE with Compressed Air Energy Storage (CAES)	• Potential reduction of fuel consumption and GHG's by an amount of 20% - 25% • Increase the efficiency of the engine	• Requires architecture modification on the DE • Complex design for control circuit and air energy management • High cost for compressed air energy storage	[49]-[55]
Continuous Variable Transmission (CVT)	• Potential reduction of fuel consumption and GHG's by an amount of 25% • Provides unlimited gear ratio	• High cost • Cannot be applied on DPG over 200 kW • Complex design and must be replaced in case of failure	[46] [47] [48]

4. Conclusion

This paper provides an overview of the latest research developments and solutions concerning mechanical, electrical and ecological optimization in the field of DE and DPG. Internal engine modifications to reduce NOx are largely mature and are present in most new engines using mechanical and ecological solutions such as EGR, Miller cycle, SAT and using external engine methods such as SCR. Tighter SOx emission requirements are leading to sales of post-combustion gas cleaning systems (scrubber solution) as an alternative to use of (expensive) low sulphur fuel. Although one post-combustion technology (Ecospec's CSNOx) has demonstrated reduction of CO_2 emissions as well as NOx and SOx reduction, it remains to be seen if effective commercial scale CO_2 reduction is feasible. High fuel prices and emission concerns have increased the focus on utilizing liquified natural gas (LNG) as fuel oil. Nowadays, utilization of LNG as fuel is a technologically feasible solution since manufacturers have designed and developed a wide range of LNG-fueled engines. Furthermore, the use of n-split diesel generator instead of more commonly used single large-sized diesel generator reveals a fuel and GHG emissions saving up to 26%. However, the use of variable diesel generators such as diesel-driven Genset-Synchro or DFIG can achieve interesting savings on fuel consumption and GHGs up to 15% and 20% but are subject to limit power (85% for Genset-Synchro) and limit speed (close to synchronous speed for DFIG). In addition, advanced diesel technology and control are summarized. In the future work, the APAE technology will be tested on a 75 kW diesel-driven Genset-Synchro generator in order to evaluate the fuel economy, valve response time for opening and closing and effect on pollutants emissions such as NOx and soot. An automated command strategy will be proposed.

Conflicts of Interest

The authors declare no conflicts of interest regarding the publication of this paper.

References

[1] Statistics Canada (2016) Population and Dwelling Counts, for Canada, Provinces

and Territories, 2016 and 2011 Censuses-100% Data. https://www12.statcan.gc.ca/census-recensement/2016/dp-pd/hlt-fst/pd-pl/Table.cfm?Lang=Eng&T=101&S=50&O=A

[2] Rezkallah, M. (2016) Design and Control of Standalone and Hybrid Standalone Power Generation Systems. PhD Thesis, École de Technologie Supérieure, Montréal.

[3] Forcione, A. and Saulnier, B. (2004) Système jumelé éolien-diesel aux Îles-de-la-Madeleine (Cap-aux-Meules) Établissement de la VAN optimale. Institut de Recherche, Hydro-Québec.

[4] Hunter, R. and Elliot, G. (1994) Wind-Diesel Systems: A Guide to the Technology and Its Implementation. Cambridge University Press, Cambridge. https://doi.org/10.1017/CBO9780511574467

[5] Maissan, J.F. (2001) Wind Power Development in Sub-Artic Conditions with Severe Rime Icing. *Circumpolar Climate Change Summit and Exposition*, Whitehorse, 19-21 March 2001, 1-17.

[6] Ibrahim, H. (2010) Étude et conception d'un générateur hybride d'électricité de type éolien-diesel avec élément de stockage d'air comprimé. PhD Thesis, Université du Québec à Chicoutimi, Québec. https://doi.org/10.1522/030145761

[7] Panwar, N.L., Kaushik, S.C. and Kothari, S. (2011) Role of Renewable Energy Sources in Environmental Protection: A Review. *Renewable and Sustainable Energy Reviews*, **15**, 1513-1524. https://doi.org/10.1016/j.rser.2010.11.037

[8] Bajpai, P. and Dash, V. (2012) Hybrid Renewable Energy Systems for Power Generation in Stand-Alone Applications: A Review. *Renewable and Sustainable Energy Reviews*, **16**, 2926-2939. https://doi.org/10.1016/j.rser.2012.02.009

[9] Dönitz, C., Vasile, I., Onder, C. and Guzzella, L. (2009) Realizing a Concept for High Efficiency and Excellent Driveability: The Downsized and Supercharged Hybrid Pneumatic Engine (No. 2009-01-1326). SAE Technical Paper. https://doi.org/10.4271/2009-01-1326

[10] International Maritime Organization (2018) Air Pollution, Energy Efficiency and Greenhouse Gas Emissions. http://www.imo.org/en/OurWork/Environment/PollutionPrevention/AirPollution/Pages/Default.aspx

[11] Reynolds, K.J. (2011) Exhaust Gas Cleaning Systems Selection Guide. Ship Operations Cooperative Program. The Glosten Associates, Washington DC.

[12] Heinrich, W., Marquardt, K.J. and Schaefer, A.J. (1986) Methanol as a Fuel for Commercial Vehicles (No. 861581). SAE Technical Paper. https://doi.org/10.4271/861581

[13] Allard, M. (2000) Issues Associated with Widespread Utilization of Methanol (No. 2000-01-0005). SAE Technical Paper. https://doi.org/10.4271/2000-01-0005

[14] Weimer, T., Schaber, K., Specht, M. and Bandi, A. (1996) Methanol from Atmospheric Carbon Dioxide: A Liquid Zero Emission Fuel for the Future. *Energy Conversion and Management*, **37**, 1351-1356. https://doi.org/10.1016/0196-8904(95)00345-2

[15] Shamsul, N.S., Kamarudin, S.K., Rahman, N.A. and Kofli, N.T. (2014) An Overview on the Production of Bio-Methanol as Potential Renewable Energy. *Renewable and Sustainable Energy Reviews*, **33**, 578-588. https://doi.org/10.1016/j.rser.2014.02.024

[16] Hikino, K. and Suzuki, T. (1989) Development of Methanol Engine with Autoignition for Low NO_x Emission and Better Fuel Economy. In: *SAE Transactions*, SAE International, Warrendale, 639-647.

https://doi.org/10.4271/891842

[17] Wang, W.G., Clark, N.N., Lyons, D.W., Yang, R.M., Gautam, M., Bata, R.M. and Loth, J.L. (1997) Emissions Comparisons from Alternative Fuel Buses and Diesel Buses with a Chassis Dynamometer Testing Facility. *Environmental Science & Technology*, **31**, 3132-3137. https://doi.org/10.1021/es9701063

[18] Elgohary, M.M., Seddiek, I.S. and Salem, A.M. (2015) Overview of Alternative Fuels with Emphasis on the Potential of Liquefied Natural Gas as Future Marine Fuel. *Proceedings of the Institution of Mechanical Engineers, Part M: Journal of Engineering for the Maritime Environment*, **229**, 365-375. https://doi.org/10.1177/1475090214522778

[19] Levander, O. (2011) Dual Fuel Engines Latest Developments. Technical Report, Wärtsilä, Concept Design, Hamburg. https://www.stg-online.org/veranstaltungen/Ship_Efficiency_2013.html

[20] Sastre, B.L. (2017) Implementation of LNG as Marine Fuel in Current Vessels: Perspectives and Improvements on Their Environmental Efficiency. Master Thesis, Universitat Politècnica de Catalunya, Barcelona.

[21] Nilsen, O.V. (2018) LNG Regulatory Update "Best Fuel of the Future". *Internationalisation Conference on LNG Project & the Baltic Sea Region LNG Cluster*, Bergen, 10-12 April 2018, 1-31. http://www.golng.eu/files/Main/20180417/2.%20Ole%20Vidar%20Nilsen%20-%20DNV%20GL.pdf

[22] Patel, N.S., Modi, M. and Patel, T. (2017) Investigation of Diesel Engine with Water Emulsifier—A Review. *International Research Journal of Engineering and Technology*, **4**, 879-883.

[23] Vellaiyan, S. and Amirthagadeswaran, K.S. (2016) The Role of Water-in-Diesel Emulsion and Its Additives on Diesel Engine Performance and Emission Levels: A Retrospective Review. *Alexandria Engineering Journal*, **55**, 2463-2472. https://doi.org/10.1016/j.aej.2016.07.021

[24] Kim, M., Oh, J. and Lee, C. (2018) Study on Combustion and Emission Characteristics of Marine Diesel Oil and Water-in-Oil Emulsified Marine Diesel Oil. *Energies*, **11**, 1830. https://doi.org/10.3390/en11071830

[25] Zhou, S., Liu, Y. and Zhou, J.X. (2014) A Study on Exhaust Gas Emission Control Technology of Marine Diesel Engine. *Advanced Materials Research*, **864-867**, 1804-1809. https://doi.org/10.4028/www.scientific.net/AMR.864-867.1804

[26] Bedford, F., Rutland, C., Dittrich, P., Raab, A. and Wirbeleit, F. (2000) Effects of Direct Water Injection on DI Diesel Engine Combustion (No. 2000-01-2938). SAE Technical Paper. https://doi.org/10.4271/2000-01-2938

[27] Wärtsilä Corporation (2006) The Engine of Industry. Wärtsilä Annual Report, Helsinki. https://www.wartsila.com/docs/default-source/investors/financial-materials/annual-reports/annual-report-2006.pdf?sfvrsn=b1b31c45_2

[28] Wang, Y., Lin, L., Roskilly, A.P., Zeng, S., Huang, J., He, Y., Yang, J., *et al.* (2007) An Analytic Study of Applying Miller Cycle to Reduce NO_x Emission from Petrol Engine. *Applied Thermal Engineering*, **27**, 1779-1789. https://doi.org/10.1016/j.applthermaleng.2007.01.013

[29] Kovács, D. and Eilts, P. (2015) Potentials of the Miller Cycle on HD Diesel Engines Regarding Performance Increase and Reduction of Emissions (No. 2015-24-2440). SAE Technical Paper. https://doi.org/10.4271/2015-24-2440

[30] Goldsworthy, L. (2002) Design of Ship Engines for Reduced Emissions of Oxides of Nitrogen. *Engineering a Sustainable Future Conference Proceedings*, Launceston, 6 August 2002, Vol.6, 1-10.

[31] Geist, M. (1998) Sulzer RTA-8T Engines: Compact Two-Strokes for Tankers and Bulk Carriers. Technology Review, Wärtsilä NSD Switzerland Ltd., Winterthur.

[32] Kech, J., Hegner, R. and Mannle, T. (2014) Turbocharging: Key Technology for High-Performance Engines. MTU Engine Technology White Paper.

[33] Park, H.K., Ghal, S.H., Kim, B.S., Kim, K.D. and Kim, J.S. (2006) NO_x Reduction of a Medium Speed Diesel Engine Using a Charge Air Moisturizer System. In: *ASME 2006 Internal Combustion Engine Division Fall Technical Conference*, American Society of Mechanical Engineers, New York, 25-29. https://doi.org/10.1115/ICEF2006-1548

[34] Jääskeläinen, H. and Addy Majewski, W. (2018) Heavy-Duty Diesel Engines with Aftertreatment. DieselNet Technology Guide. https://dieselnet.com/tech/engine_heavy-duty_aftertreatment.php

[35] Man Diesel Turbo (2018) Exhaust Gas Emission Control Today and Tomorrow. https://marine.mandieselturbo.com/docs/librariesprovider6/technical-papers/exhaust-gas-emission-control-today-and-tomorrow.pdf?sfvrsn=22

[36] Baik, J.H., Yim, S.D., Nam, I.S., Mok, Y.S., Lee, J.H., Cho, B.K. and Oh, S.H. (2004) Control of NO_x Emissions from Diesel Engine by Selective Catalytic Reduction (SCR) with Urea. *Topics in Catalysis*, **30**, 37-41. https://doi.org/10.1023/B:TOCA.0000029725.88068.97

[37] Tersus Diesel Exhaust Fluid (2017) Selective Catalytic Reduction. How It Works, https://www.tersusdef.com/about/how-selective-catalytic-reduction-scr-works

[38] Nett Technologies Inc. (2016) BlueMax™ Selective Catalytic Reduction (SCR) System. SCR Performance. https://www.nettinc.com/products/selective-catalytic-reduction-scr/bluemax

[39] Van Rens, G. and De Wilde, H. (2005) Pre- and After-Treatment Techniques for Diesel Engines in Inland Navigation. Technical Report in the Framework of EU Project CREATING.

[40] Andersson, K., Brynolf, S., Lindgren, J.F. and Wilewska-Bien, M. (2016) Shipping and the Environment: Improving Environmental Performance in Marine Transportation. Springer, Berlin.

[41] Ibrahim, S. (2016) Process Evaluation of a SO_x and NO_x Exhaust Gas Cleaning Concept for Marine Application. Chalmers University of Technology, Göteborg.

[42] University of Calgary (2018) Energy Education—Scrubber. https://energyeducation.ca/encyclopedia/Scrubber

[43] Ecospec (2015) $CSNO_X$ Emission Control. http://www.ecospec.com/marine-csnox

[44] Wolfson, R. (2012) Energy, Environment and Climate. 2nd Edition, Norton, New York.

[45] Hamilton, J.M., Negnevitsky, M., Wang, X., Tavakoli, A. and Mueller-Stoffels, M. (2017) Utilization and Optimization of Diesel Generation for Maximum Renewable Energy Integration. In: *Smart Energy Grid Design for Island Countries*, Springer, Cham, 21-70. https://doi.org/10.1007/978-3-319-50197-0_2

[46] Seelan, V. (2015) Analysis, Design and Application of Continuously Variable Transmission (CVT). *International Journal of Engineering Research and Applications*, **5**, 99-105.

[47] Meiners, D. (2013) Application of Variable Speed Diesel Generator Set for Village

Power and Wind-Diesel Applications. Report, Alaska Energy Authority, Anchorage.

[48] Kim, J., Park, F.C., Park, Y. and Shizuo, M. (2002) Design and Analysis of a Spherical Continuously Variable Transmission. *Journal of Mechanical Design*, **124**, 21-29. https://doi.org/10.1115/1.1436487

[49] Ibrahim, H., Younès, R., Ilinca, A., Ramdenee, D., Dimitrova, M., Perron, J., Arbez, C., *et al.* (2011) Potential of a Hybrid Wind-Diesel-Compressed Air System for Nordic Remote Canadian Areas. *Energy Procedia*, **6**, 795-804. https://doi.org/10.1016/j.egypro.2011.05.090

[50] Basbous, T. (2013) Hybridation pneumatique d'un moteur diesel en vue de son utilisation dans un système hybride éolien-diesel avec stockage d'énergie sous forme d'air comprimé. PhD Thesis, Université du Québec à Chicoutimi, Québec. https://doi.org/10.1522/030565288

[51] Beaulac, P. (2014) Jumelage éolien-diesel avec stockage d'air comprimé: Modélisation de la suralimentation du moteur diesel. Master of Science Thesis, Université du Québec à Rimouski, Québec.

[52] Saad, Y. (2018) Gestion optimale des systèmes hybrides pour la production de l'énergie dans les sites isolés. PhD Thesis, Université de technologie Belfort-Montbéliard, Belfort.

[53] Kang, H. and Tai, C. (2010) Demonstration of Air-Power-Assist Engine Technology for Clean Combustion and Direct Energy Recovery in Heavy Duty Application. Mack Trucks Incorporated, Detroit, MI.

[54] Foley, A. and Lobera, I.D. (2013) Impacts of Compressed Air Energy Storage Plant on an Electricity Market with a Large Renewable Energy Portfolio. *Energy*, **57**, 85-94. https://doi.org/10.1016/j.energy.2013.04.031

[55] Ibrahim, H., Ilinca, A. and Perron, J. (2008) Energy Storage Systems—Characteristics and Comparisons. *Renewable and Sustainable Energy Reviews*, **12**, 1221-1250. https://doi.org/10.1016/j.rser.2007.01.023

[56] Issa, M., *et al.* (2017) Modeling and Optimization of the Energy Production Based on Eo-Synchro Application. *Power Engineer*, **21**, 3-9.

[57] Issa, M., *et al.* (2018) Optimizing the Performance of a 500kW Diesel Generator: Impact of the Eo-Synchro Concept on Fuel Consumption and Greenhouse Gases. *Power Engineer*, **23**, 22-31.

[58] Issa, M., Fiset, J., Ibrahim, H. and Ilinca, A. (2019) Eco-Friendly Selection of Diesel Generator Based on Genset-Synchro Technology for Off-Grid Remote Area Application in the North of Quebec. *Energy and Power Engineering*, **11**, 232-247. https://doi.org/10.4236/epe.2019.115015

[59] Koczara, W. and Iwanski, G. (2009) Fuel Saving Variable Speed Generating Set. *International Conference on Clean Electrical Power*, Capri, 9-11 June 2009, 22-28. https://doi.org/10.1109/ICCEP.2009.5212087

[60] Iwanski, G. and Koczara, W. (2008) Power Management in an Autonomous Adjustable Speed Large Power Diesel Gensets. *Power Electronics and Motion Control Conference*, Poznan, 1-3 September 2008, 2164-2169. https://doi.org/10.1109/EPEPEMC.2008.4635586

[61] Kendouli, F., Nabti, K., Abed, K. and Benalla, H. (2011) Modélisation, simulation et contrôle d'une turbine éolienne à vitesse variable basée sur la génératrice asynchrone à double alimentation. *Revue des Energies Renouvelables*, **14**, 109-120.

[62] Ayodele, T.R., Ogunjuyigbe, A.S.O. and Akinola, O.A. (2017) N-Split Generator Model: An Approach to Reducing Fuel Consumption, LCC, CO_2 Emission and

Dump Energy in a Captive Power Environment. *Sustainable Production and Consumption*, **12**, 193-205. https://doi.org/10.1016/j.spc.2017.07.006

[63] Voroshilov, A.N., Khristolyubova, A.I., Khristolyubov, A.A. and Kuchak, S.V. (2013) Diesel-Generator Set Working in Parallel with Electrical Energy Storage System. 14*th International Conference of Young Specialists on Micro/Nanotechnologies and Electron Devices*, 1-5 July 2013, 288-292. https://doi.org/10.1109/EDM.2013.6641997

[64] Pichkalov, I. (2014) Optimal Coordinated Control of Diesel Generator and Battery Storage System of Stand-Alone Microgrid. 2*nd Workshop on Advances in Information, Electronic and Electrical Engineering*, Vilnius, 28-29 November 2014, 1-4. https://doi.org/10.1109/AIEEE.2014.7020331

[65] Guo, L., Fu, X., Li, X. and Wang, C. (2012) Coordinated Control of Battery Storage System and Diesel Generators in AC Island Microgrid. 7*th International Power Electronics and Motion Control Conference*, Harbin, 2-5 June 2012, Vol. 1, 112-117. https://doi.org/10.1109/IPEMC.2012.6258871

[66] Shaahid, S.M. and El-Amin, I. (2009) Techno-Economic Evaluation of Off-Grid Hybrid Photovoltaic-Diesel-Battery Power Systems for Rural Electrification in Saudi Arabia—A Way Forward for Sustainable Development. *Renewable and Sustainable Energy Reviews*, **13**, 625-633. https://doi.org/10.1016/j.rser.2007.11.017

[67] Ghasemi, A., Asrari, A., Zarif, M. and Abdelwahed, S. (2013) Techno-Economic Analysis of Stand-Alone Hybrid Photovoltaic-Diesel-Battery Systems for Rural Electrification in Eastern Part of Iran—A Step toward Sustainable Rural Development. *Renewable and Sustainable Energy Reviews*, **28**, 456-462. https://doi.org/10.1016/j.rser.2013.08.011

[68] Bernal-Agustín, J.L. and Dufo-Lopez, R. (2009) Simulation and Optimization of Stand-Alone Hybrid Renewable Energy Systems. *Renewable and Sustainable Energy Reviews*, **13**, 2111-2118. https://doi.org/10.1016/j.rser.2009.01.010

[69] Syu, J.-Y., Chang, Y.-Y., Tseng, C.-H., *et al.* (2014) Effects of Water-Emulsified Fuel on a Diesel Engine Generator's Thermal Efficiency and Exhaust. *Journal of the Air & Waste Management Association*, **64**, 970-978. https://doi.org/10.1080/10962247.2014.905508

[70] Vellaiyan, S. and Amirthagadeswaran, K.S. (2017) Emission Characteristics of Water-Emulsified Diesel Fuel at Optimized Engine Operation Condition. *Petroleum Science and Technology*, **35**, 1355-1363. https://doi.org/10.1080/10916466.2017.1330348

CHAPITRE III

Rapport technique

Détection des sous-performances dans un groupe électrogène diesel (GED)

Résumé

Dans un contexte de production d'électricité en régions éloignées, l'utilisation de groupes diesel, seuls ou en hybridation avec des sources d'énergies renouvelables, fait face à des problématiques techniques bien connues. En effet, l'instabilité électrique qui caractérise souvent les réseaux isolés, qui est due au caractère fluctuant des ressources renouvelables et aux variations de la charge, induit un fonctionnement des groupes électrogènes diesel (GED) en régime dynamique transitoire et/ou à faibles charges. De plus, un fonctionnement prolongé des GED à faibles niveaux de charge favorise la condensation des résidus de combustion sur les parois des cylindres de moteurs des GED, ce qui, au bout d'un certain temps, augmente la friction, diminue leur rendement et accroît leur consommation en carburant. Une des façons permettant de résoudre ce problème consiste à faire opérer le moteur à un régime plus élevé jusqu'à ce que la température d'opération, qui élimine ces dépôts, soit atteinte.

Le présent rapport présente les résultats de tests menés chez Innovation maritime à Rimouski pour la détection des sous-performances sur un groupe électrogène diesel de 250kW du marque C-9 de Caterpillar. Les tests sont basés sur une analyse approfondie des

gaz d'échappement. Il a été conclu que le taux de dioxyde de soufre (SO_2), le taux de soufre (S), la température des gaz d'échappement ainsi que la consommation de carburant offrent de bons indices lorsque le groupe électrogène diesel opère sous une très faible ou une faible charge (≤35%).

III.1 DESCRIPTION DE LA FICHE TECHNIQUE DE LA GÉNÉRATRICE UTILISÉE

La fiche technique de la génératrice diesel utilisée pour la détection des sous-performances est présentée dans le Tableau 4.

Tableau 4 : Spécifications techniques de la génératrice utilisée pour les tests. (Source : Caterpillar)

Modèle du moteur	**CAT C-9**	
Puissance (kW)	250	
Courant (A)	301	
Tension de sortie (V)	600	
Facteur de puissance	0,8	
Puissance apparente (kVA)	312	
Fréquence (Hz)	60	
Année de construction	2006	

III.2 DESCRIPTION DE L'INSTRUMENTATION DE LA GÉNÉRATRICE

La génératrice diesel C-9 est instrumentée par deux débitmètres à vis fonctionnant en différentiel. Les débitmètres utilisés sont de marque KRAL (modèle de série OME-13) avec une précision des valeurs mesurées en différentiel de ±0,4 % et d'un système

d'acquisition des données OP5 d'OPDAQ Systèmes. La Figure 18 illustre l'installation des débitmètres et du système d'acquisition de données. Ce dernier, enregistre en temps réel les données provenant de la génératrice (voir Tableau 5) ainsi que la consommation du carburant provenant des débitmètres.

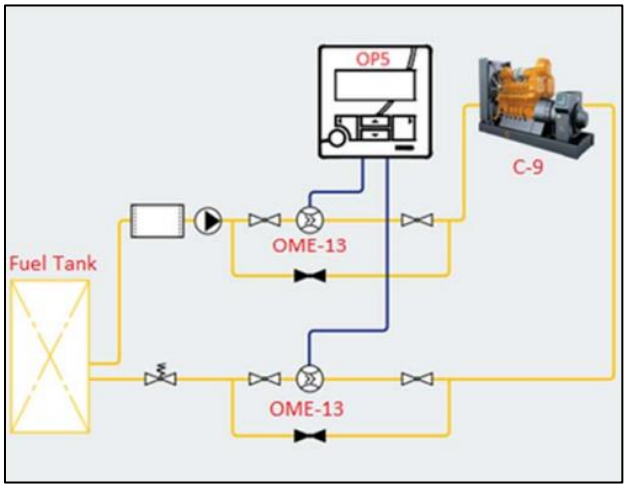

Figure 18 : Principe d'une mesure différentielle

Tableau 5 : Liste des capteurs reliés au système d'acquisition de données (l'OP5)

Numéro	Description
1	Température du moteur (ºC)
2	Vitesse de rotation du moteur (RPM)
3	Pression d'admission du moteur (kPa)
4	Température d'admission du moteur (ºC)
5	Pression d'huile du moteur (kPa)
6	Courant débité (A)
7	Tension débitée (V)
8	Puissance réactive (VAR) et puissance réelle (W)

Pour ce qui est de la mesure des puissances, la génératrice est instrumentée par un analyseur de puissance avec une précision de ±5%. Quant à l'analyseur des gaz d'échappement, un analyseur portatif professionnel du marque Testo (Testo 350 V.2) a été utilisé, Figure 19 . Les données sont enregistrées en temps réel sur un ordinateur portatif. Le

Tableau 6 montre la précision et le temps de réponse de l'analyseur du gaz utilisé.

Figure 19 : Illustration de l'analyseur des gaz utilisé (modèle Testo 350 V.2)

Tableau 6 : Précision et temps de réponse de l'analyseur utilisé (Source : Testo.com)

No.	Description	Précision	Temps de réponse
1	Température des gaz d'echappement	±1°C (0...1760°C)	
2	Dioxyde de soufre (SO2)	±5ppm (0…99 ppm) ±5 % de la valeur moyenne (100…1 999 ppm) ±10 % de la valeur moyenne (plage restante)	< 30s
3	Dioxyde de carbone (CO2)	±0,3 vol.% ±1 % de la valeur moyenne (0…25 Vol.%) ±0,5 vol.% ±1,5 % de la valeur moyenne (plage restante)	< 10s Temps de préchauffage : < 15min.
4	Oxyde d'azote (NOx)	±2 ppm (0…39,9 ppm) ±5 % de la valeur moyenne (plage restante)	< 30s
5	Dioxygène (O2)	±0,2 vol. %	< 20s
6	Monoxyde de carbone (CO)	±10 ppm (0…199 ppm) ±5 % de la valeur moyenne (200…2 000 ppm) ±10 % de la valeur moyenne (plage restante)	< 40s

La Figure 20 illustre la connexion de la sonde de mesure de l'analyseur de combustion à la conduite de l'échappement de la génératrice C-9.

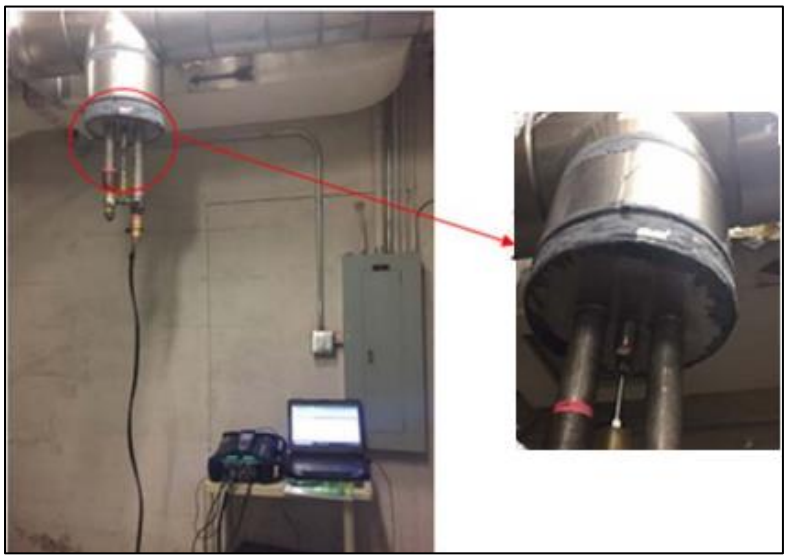

Figure 20 : Illustration du branchement de la sonde de l'analyseur de combustion des gaz d'échappement.

Cependant, pour assurer la variation de la charge, nous avons utilisé un banc de charge résistive de 250Kw et qui est relié à la génératrice C-9. Le contrôle est assuré par une armoire de contrôle manuelle illustrée dans la Figure 21. Les charges résistives sont constituées de 5 résistances de 15Kw et de 5 résistances de 35kW de type SSP avec une tolérance ±1-10%.

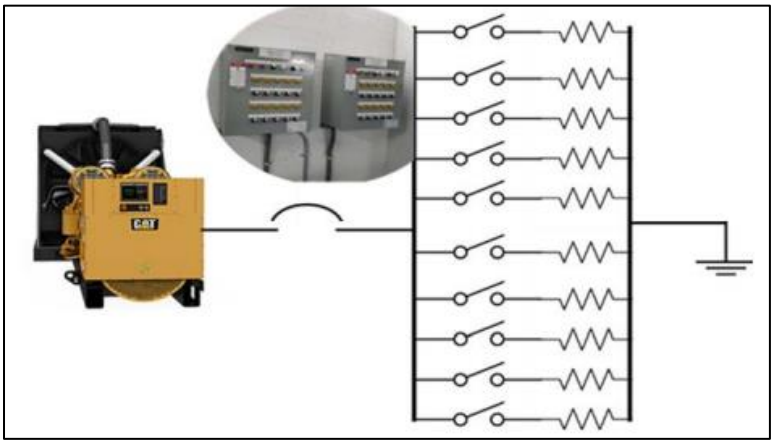

Figure 21 : Illustration simplifié du banc d'essai utilisé

III.3 MÉTHODOLOGIE DES TESTS

Dans le but d'identifier des indices pouvant servir à la détection des sous-performances ou pour prévenir le début du fonctionnement d'un GED en sous-performance, un protocole de tests a été créé. Ce protocole consiste à augmenter progressivement la charge sur un GED, à analyser la composition des gaz d'échappement ainsi que certains paramètres opérationnels afin de déterminer si des tendances peuvent indiquer un potentiel de sous-performance. L'analyse repose sur les données provenant du système d'acquisition OP-5 (voir liste des capteurs dans le Tableau 5 : Liste des capteurs reliés au système d'acquisition de données (l'OP5)) et de l'analyseur de combustion de gaz d'échappement. La durée définie pour chaque test est de 10 minutes, suivie d'une attente (stand-by à vide) d'une minute lorsque la charge appliquée est ≤ 28 %. Cependant, lorsque la charge appliquée est ≥ 30 %, l'attente à vide est maintenue pour 3 minutes au lieu d'une minute. Afin de valider la stabilité des données, le protocole de tests (voir Tableau 7) est répété 3 fois. Les tests ont été réalisés avec une température ambiante enregistrée variant de 23°C à 40°C. Les températures ambiantes enregistrées sont ajoutées dans les tableaux de résultats pour mieux

refléter l'évolution de la température ambiante en fonction de la charge appliquée dans le temps.

Tableau 7 : Description du protocole utilisé pour les trois tests

N° Test	Charge appliquée	
	(kW)	(%)
1	0	0
2	15	6
3	30	12
4	35	14
5	45	18
6	50	20
7	60	24
8	65	26
9	70	28
10	75	30
11	80	32
12	95	38
13	100	40
14	105	42
15	110	44
16	115	46
17	120	48
18	130	52

III.4 RÉSULTATS DES TESTS EFFECTUÉS

III.4.1 Mesure de la consommation de carburant en fonction de la charge appliquée

Dans cette section, les valeurs mesurées de la consommation de carburant en fonction de la charge appliquée (valeur moyenne des 3 tests) sont présentées dans le Tableau 8. L'analyse démontre que la variation de la consommation de carburant en fonction de la charge varie instantanément lors du passage d'une faible charge vers une grande charge et vice-versa. Cela permet de conclure que la courbe de consommation d'un GED par rapport à la charge pourra servir comme indicateur du niveau de charge appliqué à un GED. La Figure 22 représente la consommation moyenne (litre/heure) en fonction la charge (%). Elle permet de visualiser la consommation moyenne du moteur diesel lorsque la charge varie, ce qui correspond bien à une droite linéaire. La courbe de tendance linéaire indique clairement que la consommation moyenne augmente entre 0 % et 52 % de charge. Le coefficient de détermination R2 est de 0.9984, ce qui indique un bon ajustement de la ligne pour les données.

Tableau 8 : Investigation sur la consommation du carburant en fonction de la charge

Charge appliquée		Consommation moyenne	Température ambiante enregistrée
(kW)	(%)	(L/h)	(°C)
0	0	9	30,1
15	6	12,3	30,6
30	12	15,5	31
35	14	16,9	31,9
45	18	20,1	32,6
50	20	21,1	33,3
60	24	23,5	34,1
65	26	25,1	34,7
70	28	27	35,5
75	30	28,4	36,2
80	32	30,3	36,9
95	38	34,3	37,9
100	40	35,7	38,7
105	42	37,3	39,4
110	44	38,5	40,1
115	46	40	40,8
120	48	41,7	41,6
130	52	44	42,1

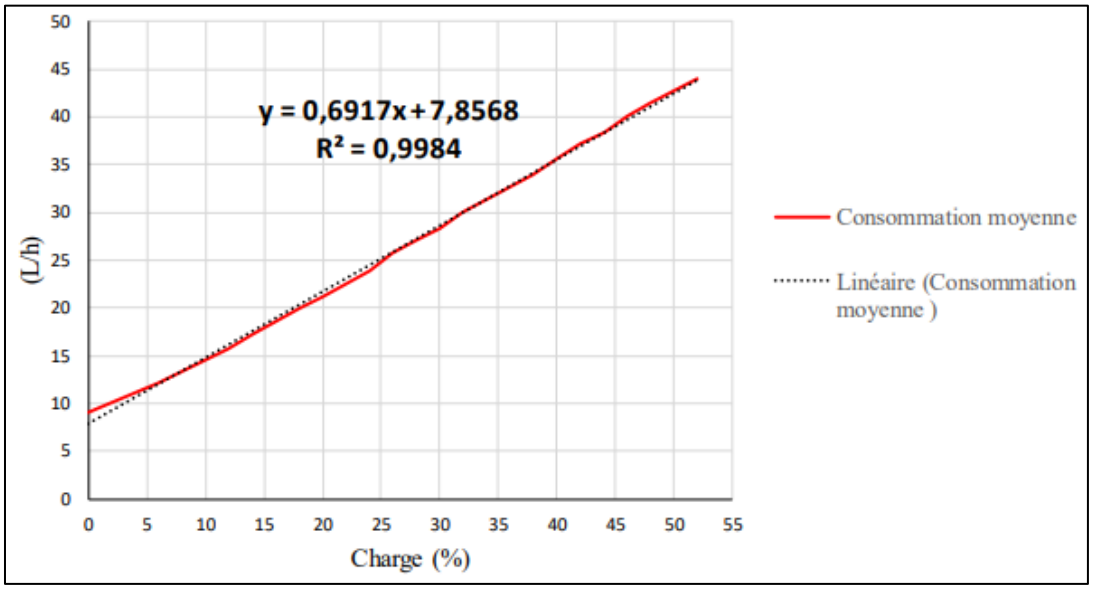

Figure 22 : Courbe de tendance pour la consommation du carburant par rapport à la charge appliquée.

III.4.2 Mesure du taux de dioxyde de soufre (SO_2) en fonction de la charge appliquée

Cette section présente les résultats de mesures du taux du dioxyde de soufre (SO_2) en fonction de la charge appliquée. Les données traitées dans cette section proviennent directement de l'analyseur de gaz d'échappement (TESTO 350). Les données du TESTO 350 sont en relation avec les données de la charge du moteur qui provient d'OP-5. Ces données sont présentées dans le Tableau 9. Il a été constaté que le taux de dioxyde de soufre peut offrir un indice important pour la détection des sous-performances dans des GED. Ceci pourrait s'expliquer par le fait que la température de combustion atteinte est au-delà d'une certaine valeur critique et/ou par le fait que l'augmentation de la prise d'air en fonction de la charge permet au taux de dioxyde de soufre de se stabiliser [81] ; [82]. La Figure 23 représente le taux de SO2 (ppm) en fonction de la charge (%). Elle permet de visualiser l'étendue de SO_2 de la génératrice diesel lorsque la charge varie. À faible charge du moteur (0 % à 30 %), le taux de SO2 (ppm) est de 28 ppm. À partir de 30 %, le taux de SO2 diminue et se stabilise entre 12 et 13 ppm.

Tableau 9 : Taux du SO_2 enregistré en fonction de la charge appliquée

Charge appliquée		Étendue (SO_2) sur 10 minutes	Moyenne enregistrée (SO_2)	Température ambiante enregistrée
(kW)	(%)	(ppm)	(ppm)	(°C)
0	0	17-27	22	30,1
15	6	22-27	23,5	30,6
30	12	22-28	24	31
35	14	21-25	22,5	31,9
45	18	20-23	22,5	32,6
50	20	20-22	21	33,3
60	24	15-17	16	34,1
65	26	12-15	14	34,7
70	28	12-15	14	35,5
75	30	12-15	12	36,2
80	32	12-15	13	36,9
95	38	12-15	13	37,9
100	40	12-15	13	38,7
105	42	12-15	13	39,4
110	44	12-15	13	40,1
115	46	12-15	13	40,8
120	48	12-15	13	41,6
130	52	12-15	13	42,1

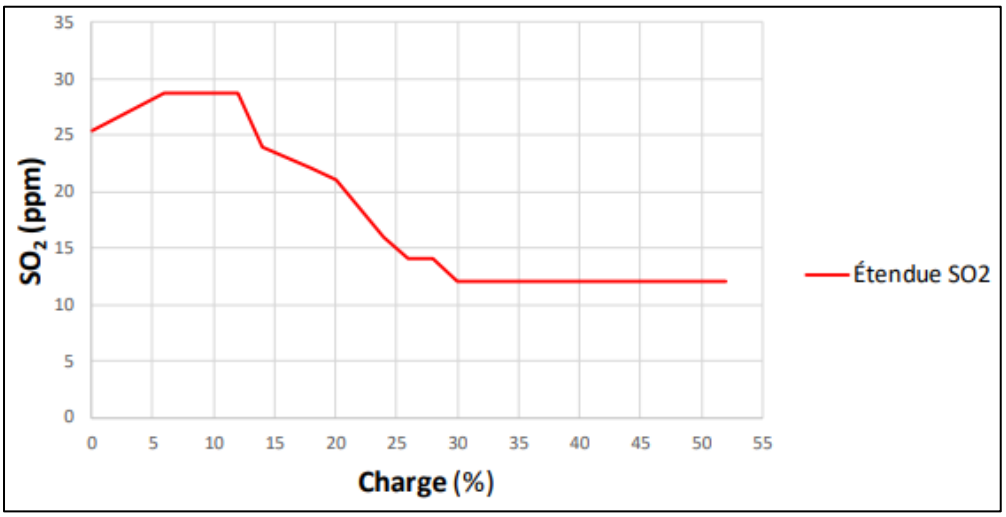

Figure 23 : Illustration de la moyenne du taux de SO_2 en fonction de la charge appliquée

La courbe de tendance exponentielle est utilisée pour illustrer le taux décroissant de SO_2 entre 0 % et 52 % de charge. Après plusieurs tentatives infructueuses, aucun modèle mathématique simple ne pouvait se superposer sur les données recueillies pour en faciliter la compréhension.

III.4.3 Mesure du taux de dioxyde de carbone (CO_2) en fonction de la charge appliquée

Les données traitées (voir

Tableau 10) concernant le taux du dioxyde de carbone ont révélé que le taux de CO_2 augmente proportionnellement avec la charge.

Tableau 10 : Taux du CO_2 enregistré en fonction de la charge appliquée

Charge appliquée		**Étendue (CO_2) sur 10 minutes**	**Température ambiante enregistrée**
(kW)	(%)	(%)	(°C)
0	0	2,78	23,1
15	6	3,57	23,9
30	12	4,21	24,8
35	14	4,35	25,3
45	18	4,7	26,1
50	20	4,9	27,4
60	24	5,04	27,9
65	26	5,11	28,8
70	28	5,21	29,3
75	30	5,27	31,2
80	32	5,33	32
95	38	5,4	32,9
100	40	5,42	34,1
105	42	5,47	35,1
110	44	5,53	36,6
115	46	5,6	37,3
120	48	5,65	38,1
130	52	5,81	38,8

La Figure 24 illustre le taux du CO_2 en fonction de la charge. Elle permet de visualiser l'étendue de CO_2 de la génératrice diesel lorsque la charge varie. La courbe de tendance logarithmique est utilisée pour illustrer le taux croissant de CO2 entre 0 % et 52 % de charge. Le coefficient de détermination R2 est de 0,9627 ce qui est considéré comme bon pour la ligne des données.

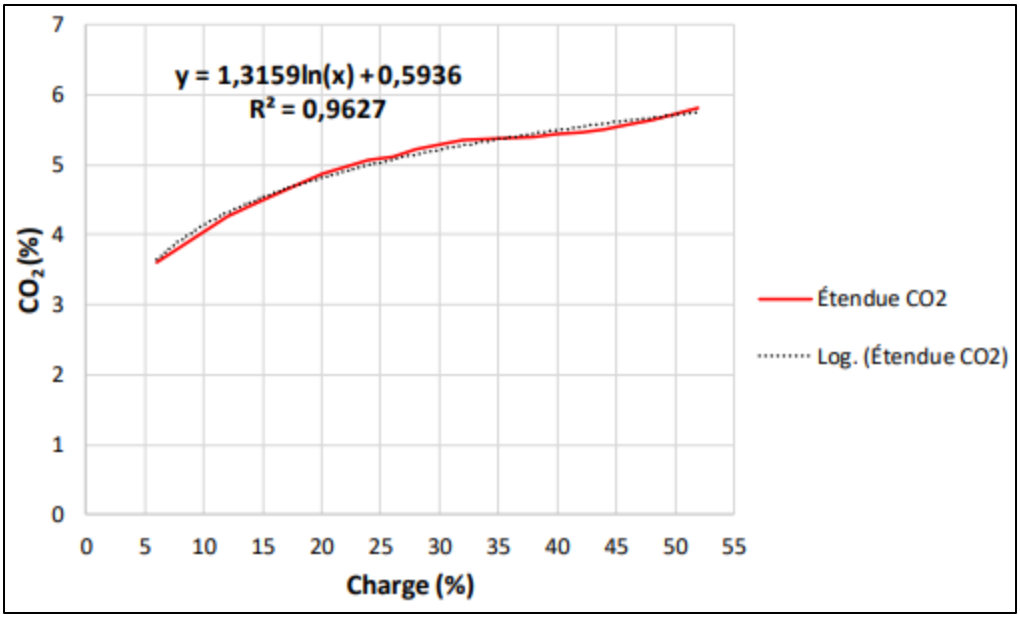

Figure 24 : Variation en pourcentage du taux de CO_2 enregistré en fonction de la charge appliquée

III.4.4 Mesure du taux de d'oxyde d'azote (NO_x) en fonction de la charge appliquée

L'analyse du taux d'oxyde d'azote (NOx) a démontré une stabilité dans les données (entre 188 et 191 ppm) lorsque la charge appliquée est entre 30 % et 48 %. Cependant, lorsque la charge appliquée atteint 52 %, le taux de dioxyde d'azote augmente davantage pour atteindre une moyenne équivalente à 209 ppm, ce qui est très proche de la moyenne à très faible charge (entre 210 et 212 ppm).

Puisqu'il est difficile de voir une tendance claire dans l'évolution des taux de NOx par rapport à la charge, il est peu probable que cette donnée soit un indicateur fiable de sous-performance. Le Tableau 11 illustre les données des tests enregistrées alors que la Figure 25 montre la variation du taux du NO_x en fonction de la charge appliquée.

Tableau 11 : Taux de NO_x enregistré en fonction de la charge

Charge appliquée		Étendue (NOx) sur 10 minutes	Température ambiante enregistrée
(kW)	(%)	(ppm)	(°C)
0	0	212	30,1
15	6	218	30,6
30	12	222	31
35	14	225	31,9
45	18	220	32,6
50	20	216	33,3
60	24	222	34,1
65	26	217	34,7
70	28	213	35,5
75	30	190	36,2
80	32	191	36,9
95	38	189	37,9
100	40	185	38,7
105	42	188	39,4
110	44	191	40,1
115	46	207	40,8
120	48	208	41,6
130	52	210	42,1

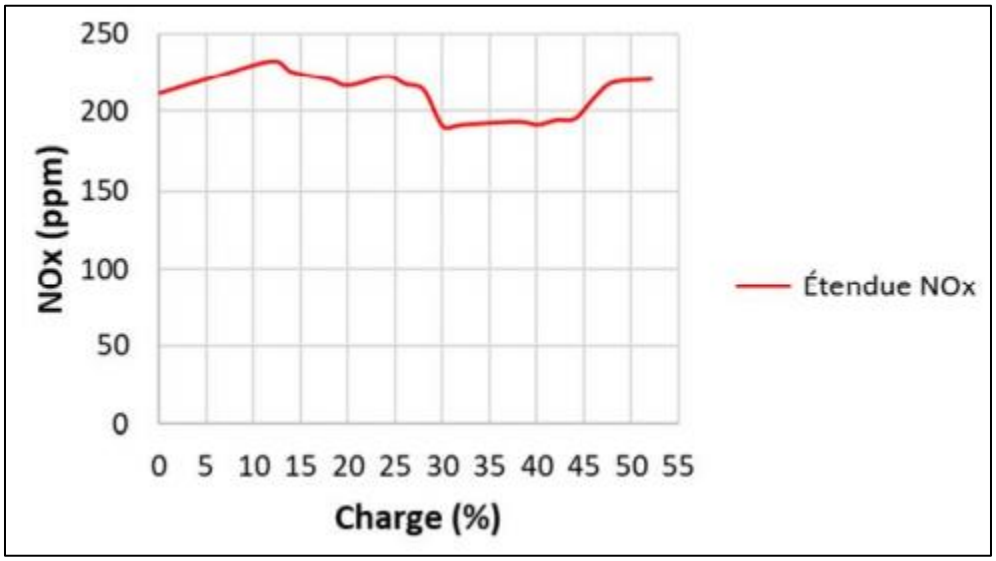

Figure 25 : Variation en ppm du taux d'oxyde d'azote en fonction de la charge

III.4.5 Mesure du taux de dioxygène (O_2) en fonction de la charge appliquée

Les mesures concernant le taux du dioxygène (O_2) en fonction de la charge ont montré une décroissance continue par rapport à la charge appliquée. Il a été constaté que plus la charge augmente, plus le taux d'O_2 diminue. Le Tableau 12 illustre la moyenne des données enregistrées alors que la Figure 26 présente la variation d'O_2 en fonction de la charge de manière graphique. Il est possible de voir qu'une faible correspondance avec une équation exponentielle existe.

Tableau 12 : Taux d'O_2 enregistrée en fonction de la charge appliquée

Charge appliquée		**Étendue (O_2) sur 10 minutes**	**Température ambiante enregistrée**
(kW)	(%)	(%)	(°C)
0	0	17,13	30,1
15	6	13,19	30,6
30	12	17	31
35	14	17	31,9
45	18	17,01	32,6
50	20	16,04	33,3
60	24	15,11	34,1
65	26	13,72	34,7
70	28	13,65	35,5
75	30	13,62	36,2
80	32	13,51	36,9
95	38	13,44	37,9
100	40	13,6	38,7
105	42	13,51	39,4
110	44	13,48	40,1
115	46	13,18	40,8
120	48	13,18	41,6
130	52	13,14	42,1

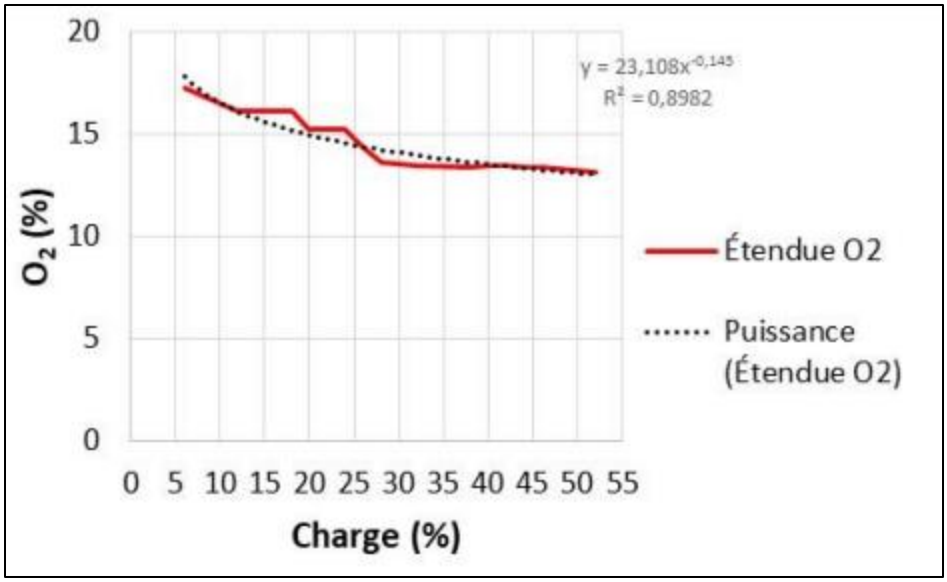

Figure 26 : L'étendue du taux d'O_2 en fonction de la charge appliquée

III.4.6 Mesure du taux de monoxyde de carbone (CO) en fonction de la charge appliquée

Les analyses concernant le taux du monoxyde de carbone (CO) ont montré une décroissance non linéaire dans les valeurs enregistrées lorsque la charge varie. En effet, il a été constaté que la réaction du monoxyde de carbone sous une très faible charge (0-25 %) varie sur une grande plage, soit entre 307 ppm et 175 ppm alors que sous une faible charge (30-40 %), le taux diminue davantage pour atteindre une moyenne de 125 ppm. Pour une charge régulière (40-52 %), le taux de monoxyde de carbone continue de diminuer pour atteindre 82 ppm. Ceci pourrait s'expliquer par les travaux menés dans l'étude de *Richard Opat et al.* [83] qui démontrent que le taux de CO est inversement proportionnel à la température de combustion et à la pression dans les cylindres. Une inflexion de la courbe à environ 24 % de charge peut montrer la transition entre la sous-performance et le fonctionnement normal du GED. Après plusieurs tentatives infructueuses, aucun modèle mathématique simple ne pouvait se superposer sur les données pour en faciliter la compréhension. Des tests supplémentaires seraient nécessaires afin de valider si l'inflexion du taux de CO représente vraiment une transition de régime de fonctionnement. Le Tableau 13 illustre la moyenne des données enregistrées alors que la Figure 27 montre l'étendue de CO en fonction de la charge.

Tableau 13 : Taux du CO enregistrée en fonction de la charge appliquée

Charge appliquée		Étendue (CO) sur 10 minutes	Température ambiante enregistrée
(kW)	(%)	ppm	(°C)
0	0	172	30,1
15	6	216	30,6
30	12	244	31
35	14	257	31,9
45	18	269	32,6
50	20	264	33,3
60	24	284	34,1
65	26	277	34,7
70	28	245	35,5
75	30	177	36,2
80	32	138	36,9
95	38	127	37,9
100	40	112	38,7
105	42	102	39,4
110	44	96	40,1
115	46	94	40,8
120	48	87	41,6
130	52	84	42,1

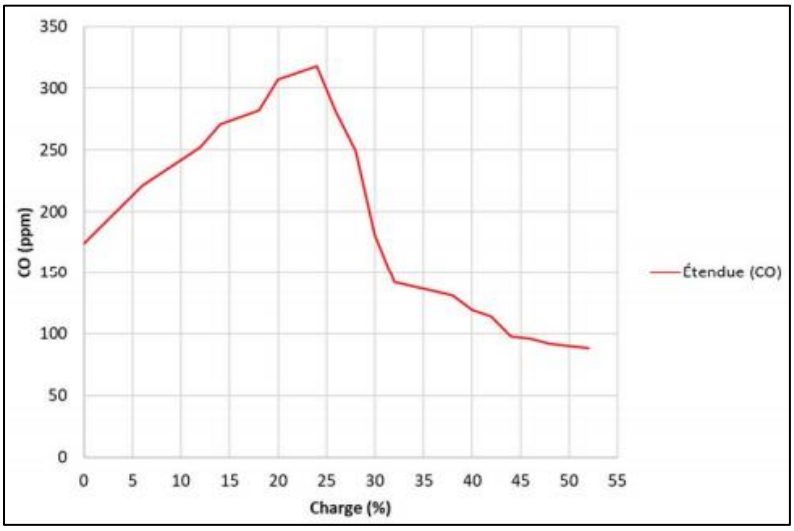

Figure 27 : Étendue du taux de monoxyde de carbone en fonction de la charge

III.4.7 Mesure de la variation de la température des gaz d'échappement en fonction de la charge appliquée

Le Tableau 14 illustre la moyenne des valeurs enregistrées alors que la Figure 28 représente la température des gaz d'échappement en fonction de la charge en (%). Elle permet aussi de visualiser l'augmentation de la température des gaz d'échappement du moteur diesel lorsque la charge augmente. Cette courbe correspond presqu'à une droite linéaire. La courbe de tendance indique clairement que la température des gaz d'échappement augmente entre 0 % et 52 % de charge. Bien que le coefficient de détermination R2 soit de 0.9373, cette courbe ne se représente pas parfaitement de façon linéaire. Dans une deuxième étape, il serait intéressant d'étudier le temps nécessaire pour évaluer la stabilité de la température des gaz d'échappement et voir si l'augmentation de la température passe par des paliers.

Tableau 14 : Température des gaz d'échappement enregistrée en fonction de la charge

Charge appliquée		**Étendue de la température des gaz d'échappement sur 10 minutes**	**Température ambiante enregistrée**
(kW)	(%)	(°C)	(°C)
0	0	223	30,1
15	6	228	30,6
30	12	242	31
35	14	262	31,9
45	18	269,7	32,6
50	20	284	33,3
60	24	305,6	34,1
65	26	319,2	34,7
70	28	322	35,5
75	30	326	36,2
80	32	327,3	36,9
95	38	329,8	37,9
100	40	337	38,7
105	42	339,8	39,4
110	44	341,4	40,1
115	46	345,5	40,8
120	48	347	41,6
130	52	353,3	42,1

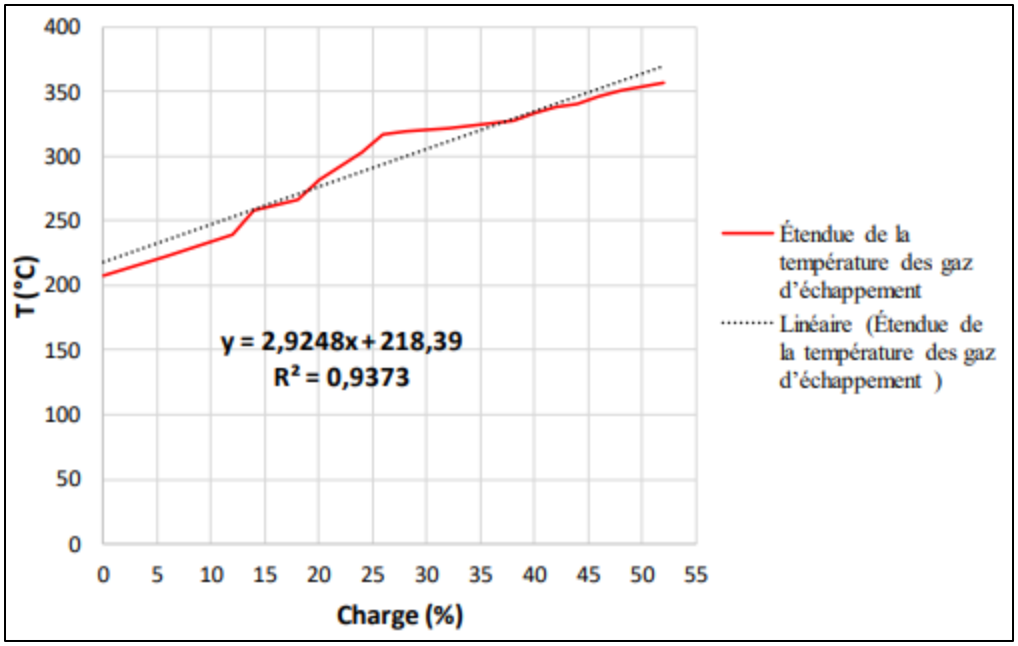

Figure 28 : Variation de la température des gaz d'échappement en fonction de la charge appliquée

III.4.8 Mesure du taux de soufre (S) dans les gaz d'échappement en fonction de la charge

Finalement, dans une dernière étape d'analyse des données, le taux de soufre dans les gaz d'échappement est considéré comme le meilleur indice pour la détection des sous-performances. Les données ont révélé que le taux de soufre se stabilise à 0,1 % lorsque la charge appliquée est ≥ 25 %. Il est donc possible de croire que cette stabilisation coïncide avec la combustion complète du soufre et que le moteur sortirait du régime de sous-performance. Toutefois, ce résultat peut être dû au fait qu'un carburant à faible teneur en soufre est utilisé et des validations supplémentaires avec des carburants à haut taux de soufre devraient être effectuées. Le Tableau 15 illustre le taux de soufre enregistré alors que la Figure 29 illustre la variation du taux de soufre. La relation par palier entre le soufre et la charge ne se prête pas à un modèle mathématique simple pour sa compréhension.

Tableau 15 : Taux du soufre enregistré dans les gaz d'échappement en fonction de la charge appliquée

Charge appliquée		Taux de soufre dans les gaz d'échappement	Température ambiante enregistrée
(kW)	(%)	(%)	(°C)
0	0	0,3	23,1
15	6	0,2	23,9
30	12	0,2	24,8
35	14	0,2	25,3
45	18	0,2	26,1
50	20	0,2	27,4
60	24	0,1	27,9
65	26	0,1	28,8
70	28	0,1	29,3
75	30	0,1	31,2
80	32	0,1	32
95	38	0,1	32,9
100	40	0,1	34,1
105	42	0,1	35,1
110	44	0,1	36,6
115	46	0,1	37,3
120	48	0,1	38,1
130	52	0,1	38,8

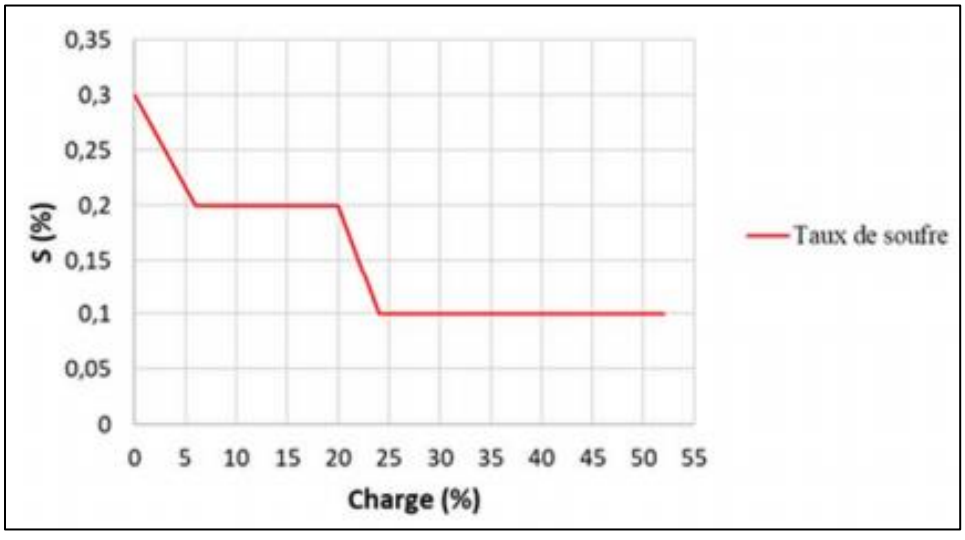

Figure 29 : Variation du taux de soufre dans les gaz d'échappement en fonction de la charge appliquée

III.5 CONCLUSION

L'objectif principal de cette investigation pratique consistait à identifier des indicateurs possibles liés à la sous-performance sur un groupe électrogène diesel de 250 kW. L'approche proposée repose sur des analyses de gaz, notamment le taux de dioxyde de soufre (SO2) et le taux de soufre (S), ainsi que sur le suivi de la température des gaz d'échappement.

Le banc d'essais réalisé chez Innovation maritime a permis de valider expérimentalement certaines hypothèses. Globalement, les résultats obtenus se sont avérés intéressants. Les remarques et les conclusions les plus pertinentes que l'on peut tirer de ces travaux de recherche peuvent être résumées par les quelques points suivants :

- Parmi les gaz mesurés, le taux de dioxyde de soufre (SO2) et le taux de soufre (S) offrent les meilleurs indices pour le fonctionnement d'un GED sous une faible charge. La température des gaz d'échappement est aussi un bon indicateur.

- Les concentrations de SO_2 (ppm) et le pourcentage de soufre (S) apparaissent, à cette étape, comme les meilleurs indices, car leurs valeurs se stabilisent et restent constantes lorsque la charge appliquée est ≥ 30 %, tandis que la température des gaz augmente proportionnellement par rapport à la charge appliquée.

- La consommation de carburant peut s'avérer un indice important pour la détection d'un fonctionnement sous une faible charge. Il s'agit d'associer la courbe de la consommation du groupe électrogène diesel en fonction de la charge (cette courbe est souvent fournie dans les spécifications techniques de la génératrice à 15 °C ou 16 °C par le manufacturier). Cependant, une attention devra être portée à la température ambiante, car la consommation pourrait être affectée en fonction de celle-ci.

CHAPITRE IV

ARTICLE 2

A Review and Economic Analysis of Different Emission Reduction Techniques for Marine Diesel Engines

Publié dans Open Journal of Marine Science, 2019

Volume 9:148-171 / ISSN: 2161-7392

Résumé

L'objectif de cet article est de présenter les normes adoptées par l'organisation Maritime Internationale (OMI) en Avril 2018 concernant la réduction des empreintes écologiques émis par les navires marchands ainsi que la stratégie introduite pour permettre aux armateurs et aux chantiers navales de prendre les bonnes démarches afin d'optimiser les moteurs et les génératrices diesel existants et/ou à venir.

Nous survolons les principales sources polluantes émises par les GED et les moteurs de propulsion et nous présentons les différentes solutions possibles pour répondre aux normes adoptées par l'OMI. Les avantages et les inconvénients de chacune de ses technologies sont aussi présentés suivi d'une analyse économique détaillée pour assurer un rétrofit des GED et des moteurs diesel (Catégorie 3) existants à bord des navires.

Après une étude techno-économique approfondie, les résultats ont démontré que l'utilisation des moteurs et des GED avec la possibilité de fonctionner en bicarburant (diesel/Methanol) coute le moins cher, alors que les systèmes de lavage de gaz sont les plus chers à exploiter et à maintenir. Il a été démontré aussi que l'utilisation d'un catalyseur pour réduire les émissions du NO_x par 95% vient en deuxième position au niveau des prix à exploiter (après les laveurs de gaz) alors que l'utilisation des gaz naturels liquéfiés ou le méthanol offrent une très bonne réduction des GES et une réduction de coût de 31% annuellement par rapport à l'utilisation du fioul lourd. Toutefois, ils sont confrontés à des problèmes techniques au niveau du stockage et de l'exploitation due à la grosseur de leurs réservoirs de stockage (4 fois plus grands).

Pour conclure, il a été aussi démontré que le jumelage de plusieurs techniques peut s'avérer intéressante pour optimiser les moteurs diesel de propulsion et des GED existant à bord des navires marchands.

Scientific Research Publishing

Open Journal of Marine Science, 2019, 9, 148-171
http://www.scirp.org/journal/ojms
ISSN Online: 2161-7392
ISSN Print: 2161-7384

A Review and Economic Analysis of Different Emission Reduction Techniques for Marine Diesel Engines

Mohamad Issa[1*], Hussein Ibrahim[2], Adrian Ilinca[3], M. Yasser Hayyani[3]

[1]Department of Applied Sciences, Institut Maritime du Québec, Rimouski, Canada
[2]Department of Research and Development, Institut Technologique de Maintenance Industrielle, Sept-Îles, Canada
[3]Department of Mathematics, Informatics and Engineering, Université du Québec à Rimouski, Rimouski, Canada
Email: *missa@imq.qc.ca

How to cite this paper: Issa, M., Ibrahim, H., Ilinca, A. and Hayyani, M.Y. (2019) A Review and Economic Analysis of Different Emission Reduction Techniques for Marine Diesel Engines. *Open Journal of Marine Science*, **9**, 148-171.
https://doi.org/10.4236/ojms.2019.93012

Received: June 22, 2019
Accepted: July 27, 2019
Published: July 30, 2019

Abstract

The maritime industry is currently facing the challenges of adopting new technologies and operational practices with stricter international, national and local rules in order to reduce exhaust gas emissions from ships. The most objective of regulations introduced and presented by the Worldwide Sea Organization such as International Maritime Organization (IMO) and the US Environmental Protection Agency (EPA) is to lessen the commitment shipping makes to worldwide and local discharges. This paper analyzes emissions from marine engines and the process of waste exhaust gas formation and provides a summary of the emission reduction technologies to satisfy MARPOL NO_x tier III and EPA tier IV rules. The results showed the possibility of achieving a valuable emission reduction percentage if future diesel engines are equipped with pre-treatment, internal-treatment and/or post-treatment techniques. Economics impact for medium and low speed for category 3 marine diesel engines is also presented.

Keywords

Air Pollution, GHG, IMO Requirements, Tier III, Tier IV, Scrubber, SCR, Exhaust Gas Emissions

1. Introduction

In recent years, marine diesel engine manufacturers have had to address the challenge of tightening controls on baneful exhaust gas emissions obligatory by regional, national and international authorities responding to concern over atmospheric pollution and its impact on human health and climate amendment.

International Maritime Organization (IMO) regulations concerning gas oxides had planned to accomplish emissions reduction emitted by diesel engines (DE) through three tiers [1].

Tier I for vessels launched after first of January 2000, tier II, for vessels launched after first of January 2011 with 15% exhaust gas emissions reduction of tier I, while tier III for vessels launched after first of January 2016 with 85% exhaust gas emissions reduction of tier I [2]. The current allowable NO_x discharge level as per IMO control relies upon the speed class of the engine and ranges [3]. Besides, the regulations for the prevention of Air pollution from vessels (Annex VI) additionally forced a 1.5 percent Sulphur limit on marine power engines in Emission Control Areas (ECAs) viable since 2006, this limit decreased to 1.0% Sulphur compelling from first of July 2010 and was additionally diminished to 0.1% Sulphur starting on January 2015 [4]. Furthermore, in May 2004, the US Environmental Protection Agency (EPA) signed the final rule introducing Tier IV emission standards, which are phased-in over the period 2008-2015. The tier IV rules necessitate that outflows of particulate matter (PM) and NO_x be additionally decreased by 99% [5]. **Figure 1** shows the emissions regulations

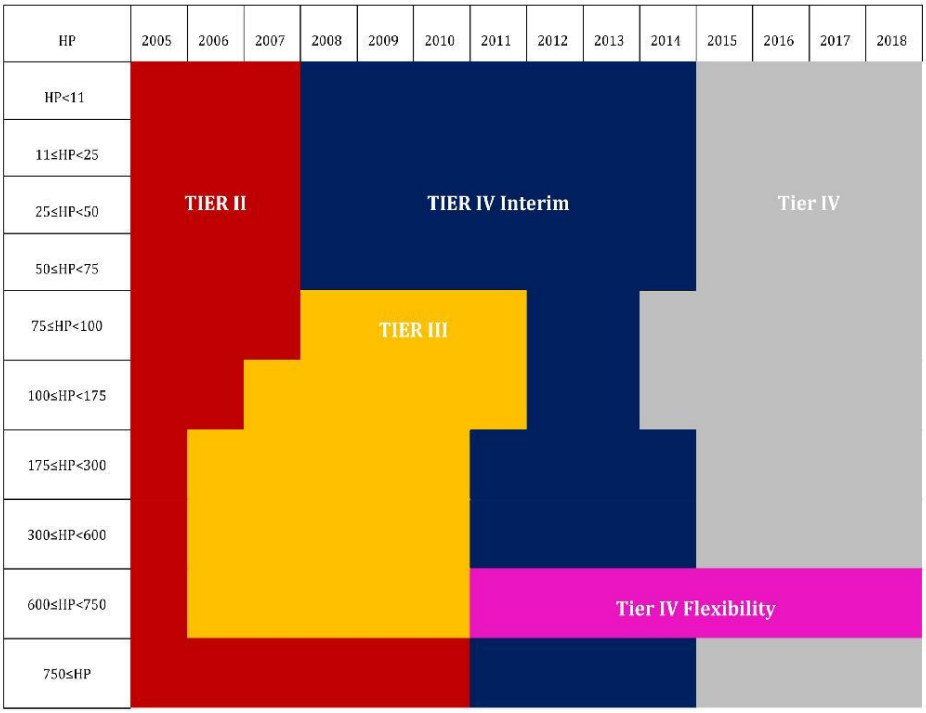

Figure 1. Implementation of Tiers II-IV for nonroad diesel engines over the last decade.

implemented over the last two decades on different diesel engines size and culminated in 2015 with Tier IV final.

It should be noted here that Tier 4 Flexibility rules allow pre-approved equipment manufacturers to use the previous-Tier engines in lieu of Tier 4 Interim or Tier 4 final engines for up to a seven-year phase-in period in order to provide equipment manufacturers with some control over their transition to the new emission standards.

However, emergency standby power (ESP) has been exempted from EPA tier IV because tier III already decreases over 85 percent exhaust gas emissions that occurred through in-engine structure upgrades and because of ESP's runs for a short period of time during a year. For application other than ESP, diesel power generators are phased-in two steps, starting with tier IV interim in 2011 and tier IV final rules by 2015 (**Figure 2**). Moreover, in order to achieve the level of emission control required to meet tier IV interim and tier IV final rules, some form of exhaust after-treatment will be required.

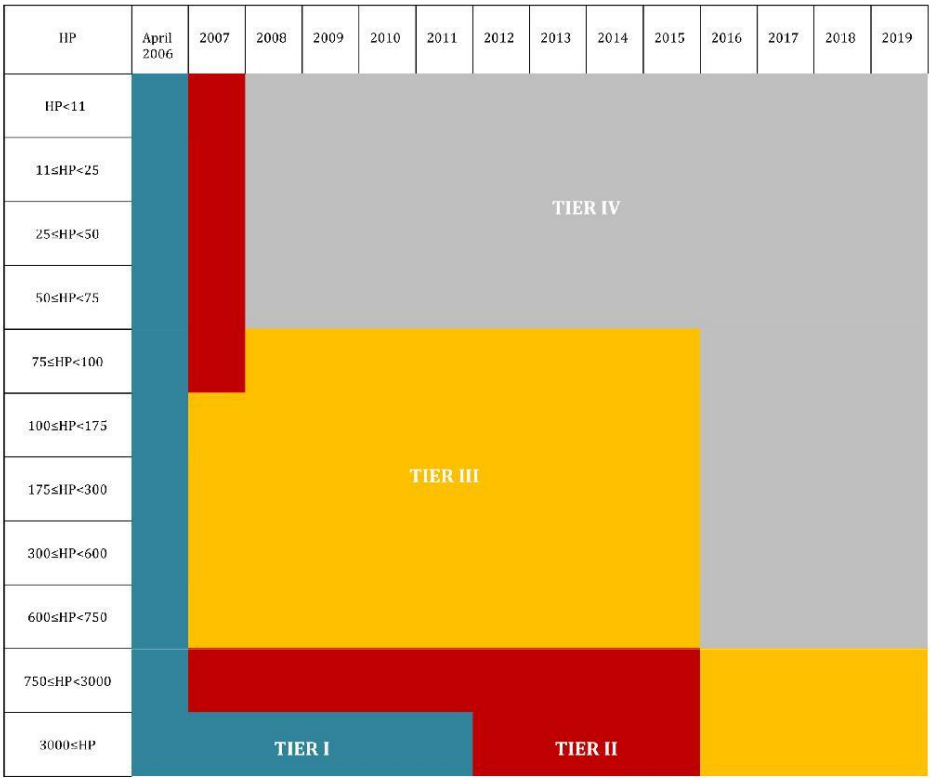

Figure 2. Implementation of Tiers I-IV for diesel power generators over the last years.

The structure of the present paper is as follows. Section 2 presents the main pollutants from marine diesel engines, particularly nitrogen oxides (NO_x), Sulphur Oxides (SO_x) and smoke in general. In Section 3, NO_x and SO_x emissions control technologies such as internal-treatment and add-on technologies are presented. In Section 4 we evaluate the economic impact of the selected technology for category 3 marine DEs in order to determine the estimated cost of compliance with potential future emission regulations. Finally, Section 5 provides a conclusion of our study.

2. Exhaust Gas Emissions from Marine Diesel Propulsion Engines

Marine diesel propulsion engines are characterized by their speed (Low, Medium or High) and stroke numbers. According to Kristensen H.O. [6], the following engines are used for propulsion: 1) Low speed two stroke DE (50 - 300 RPM), 2) Medium speed four stroke DE (300 - 1000 rpm), 3) High speed four stroke DE (1000 - 3000 rpm), and 4) Gas turbine (very high rpm > 5000 rpm). These DEs run with air excess. Diesel is injected into the cylinder chamber at high pressures, which is compressed by moving cylinders. This compression increments sufficiently the air temperature in the cylinder chamber allowing the fuel to ignite. However, combustion creations have a significant percentage of nitrogen and oxygen due to the air reaction (1) [7].

$$C_aH_b + (O_2 + 3.75N_2) \rightarrow CO_2 + H_2O + N_2 + O_2 + \text{Other} \quad (1)$$

Additional exhaust gas emissions from marine diesel engines largely comprise oxides of Sulphur, carbon dioxide and water vapour, with a few quantities of carbon monoxide, partially reacted and non-combusted PM and hydrocarbons (HC). Classic exhaust gas emissions from a low speed DE are shown in **Figure 3**, while **Figure 4** illustrates the typical content of the exhaust gas emissions from a

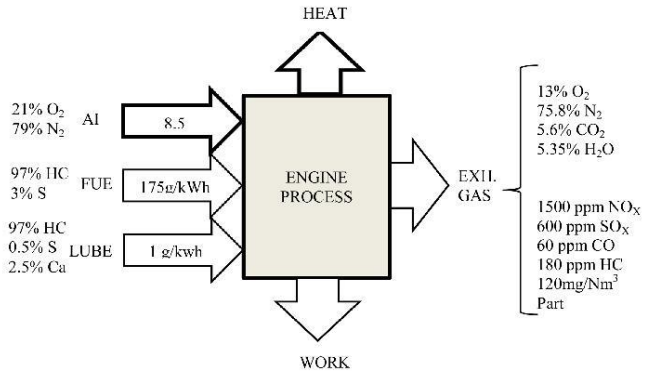

Figure 3. Typical exhaust gas emissions from a 41 MW low speed DE [9].

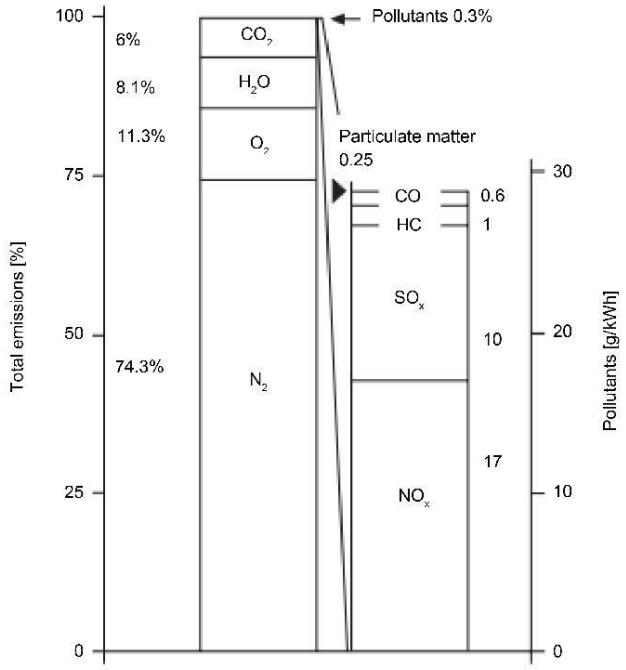

Figure 4. Typical exhaust gas composition of a medium speed four strokes 18 MW DE burning heavy fuel oil (HFO) with 3% Sulphur content [9].

medium speed DE burning heavy fuel oil with a mean of 3 percent Sulphur content [8].

According to **Figure 4**, the principle emissions are nitrogen (N_2), Oxygen (O_2), water (H_2O) and carbon dioxide (CO_2). Among these gases, carbon dioxide is considered as potential source for greenhouse gas (GHG) development. Different studies have evaluated that 3 to 4 percent of universal CO_2 emissions are attributable to marine vessels [10]. A 10 percent reduction in cruise speed is an effective operational methodology that offers a significant reduction in CO_2 and fuel consumption up to 20 percent over the same distance [11]. Below are described the main pollutants emitted by a marine diesel engine which contribute to air pollution and human health risks.

2.1. Nitrogen (N_2) and Oxygen (O_2)

Nitrogen and Oxygen are not poisonous. N_2 and O_2 are the main components of both air intake and exhaust emissions from engines. Nitrogen which forms 78 percent by volume of intake air, mostly do not react during the combustion operation, despite a very small portion will react chemically creating diverse oxides

of nitrogen (NO_x). O_2 which forms 21 percent of the intake air, will be moderately transformed by the combustion operation, therefore, the free O_2 of the exhaust will depend on the excess air ratio along which engine is operated [12].

2.2. Carbon Dioxide (CO_2) and Water Vapor (H_2O)

The production of both carbon dioxide and water vapor depends on the quantity of fuel burned and the fundamental composition of the fuel burned. CO_2 and H_2O vapor will be created in all combustion forms such as completed or nearly completed. Carbon dioxide is considered as a GHG that absorbs and transmits radiation inside the thermal infrared spectrum length [13].

2.3. Micro Pollutants

In the context of DE emissions, micro pollutants will enclose organic and heavy metals micro pollutants. Organic micro pollutants generally consist of dioxins, furans and polyaromatic hydrocarbons (PAH). However, PAH is well identified and known as a carcinogen for humans and is well documented. Furthermore, polychlorinated dibenzofurans (PCDF) has been reported as highly toxic and has been identified in the engine exhaust system. Heavy metals such as copper, mercury, cadmium, chromium, nickel and zinc are highly toxic and can cause serious damage by reducing the diversity of aquatic ecosystems, over fish kills to cancer in humans.

2.4. Sulphur Oxides (SO_X)

Sulphur oxides are related precisely from the Sulphur content of the used fuels. Oxidation of the Sulphur inside the combustion chamber allows the formation of the Sulphur dioxide (SO_2) and a smaller proportion of the Sulphur trioxide (SO_3). SO_x have bad odor and are a bigger source of acid rain. SO_x represent around 60% of universal transport SO_x emissions and symbolize dangerous source to human health. New strict regulations to reduce SO_x emissions are adopted recently such as the regulation 14 of the MARPOL Annex VI which imposes Sulphur limitations to the fuel used for marine applications.

2.5. Oxides of Nitrogen (NO_X)

The development of nitrogen oxides is caused by the oxidation of molecular nitrogen in the combustion air or by the oxidation of organic nitrogen in the fuel. Depending on the fuel used, important portion of the total nitrogen oxides emissions, are related for engines using HFO. It is known that the evolution of nitrogen oxides growths with the combustion temperature. As a result, slow speed marine DE produce high level of NO_x compared to a medium or high-speed marine DE. This can be explained by the fact that slow speed marine DE requires a longer time period for his combustion process so there is greater time ready for use for NO_x development. Nitrogen oxides aims to acid rain and its oxidation in the atmosphere leads to the creation of fine nitrate particles, which can pose a sig-

nificant danger to human health.

3. NO_X and SO_X Emissions Control Technologies

Emission control technologies for oxides of nitrogen can be divided through two categories: internal modification to the DE and add-on technologies. Add-on technologies include pre-treatment and post-treatment techniques.

Internal modifications to the DEs are commonly desirable to exhaust treatment. However, external treatment brings several disadvantages such as costs, zone restraints and extended fuel consumption which has direct environmental impact, particularly on GHG as well as financial. While emission control technologies for NO_x can be achieved by internal modifications to the DE or by add-on technologies, there is no consequence on Sulphur oxides emissions by bringing measures within the DE. Currently, there is one way to minimize the SO_x emissions by applying after-treatment technology or using low Sulphur content fuel such as liquified natural gas, biofuels and light marine fuel oil (LMFO). **Figure 5** illustrates the DE-NO_X and SO_x reduction emissions based on pre-treatment, internal treatment and post treatment technologies.

3.1. Marine Diesel Engine Emissions Reduction Solutions Using Pre-Treatment Technologies

Pre-treatment is the easiest and fastest way to comply with the emissions regulation recently adopted by the IMO. However, low-Sulphur substitute fuel such as methanol and liquified natural gas (LNG) face several challenges in terms of adaptability on board. In terms of engineering, they require dual-fuel engines and additional special fuel storage tanks.

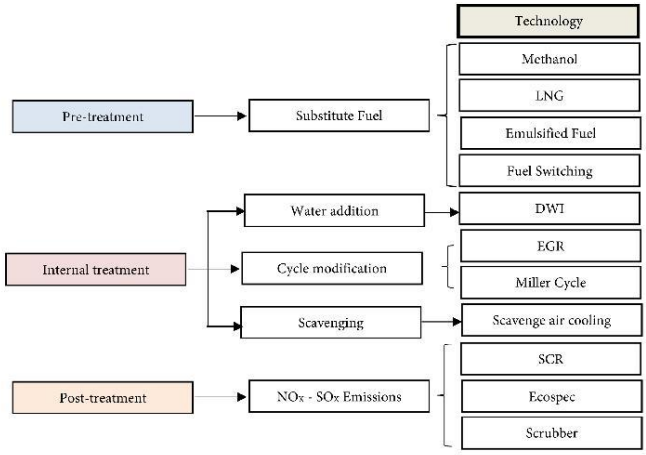

Figure 5. Methods of reducing SO_x and NO_x emissions from marine diesel engines using pre-treatment, internal-treatment and post treatment solutions [14].

Methanol has the advantage to reduce SO_x, NO_x and PM emissions by an amount of about 99%, 60% and 95% compared to heavy fuel oil (HFO) for marine use, while LNG has the advantage to reduce SO_x, NO_x, CO_2 and PM by 98%, 86%, 11% and 96% respectively [15], **Figure 6**. However, methanol raises the possibility of corrosion and must be faced with adequate upgrading of fuel storage tanks. On the other hand, LNG retains about 85% of the energy stocked per unit volume compared to traditional oil fuel. One of the most vital challenges of the use of LNG as a marine fuel, is the higher size of his tanks (3 - 4 times greater) than the marine diesel oil tanks [16]. This further increases the costs of installations for a retrofit. Recently, a study conducted and published by DNV-GL [17], confirms that LNG-fueled fleet will increase very-quickly over the next years, especially in zones with existing bunkering abilities. Moreover, a previous study assessed by Wärtsilä in order to evaluate the advantages of changing from HFO fueled engine equipped with a Sea scrubber to LNG fueled engine [18] has shown additional savings from the annual machinery cost (maintenance, oil lubricating, scrubber and SCR with annual capital) by an amount of 500 $/kW. Furthermore, the expansion in navigation time in emission control areas (ECAs) where high quality fuel is required will add more economic interests to LNG than HFO-powered engines where stricter emission regulations are approved and implemented. **Figure 7** shows price comparison between HFO and LNG for three engine grades conforming to the current fuel price (January 2019), is about 15.3$ US/MMBtu for HFO and 11.6$ US/MMBtu for LNG.

Emulsified fuel relies on decreasing the temperature in the combustion chamber by adding water to the fuel. Emulsified fuel offers the advantage for a better atomization and a better distribution of the fuel inside the combustion chamber resulting in a complete combustion. Emulsified fuel has the advantage to reduce the nitrogen oxides emissions and PM. However, it also motives corrosion of engine components and the short common of oil-water separation

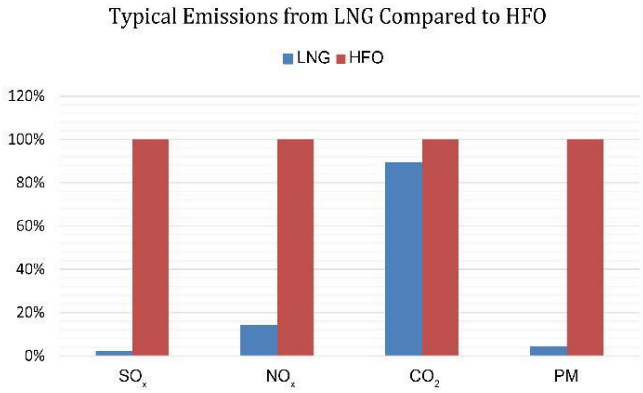

Figure 6. Relative gas emissions for LNG and HFO

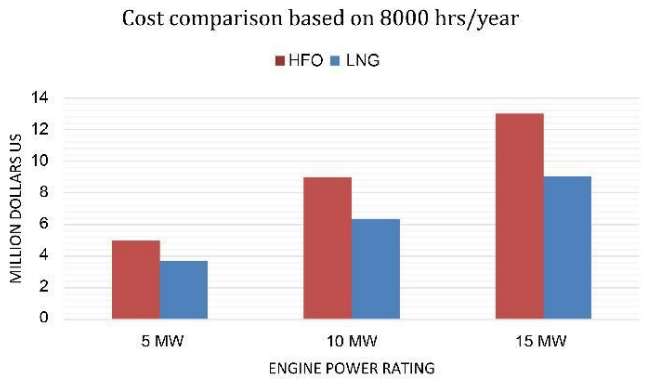

Figure 7. Price comparison between LNG and HFO for different marine engine grades.

phenomenon [19]. To conclude this section, many DE manufacturers such as Wärtsila and MAN B&W have developed DEs that can be run on natural gas, marine diesel oil (MDO) or heavy fuel oil (HFO). This is known as fuel switching technology or dual-fuel technology [20]. The dual-fuel technology provides shipowners and operators with outstanding benefits. In gas mode, without any secondary exhaust gas purification systems, the engine is already compliant with IMO Tier III regulations [21]. Furthermore, dual-fuel technology offers reduced emissions of SO_x and CO_2 as well as smokeless operation in gas mode. On the other hand, dual-fuel technology allows the operator to select the type of fuel to be used based on the market price variation. However, there are several disadvantages [22]. First, a spark ignited gas engine's power output is lower than that of a diesel engine of similar size. This translates during initial installation into a higher capital investment. There are also high maintenance costs for the spark ignition system. While many producers continue to provide in the development of longer-life spark plugs, there is still concern about their operating life. Furthermore, spark ignited engines run hotter than their diesel complements, resulting in significantly higher valve seat wear rates. **Table 1** summarizes the benefits and limitations between alternative fuels for marine use considered as pre-treatment solutions.

3.2. Marine Diesel Engine Emissions Reduction Solutions Using Internal-Treatment Technologies

Internal treatment consists of a direct modification in the diesel engine. This is done by the DE manufacturers and may require modifications in the injectors design such as the use of direct water injection (DWI) and/or engine cycle such as the use of Miller cycle and/or combustion chamber such as the use of scavenge air temperature. All these technologies have a positive impact on the reduction of NO_x and PM and can further achieve the standards set out in Annex VI of the MARPOL convention.

Table 1. Benefits and limitations between the alternative fuels for marine application.

Technology	Benefits	Limitations	References
Emulsified Fuel	• Allows significant NO_x reduction by an amount of 80%	• Increase the fuel consumption by 3% to achieve the same output • Corrosive	[19]
Methanol	• Renewable resource • Biodegradable • Allows NO_x reduction by an amount of 60% and fuel consumption by 2% - 3%	• Corrosive • Toxic • Burns with non-luminous flame • Cost • Miscible with water	[15] [16] [17] [18]
LNG	• Has environmental benefits through an average reduction of SO_x, NO_x, and PM • Lower operating cost	• Highly flammable • Requires huge investments for storage and installation • High CO_2 emissions	[15] [16] [17] [18]
Fuel Switching	• Allows much lower emissions of oxides of nitrogen and PM • Can be designed to operate interchangeably on natural gas with diesel pilot or on 100% diesel fuel	• High capital cost in general • Requires high maintenance for the spark ignition system	[20] [22]

DWI technology uses an injector composed of two parts, one to spray water and the other to inject fuel oil. During the fuel injection phase, the water-fuel density 0.4 - 0.7 high pressure water is injected into the combustion chamber and the mixture of water and combustion gas is completed, allowing a reduction of combustion temperatures and NO_x emissions by up to 60 percent [23]. Another advantage of using this technology appears in the fact that it does not require an extra space or additional cost and can be integrated for a medium speed marine diesel engine. However, this technology can bring to lightly more fuel consumption rate by 2% approximately. On the other hand, Miller cycle was initially proposed by Ralph Miller in 1947 and consists to use the Early Intake Valve Closing (EIVC) to achieve internal cooling before compression in order to reduce the compression cycle work [24]. The Miller cycle is considered as a cold cycle and allows a lower NO_x emission up to 40% - 60% and increase the efficiency of the engine [25]. Furthermore, Miller cycle can be used on four stroke marine diesel engine to complete low scavenge air temperature [26]. By reducing the scavenge air temperature, combustion temperatures and NO_x are also reduced. According to Holtbecker, M. [27], for each 3˚C reduction, nitrogen oxide decreases approximatively by 1 percent. Moreover, internal engine technology such as Exhaust Gas Recirculation (EGR) results in combustion temperature reduction and small NO_x composition. It is considered as the principal technology to reduce NO_x from DE. **Figure 8** illustrates the schematic diagram of EGR technology [28]. The resulting combination of exhaust gas with the fresh air

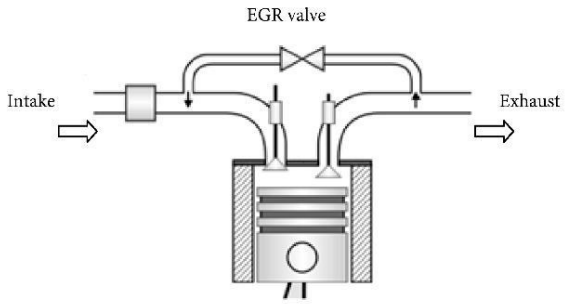

Figure 8. Schematic diagram of EGR [29].

has a low volume calorific value, which reduces the combustion chamber temperatures, and allows NO_x less formation by 40 percent and more. However, the production of PM is increased due to the reduction of oxygen in the combustion chamber when applying EGR [29]. The deliberate reduction in the cylinder's oxygen available will reduce the engine's peak power. For this reason, when full power is required, the EGR is usually shut down, so in this situation, the EGR approach to controlling NO_x fails. **Table 2** summarizes the benefits and limitations of the selected Internal-treatment technologies.

3.3. Marine Diesel Engine Emissions Reduction Solutions Using Post-Treatment Technologies

Today, post-treatment technologies are considered the most suitable solutions for maritime industry to reduce NO_x and SO_x emissions from the exhaust gas engine. They can be integrated into service ships that were launched before the adoption of tier II or tier III and use heavy fuel oil (HFO) with 3% Sulphur content. In terms of efficiency, Seawater scrubbers such as open-loop, closed-loop and Ecospec scrubbers offers up to 99% and 60% abatement of SO_x and NO_x [30] [31], allowing shipowners to continue to use the HFO which is cheaper to buy than light fuel oil (LFO) with 0.1% Sulphur content. The open loop scrubber is the easiest system, where water is supplied from the sea, pumped, filtered and sprayed into the scrubber using nozzles that diffuse water into droplets. However, open loop scrubber is only profitable if the water is alkaline. This can be accomplished by adding an alkali chemistry or by using seawater with a natural alkalinity extracted from the bicarbonate ion (HCO_3^-) existing in the seawater [31] [32]. The water is released back into the sea after particular matters are eliminated. Operation of the open loop scrubber system in fresh water can restrict scrubbing of SO_x due to the weak alkalinity of the water. For this, it is therefore more interesting to use a closed-loop scrubber, where, fresh water treated with an alkaline chemical like caustic soda is employed for neutralization. Fresh water scrubbers are used when high efficiency cleaning is required or when the varying alkalinity associated with seawater prevents the use of marine scrubbers.

Table 2. Benefits and limitations of the selected internal-treatment solutions.

Technology	Benefits	Limitations	References
DWI	• Potential reduction of NO_x by an amount of 60% • Can be applied for Medium Speed Marine Diesel Engine	• Increase the fuel consumption by 2% - 3%	[23]
Miller Cycle	• Increase efficiency of the engine • Potential reduction of NO_x by an amount of 40% - 60%	• Requires high maintenance • High cost	[24] [25] [26]
Scavenge Air Temperature	• Potential reduction of NO_x by an amount of 60% • Reduce number and size of exhausts ports	• Cylinder head complex • Additional maintenance is required	[27]
Exhaust Gas Recirculation (EGR)	• Allows NO_x emission reductions by 30% • Low operating cost	• Cannot be employed at high loads because it would reduce peak power output • Increase the production of PM	[28] [29]

Nevertheless, closed loop fresh water scrubber systems have much smaller discharge rates than open loop sea scrubber systems by an amount approximately of 0.1 to 0.3 m^3/MWh and occur a smaller volume of effluent [33]. Moreover, closed loop fresh water scrubber system can periodically be operated in zero discharge mode without discharging any overboard wash water. Despite their advantages, open loop scrubber are affected by corrosion (salt water), while closed loop scrubber requires more space to hold wastewater and hazardous chemical solutions [34] [35] [36]. Both systems require additional electric power for pumping and managing wastewater by an amount of 150 kW. On the other hand, Ecospec Marine of Singapore proposed their $CSNO_x$ scrubber system which allows significant reductions in NO_x, SO_x and CO_2 in a single process [37]. It consists of two stages. The first stage is an open-loop wet scrubber related to a wash water handling techniques, while the second stage uses seawater conditioned by ultra-low frequency (ULF) waves resulting in alkaline seawater that allegedly absorbs the SO_x, NO_x and CO_2. However, maintenance and repair costs are expected to be 4 percent of the cost of the equipment each year. Supplementary engineer is pretended to spend partially half time on scrubber operations for operations. The engineer's cost will vary significantly depending on the ship's flag. Furthermore, scrubber installation is challenging for new buildings and retrofits alike. Significant considerations include:

- Weight and balance: weights depending on the scrubber rating and type will

vary significantly. The primarily weights of concern are the scrubbers themselves and even a 20 ton wet weight could be considerable concern for ships stability.

- Systems for water handling: These systems can be important for any of the wet systems, but especially for open loop scrubber. For example, an open loop scrubber 50 MW plant will require 4500 cubic meters of wash water an hour. This wash water would require a running capacity of about 500 kW and a pipe of 760 mm (30 inch diameter).
- Backpressure to exhaust: Most engines can tolerate ~3.0 kPa backpressure without significant power degradation or adverse effects. For each additional 3 kPa of back pressure, exceeding the ratio will degrade performance by 1%.
- Electrical power: these systems' needs can reach 2% of nominal power significantly. Additional generator must be taken into consideration.
- Arrangements for machinery and stacking: for retrofits, it will be a significant challenge to fit the scrubber into existing spaces.

Otherwise, Selective Catalytic Reduction (SCR) technology offers the largest reduction of nitrogen oxide up to 90 percent on Des [38] [39]. The functioning principle is that the waste exhaust gas is combined with ammonia (NH_3) or urea before passing over a special catalyst layer at a high temperature between 300˚C - 400˚C, reducing the NO_x to N_2 and water (H_2O) (2) and (3).

$$4NO + 4NH_3 + O_2 \rightarrow 4N_2 + 6H_2O \quad (2)$$

$$6NO_2 + 8NH_3 \rightarrow 7N_2 + 12H_2O \quad (3)$$

According to Wärtsilä manufacturer, SCR is the best technology to achieve tier III compliance. **Table 3** summarizes the benefits and limitations of the selected Post-treatment technologies.

4. Economic Analysis of the Selected Technologies

Each technology mentioned above has their advantages and disadvantages. In order to give a potential estimated cost to the selected method, a typical model of low and medium speed for category 3 marine diesel engines (MDE) were chosen among various DE manufacturer's which are characterized by their cylinder's displacement at or above 30 liters per cylinder, used for propulsion power on ocean going vessels such as container ships, oil tankers, bulk carriers and cruise ships, see **Table 4**. These include fuel emulsions, DWI, EGR, SCR, fuel switching (for new construction vessels) and scrubbers. With regard the fuel switching, we have considered the fact that new vessels will be built with further distillate fuel storage systems over existing vessels. Prices include an LFO separator, a three-way valve, an HFO/LFO blending unit, filters, a viscosity meter and various pumps and piping.

4.1. Methodology for Estimating Cost

We did not define a single model's costs to estimate the economic impact of all

Table 3. Benefits and limitations of the selected post-treatment solutions.

Technology	Benefits	Limitations	References
SCR	• Potential reduction of NO_x by an amount of 95% • Relatively simple installation	• Expensive • Catalyst may suffer from erosion caused by flue gases • Requires enough space that can be complex or not feasible for retrofit applications	[38] [39]
Open loop scrubber	• High Sulphur dioxide (SO_x) removal efficiency (up to 98%) • Offers the possibility to use the cheaper bunker fuel than medium or low Sulphur fuel • Reduce the PM by 60%	• Subject to corrosion (seawater) • Requires regular maintenance • Requires additional electric power to run seawater and pumps • Not suitable for vessels operating in fresh water • Increases ship fuel consumption	[34] [35] [36] [37]
Closed loop scrubber		• Requires storage space to hold waste water and hazardous chemical solutions • High consumption of fresh water • Crews must be trained to manipulate waste water and chemical solutions	[34] [35] [36] [37]
Ecospec CSNOx	• Potential reduction of NO_x by 65% • Potential reduction of SO_x by 99% • Potential reduction of CO_2 by 77% • Possibility to continue using heavy fuel oil (HFO)	• High investment cost • Requires additional generator power • Machinery and stacking arrangements: for retrofits, fitting this equipment into existing spaces will be a major challenge	[34] [35] [36] [37]

Table 4. Technical characteristics for category 3 marine diesel engines for medium and low speed categories.

Speed	**Medium**	**Medium**	**Medium**	**Low**	**Low**	**Low**
Engine power (kW)	4500	9500	18,000	8500	15,000	48,000
Cylinders	9	12	16	6	8	12
Liter/cylinder	35	65	95	380	650	1400
Engine speed (rpm)	650	550	500	130	110	100

the considered technology. Component manufacturer costs have been estimated from different sources, including information from marine diesel engine manu-

facturers and previous work done by the author of Costs of Emission Reduction Technologies for Category 3 Marine Engines. Costs include hardware and fixed costs.

Fixed costs reflect the need for manufacturers to focus on adapting emission controls to specific applications for marine diesel engines, with significant engine calibration required to optimize these controls over a wide range of ship types and operating conditions. Fixed cost/engine was supplied by EPA.

Hardware charges furnished by a supplier other than engine manufacturer are subject to a 29% mark up, which is an average supplier mark up of new engine sales technologies [40] [41].

However, for the estimated emission reduction, a load factor of 0.768 is calculated at 11% of the baseline emissions for 6000 hours per year over 5 years. Baseline NO_x emission rates for medium speed motors are 14 g/kWh and 18.1 g/kWh for slow speed motors. This calculates emission reductions in metric tons as follows:

- Slow speed engines: 18.1 g/kWh × Power (kWh) × 0.768 × 6000 hours/yr × 5 years/1,000,000g metric tonne × 11% (4)
- Medium speed engines: 14 g/kWh × Power (kWh) × 0.768 × 6000 hours/yr × 5 years/1,000,000g metric tonne × 11% (5)

4.1.1. Emulsified Fuel

Costs for emulsified fuel include water storage tank costs, heat exchanger, ultrasonic homogenizer, distilled water and various pumps and pipes. These are detailed in **Table 5**. It is supposed that the water tank is made of cold rolled steel

Table 5. Cost of emission reduction technologies using emulsified fuel.

Speed	Medium	Medium	Medium	Low	Low	Low
Engine power (kW)	4500	9500	18,000	8500	15,000	48,000
Component Cost						
Water Tank	$1132	$1767	$2610	$1611	$2240	$4386
Ultrasonic Homogenizer	$37,500	$56,000	$75,000	$56,000	$75,000	$112,200
Heat Exchanger	$9400	$11,700	$14,000	$11,700	$14,000	$16,400
Pump/Piping	$4700	$5600	$6600	$5600	$6600	$7500
Total Component Cost	$52,732	$75,067	$98,210	$74,911	$97,840	$140,486
Assembly Labor (hr)	240	320	400	320	400	480
Cost ($23.85/hr)	$5723	$7631	$9538	$7631	$9538	$11,446
Overhead@40%	$2289	$3052	$3815	$3052	$3815	$4578
Total Assembly Cost	8012	10,683	13,354	10,683	$13,354	$16,025
Total Variable Cost	$60,744	$85,750	$111,564	$85,594	$111,194	$156,511
Markup@29%	$17,616	$24,867	$32,354	$24,822	$32,246	$45,388
Total Hardware	$78,361	$110,617	$143,918	$110,417	$143,441	$201,899
Fixed Cost/Engine	$8103	$8103	$8103	$8103	$8103	$8103
Total Costs	$86,464	$118,720	$152,021	$118,520	$151,544	$210,001
Cost per kW	**$19.2**	**$12.5**	**$8.4**	**$13.9**	**$10.1**	**$4.4**

1 mm thick and estimates water storage during emission control area (ECA) operation for 250 hours of normal operation.

4.1.2. Direct Water Injection (DWI)

DWI contains charges for a low and high-pressure module, water storage tank, water injectors, flow fuses control unit and the related piping. **Table 6** shows costs the detailed information.

4.1.3. Selective Catalytic Reduction (SCR)

Selective Catalytic Reduction charges include reactor, the urea tank, dosage pump, injectors, control system, a bypass valve, cleaning probe and the acoustic horn. Retooling charges are for redesign of the exhaust system to entertain the SCR system. **Table 7** shows costs the detailed information.

4.1.4. Exhaust Gas Recirculation (EGR)

EGR charges contain a sludge tank, supply pump, piping, waste pump, a recirculation pump, an EGR Valve, separator, a scrubber system and control system.

Table 6. Cost of emission reduction technologies using DWI.

Speed	Medium	Medium	Medium	Low	Low	Low
Engine Power (kW)	4500	9500	18,000	8500	15,000	48,000
Component Cost						
Water Tank	$1132	$1767	$2610	$1611	$2240	$4386
Low Pressure Module	$4700	$7000	$9500	$9500	$19,000	$3800
High Pressure Module	$9500	$14,000	$19,000	$19,000	$38,000	$75,000
Piping	$5600	$7500	$9500	$9500	$14,000	$19,000
Flow Fuses (each)	$1900	$1900	$1900	$1900	$1900	$1900
Water Injectors (each)	$2400	$2400	$2400	$2400	$2400	$2400
Number per Cylinder	1	2	3	3	6	12
Control Unit/Wiring	$9500	$11,300	$13,000	$11,300	$13,000	$15,000
Total Component Cost	$69,132	$144,767	$260,010	$128,311	$292,640	$736,386
Assembly Labor (hr)	500	750	1000	1000	1500	2000
Cost ($23.85/hr)	$11,923	$17,885	$23,846	$23,846	$35,769	$47,692
Overhead@40%	$4769	$7154	$9538	$9538	$14,308	$19,077
Total Assembly Cost	$16,692	$25,039	$33,384	$33,384	$50,077	$66,769
Total Variable Cost	$85,825	$169,805	$293,395	$161,696	$342,717	$803,155
Markup@29%	$24,889	$49,244	$85,084	$46,892	$99,388	$232,915
Total Hardware	$110,714	$219,049	$378,479	$208,588	$442,105	$1,036,070
Fixed Cost/Engine	$74,891	$74,891	$74,891	$74,891	$74,891	$74,891
Total Costs	$185,605	$293,940	$453,371	$283,479	$516,997	$1,110,960
Cost per kW	**$41.2**	**$30.9**	**$25.2**	**$33.4**	**$34.5**	**$23.1**

Table 7. Cost of emission reduction technologies using SCR.

Speed	Medium	Medium	Medium	Low	Low	Low
Engine Power (kW)	4500	9500	18,000	8500	15,000	48,000
Component Cost						
Urea Tank	$1194	$1868	$2765	$1690	$2356	$4636
Reactor	$200,000	$295,000	$400,000	$345,000	$560,000	$1,400,000
Dosage Pump	$9500	$11,300	$13,000	$11,300	$13,000	$15,000
Piping	$4700	$5600	$6600	$5600	$7500	$9500
Injectors (each)	$2400	$2400	$2400	$2400	$2400	$2400
Number of Injectors	3	6	8	12	16	24
Bypass Valve	$4700	$5600	$6600	$5600	$6600	$7500
Acoustic Horn	$9500	$11,300	$13,000	$11,700	$14,000	$16,400
Control System	$14,000	$14000	$14,000	$19,000	$19,000	$19,000
Cleaning Probe	$575	$575	$575	$900	$900	$900
Total Component Cost	$251,369	$359,643	$475,740	$429,390	$661,556	$1,530,336
Assembly Labor (hr)	1000	1200	1500	1200	1600	2000
Cost ($23.85/hr)	$23,846	$28,615	$35,769	$28,615	$38,154	$47,692
Overhead@40%	$9538	$11,446	$14,308	$11,446	$15,262	$19,077
Total Assembly Cost	$33,384	$40,061	$50,077	$40,061	$53,416	$66,769
Total Variable Cost	$284,753	$399,704	$525,816	$469,452	$714,971	$1,597,106
Markup@29%	$82,578	$115,914	$152,487	$136,141	$207,342	$463,161
Total Hardware	$367,332	$515,618	$678,303	$605,593	$922,313	$2,060,266
Fixed Cost/Engine	$22,699	$22,699	$22,699	$22,699	$22,699	$22,699
Total Costs	$390,031	$538,317	$701,002	$628,292	$945,012	$2,082,965
Cost per kW	**$86.7**	**$56.7**	**$38.9**	**$73.9**	**$63**	**$43.4**

Based on an average EGR rate of 20 percent, sludge is supposed to grow at 0.005 g/kWh with a sludge density of 1300 kg/m^3. The sludge tank is intended to be made of 1mm thick cold rolled steel. The tank will hold sludge from engine operation over 500 hours. **Table 8** illustrates the cost of emission reduction technologies using the exhaust gas recirculation.

4.1.5. Seawater Scrubber

Scrubber charges contain the sludge tank, supply pump, a waste pump, a recirculation pump, an SO_2 monitor, oil and water separator, the scrubber system and control system. Sludge tank acquires a sludge buildup rate of 0.25 g/kWh and a sludge density of 1300 kg/m^3.

It is envisioned to be made of cold rolled steel 1mm thick and will hold sludge generated from engine operation over 500 hours. **Table 9** illustrates the cost of emission reduction technologies using the seawater scrubber.

Table 8. Cost of emission reduction technologies using EGR.

Speed	Medium	Medium	Medium	Low	Low	Low
Engine Power (kW)	4500	9500	18,000	8500	15,000	48,000
Component Cost						
Sludge Tank	$268	$345	$435	$511	$635	$859
Supply Pump	$1900	$2600	$3600	$2600	$4400	$7000
Waste Pump	$1900	$2800	$3800	$2800	$4700	$7500
Recirculation Pump	$1900	$2800	$3800	$2800	$4700	$7500
Scrubber Unit	$23,500	$35,000	$56,000	$32,700	$56,000	$112,200
EGR Valve	$7000	$9500	$11,700	$9500	$11,700	$14,000
Separator	$1900	$2800	$3800	$2800	$3800	$4700
Piping	$2800	$3800	$4700	$3700	$4700	$5600
Control System	$4700	$4700	$4700	$4700	$4700	$4700
Total Component Cost	$45,868	$64,345	$92,535	$62,111	$95,335	$164,059
Assembly Labor (hr)	200	300	400	300	400	500
Cost ($23.85/hr)	$4769	$7154	$9538	$7154	$9538	$11,923
Overhead@40%	$1908	$2862	$3815	$2862	$3815	$4769
Total Assembly Cost	$6677	$10,015	$13,354	$10,015	$13,354	$16,692
Total Variable Cost	$52,545	$74,361	$105,888	$72,127	$108,689	$180,751
Markup@29%	$15,238	$21,565	$30,708	$20,917	$31,520	$52,418
Total Hardware	$67,783	$95,925	$136,596	$93,044	$140,208	$233,169
Fixed Cost/Engine	$17,889	$17,889	$17,889	$17,889	$17,889	$17,889
Total Costs	$85,672	$113,814	$154,485	$110,932	$158,097	$251,058
Cost per kW	**$19**	**$12**	**$8.6**	**$13.1**	**$10.5**	**$5.2**

4.1.6. Fuel Switching

In this section, hardware charges related to fuel switching are presented. We pretend that the ships have sufficient storage tank capacity for fuel switching and all the appropriate equipment to achieve fuel switching in an Emission Control Area (ECA). The Air Resources Board (ARB) evaluates that 78% of all ships fall into this category based on their survey. **Table 10** shows the cost of emission reduction technologies using the fuel switching.

Economics impact for low and medium speed for category 3 marine diesel engines are shown in **Figure 9** (for low speed marine engines) and in **Figure 10** (for medium speed marine engines), where they are associated to kW/hour and kg fuel burned commonly for different engine grades and different emission reduction technology.

Based on the analysis and calculations, fuel switching technologies is the least

Table 9. Cost of emission reduction technologies using seawater scrubber.

Speed	Medium	Medium	Medium	Low	Low	Low
Engine Power (kW)	4500	9500	18,000	8500	15,000	48,000
Component Cost						
Supply Pump	$9500	$14,000	$19,000	$14,000	$23,500	$37,500
Sludge Tank	$350	$481	$641	$637	$818	$1256
Piping	$4700	$5600	$6600	$5600	$7500	$9500
Waste Pump	$9500	$11,300	$13,000	$11,300	$13,000	$15,000
Recirculating Pump	$9500	$11,300	$13,000	$11,300	$13,000	$15,000
Scrubber	$215,000	$355,000	$550,000	$340,000	$500,000	$1,125,000
Separator	$7000	$8000	$9000	$8000	$9000	$10,000
SO2 monitor	$9500	$9500	$9500	$9500	$9500	$9500
Control System	$28,000	$28,000	$28,000	$28,000	$28,000	$28,000
Total Component Cost	$293,050	$443,181	$648,741	$428,337	$604,318	$1,250,756
Assembly Labor (hr)	600	800	1000	1000	1500	2000
Cost ($23.85/hr)	$14,308	$19,077	$23,846	$23,846	35,769	$47,692
Overhead@40%	$5723	$7631	$9538	$9538	$14,308	$19,077
Total Assembly Cost	$20,031	$26,708	$33,385	$33,385	$50,077	$66,769
Total Variable Cost	$313,081	$469,888	$682,126	$461,722	$654,395	$1,1317,525
Markup@29%	$90,794	$136,268	$197,817	$133,899	$189,774	$382,082
Total Hardware	$403,875	$606,156	$879,943	$595,621	$844,169	$1,699,608
Fixed Cost/Engine	$17,889	$17,889	$17,889	$17,889	$17,889	$17,889
Total Costs	$421,763	$624,045	$897,831	$613,510	$862,058	$1,717,497
Cost per kW	**$93.7**	**$65.7**	**$49.9**	**$72.2**	**$57.5**	**$35.8**

expensive among the different technologies presented in this review, while sea water scrubbers remain the most expensive technology to adopt.

It can also be seen that the prices vary proportionally depending on the power rate of the engine but in the case of the DWI technique, the cost of adaptation on a 15,000 kW (for low speed) is slightly higher than that of 8500 kW due to the number of hours required for assembly and installation, while it is also higher than that of 48,000 kW because the cost of 48,000 kW is twice that of 15,000 kW but 3, 2 times bigger in terms of power allowing a cost reduction cost by an average of 33%. However, a combination of two or three technologies may prove attractive for shipowners to achieve significant emission reductions. In the future, the integration of multiple technologies will be the research direction of many vessels equipped with a marine diesel engine.

Table 10. Cost of emission reduction technologies using the fuel switching.

Speed	Medium	Medium	Medium	Low	Low	Low
Engine Power (kW)	4500	9500	18,000	8500	15,000	48,000
Component Cost						
Additional Tank	$3409	$5511	$8341	$4562	$6548	$13,733
LFO Separator	$2800	$3300	$3800	$3800	$4200	$4700
HFO/LFO Blending Unit	$4200	$4700	$5600	$4700	$5600	$6600
3-Way Valve	$950	$1400	$1900	$1400	$1900	$2800
LFO Cooler	$2400	$2800	$3300	$2800	$3800	$4700
Filters	$950	$950	$950	$950	$950	$950
Viscosity Meter	$1400	$1400	$1400	$1400	$1400	$1400
Piping/Pumps	$2000	$2000	$2000	$2000	$2000	$2000
Total Component Cost	$8012	$10,683	$16,025	$10,683	$16,025	$20,031
Assembly Labor (hr)	240	320	480	320	480	600
Cost ($23.85/hr)	$5723	$7631	$11,446	$7631	$11,446	$14,308
Overhead@40%	$2289	$3052	$4578	$3052	$4578	$5723
Total Assembly Cost	$8012	$10,683	$16,025	$10,683	$16,025	$20,031
Total Variable Cost	$26,121	$32,744	$43,316	$32,295	$42,423	$56,914
Markup@29%	$7575	$9496	$12,562	$9366	$12,303	$16,505
Total Hardware	$33,696	$42,240	$55,877	$41,661	$54,725	$73,419
Fixed Cost/Engine	$1233	$1233	$1233	$1233	$1233	$1233
Total Costs	$34,929	$43,473	$57,110	$42,894	$55,958	$74,652
Cost per kW	**$7.8**	**$4.6**	**$3.2**	**$5.0**	**$3.7**	**$1.6**

5. Conclusions

Ship emissions are one of the major issues affecting those interested in the maritime domain, as they have a negative impact on the marine environment. In this paper, a review and economic impact analysis of different emission reduction techniques for marine diesel engines have been presented.

According to **Figure 9** and **Figure 10**, using fuel switching technique as pre-treatment technology onboard ships appeared the best methods at long-term from the point of view of cost, while sea water scrubbers as post-treatment technology will be costly and add more ship operating cost. On the other hand, pre-treatment technologies such as the use of Methanol or LNG as marine fuel compared to HFO, reduce dependency on conventional fuels and have environmental benefits through an average reduction. However, due to the fact that both gases have significant differences in terms of characteristics and properties than

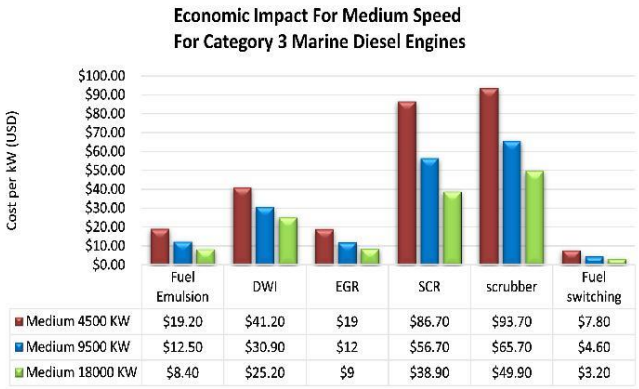

	Fuel Emulsion	DWI	EGR	SCR	scrubber	Fuel switching
Medium 4500 KW	$19.20	$41.20	$19	$86.70	$93.70	$7.80
Medium 9500 KW	$12.50	$30.90	$12	$56.70	$65.70	$4.60
Medium 18000 KW	$8.40	$25.20	$9	$38.90	$49.90	$3.20

Figure 9. Cost per kW (USD) for a medium speed for category 3 marine diesel engines.

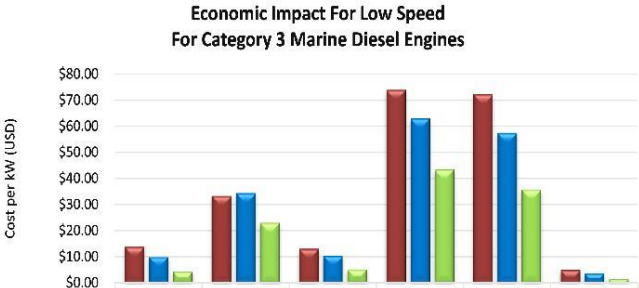

	Fuel Emulsion	DWI	EGR	SCR	scrubber	Fuel switching
Low 8500 KW	$13.90	$33.40	$13	$73.90	$72.20	$5.00
Low 15000 KW	$10.10	$34.50	$11	$63.00	$57.50	$3.70
Low 48000 KW	$4.40	$23.10	$5	$43.40	$35.80	$1.60

Figure 10. Cost per kW (USD) for a low speed for category 3 marine diesel engines.

conventional marine fuels, they are subject to storage challenges and require high capital cost in order to integrate them aboard ships in service. Appropriate integration for these gases as marine fuel is suitable for future ships to come.

It also was shown that internal-treatment technologies such as EGR and DWI in order to reduce oxides of nitrogen are mostly mature and are present in new marine DEs. The most advanced technology that can come in force with internal-treatment is the post-treatment, principally using SCR. However, due to the high price of reactor and the storage of urea in proportion to the fuel carried, SCR becomes the second most expensive technique after the scrubber.

Finally, the combination of two or three technologies is possible and can offer new solutions with high efficiency from the viewpoint of environmental and economic issues.

Conflicts of Interest

The authors declare no conflict of interest regarding the publication of this paper.

References

[1] Seddiek, S. and Elgohary, M. (2014) Eco-Friendly Selection of Ship Emissions Reduction Strategies with Emphasis on Sox and NOx Emissions. *International Journal of Naval Architecture and Ocean Engineering*, **6**, 737-748. https://doi.org/10.2478/IJNAOE-2013-0209

[2] Lin, B and Lin, C.Y. (2006) Compliance with International Emission Regulations: Reducing the Air Pollution from Merchant Vessels. *Marine Policy*, **30**, 220-225. https://doi.org/10.1016/j.marpol.2005.01.005

[3] International Maritime Organization (2015) Third IMO GHG Study 2014. Report, International Maritime Organization, London.

[4] Hermann, R.R. (2017) Drivers for Environmental Technologies Selection in the Shipping Industry: A Case Study of the North European Sulphur Emission Control Area. *International Journal of Environmental Technology and Management*, **20**, 139-162. https://doi.org/10.1504/IJETM.2017.10010687

[5] Ueno, C. (2010) Understanding Tier 4 Interim and Tier 4 Final. MTU onsite Energy. https://www.mtu-online.com/uploads/tx_templavoila/WhitePaper_Tier4i_and_Tier4_02.pdf

[6] Kristensen, H.O. (2012) Energy Demand and Exhaust Gas Emissions of Marine Engines. *Clean Shipping Currents*, **1**, 18-26.

[7] Lamas, M.I. and Rodriguez, C.G. (2012) Emissions from Marine Engines and NOx Reduction Methods. *Journal of Maritime Research*, **9**, 77-81.

[8] Woodyard, D. (2009) Pounder's Marine Diesel Engines and Gas Turbines. Ninth Edition, Elsevier, Oxford, 61-87.

[9] Man Diesel Turbo (2009) Exhaust Gas Emission Control Today and Tomorrow. https://marine.mandieselturbo.com/docs/librariesprovider6/technical-papers/exhaust-gas-emission-control-today-and-tomorrow.pdf?sfvrsn=22

[10] Cariou, P. (2011) Is Slow Steaming a Sustainable Means of Reducing CO_2 Emissions from Container Shipping? *Transportation Research Part D: Transport and Environment*, **16**, 260-264. https://doi.org/10.1016/j.trd.2010.12.005

[11] Kuiken, K. (2017) Diesel Engines: For Ship Propulsion and Power Plants from 0 to 100,000Kw. In: *Regulations for Propulsion Engines*, *Classification*, *Repair and Damage*, 3rd Edition, Onnen Target Global Energy Training, Netherlands, 398-424.

[12] Kristensen, H.O. (2015) Energy Demand and Exhaust Gas Emissions of Marine Engines. Mitigating and Reversing the Side-Effects of Environmental Legislation on RO-RO Shipping in Northern Europe. Report, Technical University of Denmark, Denmark.

[13] Rudzki, A and Carran, A. (2014) Assessment of Current and Future Air Pollutant Emission Reduction Technologies for Marine Diesel Engines. Report, Defense Research and Development Canada, Atlantic Research Centre, Victoria, Canada. https://apps.dtic.mil/dtic/tr/fulltext/u2/a603708.pdf

[14] Issa, M., Ibrahim, H., Lepage, R. and Ilinca, A. (2019) A Review and Comparison on Recent Optimization Methodologies for Diesel Engines and Diesel Power Genera-

tors. *Journal of Power and Energy Engineering*, **7**, 31-56.
https://doi.org/10.4236/jpee.2019.76003

[15] Elgohary, M, Seddiek, S. and Salem, A.M. (2015) Overview of Alternative Fuels with Emphasis on the Potential of Liquified Natural Gas as Future Marine Fuel. *Proceedings of the Institution of Mechanical Engineers, Part M: Journal of Engineering for the Maritime Environment*, **229**, 365-375.
https://doi.org/10.1177/1475090214522778

[16] Sastre, B.L. (2017) Implementation of LNG as Marine Fuel in Current Vessels: Perspectives and Improvements on Their Environmental Efficiency. Master Thesis, Universitat Politècnica de Catalunya, Spain.

[17] Nilsen, O.V. (2018) LNG Regulatory Update "Best Fuel of the Future". *Internationalisation Conference on LNG Project & the Baltic Sea Region LNG Cluster*, Bergen, Norway, 10-12 April 2018.
http://www.golng.eu/files/Main/20180417/2.%20Ole%20Vidar%20Nilsen%20-%20DNV%20GL.pdf

[18] Levander, O. (2011) Dual Fuel Engines Latest Developments. Technical Report, Wärtsilä, Concept Design, Hamburg.
https://www.stg-online.org/veranstaltungen/Ship_Efficiency_2017.html

[19] Zhou, S., Liu, Y. and Zhou, J.X. (2014) A Study on Exhaust Gas Emission Control Technology of Marine Diesel Engine. *Advanced Materials Research*, **864**, 1804-1809.
https://doi.org/10.4028/www.scientific.net/AMR.864-867.1804

[20] Wärtsilä Engines (2017) Wärtsilä 20DF Four-Stroke Dual-Fuel Engine. Report, Wärtsilä, Helsinki, Finland.
https://cdn.wartsila.com/docs/default-source/product-files/engines/df-engine/brochure-o-e-w20df.pdf?utm_source=engines&utm_medium=dfengines&utm_term=w20df&utm_content=brochure&utm_campaign=msleadscoring

[21] Zheng, Z., Yao, M.F., Zhang, B. and Chen, Z. (2005) Experimental Study on Performance and Emissions Characteristics of HCCI Operation for DME/Methanol Dual Fuel. *Transactions of CSICE*, **23**, 32-36.

[22] Martz, J. (2011) Focusing on Dual-Fuel Engine Benefits. Consulting-Specifying Engineer Magazine and Newsletters.
https://www.csemag.com/articles/focusing-on-dual-fuel-engine-benefits

[23] Wärtsilä Corporation (2006) The Engine of Industry. Wärtsilä Annual Report, Helsinki, Finland.
https://www.wartsila.com/docs/default-source/investors/financial-materials/annual-reports/annual-report-2006.pdf?sfvrsn=b1b31c45_2

[24] Wang, Y., Lin, L., Roskilly, A., Zeng, S., *et al.* (2007) An Analytic Study of Applying Miller Cycle to Reduce NOx Emission from Petrol Engine. *Applied Thermal Engineering*, **27**, 1779-1789. https://doi.org/10.1016/j.applthermaleng.2007.01.013

[25] Kovacs, D. and Eilts, P. (2015) Potentials of the Miller Cycle on HD Diesel Engines Regarding Performance Increase and Reduction of Emissions. SAE International, No. 2015-24-2440. https://doi.org/10.4271/2015-24-2440

[26] Goldsworthy, L. (2002) Design of Ship Engines for Reduced Emission of Oxides Nitrogen. *Engineering a Sustainable Future Conference Proceeding*, Australian Maritime College, Launceston.

[27] Geist, M. (1998) Sulzer RTA-8T Engines: Compact Two Stroke for Tankers and Bulk Carriers. Report, Wärtsilä NSD Switzerland Ltd., Winterthur.

[28] Kech, J., Hegner, R. and Mannle, T. (2014) Turbocharging: Key Technology for High-Performance Engines. MTU Engine Technology White Paper.

[29] Agarwal, D., Singh, S.K. and Agarwal, A.K. (2011) Effect of Exhaust Gas Recirculation (EGR) on Performance, Emissions, Deposits and Durability of a Constant Speed Compression Ignition Engine. *Applied Energy*, **88**, 2900-2907. https://doi.org/10.1016/j.apenergy.2011.01.066

[30] Andersson, K., *et al.* (2016) Shipping and the Environment. In: Andersson, K., Brynolf, S., Lindgren, J. and Wilewska-Bien, M., Eds., *Shipping and the Environment*, Springer-Verlag, Berlin, Heidelberg. https://doi.org/10.1007/978-3-662-49045-7_1

[31] Ibrahim, S. (2016) Process Evaluation of a Sox and NOx Exhaust Gas Cleaning Concept for Marine Application. Master of Science Thesis, Chalmers University of Technology, Sweden.

[32] Ecospec Global Technology Pte Limited (2015) CSNOx-Ultra Low Frequency, Singapore. http://www.ecospec.com/marine-csnox

[33] International Maritime Organization (2018) Marine Environment Protection Committee on Its Fifty-Eighth Session. Marine Environment Protection Committee. MEPC 58/23, United Kingdom. http://ec.europa.eu/environment/waste/ships/pdf/report_mepc58.pdf

[34] Reynolds, K.J., Caughlan, S.A. and Strong, R.S. (2011) Exhaust Gas Cleaning Systems-Selection Guide. Report, U.S. Department of Transportation. File No. 10047.01.

[35] Entec UK Limited (2005) Service Contract on Ship Emissions. Assignment, Abatement and Market Based Instruments. Final Report, European Commission Directorate General Environment.

[36] Issa, M., Beaulac, P., Ibrahim, H. and Ilinca, A. (2019) Marinization of a Two-Stage Mixed Structured Packing Scrubber for Sox Abatement and CO_2 Capture. *International Journal of Advanced Research*, **7**, 73-82. https://doi.org/10.21474/IJAR01/8793

[37] Chew, H.H. (2012) U.S. Patent No. 8,241,597. U.S. Patent and Trademark Office, Washington DC.

[38] Cimino, S., Lisi, L. and Tortorelli, M. (2016) Low Temperature SCR on Supported MnO_x Catalysts for Marine Exhaust Gas Cleaning: Effect of KCl Poisoning. *Chemical Engineering Journal*, **283**, 223-230. https://doi.org/10.1016/j.cej.2015.07.033

[39] Ballinger, T., Cox, J., Konduru, M., De, D., Manning, W. and Andersen, P. (2009) Evaluation of SCR Catalyst Technology on Diesel Particulate Filters. *SAE International Journal of Fuels and Lubricants*, **2**, 369-374. https://www.jstor.org/stable/26273395 https://doi.org/10.4271/2009-01-0910

[40] Jack Faucett Associates (1985) Update of EPA's Motor vehicle Emission Control Equipment Retail Price Equivalent. Calculation Formula, Final Report.

[41] United States Environmental Protection Agency (2009) Costs of Emission Reduction Technologies for Category 3 Marine Engines. Final Report, Assessment and Standards Division Office of Transportation and Air Quality.

CHAPITRE V

ARTICLE 3

Marinization of a Two-Stage Mixed Structured Packing Scrubber for SO_x Abatement and CO_2 Capture

Publié dans International Journal of Advanced Research, 2019

Volume 7:73-82 / ISSN: 2320-5407

Résumé

Dans cet article, une enquête pratique en laboratoire sur le lavage des gaz d'échappement à l'aide des solutions d'amines provenant d'un GED sont présentés. Les tests ont été réalisés en deux étapes. En première lieu, les tests ont été menés dans le laboratoire du centre de recherche d'innovation maritime sur un GED de 250 kW avec une charge allant jusqu'à 52%. Par la suite, les tests ont été conduit au sein de l'entreprise Genset-Synchro sur un GED de 250 kW avec une charge allant jusqu'à 85%.

L'objectif principal de cette recherche est d'évaluer le rendement d'un système de lavage de gaz lorsque le fioul utilisé contient 0,5% de Soufre et d'évaluer s'il sera possible de répondre à la norme IMO qui oblige les navires marchands d'utiliser un fioul avec 0,1% en teneur de soufre à partir de 2030. Pour faire, deux bancs d'essais ont été développés. Ils sont constitués d'une colonne de garnissage à deux étages et raccordée directement à la sortie de l'échappement du GED. Le premier étage de l'épurateur est alimenté par une solution

d’hydroxyde de sodium, utilisé comme absorbeur de SOx, alors que dans le deuxième étage de la colonne, est alimentée par une solution d’amine afin d’absorber le CO_2. Les résultats ont révélé une diminution significative du SOx par 89%, tandis que le CO2 a connu une diminution de 49%. Toutefois, une chute de pression de 17% a été remarquée lorsque le GED est soumis sous une grande charge due à l’encrassement des emballages structurés.

Journal Homepage: -www.journalijar.com
INTERNATIONAL JOURNAL OF ADVANCED RESEARCH (IJAR)
Article DOI:10.21474/IJAR01/8793
DOI URL: http://dx.doi.org/10.21474/IJAR01/8793
ISSN NO. 2320-5407

RESEARCH ARTICLE

MARINIZATION OF A TWO-STAGE MIXED STRUCTURED PACKING SCRUBBER FOR SOX ABATEMENT AND CO2 CAPTURE.

Mohamad Issa[1], Philippe Beaulac[2], Hussein Ibrahim[3] and Adrian Ilinca[2].

1. Institut Maritime du Québec, Department of applied sciences, Rimouski, Canada.
2. Université du Québec à Rimouski, department of engineering, Rimouski, Canada.
3. Institut Technologique de Maintenance Industrielle (ITMI), Sept-Îles, Canada.

Manuscript Info

Manuscript History
Received: 03 February 2019
Final Accepted: 05 March 2019
Published: April 2019

Key words:-
SOx reduction, IMO requirements, Wet scrubbers, packed beds, Pressure drop, CO2 capture.

Abstract

In this paper, a practical investigation to evaluate the impact of a two-stage mixed structured packing scrubber for SO_x abatement and CO_2 capture using amine solutions is presented. The practical test consists to connect the two-stage packing column to the diesel engine (DE) exhaust outlet. The first stage of the scrubber, fed with a sodium hydroxide solution, served as a SO_X absorber, where the liquid flow rate and the sodium concentration are the operating variables. Gasses are then transported from the first stage to the second stage, where they encounter an amine solution that can be recycled in a closed loop to absorb residual CO_2 streams. Tests are conducted with a 250kW diesel generator (DG) filled with a 0,5% Sulphur content fuel. Results revealed a significant decrease of SO_X by an amount of 89% while CO_2 capture has shown a decrease by an amount of 49%. However, drop pressure was detected when DG operates at high loads due to the fouling structured packing.

Introduction:-

Maritime transport emissions represent around 10-15% of global Sulphur oxide (SO_x) and nitrogen oxide (NOx) emissions, and approximately 3,1% of global carbon dioxide (CO_2) emissions [1], [2]. However, several studies confirmed that air pollutants could travel thousands of mile before deposition and contamination took place [3]. At the end 1980s, the international maritime organization (IMO) began its work and research on prevention of air pollution from ships and has adopted in 1997 the air pollution Annex VI (MARPOL convention).

This Annex came into force on 19 May 2005 after achieving the essential number of endorsers [4]. The Annex includes the establishment of emission control areas (ECAs) to scale down emissions in specified sea zones with a gradual reduction in emissions of NO_X, SO_X and particulate matter (PM), figure 1 [5], [6]. Since then, several measures have been taken into consideration. A tier system has been adopted to reduce NO_X levels, while SO_X will be reduced from current 3, 50% to 0, 50% beginning from 1 January 2020 in international waters and to 0,1% for ECA. Table 1 summarizes the regulatory requirements to reduce ship emissions of Sulphur oxides for ship categories 1, 2 and 3, [7].

Corresponding Author:-Mohamad Issa.
Address:-Institut Maritime du Québec, Department of Applied Sciences, Rimouski, Canada.

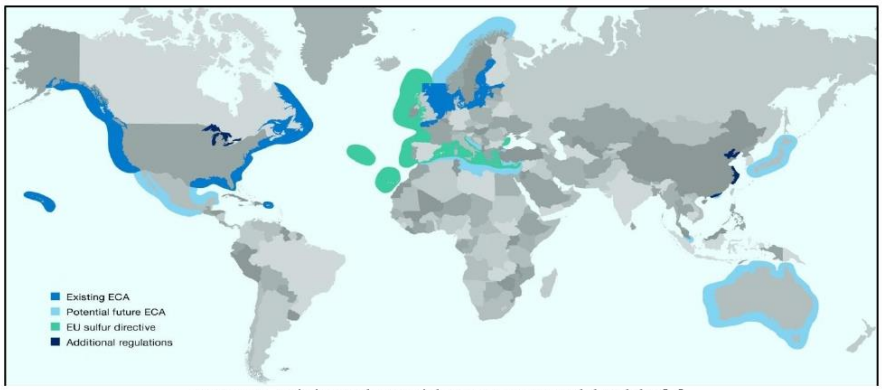

Figure 1:- Existing and potential new ECAs around the globe [6].

However, there are different feasible methods to meet Annex VI requirements. This can be accomplished by switching to a low-sulfur fuel or by applying exhaust after-treatment through absorption. As an alternative to low-sulfur fuel, MARPOL Annex VI recognizes exhaust gas cleaning systems (EGCS) that reduces sulfur emissions as efficiently as they do with low-sulfur fuel. The cost and benefit analysis of EGCS versus fuel changes was examined in [8-12]. Results have encouraged shipowners to choose primarily the EGCS option due to the ascending fuel price.

Table 1:- Low Sulfur Phase-In Dates [7].

Starting year (January 1st)	Category 3 ships				Category 1 & 2 ships
	Oceans	Emission Control Areas	EU Ports	California Coastal	
2010	4,5%	1,0%	0,1%	0,5%*	0,05%
2012	3,5%	1,0%	0,1%	0,1%	0,0015%
2015	3,5%	0,1%	0,1%	0,1%	0,0015%
2020-(2025)**	0,5%	0,1%	0,1%	0,1%	0,0015%

0, 5%*: Marine Gas Oil, or 0, 1% Marine Diesel Oil

(2025): Implementation of Oceans limit at 0, 5% Sulphur**

In the last decade, application of absorbers for Sulphur dioxide (SO_2) elimination has increased considerably in marine transport and they are generally called scrubbers [13]. Scrubbers are categorized as dry scrubbers, using dry lime and other calcium-based pH control minerals, or as wet scrubbers using an alkaline solution, figure 2 [14]. The open loop scrubber is the easiest system, where water is supplied from the sea, pumped, filtered and sprayed into the scrubber using nozzles that diffuse water into droplets. However, open loop scrubber is only profitable if the water is alkaline. This can be accomplished by adding an alkali chemistry or by using seawater with a natural alkalinity extracted from the bicarbonate ion (HCO_3^-) existing in the seawater [14]. The water is released back into the sea after particular matters are eliminated. Figure 3 illustrates a schematic of an open loop wet scrubber [15]. However, operation of the open loop scrubber system in fresh water can restrict scrubbing of SO_X due to the weak alkalinity of the water [16].

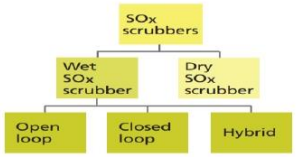

Figure 2:-The hierarchy of SO_X Scrubber systems [14].

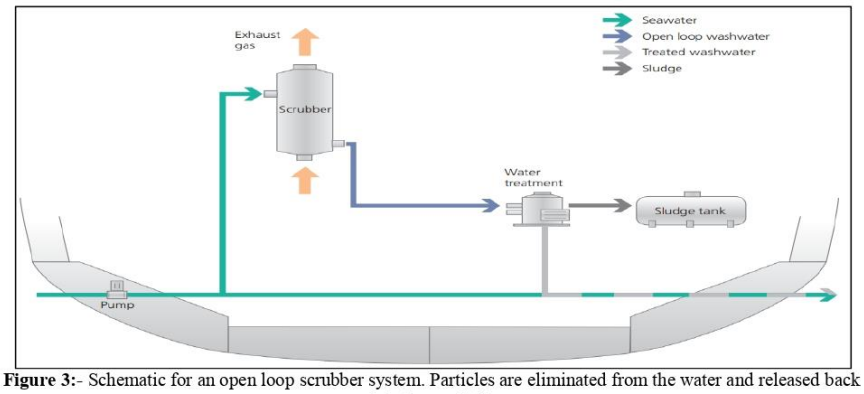

Figure 3:- Schematic for an open loop scrubber system. Particles are eliminated from the water and released back into the sea [15].

For this, it is therefore more interesting to develop closed loop technology for shipowners sailing in fresh water such as the St. Lawrence River (Canada) and the Great Lakes (USA and Canada). Fresh water treated with an alkaline chemical like caustic soda is employed for neutralization in a closed loop scrubber system (including hybrid SO_X scrubbers when operating in closed loop mode). Fresh water scrubbers are used when high efficiency cleaning is required or when the varying alkalinity associated with seawater prevents the use of marine scrubbers [16]. Nevertheless, closed loop fresh water scrubber systems have much smaller discharge rates than open loop sea scrubber systems by an amount approximately of 0,1 to 0,3 m^3/MWh and occurs a smaller volume of effluent [17]. Moreover, closed loop fresh water scrubber system can periodically be operated in zero discharge mode without discharging any overboard wash water. Figure 3 shows the schematic for a closed loop fresh water scrubber system [15].

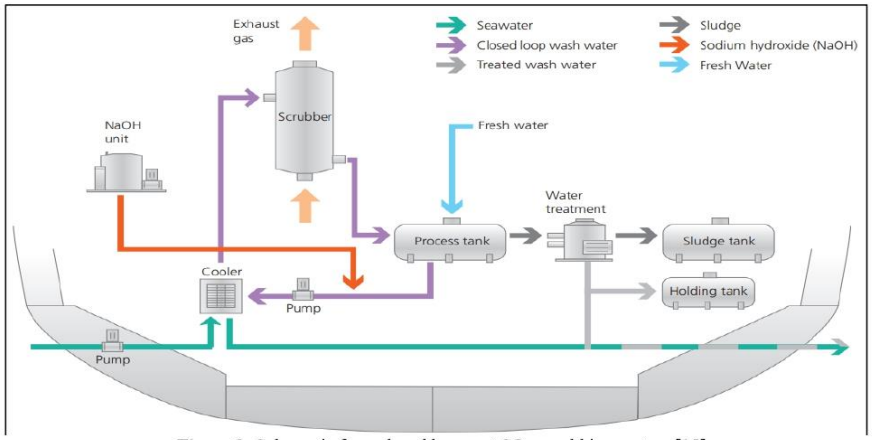

Figure 3:-Schematic for a closed loop wet SO_X scrubbing system [15].

Finally, hybrid wet SO_X scrubber systems either can operate in open loop mode or closed loop mode offering advantages that sodium hydroxide is used only when required, reducing handling and storage costs. However, hybrid wet SO_X scrubber systems have more complex design. On the other hand, dry SO_X scrubber systems have

been generally applied in land-based industry since 1970. Dry SO_X scrubber use calcium hydroxide granules ($Ca(OH)_2$) which react with sulfur oxides to form gypsum ($CaSO_4$-$2H_2O$). Contrary to wet SO_X scrubbers, dry scrubbers do not require wash water treatment making them ideal for areas where there is an increased sensitivity to discharge to the sea. However, as with closed loop operation of a wet system, consumables need to be stored and handled. Granules used must also be stored offshore before disposal.

The objective of this paper is to evaluate the effect of a vertical two-stage mixed structured closed loop-packing scrubber using a sodium hydroxide solution for SO_X abatement and CO_2 capture in aqueous Monoethanolamine (MEA) solutions. Indeed, the closed loop technology is much more interesting to develop for shipowners sailing in fresh waters and who have hybrid or closed loop with a 0,5% sulfur content fuel. Attention was given to the drop pressure in the scrubber column due to the fouling structured packing and on the level of SO_X abatement and CO_2 capture.

Experimental:-

The experimental setup is based on the absorption principle of contacting the gas phase with the liquid phase at room temperature and atmospheric pressure. A vertical two-stage gas-liquid counter-current packed bed (1) is used as absorbers and connected to the diesel engine exhaust outlet (Fig.4). The scrubber consists of an inox steel column (2), which is assembled up to a nominal height of 200cm around the 250kW diesel generator's main exhaust gas (3). The stainless steel fan (4), which is specifically designed to operate at high temperatures (up to 400°C), is connected to the main exhaust of the diesel engine, the main purpose of which is to redirect the part of the gasses emitted to two heat exchangers (5), in order to reduce the temperature of the gasses below 115°C, so that the amine solution can have an effect on the CO_2 capture. To adjust and control the amount of gas passing through the packaging column (10 l/min), a needle valve (6) with a rotameter (7) are used. Additionally, two pumps were used, the first (8) to feed the packing column with NaOH solution (0,1l/min) to capture the SO_x, while the second (9) was used to feed the second packing column with a Monoethanolamine (MEA) solution (0,1l/min) to reduce CO_2 emissions. Finally, at the inlet and outlet of the column, gas sensors (10) are installed to assess the CO_2 and SO_x levels before and after treatment with a differential pressure drop sensors (11).

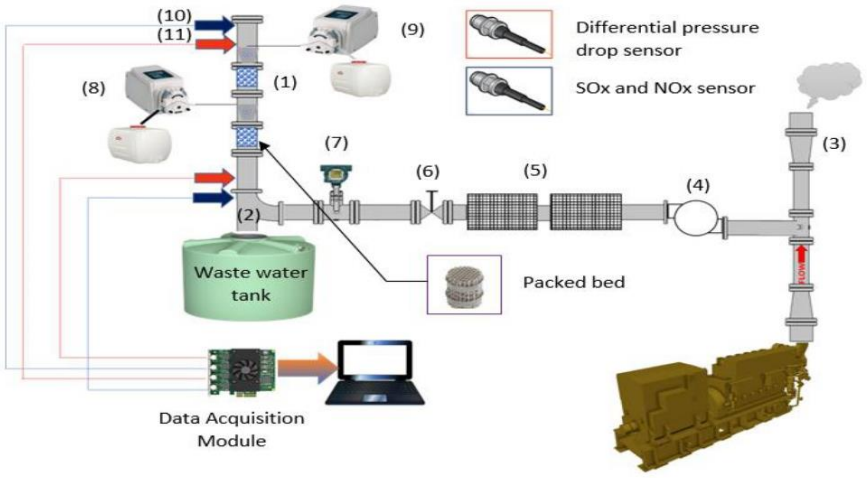

Figure 4:-Experimental setup representing the various components to assess the impact on the reduction of SO_X and CO_2 emissions.

Table 2 summarizes the fluid properties, the range of operating conditions and the specifications of the packed bed, while table 3 illustrates the technical specifications of the diesel generator used during the test.

Table 2:- Operational conditions and system properties ranges

Parameter	Value/Range
Gas velocity, U_g	0,0016 - 0,10m/s
Liquid velocity, U_l	0,0025 – 0,005m/s
Liquid surface tension, σ_L	0,072N/m
Gas density, ρ_g	1,2Kg/m^3
Bed porosity, ε	0,395
Bed length, L	0,3m
Column diameter, D	0,058m
Diesel Sulphur Content	0,5%
Applied Load for testing	30%, 50% and 85%

The installation was conducted in a liquid phase recycling approach supplied and controlled by two peristaltic pumps. Two multipoint liquid distributors were used, consisting of 9 needle orifices with an internal diameter of 1mm for NaOH and MEA supply. The evolution of gas state for SO_X and CO_2 as well pressure drops through the bed were measured in real time and transferred to the PC via a data acquisition system

Table 3:- Generator set specifications according to Caterpillar manufacturer

Description	Value/Range
Genset power rating with fan@0,8p.f.	250kW
Open generator set	1800rpm/60Hz/600V
Fuel consumption@100% load with fan	71L/hr
Fuel consumption@75% load with fan	57,6L/hr
Fuel consumption@50% load with fan	39,2L/hr
Exhaust stack gas temperature	426°C

Results and discussion:-

Evaluation of the SO_X and CO_2 content at the outlet of the scrubber without the intervention of the NaOH and MEA solutions for different applied loads

The main purpose of this section is to assess the amount of SO_x in the inlet of scrubber as well as the CO_2 level after combustion at 30%, 50% and 85% of applied loads. A SO_2-B4 sensor from alphasense air manufacturer was used for SO_2 detection, while a MH-410D sensor from winsensor manufacturer for CO2 detection was employed. Table 4 shows the SO_X and CO_2 level at the outlet scrubber. In addition, photos were taken with a thermal camera to assess temperature variation in heat exchangers in order to ensure a reduction in exhaust gas temperature as shown in figure 5 (a), (b) and (c).

Table 4:- Evaluation of the SO_X and CO_2 levels at different loads during 8 minutes of test.

Applied load (%)	Q_{Gas} (L/min.)	SO_X (ppm)				CO_2 (ppm)			
		2 min.	4 min.	6 min.	8 min.	2 min.	4 min.	6 min.	8 min.
30	10	44	43	42	42	1,09	1,08	1,08	1,08
50		33	32	33	33	0,97	0,97	0,97	0,97
85		18	19	20	20	0,78	0,78	0,78	0,78

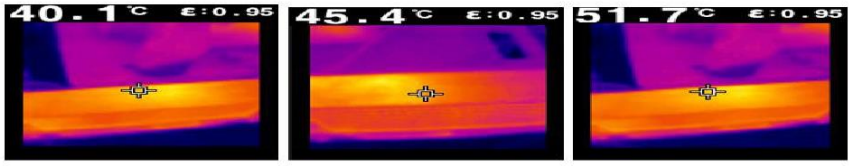

(a) (b) (c)

Figure 5:-Temperature in the heat exchanger at 30% of load in (a) , at 50% of load in (b) and 85% of load in (c).

77

According to table 4, we can notice that the SOx and CO2 levels are lower when the charge increases. This can be explained by the fact that the combustion becomes better and the majority of the particles are burned under high loads.

Evaluation of the SOx content at the outlet of the scrubber with the intervention of the NaOH solution for different applied loads

SO_2 associates with a salt in freshwater scrubbers and therefore does not react with the natural seawater bicarbonate. There are the coming reactions:

$$2NaOH + SO_2 \rightarrow Na_2SO_3 + H_2O \text{ (Sodium Sulfite)} \quad (1);$$
$$Na_2SO_3 + SO_2 + H_2O \rightarrow 2NaHSO_3 \text{ (Sodium Hydrogen Sulfite)} \quad (2);$$
$$SO_2 \text{ (Gas)} + H_2SO_4 \rightarrow NaHSO_4 + H_2O \text{ (Sodium Hydrogen Sulfate)} \quad (3);$$
$$2NaOH + H_2SO_4 \rightarrow Na_2SO_4 + 2H_2O \text{ (Sodium Sulfate)} \quad (4).$$

A freshwater scrubber usually discharges 250 times less water than an open loop seawater scrubber. The bleed off is significantly smaller for fresh water units (0.1-0.3m^3/MWh) and as a result, the concentration of pollutants is higher, making washwater cleaning easier [18].

Table 5 shows the results of the reduction, followed by a comparison before and after NaOH's intervention, see table 6 and figure 6. It should be noted that only 0.1 liters of NaOH solution has been injected into the packing column.

Table 5:-Evaluation of the SO_X abatement with NaOH intervention

Applied load (%)	Q_{Gas} (L/min.)	SO_X (ppm)				Pump (NaOH solution) l/min.
		2 min.	4 min.	6 min.	8 min.	
30	10	5,77	5,16	5,09	5,11	0,1
50		3,27	3,45	3,35	3,34	
85		1,89	1,90	1,89	1,88	

In order to compare results, we calculated the average of SO_X emissions before and after NaOH intervention and this for eight minutes of testing. Table 6 shows the average of SO_x emissions, while figure 6 shows the comparison.

Table 6:-Evaluation of the average of SO_X emissions before and after NaOH intervention

Without intervention of NaOH							With the intervention of NaOH				
Applied load (%)	Q_{Gas} (L/min.)	SO_X (ppm)				Average (ppm)	SO_X (ppm)				Average (ppm)
		2 min.	4 min.	6 min.	8 min.		2 min.	4 min.	6 min.	8 min.	
30	10	44	43	42	42	42,75	5,77	5,16	5,09	5,11	5,28
50		33	32	33	33	32,75	3,27	3,45	3,35	3,34	3,35
85		18	19	20	20	19,25	1,89	1,90	1,89	1,88	1,89

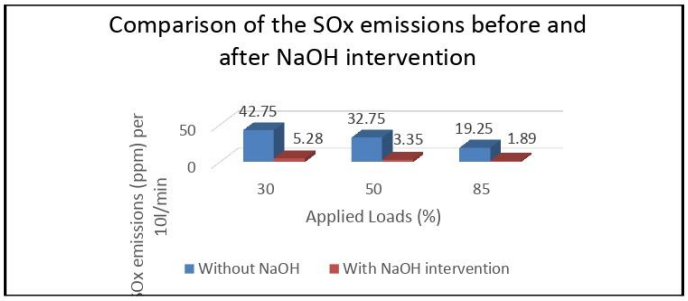

Figure 6:- Influence of the NaOH intervention on the SO_X abatement with a 0,5% sulfur content fuel.

According to table 6 and figure 6, the reduction of the SO_X emissions is 89% when the scrubber is fed with the NaOH solution. It can also be noted that due to better combustion in the piston chamber, the SO_X emission rate is further reduced at high load. However, an increase in pressure drop in the packing column has been detected due to the fouling structured packing under a high load. Figure 7 shows the microscopic Sulphur particles stuck on the packed bed causing an increase in the pressure drop.

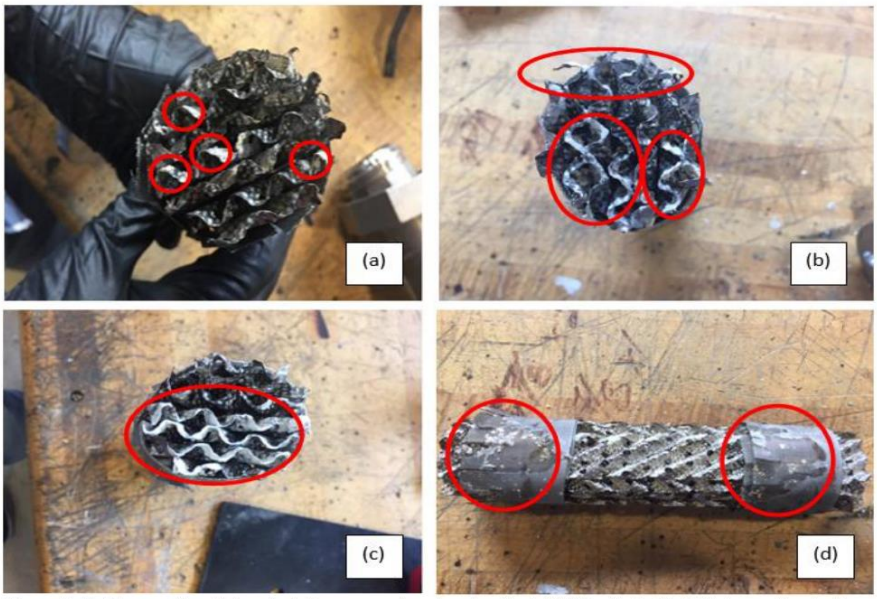

Figure 7:- in (a) a small particles of sulphur appeared under a low load (30%) with the NaOH intervention; in figure 3(b) the particles of sulphur appeared more on the packed bed under a load of 50%, whereas in figure 3(c) and 3(d) the particles are thicker and further blocks the flow of exhaust gas creating an increase in pressure drop.

Pressure drop

The overall pressure drop consists of gas-liquid interactions and static head of the liquid phase in the packed beds with gas-liquid simultaneous flow. According to table 7, the pressure drop (inlet Vs outlet of the scrubber) increase by 9,93% after 3 minutes of operation between a low load (30%) and a medium load (50%), while it is 16,6% under a high load (85%). This can be explained by the increase in the flow and pressure of exhaust gasses when the load increase. Furthermore, the amount of the sodium sulfate (Na_2SO_4) increases further due to the reaction causing the fouling of the packed beds in the column. Figure 8 shows the pressure drop across the different applied loads.

Table 7:-Evaluation of the pressure drop (ΔP) in the column at different loads

Time (s)	Pressure drop evolution (ΔP)		
	30% of load	50% of load	85% of load
0	0	0	0
20	4	5	6
40	8	9	10,5
60	12	12,6	13
80	12,22	13	13,6
100	12,41	13,2	13,99
120	12,65	13,9	14,4
140	12,88	14	14,96
160	12,97	14,37	15,22
180	12,97	14,4	15,55
200	12,98	14,4	15,69

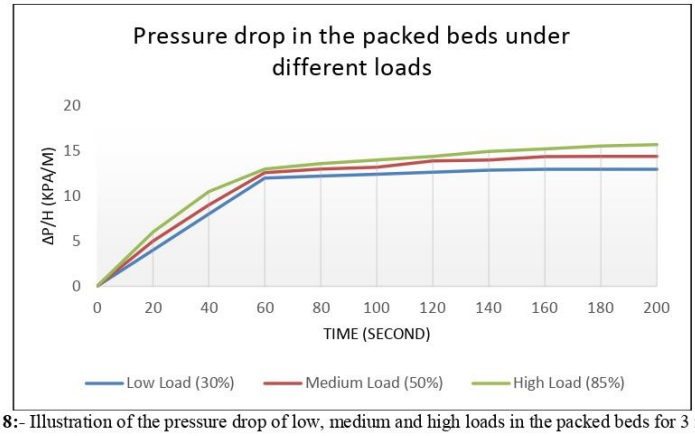

Figure 8:- Illustration of the pressure drop of low, medium and high loads in the packed beds for 3 minutes.

Evaluation of the CO_2 content at the outlet of the scrubber with the intervention of the monoethanolamine (MEA) solution for different applied loads

Carbon dioxide is considered as potential source for greenhouse gas (GHG) development. Different studies have evaluated that 3 to 4 percent of universal CO_2 emissions are attributable to marine vessels [19]. A 10 percent reduction in cruise speed is an effective operational methodology that offers a significant reduction in CO_2 and fuel consumption up to 20 percent over the same distance [20].

In this section, attention is given to reduce the carbon dioxide level at the exit of the scrubber by injecting a 0,1l/min of MEA solution. The following reversible reaction provides the basic reaction chemistry for an aqueous Monoethanolamine solution and CO_2 [21]:

$$C_2H_4OH\,NH_2 + CO_2 + H_2O \underset{Cold}{\overset{Hot}{\rightleftarrows}} C_2H_4OH\,NH_3^+ + HCO_3^- \quad (5)$$

This is an exothermic reaction and per mole of CO_2 absorbed in MEA solution, 72KJ of thermal energy is released. Absorption normally occurs around 50°C [21].

Table 8 shows the results of the reduction with a comparison before and after MEA solution intervention. It should be noted that only 0.1 liters of MEA solution has been injected into the packing column. Figure 9 illustrates the percentage reduction of the CO_2 after MEA solution intervention.

Table 8:-Evaluation and Comparison of the CO_2 reduction using MEA solution

Without the intervention of MEA solution							With the intervention of MEA solution				
Applied load (%)	Q_{Gas} (L/min.)	CO_2 (%)				Average (%)	CO_2 (%)				Average (%)
		2 min.	4 min.	6 min.	8 min.		2 min.	4 min.	6 min.	8 min.	
30	10	0,78	0,78	0,78	0,78	0,78	0,36	0,36	0,36	0,36	0,36
50		0,97	0,97	0,97	0,97	0,97	0,48	0,48	0,48	0,48	0,48
85		1,09	1,08	1,08	1,08	1,082	0,59	0,58	0,58	0,58	0,582

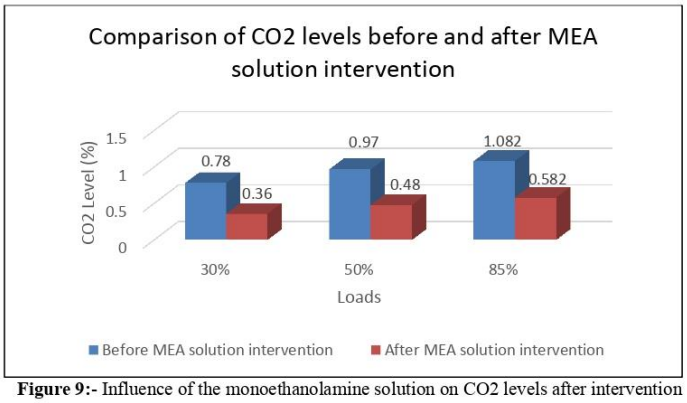

Figure 9:- Influence of the monoethanolamine solution on CO2 levels after intervention

According to table 8 and figure 9, the CO2 rate has decreased by an average of 49%. However, CO2 level increased with the load. This can be explained by the fact that the turbo absorbs a larger amount of air when the load increases.

Conclusion:-

Ship emissions are one of the major issues affecting those interested in the maritime domain, as they have a negative impact on the marine environment. The present paper discussed the various wet scrubber technologies, which could carry out to reduce those emissions.

A two-stage packed bed closed loop scrubber systems for sulfur abatement and CO2 capture was examined. For the evaluation of the efficiency of the system, a soda solution (NaOH) for sulfur abatement and monoethanolamine solution for CO2 capture were used. Tests are conducted using a 250KW diesel generator filled with a 0, 5% sulfur content fuel. The results showed the possibility to achieve valuable emission reduction percentage for the SO_X and CO_2 by an average of 89% and 49%. However, the accumulation of the sodium sulfate (Na_2SO_4) in the packed bed due to the chemical reaction between the SO_x and the NaOH solution, served further to the pressure drop in the scrubber by an amount of 17%.

On the other hand, the application of this methodology by ship operators allows them to meet the requirements set by IMO established in 2015 and that is to burn fuel with a sulfur content of less than 0,1% percent in ECAs starting by January 2020.

References:-

1. Smith, T. W. P., Jalkanen, J. P., Anderson, B. A., Corbett, J. J., Faber, J., Hanayama, S., ... & Raucci, C. (2015). Third IMO GHG Study.
2. Lindstad, H. E., & Eskeland, G. S. (2016). Environmental regulations in shipping: Policies leaning towards globalization of scrubbers deserve scrutiny. Transportation Research Part D: Transport and Environment, 47, 67-76.
3. Lindstad, H., Sandaas, I., & Strømman, A. H. (2015). Assessment of cost as a function of abatement options in maritime emission control areas. Transportation Research Part D: Transport and Environment, 38, 41-48.
4. American Bureau of Shipping (2018). ABS Advisory on Exhaust Gas Scrubber Systems. https://ww2.eagle.org/content/dam/eagle/advisories-and-debriefs/exhaust-gas-scrubber-systems-advisory.pdf (accessed 29 January 2019).
5. International Maritime Organization. Air Pollution, Energy Efficiency and Greenhouse Gas Emissions.http://www.imo.org/en/OurWork/Environment/PollutionPrevention/AirPollution/Pages/Default.aspx (2018, accessed 22 January 2019).
6. Elgohary, M. M., Seddiek, I. S., & Salem, A. M. (2015). Overview of alternative fuels with emphasis on the potential of liquefied natural gas as future marine fuel. Proceedings of the Institution of Mechanical Engineers, Part M: Journal of Engineering for the Maritime Environment, 229(4), 365-375.
7. Reynolds, K. J. (2011). Exhaust gas cleaning systems selection guide. Ship operations cooperative program. The Glosten Associates.
8. Wang, C., Corbett, J. J., & Winebrake, J. J. (2007). Cost-effectiveness of reducing sulfur emissions from ships.
9. Caiazzo, G., Di Nardo, A., Langella, G., & Scala, F. (2012). Seawater scrubbing desulfurization: A model for SO2 absorption in fall-down droplets. Environmental Progress & Sustainable Energy, 31(2), 277-287.
10. Yang, Z. L., Zhang, D., Caglayan, O., Jenkinson, I. D., Bonsall, S., Wang, J., ... & Yan, X. P. (2012). Selection of techniques for reducing shipping NOx and SOx emissions. Transportation Research Part D: Transport and Environment, 17(6), 478-486.
11. Jiang, L., Kronbak, J., & Christensen, L. P. (2014). The costs and benefits of sulphur reduction measures: Sulphur scrubbers versus marine gas oil. Transportation Research Part D: Transport and Environment, 28, 19-27.
12. Ciatteo, V., Giacchetta, G., & Marchetti, B. (2014). Dynamic model for the economical evaluation of different technical solutions for reducing naval emissions. International Journal of Productivity and Quality Management, 14(3), 314-335.
13. Andersson, K., Baldi, F., Brynolf, S., Lindgren, J. F., Granhag, L., & Svensson, E. (2016). Shipping and the Environment. In Shipping and the Environment (pp. 3-27). Springer, Berlin, Heidelberg.
14. Ibrahim, S. E. R. W. A. H. (2016). Process evaluation of a SOx and NOx exhaust gas cleaning concept for marine application. Chalmers University of Technology, Gothenburg Google Scholar.
15. Lloyd's Register (2012). Understanding exhaust gas treatment systems: Guidance for shipowners and operators. London, United Kingdom, 2012.
16. Reynolds, K. J. (2011). Exhaust gas cleaning systems selection guide. Ship operations cooperative program. The Glosten Associates.
17. MEPC (2008). 58/23 Annex 16, Report of the Marine Environment Protection committee on its fifty-eight session, International Maritime Organization.
18. Eelco den Boer & Marten 't Hoen. Scrubbers- An economic and ecological assessment. Report, Delft, CE Delft, March 2015. Publication code: 15.4F41.20. https://www.nabu.de/downloads/150312-Scrubbers.pdf
19. Cariou P. Is slow steaming a sustainable means of reducing CO2 emissions from container shipping? Transportation Research Part D: Transport and Environment (2011); 16(3):260-264
20. Kuiken K. Diesel engines: for ship propulsion and power plants from 0 to 100,000Kw. In: Regulations for propulsion engines, classification, repair and damage. Third ed. Netherlands: Onnen Target Global Energy Training, 2017, pp. 398-424.
21. Yeh, J. T., Pennline, H. W., & Resnik, K. P. (2001). Study of CO2Absorption and Desorption in a Packed Column. Energy & Fuels, 15(2), 274–278.

CHAPITRE VI

ARTICLE 4

Modeling and Optimization of the Energy Production Based on Eo-Synchro Application

Publié dans Institution of Diesel and Gas Turbine Engineers Journal (IDGTE, Londres), 2017

Volume 3:03-09 / No. 620- Technical Paper

Résumé

L'objectif de cet article est de décrire le principe de fonctionnement de la nouvelle technologie électrique d'Eo-Synchro connue aussi sous le nom de Genset-Synchro , de présenter sa conception mécanique et électrique, son principe de fonctionnement et son impact sur la consommation du carburant lorsqu'elle est intégrée sur un GED.

Il a été démontré dans des tests pratiques menés au sein de l'entreprise Genset-Synchro à Lévis, qu'il est possible d'atteindre des économies allant jusqu'à 12% lorsque la charge appliquée est inférieure ou égale à 35%, alors que cette économie diminue pour atteindre 2-3% lorsque la charge appliquée est de 80%. Les tests ont été menés sur un GED de 80kW de marque John-deer sous une température ambiante de 21ºC avec des bancs de charges résistifs. Une simulation mathématique basée sur les résultats obtenus, démontre que pour un même GED opérant dans le nord dans une communauté isolée avec un profil de charge variant entre 25% et 45% peut assurer une économie annuelle d'ordre de 216 milles litres de carburant par année.

Modeling and optimization of the energy production based on Eo-Synchro application

Authors: Mohamad ISSA [a,1], Éric DUBÉ [b,2], Mohammadjavad MOBARRA [a,3], Jean FISET [b,4], Adrian ILINCA [a,5]

[a] Laboratoire de Recherche en Énergie Éolienne, Université du Québec à Rimouski, 300 allée des ursulines, Rimouski, Québec G5L 3A1, Canada

[b] Entreprise EO-SYNCHRO, Département De la Recherche et Du Développement, 201 Rue Monseigneur Bourget, Lévis, Québec, G6V 6Z9, Canada

[1] missa@imq.qc.ca [2] Edube01@videotron.ca
[3] Pooria_mobarra@hotmail.com
[4] Jfiset@eo-synchro.com [5] Adrian_ilinca@uqar.ca

Abstract

In this paper, we are studying an innovative solution to reduce fuel consumption and production cost for electricity production by diesel generators. The solution is particularly suitable for remote areas where the cost of energy is very high not only of inherent cost of technology but also due to transportation cost. After a brief description of power generation based on a conventional synchronous alternator, the attention is focused on the Eo-Synchro concept. Then an innovative approach for optimizing the energy is proposed; it is based from the fact that the structure that contains the stator windings of the alternator is mounted on roller bearings which allows its free rotation around the axis of the rotor, consequently stopping the rotor structure from being static and aims to minimize the unit cost of electricity. Our model yields improved performance on fuel saving at all generator load stages compared to the conventional model. Experimental results on a 75kW Diesel Generator (DG) validate the performance of the proposed model.

Keywords

Diesel generator, power generation system, electrical machines, control of rotor speed, control of stator speed, Eo-Synchro concept, fuel saving.

1. Introduction

Most of the remote and isolated communities or technical installations (communication relays, meteorological systems, tourist facilities, farms, etc) that are not connected to national electric distribution grids rely on diesel engines to generate electricity [1]. In Canada, approximately 200,000 people live in more than 300 remote communities (Yukon, Northwest Territories, Nunavut, etc) that use diesel generated electricity, which is responsible for the emission of 1.2 million tons of greenhouse gases annually [2]. In Quebec alone, there are over 14,000 subscribers scattered in about forty communities that are not connected to the main electrical grid. Each community constitutes an autonomous network that uses diesel generators for electricity production [3]. The diesel power generating units, while requiring relatively little investment, are generally expensive to exploit and maintain, particularly when they are functioning regularly at partial load [4]. The use of diesel power generators under weak operating factors accelerates wear and increases fuel consumption [5]. During the past several years, the oil prices have achieved historic highs, peaking at 147$CAD/barrel in July 2008, averaging over 100$/barrel during 2011, averaging over 110$/barrel until October 2014, and then it fell to 80$/barrel. Recently, the oil price is around 45$/barrel. Despite this considerable drop, the diesel fuel prices are losing only a few cents in some provinces in Canada. According to Statistic Canada, in St. John's Newfoundland, the diesel fuel lost only 5.7¢/L, and in Whitehorse in Yukon increased by 3.5¢/L and in Yellowknife in Northwest Territories was set to rise up to 9.3¢/L in October 2014 compared to 2013. According to Statistics Canada (http://www5.statcan.gc.ca), the decline in crude oil prices is not felt at the pump in this region. However, the pump price gasoline only decreased by 11.8¢/L from a high of $112 per barrel to a low of $35 per barrel in December 2015. Therefore, the decrease in oil prices has not greatly affected the price of diesel fuel, which implies that the electrical energy produced using only oil and energy source will always remain expensive, at any cost per barrel [6]. According to Hydro Quebec, extending the main grid to these isolated areas will cost around (1M $/km), which is impossible to do with the actual economic crisis.

There are two types of DGs. The first type consists of a Diesel Engine (DE) running at a fixed speed coupled with a Synchronous Generator (SG); this solution has the advantage of simplicity. However, there are some drawbacks, including high level of noise regardless of the power level required by the load, high level of greenhouse gases emission (GHG) even when load power demand is low and over dimensioning in case of non-linear or unbalanced loads. The second type of DG operates with a variable speed. In this option the DE is coupled with an electrical generator operating at variable speed. This concept is able to reduce fuel consumption and reduce the cost of DG power generation [7]. Currently, most existing

DGs in remote areas operate at a constant rotational speed due to the restriction of the constant frequency required at the terminals of the generator. This operating mode causes high fuel consumption, as well as increases the maintenance costs [6]. To overcome these drawbacks, variable speed DGs are being proposed as an alternate configuration (Pena et al, 2008). Compared to the fixed speed DGs, variable speed DGs, are more efficient but costly, due to the use of power converters or mechanical transmissions.

In our project, we investigate another possibility that, when coupled to a DG operating in a power unit (Figure 1), the alternator with the Eo-Synchro application features can operate at variable speeds without the need for costly power electronics components to generate a constant frequency at the generator terminals. Per its configuration, the system can compensate for a lower or higher heat motor speed with no perturbation on the wave quality of the electricity being generated. It can operate in instant and/or prolonged mode, depending on the desired application. The system can therefore be used to compensate brief speed fluctuations or extended under-speed use while still compensating for intermittent and brief speed fluctuations [7, 8].

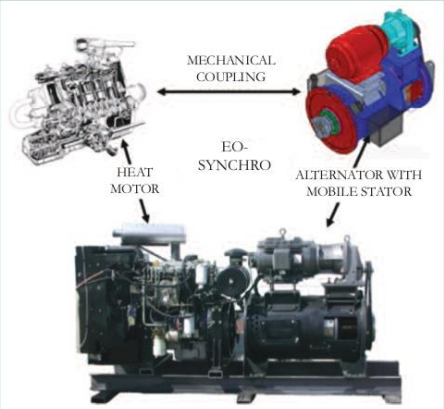

Figure 1 Illustration of alternator with mobile stator (Eo-Synchro application) coupled to heat motor

The project was developed by Concept Fiset Inc and was performed by the project partners Renewable Energy Research Laboratory of University of Quebec at Rimouski. The Eo-Synchro concept has three international patents including Canada [7, 8] , the United States [9] and Australia [10].

2. Objectives and methodology

A conventional DG consists of an engine connected directly to a synchronous alternator to produce electricity [11]. Since the electricity produced must be at a fixed frequency, normally 50Hz or 60Hz, the engine must rotate at a constant speed (typically 1,500rpm for 50Hz or 1,800rpm for 60Hz), no matter what the power demand is. One solution to save fuel in a diesel generator is to enable the engine to operate at variable speeds in direct relation to the electrical load demand [12]. In a previous work [13], Peter Dengler and Marcus Geimer from Karlsruhe Institute of Technology demonstrated that using an electronic converter is an easier way to provide a system at variable engine speed but at constant electric frequency (VSCF). These devices are already available on the market for other purposes, but a system with a generator in VSCF technology is still not established in the market as their higher investment costs are not yet proved to be economically justified by lower fuel consumption [13]. The objective of this study is to demonstrate that the Eo-Synchro application is able to reduce the fuel consumption and to reduce the cost of DG power generation. The structure of the present article is as follows. Section 3. presents the design approach of the active power generation by a synchronous alternator in general followed by the mechanical concept of Eo-Synchro and its principle control. In Section 4. we present the bench test and discuss the results obtained in order to demonstrate the efficiency of Eo-Synchro technology for generator applications. In Section 5. we provide a preliminary conclusion of our study and a perspective for future work.

3. The design approach

3.1 Three phase synchronous alternator

The active power which is supplied by a three-phase synchronous generator is given by:

$$P = \frac{E_0 \, E_b}{X_s} \sin\delta \quad (1)$$

where:

P = *active power provided per phase (W);*

E_0 = *induced voltage per phase (V);*

E_b = *voltage across terminal per phase (V);*

X_s = *synchronous resistance per phase (Ω);*

δ = *internal phase difference angle between E_0 and E_b, in electrical degree.*

Parameters E_0 and E_b are normally controlled by an Automatic Voltage Regulator (AVR). This unit is integrated with the alternator and maintains the voltage produced by the alternator at a present value [14]. The magnetic field of the alternator must rotate at the rated speed, that is 60Hz in North America. When connecting an alternator to a public electricity grid, the electricity grid one must be considered to be extremely large. Such a grid, to which hundreds of alternators and thousands of various loads are connected, consequently imposes a voltage and a fixed frequency to any apparatus that is connected. According to this principle, when synchronizing an alternator on an infinite grid, the induced voltage E_0 is equal to and in phase with the voltage E_b of the grid. Therefore, according to the above equation, the voltages E_0 and E_b being fixed by the grid and the reactance Xs being specific to the structure of the alternator, the only parameter which could modify the active power P provided by the alternator, is the electrical phase angle δ between the stator and rotor electrical field. This electrical angle δ is associated with the mechanical angle α through the following equation:

$$\delta = \frac{p\,a}{2} \quad (2)$$

Where p is the number of poles.

When the motor develops a torque, the poles of the rotor move backward of the poles of the stator.

In a standard synchronous alternator, the stator is stationary. If a torque is applied to the rotor, its axis has a tendency to deviate from the central axis of the stator. Figure 2 confirms this principle for a synchronous motor however, it is applied as well to a synchronous alternator.

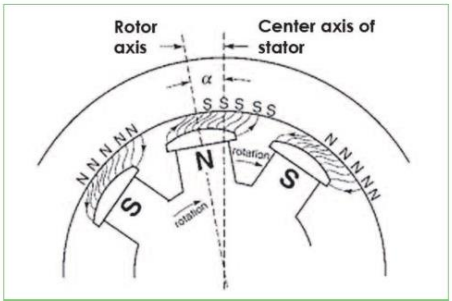

Figure 2 When the motor develops a torque, the poles of the rotor move backward of the poles of the stator. The angle δ between the axis of the rotor and the central axis of the stator is a measurement of the torque produced [15].

The difference rests on the fact that the torque is applied to the shaft of the machine (generator mode) and is not generated by the machine (motor mode). According to Figure 3 the maximum power provided by an alternator is obtained at an electrical phase difference angle δ of 90°. However, for stability reasons [14], the wattage rating of an alternator is reached at an electrical phase difference angle δ of 30°, ie a mechanical phase difference angle α of 15° for a 4-pole alternator.

The rotating speed of the electric field is equal to:

$$n_{sync} = \frac{120\,f}{p} \quad (3)$$

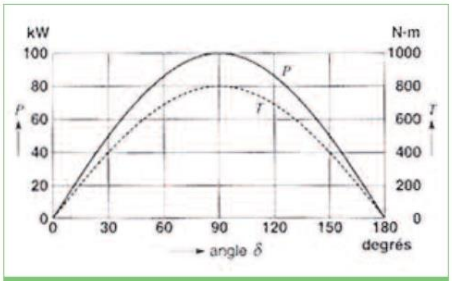

Figure 3 Power and torque in terms of the internal angle δ for a 40kW synchronous motor, 1,200rpm, 60Hz. The maximum power is 100kW.

In the case of a 4-pole alternator which operates at 60Hz, the rotating speed of the electric field inside the stator (also called synchronous speed) is 1,800rpm. In a synchronous alternator, the rotating speed of the stator field must be identical to the rotating speed of the rotor field. The two fields are therefore stationary with respect to one another and rotate at a constant speed. From a mechanical point of view, if free rotation of the stator is possible, the equation which describes the synchronous speed n in rpm is the following:

$$n_{sync} = n_{rotor} - n_{stator} \quad (4)$$

and by transmutation,

$$n_{stator} = n_{rotor} - n_{sync} \quad (5)$$

When a negative value of nstator occurs, it means that the stator rotates mechanically in the opposite direction with respect to the rotor [16]. Therefore, to maintain a synchronous speed of 1,800rpm, if the rotor rotates at 1,650rpm, the stator must rotate in the opposite direction at 150rpm so that the resulting speed is 1,800rpm. If the rotor rotates at 1,800rpm, the stator must remain mechanically stationary. If the rotor rotates at 1,950rpm, the stator must rotate at 150rpm in the same direction as the rotor. In a standard alternator, where the stator is stationary (n_{stator} = 0rpm) and the rotor is rotating, the synchronous speed then corresponds exclusively to the mechanical speed of the rotor. Therefore, for a 4-pole synchronous alternator, to have a frequency of 60Hz, the rotor must rotate at a constant and stable mechanical speed of 1,800rpm. In a production generator unit which uses a standard synchronous alternator, control of the mechanical speed of the rotor is therefore of prime importance to maintain an optimum phase angle, with an optimum power supply. In practice, this control is exercised at the level of the opening of the governor valves of a turbine in the case of a hydro-electric power station or from the angle of attack of the blades (pitch) in the case of a wind power turbine for example.

3.2 The Eo-Synchro concept as applied to power units

The Eo-Synchro application is a power unit control system with a highly original approach for power generation based on an innovative alternator design. Modifications to the structure holding the stator windings are the leading principle behind the Eo-Synchro application where this structure now rotates freely in reference to the rotor and frame. An auxiliary motor, driven by a dedicated automatic controller, dictates the desired position, speed or acceleration of the stator structure. This concept ensures regular wave quality regardless of speed variations of the rotor. No energy goes through power electronic equipment as in conventional technologies [8, 9, 10].

3.2.1 Rotating stator concept

To generate electricity in a power unit, a synchronous alternator transforms the mechanical energy coming from a heat motor into electrical energy [17]. When this alternator incorporates the Eo-Synchro concept by allowing the mechanical rotation of the stator windings, the synchronous speed of this alternator can remain constant through:

- Control of rotor speed only (existing design)
- Control of stator speed only (new design) [8, 9, 10]
- Control of both speeds simultaneously (new design) [8, 9, 10]

With the Eo-Synchro design, it becomes possible to control the synchronous speed of a 3-phase alternator by controlling the mechanical speed of the stator (control of stator speed only). In addition, because the Eo-Synchro application is entirely independent from the drive mechanism, it can be adapted to any type of rotor speed control and integrated into any type of power generation unit (reciprocating engine, wind turbine, hydraulic turbine, gas turbine, etc).

Figure 4 shows a prototype of the Eo-Synchro alternator, rated at 75kW. Rotor speed can vary from 1,575 to 2,025rpm. The main system components are identified in Figure 5.1 and 5.2.

Figure 4 The concept and prototype of Eo-Synchro

For this prototype, a three-phase synchronous alternator was modified to allow the stator windings to rotate around the rotor. No other modifications were made on the alternator rotor. The stator windings also remain the same.

The stator drive (compensating motor) is mounted in a casing affixed to the top of the casing of the synchronous motor using an assembly means comprising of brackets and bolts such that the output shaft of the stator drive is aligned in a parallel orientation with the stator shaft [8, 9, 10]. The output shaft of the stator drive and the stator shaft are connected using a timing belt and pulleys. The bottom pulley is fitted to the distal end of the stator shaft extending outside the casing of the synchronous alternator and the top pulley is fitted to the output shaft of the stator drive such that both pulleys are vertically aligned with one another. The timing belt links the two pulleys for one to drive the other.

3.2.2 Stator speed control

In the illustrated system (Figure 6) the controlling unit receives a feedback signal from an encoder which senses the position, or the speed of the stator. In this case, the encoder is positioned on the rotor to sense the position, and thereby the speed, of the rotor. The controlling unit also reads the produced alternating current as a feedback. From the received feedback signal and/or alternating current, the controlling unit produces the control signal which is inputted to the variable speed drive to control the rotation of the stator drive (compensating motor) and thereby of the stator of the synchronous alternator.

The controlling unit may use the feedback signal, the reading of the alternating current, or a combination of both. The

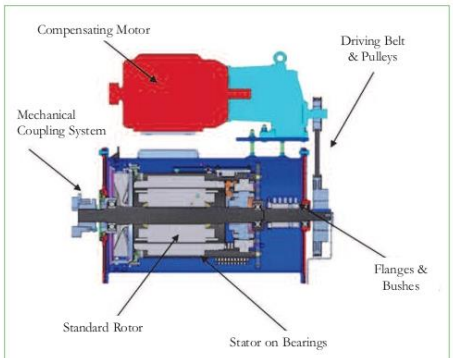

Figure 5.1 Main components of the Eo-Synchro concept

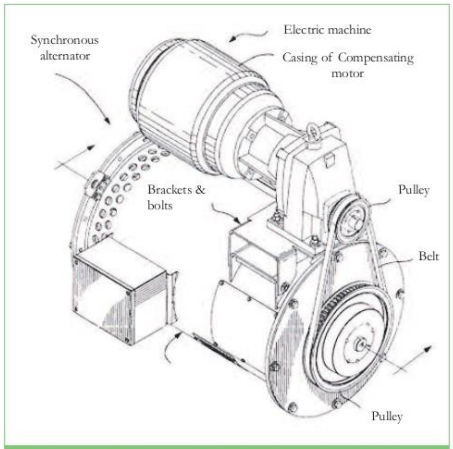

Figure 5.2 A perspective view of the mechanical components of an example configuration of the electrical generator using the Eo-Synchro concept

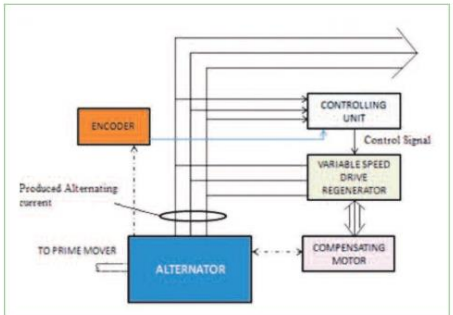

Figure 6 A schematic view illustrating an electrical generation system for producing electric current with a regulated frequency

controlling unit can be provided as a programmable logic controller, a computer or any other processing unit for example. The variable speed drive is typically powered using the electric current produced by the alternator and the frequency regulation consequently consumes part of the produced power, but the total balance of produced electric power remains positive. By controlling the rotation of the stator about the rotor, the relative speed, and thereby the frequency of the generated electric current, can be regulated [18]. For example, in a typical wind turbine generator (Figure 7), a 60Hz alternating current is generated in a 4-pole-3-phase alternator that rotates at 1,800rpm [19].

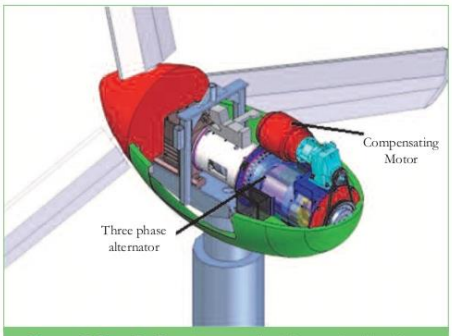

Figure 7 The Eo-Synchro applied in a wind turbine

When the wind is strong, the speed of the prime mover, ie the wind turbine, may rotate faster, at 2,000rpm for example. In order to compensate for such a higher rotation speed of the rotor, the stator is rotated at 200rpm in the direction of rotation of the rotor. The relative speed between the rotor and the stator is thus 1,800rpm (2,000rpm -200rpm: 1,800rpm). If the speed of the rotor decreases due to weak winds for example, eg at 1,500rpm, the stator is rotated at 300rpm in the direction opposite to the rotor. The relative speed is thus 1,800rpm (1,500rpm +300rpm: 1,800rpm).

4. Eo-Synchro application for power units

In order to demonstrate the efficiency of Eo-Synchro technology for a generator application, we performed bench testing in an R&D pilot facility of an industry leading generator supplier in collaboration with the Renewable Energy Research Laboratory at the University of Quebec in Rimouski, Canada. The following is a summary of the bench test work performed.

4.1 Description of the test bench

Figure 8 shows the schematic of the bench test studied. It consists of DE as a prime mover coupled to an SA. A compensating motor mounted on the top of the alternator and coupled to a drive provides the necessary rotation speed of the stator of the SA. The DE was instrumented by a torque sensor and speed sensor. This allowed us to measure the mechanical power supplied to the SA. Also, the output of the SA was instrumented with the global output. We were able to measure the current and voltage of each line with the PF and the total harmonic distortion (TDH) of the current and voltage.

Y1: CURRENT
VOLTAGE
POWER
PF
THD

Y2: CURRENT
VOLTAGE
POWER
PF
THD

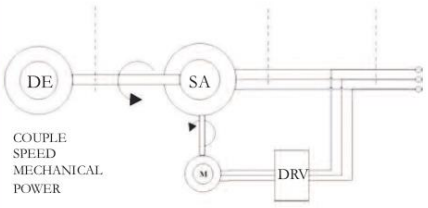

Figure 8 Schematic of the bench test

Figure 9 shows the main components of the bench test and their technical characteristics. All tests were performed with a mechanical power between 20kW and 60kW at 600V and a speed ranging from 1,400rpm to 1,800rpm.

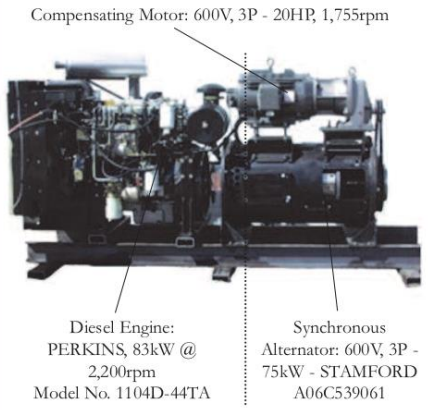

Figure 9 Main components of the bench test

4.2 About the tests

We started the tests without introducing the compensating motor (stator fixed) in order to evaluate the engine fuel consumption at different applied loads. Table 1 illustrates the different applied loads and fuel consumption in g/kWh. Subsequently, we performed the same tests mentioned above but with the application of Eo-Synchro technology. Table 2 illustrates the fuel consumption results with stator speed control.

Table 1 Evaluation of fuel consumption with a blocked stator

Blocked Stator Without Eo-Synchro Intervention			
Load (%)	Load (kW)	Consumption g/kWh	Engine speed (rpm)
100	60	262,7	1655
90	54	289,6	1585
80	48	286,7	1550
70	42	270,5	1550
60	36	262,5	1550
50	30	265,3	1525
40	24	311,7	1500
30	18	346,7	1500

Table 2 Evaluation of fuel consumption with Eo-Synchro

With Eo-Synchro System			
Load (%)	Load (kW)	Consumption g/kWh	Engine speed (rpm)
100	60	Uncompleted test, spyder had broken	
90	54	265,9	1600
80	48	266,1	1600
70	42	270,4	1525
60	36	263,3	1500
50	30	250,7	1480
40	24	272,8	1430
30	18	312,1	1430

4.3 Results comparison

First, it is important to note that both tests were done off-grid and the THD of the output current was below 2%. As observed in Table 1 and 2, when the Eo-Synchro technology is applied, fuel consumption decreases significantly when the engine is running at low load (40% and less). However, we must note that variable speed generators in remote area applications will regularly run at lower loads. Figure 10 illustrates a typical load for a remote area using a DE as a primary electricity source [20].

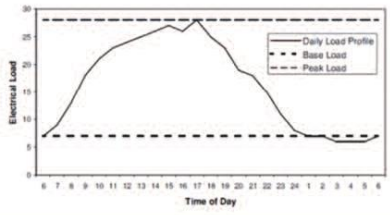

Figure 10 Example of a typical electrical daily load profile in a remote area. The peak load for any community occurs during the daytime hours when residents, businesses and manufacturers consume electricity at their peak demand.

Table 3 shows the fuel consumption difference between the conventional generator model (stator is fixed) and when Eo-Synchro technology is applied. As we can see, results obtained at 60% and 70% of applied loads are highlighted in red because they are very close to a conventional generator with a blocked stator. However, when the load is increased to 80%, we achieved a significant gain of 7% on fuel consumption followed by 8% for a load of 90%. Unfortunately, the test was suspended at 100% when the load was increased to 100% because the spyder had broken.

Table 3: Efficiency of the consumption variation

Consumption Variation	
Loads (%)	Blocked Stator Vs Eo-Synchro
100	-
90	+8,18%
80	+7,18%
70	-0,40%
60	-0,30%
50	+5,50%
40	+12,48%
30	+9,98%

Figure 11 further illustrates the effect the Eo-Synchro technology can have on improving DE fuel consumption for different loads.

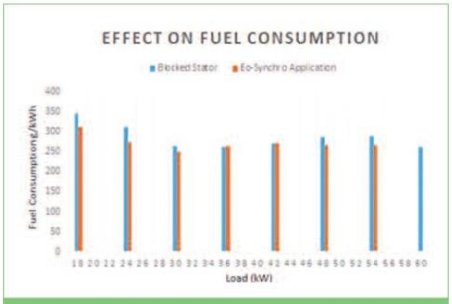

Figure 11 Effect of the Eo-Synchro application on fuel consumption.

5. Conclusion

This article presented the innovative features of the Eo-Synchro technology which originate from a rotational non-fixed stator design and a fuel savings evaluation for a DE generator application that can be achieved by controlling the rotation of the stator. A decrease of the heat losses to the DE exhaust is facilitated by allowing for lower engine operating speed at low power load with the Eo-Synchro technology. For this reason significant fuel savings of up to 12% can be obtained at low DE generator power loads (40%). The maximum gas pressure in the combustion chamber has to stay below a certain threshold and limits the intake pressure and therefore the fuel savings can be realized. This is why the fuel economy is higher for lower loads. Based on our results, for a 1MW DE generator unit, the fuel saving are projected to be 23g per kWh at 90% load. For an 1MW unit producing 1,000kWh, fuel savings would be 23kg/h. For equivalent purposes, as 1 liter of fuel weighs approximately 0.85kg, we can assume fuel saving of 27 liters/h, which represents

an annual fuel saving of 216,500 liters (57,190 US gallon) over 8,000 hours of annual operation. However, in the present paper, only an evaluation of fuel consumption based on 75kW DE has been demonstrated. Current estimation aims at bounding the hoped fuel economy for a 1MW DE.

While the present paper presents the original aspect of Eo-Synchro technology and theoretical results that are valid for a small DE, some preliminary experimental results under a 500kW DE were conducted under a new test bench by PhD researchers at University of Quebec in Rimouski and will be published shortly. The published experimental results cover a mathematical model to characterize the generated power model and the results of fuel economy savings obtained. ■

Nomenclature

DE	Diesel Engine
DG	Diesel Generator
VSCF	Variable Speed @ Constant Frequency
SA	Synchronous Alternator
DRV	Drive
SG	Synchronous Generator
GHG	Green House Gases emission
PF	Power Factor
TDH	Total Distortion Harmonic

References

[1] Ibrahim H, Younes R, Basbous T, Ilinca A, Dimitrova M. Optimization of diesel engine performances for a hybrid wind-diesel system with compressed air energy storage. Energy 2011;36:3079—91.

[2] Liu W, Gu S, Qiu D. Techno-economic assessment for off-grid hybrid generation systems and the application prospects in China, http://www.worldenergy.org/wecgeis/publications.

[3] Ibrahim H, Ilinca A. Younes R, Basbous T. Study of a hybrid wind-diesel system with compressed air energy storage, electrical power conference 2007, "Renewable and alternative energy resources", EPC2007. Montreal, Canada: IEEE Canada; 2007. October 25-25, 2007

[4] Hunter R, Elliot G. Wind-diesel systems-a guide to the technology and its implementation. Cambridge (UK): Cambridge University Press; 1994.

[5] Forcione A. Système jumelé éolien-Diesel aux iles-de-la-Madeleine (Cap-auxMeules)-Établissement de la VAN optimale. Institut de Recherche, HydroQuébec, Février; 2004.

[6] MiloudRezkallah 2016. Design and control of standalone and hybrid standalone power generation systems. Thèse de doctoratélectronique, Montréal, École de technologiesupérieure.

[7] Fiset Jean, Canadian Intellectual Property Office -Patent no.2580360: Energy Transfer Apparatus

[8] Fiset Jean, Canadian Intellectual Property Office -Patent no.2697420 :Mechanical Regulation Of Electrical Frequency In An Electrical Generation System

[9] Jean Fiset, Tony Durand, United States Patent & Trademark Office - Patent no. US8258641B2:Mechanical Regulation Of Electrical Frequency In An Electrical Generation System

[10] Jean Fiset, Tony Durand, Australian Patent - Patent no. 2008291635:Mechanical Regulation Of Electrical Frequency In An Electrical Generation System

[11] TiberiuTudorache, and Cristian Roman: The Numerical Modeling of Transient Regimes of Diesel Generator Sets. ActaPolytechnicaHungarica, vol. 7(2), 2010.

[12] ChemNayar : Innovative Remote Micro-Grid Systems. International Journal of Environment and SustainabilityISSN 1927-9566 | Vol. 1 No. 3, pp. 53-65 (2012), Regen Group Pty Ltd, Curtin University of Technology, Western Australia, Australia

[13] Peter Dengler and Marcus Geimer : Potential of Reduced Fuel Consumption of Diesel Electric APUs at Variable Speed in Mobile Applications - Peter Dengler and Marcus Geimer Karlsruhe Institute of Technology

[14] WILDI, T. SYBILLE, G., Électrotechnique, 4e édition, PUL 2005.

[15] Geoff Klempner and IsidorKerszenbaum, Handbook of Large Turbo-Generator Operation & Maintenance. Chapter One: Principles of operation of synchronous machine.

[16] Marian Kazmierkowski, The Electric Generators Handbook : Synchronous Generators, Ion Boldea 2006

[17] L.L.J. Mahon, Diesel Generator Handbook 1992

[18] HAU, E., Wind Turbines, 2nd edition, Springer 2006

[19] NREL, Advanced Control Design and Field Testing for Wind Turbines at the National Renewable Energy Laboratory, NREL/CP-500-36118, 2004

[20] MIA M. DEVINE, Analysis Of Electric Loads And Wind-Diesel Energy Options For Remote Power Stations in Alaska, M.S., University Of Massachusetts, February 2005.

CHAPITRE VII

ARTICLE 5

Modeling and Optimization of the Energy Production Based on Eo-Synchro Application

Publié dans Power Engineer Journal (IDGTE, Londres), 2018

Volume 2:22-31 / No. 624- Technical Paper

Résumé

L'objectif principal de cet article est d'évaluer si le concept Genset-Synchro peut maintenir les mêmes résultats obtenus sur le premier prototype de 80 kW mais cette fois-ci en employant une génératrice de 500 kW d'une part, et d'évaluer le taux des émissions des gaz d'échappement (GES) ainsi que le taux de distorsion harmonique en tension et en courant lorsque le stator est en mouvement.

Des charges capacitives et inductives ont été ajoutées pour tester davantage la qualité des signaux de sortie. Le facteur de puissance a été maintenue à 97% et deux vitesses statoriques ont été analysées (voir le 250 rpm et le 300 rpm).

Les résultats ont démontré qu'il est possible de maintenir une économie moyenne en carburant sur toutes les charges par 8,1% et une baisse dans les émissions de gaz d'échappement par

7,2%. Toutefois, le taux d'harmonies en tension a été légèrement supérieure lorsque le stator est en mouvement à 250 rpm et 300 rpm.

Sous une faible charge, le taux de distorsion harmonique passait de 5,5% à 5,8%, sous une moyenne charge le taux de distorsion harmonique passait de 9,6% à 10,2% et sous une grande charge le taux de distorsion harmonique passait de 12,7 à 13,1%.

Il a été conclu que les vibrations due à la rotation du stator sont les causes de cette augmentation de distorsion harmonique. Pour ce qui est du taux de distorsion harmonique en courant, il est resté inchangé. Les tests ont été menés sous une température ambiante à 22ºC.

Finalement, une analyse théorique basée sur les résultats obtenus démontre qu'il est possible pour la mine Raglan située dans l'extrême Nord du Québec de réaliser des économies en carburant d'ordre de 1,120 000 litres de diesel par année si le central électrique alimentant la mine sera doté de la technologie Genset-Synchro.

Optimizing the performance of a 500kW Diesel Generator: Impact of the Eo-Synchro concept on fuel consumption and greenhouse gases

Authors: Mohamad ISSA [a,1], Jean FISET [b,1], Mohammadjavad MOBARRA [a,2], Hussein IBRAHIM [a,3], Adrian ILINCA [a,4]

[a] Laboratoire de Recherche en Énergie Éolienne, Université du Québec à Rimouski, 300 allée des ursulines, Rimouski, Québec G5L 3A1, Canada
[b] Entreprise EO-SYNCHRO, Département De la Recherche et Du Développement, 201 Rue Monseigneur Bourget, Lévis, Québec, G6V 6Z9, Canada

[a1] missa@imq.qc.ca [a2] Pooria_mobarra@hotmail.com [a3] Hussein.Ibrahim@itmi.ca [a4] Adrian_ilinca@uqar.ca
[b1] Jfiset@eo-synchro.com

Abstract

The power generation for many remote areas such as telecommunications infrastructures, mining facilities and isolated residential areas, is historically ensured with Diesel engine generators. The economical cost of energy is therefore very high not only due to inherent cost of fuel but also due to transportation and maintenance costs. The environmental cost of energy is also high as the use of fossil fuels for electricity generation is a significant source of greenhouse gas emissions. On the other hand, the shipping industry is under great pressure to reduce its environmental impact. If no measures are taken, CO_2 emissions are projected to increase 50-250% by 2050, while the Paris convention requires a significant reduction to achieve 2°C global warming target. Moreover shipping already contributes to 15% of the global NO_X emissions, which is also projected to increase if no measures are taken. In previous work, we have explored and evaluated a new technique based on the Eo-Synchro concept to reduce fuel consumption and minimize the unit cost of electricity; a general savings of 7% of fuel consumption was found when the Eo-Synchro concept was applied on a 75KW Diesel Generator (DG). As a continuity of these previous works, experimental tests have been carried out on a 500KW DG to evaluate the performance of fuel consumption and gaseous emission characteristics when the Eo-Synchro concept is applied. The experimental results show a significant fuel saving up to 15% can be obtained at low power loads and up to 5% at high power loads. On the other hand, the emission of nitrogen oxides (NO_X) and of carbon dioxide (CO_2) are 5,8% lower when the Eo-Synchro concept is used. The results for the other emissions are also shown in the figures and tables. Based on our results, an assessment of fuel savings and greenhouse gases reduction is presented for an off-grid mine site located in the Canadian North. A savings of 4% on fuel consumption and GHG emissions has been registered at high power loads.

Keywords: Diesel engine, diesel generator, Eo-Synchro concept, performance, emissions, greenhouse gases. power ship, off-grid mine.

1 Introduction

Motor generators are a wide class of electric power systems, which includes plants of the diesel generator (DG) type, gasoline engine generator plants, marine and other shaft generator plants, wind farms, and a number of other power generating systems [1]. Of the above mentioned systems, the most widely used plants are those of the DG type. They, having high reliability, a long service life, and durability, are indispensable as autonomous sources of primary or backup power supply for both marine vessels and onshore facilities. Classic gensets based on internal combustion engines are equipped with synchronous generators; therefore fixed speed operation is required. They operate at low efficiency during low load operation (figure 1). It is not critical in emergency power applications, but very important in continuously operated systems, where fuel consumption is a significant economic and logistic aspect. In fact, remote areas with relatively small communities generally show significant variation between the time of peak loads and the time of minimum loads. A typical example of a load profile of a remote community in Western Australia is shown below in figure 2 [2].

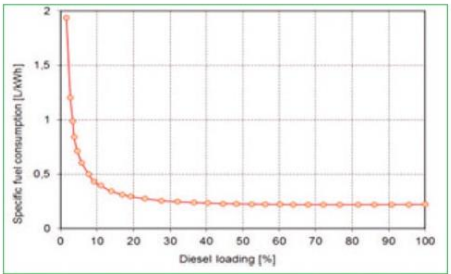

Figure 1 Example of a variation of a diesel fuel consumption with loading [2]

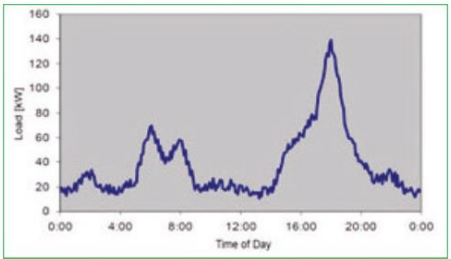

Figure 2 Typical load profile of a remote community in Australia

Diesel-powered electric generators are typically sized to meet the peak demand during the evening but must run at very low loads during "off-peak" hours during the day and night. This low-load operation results in poor fuel efficiency and increased operation and maintenance costs [3]. Moreover, low load operation of a diesel genset at synchronous speed reduces the engine lifetime, by incomplete combustion of the fuel; therefore an additional dump load is required to improve the combustion process. The efficiency and fuel combustion at low load conditions can be improved by use of load adaptive adjustable speed operation of the genset [4]. Power electronics based designs use an engine driven generator along with power transistor (or controllable thyristors) inverters in back-to-back intermediate circuit connection, power electronics filters and a control scheme to create resulting voltage and current waveforms comparable to that generated by a fixed speed synchronous genset. The line side inverter provides constant voltage and frequency output during most load conditions and may also provide fault protection. In the solution with AC voltage output of the line side inverter and varying rotational speed there is a problem of rapid load changes which may cause a voltage collapse [5].

In some remote locations, a dual diesel generator system is employed. When the load is light, the smaller generator is used; as the load increased, the manual switch is transferred to the larger generator. This approach results in some fuel savings, however managing this dual system is time consuming and impractical [3]. High fuel costs have translated into tremendous increases in the cost of energy generation [3]. In Quebec for example, as the fuel should be delivered to remote locations, some of them reachable only during summer periods by barge, the cost of electricity produced by diesel generators reached in 2007 more than 50 cent/kWh in some communities, while the price for selling the electricity is established, as in the rest of Quebec, at approximately 6 cent/kWh [6]. The deficit is spread among the Quebec population and the total consumption of the autonomous grids is far from being negligible. Moreover, the electricity production by the diesel is ineffective, presents significant environmental risks (spilling of fuel and lubricants), contaminates the local air and largely contributes to GHG emissions.

In all, we estimate at 140,000 tons annual GHG emission resulting from the use of diesel generators for the customers of the autonomous networks in Quebec. This is equivalent to the GHGs emitted by 35,000 cars during one year.

Based on these economic and environmental concerns, this paper proposes and investigates the use of the Eo-Synchro concept on a diesel generator, so as to minimise the performance indices of life cycle cost, net fuel consumption, net CO_2 emissions, dump energy and reliability of DGs. The rest of the paper is organised as follows : section 2 presents the different factors that influence the efficiency of DGs ; section 3 presents a brief review of the Eo-Synchro concept and the relationship between the magnetic field induced and speed governor in a DG ; section 4 presents the bench test and discusses the results obtained on a 500KW DG ; section 5 presents the case study for on off-grid mining based on the Canadian north and section 6 provide a conclusion and a perspective for the future work.

2 Factors influencing the efficiency of Diesel Generator

2.1 Design Engine Efficiency

A diesel generator set is a combination of two major components: the engine (the driver) and the alternator (driven by the engine to produce power). Thus the efficiency of diesel generator sets is expressed as a combined efficiency of these two sub-components. Typically, the combined efficiency of diesel generator sets varies between 30-55% (for large low speed units) while stand-alone efficiency of diesel engine and alternator ranges between 35-50% and 85-95% respectively [7]. The wide range of engine efficiency is mainly attributed to design, size or capacity, mechanism for fuel control, operating speed, type of cooling mechanism, and material of construction. However, the efficiency during operation deviates from the design value because of load conditions, ambient conditions, and operation and maintenance (O&M) practices [8]. In order to analyze the efficiency pattern of diesel engines, efficiency information for a sample number of models [9] was analysed as shown in figure 3.

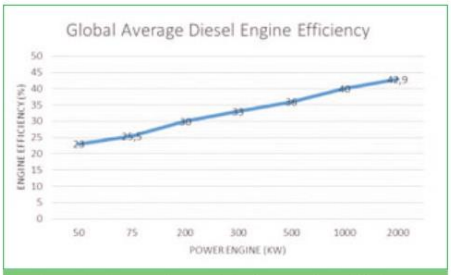

Figure 3 Comparison of design engine efficiency for a sample number of models

The analysis shows an increase in engine efficiency with increase in size of the sets. For up to 50 kW to 1000 kW categories, efficiency varies between 20% and 40%, This is due to a wide variety of engine types and technologies (such as number of strokes, cylinders, fuel injection system, cooling type) adopted by manufacturers. Variation in efficiency is much lower in larger diesel generator sets (above 300kW or 375kVA). This is largely because scope for technology improvements increases with increase in size of the sets. This provides manufacturers with several options

efficiency is much lower in larger diesel generator sets (above 300kW or 375kVA). This is largely because scope for technology improvements increases with increase in size of the sets. This provides manufacturers with several options for improvement in engine design, engine geometry, and sophisticated fuel control mechanism.

2.2 Fuel Engine Efficiency

Fuel efficiency is another metric of expressing the efficiency performance of a diesel generator set and it is directly linked to energy efficiency of the diesel generator (combined efficiency of engine and alternator). Specific Fuel Consumption (SFC) expressed in litre/hour or gm/kWh is an indication of the quantity of diesel required to generate one unit of electricity. The variation in SFC is influenced by operational factors such as loading, O&M practices, and ambient conditions. The following are the observations on parameters affecting the SFC of diesel generator sets [7]:

- SFC varies with size: the SFC becomes better in larger sized sets, specifically over 500 KVA categories. For example, a 500KVA diesel generator at 100% loading has typically 12% better SFC than a 25KVA set at the same loading. For diesel generators capacity beyond 800KVA, SFC continues to improve as size increases to 2MW, 4MW, 6MW and greater.
- SFC varies with loads: SFC is typically optimum at 75-80% loading of the rated capacity. SFC worsens substantially at 25% load or below for all capacity ratings. For instance, a 500KVA set is observed to have 20% better SFC at 75% than at 25% loading.

2.3 Transmission Loss

From engine shaft to load, there are transmission losses of around 10% at full load rating [10]. The power efficiency of the generator is usually considered to be around 96%, where power efficiency is defined to be its output power dividing by its input shaft power. Power loss is typically assumed to be neglectable when it comes to the switchboard, while the power efficiency of power converter (transformer) is assumed to be around 98%-99.5%. Meanwhile, the power efficiency of electric motors is around 96%. However, all these values are specified on product's data sheet at rated conditions by manufacturers. This is because many notable regulatory bodies and trade organizations have tried to establish international standards for the way in which efficiency is calculated and stated on product data sheets. As a result, power supply efficiency is usually specified based on the operating conditions that are most favourable to the figure concerned, for example, at maximum rated load. However, for the rest of the time, it will be operating below full load, and efficiency is likely to be much lower than the stated figure. To assess the impact on heat generation within a product, one need to dig deeper into the data sheet and find the efficiency vs. load curve, if one is provided. Figure 4 shows an example of converter efficiency against load percentage. Across a wide span of load range from 40% to around 100%, there exists relatively flat efficiency. However, converter efficiency degrades significantly as load percentage drops to 40% and below where converter efficiency approaches 77% at close to 0% load.

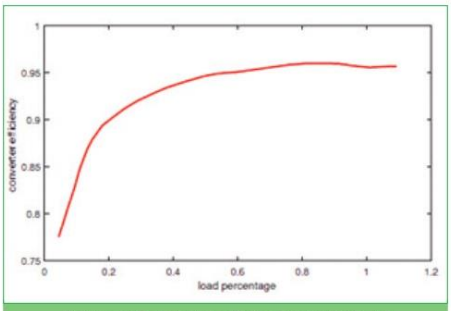

Figure 4 Converter efficiency again load percentage [10]

3 The Eo-Synchro Concept and relationship between the magnetic field induced and speed governor in a diesel engine

3.1 The Eo-Synchro concept: A brief review

The Eo-Synchro concept is a control system which proposes a highly original approach based on a new alternator design. The concept employs a new non-static stator where the stator rotates around the axis of the rotor. A motor mounted on the alternator provides full control of the position and the rotational speed of the stator [11]. Figure 5 shows a prototype of the Eo-Synchro alternator, rated at 75 kW.

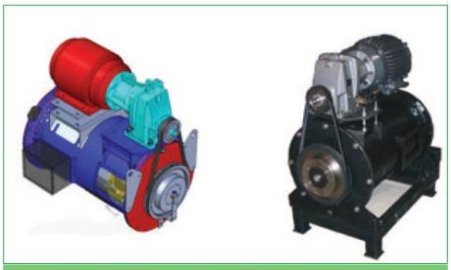

Figure 5 The concept and prototype of Eo-Synchro [11]

In our previous work [11], we have demonstrated the positive effect of the Eo-Synchro concept on fuel consumption when applied to a 75KW DG. A general fuel consumption savings saving of 7% was found for the different ranges of the applied loads. In the following section (III.2), we discuss the relationship between the magnetic field induced and the speed governor's reaction according to the applied loads when the stator is fixed, followed by an explanation of the Eo-Synchro concept as a variable speed generator.

3.2 Relationship between the magnetic field induced and speed governor in a diesel generator

A synchronous electrical generator is designed to be operated at a constant speed. i.e. synchronous speed. When

the generator rotor is rotated, the magnetic flux of the generator rotor induces a voltage in the generator stator windings, called the generator terminal voltage [12]. When the speed of the generator rotor is constant and the excitation is constant, the generator terminal voltage will be constant. The magnitude of the generator terminal voltage is a function of the strength of the magnetic field of the generator rotor, since the generator rotor is being rotated at constant speed, which is the synchronous speed. To do so, an Automatic Voltage Regulator (AVR) adjusts the magnetic fields as needed. During heavy power demands, voltage decreases causing the AVR to increase the magnetic field. Conversely, when power demands are low, the AVR tempers the field. Mechanical power is given by P = Torque x Rotational speed. Speed is normally regulated to be a constant value in order to keep the voltage and frequency constant. Torque varies as required to supply the mechanical power that is converted to electrical power. If the generator requires more torque, the fuel flow must increase to supply the additional power. Power available from burning fuel is proportional to fuel mass per unit of time. As electrical load increases the mechanical load increases. If the throttle position were fixed the speed would drop. The governor opens the throttle to allow more fuel in to maintain speed at set point.

3.3 The Eo-Synchro concept as variable speed generator

Applying the Eo-Synchro concept by allowing the free rotation of the stator, the diesel generator set (DGS) can be operated at variable speed. The synchronous speed of the alternator can remain constant through three different methods of speed control :

- Rotor speed only;
- Stator speed only;
- Both speeds simultaneously.

A number of sources reported that variable speed diesel generator is more efficient than constant speed diesel generator. The minimum recommended continuous load for a constant speed diesel engine is about 40%, this value is approximately 23% for a variable speed diesel engine [15]. The main advantage of the operation of engines at variable speed is the ability to reduce fuel consumption and to generate more power from the diesel engine without exceeding its rated torque. The best fuel consumption by considering the restriction such as rated torque and engine speed can be achieved when the DG set operates at or near to its rated torque. In order to reduce the fuel consumption, the diesel engine has to be operated based on its fuel efficiency map. It can be provided by experimental analysis and extracting the fuel efficiency map for a 500KW variable speed DGS used in this study by controlling the stator speed only as presented in figure 6.

4 Test bench

Figure 7 shows the bench test studied. It consists of a diesel engine (DE) as a prime mover coupled to an synchronous alternator (SA). The model tested is the genset 3412C 500KW manufactured by Caterpillar.

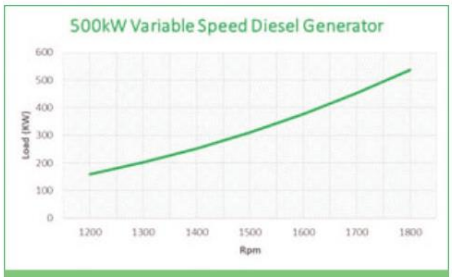

Figure 6 Optimal rotational speed versus load curve

The DE was instrumented by a torque sensor and speed sensor. This allowed us to measure the mechanical power supplied to the SA. Also, the output of the SA was instrumented with the global output. We were able to measure the current and voltage of each line with the power factor (PF) and the total harmonic distortion (THD) of the current and voltage. Tests were performed with a mechanical power between 134KW and 537KW at 600V and a speed ranging from 1200rpm to 1800rpm. To finish, we integrated the industrial combustion analyzer TESTO 300 to analyze the greenhouse gas (GHG) emissions emitted by the engine. Figure 8 shows the schematic of the bench test studied.

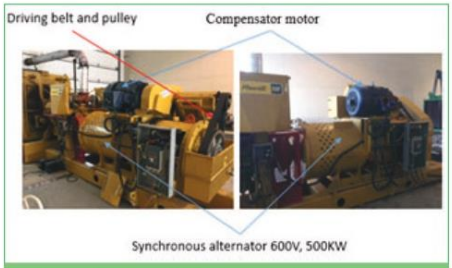

Figure 7 Genset 3412C adapted to Eo-Synchro concept

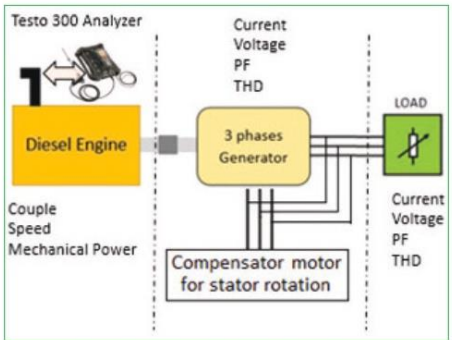

Figure 8 Schematic of the bench test

4.1 Results obtained concerning the fuel consumption

In order to evaluate the fuel consumption of the 3412C genset at different loads, we used a fuel tank load cell and we made the first test without introducing the compensator motor. Table 1 shows the fuel consumed when the stator is fixed.

Blocked stator without Eo-Synchro intervention

Load (%)	Load (KW)	Engine speed (rpm)	BSFC g/kW-hr	Fuel rate (L/hr)
25	134,2	1200	234.4	39
40	214,8	1323	231.7	60
50	268,5	1424	228.2	74
60	322,2	1518	224.0	87
70	375,9	1600	219.9	98
80	429,6	1680	220.0	113
90	483.0	1725	221.2	128
95	510,5	1755	222.2	135
100	537.0	1800	223.1	142

Table 1 Evaluation of fuel consumption with a blocked stator (conventional mode)

Subsequently, we performed the same tests mentioned above but with the application of Eo-Synchro technology. Tests were performed by applying a fixed speed stator rotating at 200rpm. Table 2 illustrates the fuel consumption results when stator rotation is applied.

With Eo-Synchro (stator runs at 200 rpm)

Load (%)	Load (KW)	Engine speed (rpm)	BSFC g/kW-hr	Fuel rate (L/hr)
25	134,2	1200	205.1	33
40	214,8	1250	208.0	54
50	268,5	1350	215.6	70
60	322,2	1470	220.0	85
70	375,9	1550	219.1	96.9
80	429,6	1605	209.0	107
90	483.0	1700	212.3	123
95	510,5	1725	215.7	131

Table 2 Evaluation of fuel consumption with Eo-Synchro concept (with rotating stator)

As we can see, the load tests can not exceed 95%. This can be explained by the fact that the compensator motor is powered by the main generator and absorbs a power equivalent to 27KW. Table 3, shows the fuel consumption difference between the conventional DG and when Eo-Synchro technology is applied.

Blocked Stator Vs Eo-Synchro

Load (%)	Load (KW)	Difference (%)
25	134,2	+15.4
40	214,8	+10
50	268,5	+5.4
60	322,2	+2.29
70	375,9	+1.12
80	429,6	+5.30
90	483	+3.90
95	510,5	+2.96

Table 3 Fuel Consumption Variation

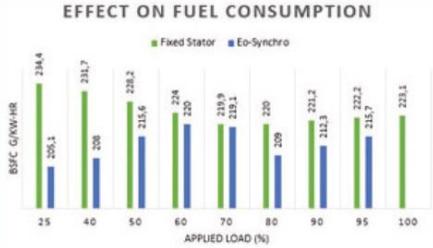

Figure 9 Effect of the Eo-Synchro on fuel consumption applied to the 3412C, 537KW, 600V, 60Hz

Figure 9 further illustrates the effect of the Eo-Synchro technology can have on improving DE fuel consumption for different loads.

According to the table 3 we can consider that the Eo-Synchro technology has a positive impact on fuel consumption on the 3412C DG. An average saving of 5.8% was found for the different loads while the highest fuel consumption improvement was registered at 25% of applied load and the lowest at 70%. This can be explained that most of the DG are designed and optimized to run between 70 and 80 percent of total load rating.

4.2 Results obtained concerning the GHG emissions

In order to evaluate the GHG emissions emitted by the DE, we used the industrial combustion analyzer "TESTO 300". We recorded the data collected for carbon dioxide (CO_2), sulfur oxide (SOx), nitrogen oxide (NOx) and particulate matter (PM). Tests were performed for conventional operation (Fixed stator) and with the Eo-Synchro concept for different loads at 25°C and number 2 diesel fuel with 35° API (American Petroleum Institute gravity) and LHV (Lower Heating Value) of 18 390btu/lb. Table 4 shows the results for conventional operation while table 5 shows the results with the Eo-Synchro concept.

In order to make a comparison on the value of the carbon dioxide emissions, we created table 6 to compare the emission results and calculate the rate of change by percent. We

GHG emissions with conventional mode

Load (%)	CO_2 (Kg)	SOx (Kg)	NOx (Kg)	PM (Kg)
25	106.860	0.1660	0.0858	0.0039
40	164.400	0.25548	0.1320	0.0060
50	202.760	0.3150	0.1628	0.0074
60	238.380	0.3704	0.1914	0.0087
70	268.520	0.4172	0.2156	0.0098
80	309.620	0.4811	0.2486	0.0113
90	350.720	0.5450	0.2816	0.0128
95	369.900	0.5748	0.2970	0.0135
100	389.080	0.6046	0.3124	0.0142

Table 4 GHG emissions for 3412C DG

GHG emissions with rotational stator

Load (%)	CO_2 (Kg)	SOx (Kg)	NOx (Kg)	PM (Kg)
25	90.420	0.1405	0.0726	0.0033
40	147.960	0.2299	0.1188	0.0054
50	191.800	0.2980	0.1540	0.0070
60	232.900	0.3619	0.1870	0.0085
70	265.506	0.4126	0.2131	0.0096
80	293.180	0.4556	0.2354	0.0107
90	337.020	0.5237	0.2706	0.0123
95	358.940	0.5577	0.2882	0.0131

Table 5 GHG emissions for 3412C DG with Eo-Synchro intervention

Blocked Stator Vs Eo-Synchro

Load (%)	Load (KW)	Difference (%)
25	134,2	-15.48
40	214,8	-10.00
50	268,5	-5.400
60	322,2	-2.29
70	375,9	-1.12
80	429,6	-5.30
90	483	-3.90
95	510,5	-2.96
Average of :		-5.8096

Table 6 Improved of CO2 emissions at different load

performed in the same way the emissions for sulfur oxide (table 7 and figure 11), nitrogen oxide (table 8 and figure 12) and for particulate matter (table 9 and figure 13).

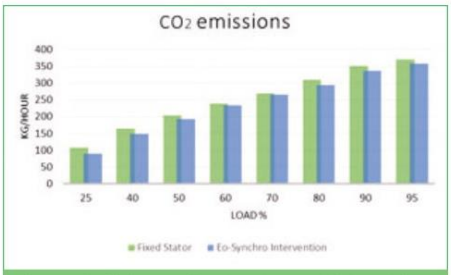

Figure 10 Efficiency of Eo-Synchro on CO2 emissions

Blocked Stator Vs Eo-Synchro

Load (%)	Load (KW)	Difference (%)
25	134,2	-15.36
40	214,8	-10.01
50	268,5	-5.39
60	322,2	-2.29
70	375,9	-1.10
80	429,6	-5.30
90	483	-3.90
95	510,5	-2.97
Average of :		-5.79

Table 7 Improved of SOx emissions at different load Blocked Stator Vs Eo-Synchro

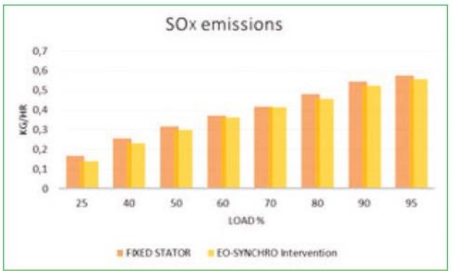

Figure 11 Efficiency of Eo-Synchro on SOx emissions

According to the tables 6, 7, 8 and 9, the Eo-Synchro technology has a positive impact on GHG emissions. We could see a 5.8% decrease compared to the conventional operation and this can be explained by the fact that we have a reduction in fuel consumption. Table 6 shows the difference between value and overall average for all loads.

4.3 Results obtained concerning the total harmonic distorsion (THD)

Analyzing the compilation presented in table 10 and figures 14 and 15, it can be observed that the voltage harmonics

and current harmonics have nearly constant values between conventional operation (fixed stator) and the Eo-Synchro technology. This confirms that the generator meets specified requirements in the standard PN-EN 61000-3 regarding harmonic distortion even with the modifications to allow rotation of the stator.

Blocked Stator Vs Eo-Synchro

Load (%)	Load (KW)	Difference (%)
25	134,2	-15.38
40	214,8	-10.00
50	268,5	-5.40
60	322,2	-2.29
70	375,9	-1.15
80	429,6	-5.30
90	483	-3.90
95	510,5	-2.96
Average of :		-5.79

Table 8: Improved of NOx emissions at different load

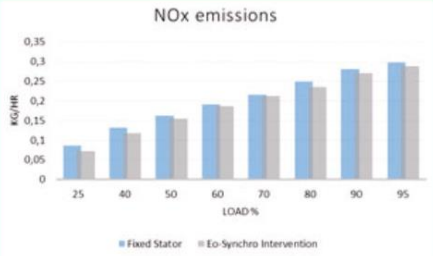

Figure 12 Efficiency of Eo-Synchro on NOx emissions

Blocked Stator Vs Eo-Synchro

Load (%)	Load (KW)	Difference (%)
25	134,2	-15.38
40	214,8	-10.00
50	268,5	-5.40
60	322,2	-2.29
70	375,9	-2.04
80	429,6	-5.30
90	483	-3.90
95	510,5	-2.96
Average of :		-5.90

Table 9 Improved of PM emissions at different load

Voltage and current harmonics comparison

	Fixed Stator		*Eo-Synchro Tech*	
Load (%)	Current (%)	Voltage (%)	Current (%)	Voltage (%)
25	1,45	4,5	1,7	4,9
40	1,50	8,5	1,4	8,7
50	1,44	9,3	1,42	9,4
60	1,42	9,8	1,4	10,3
70	1,47	11,5	1,5	11,6
80	1,8	13,6	1,5	13,1
90	1,8	14	1,5	13,9
95	1,8	14,3	1,5	14,3

Table 10 Voltage and current THD comparison between all loads

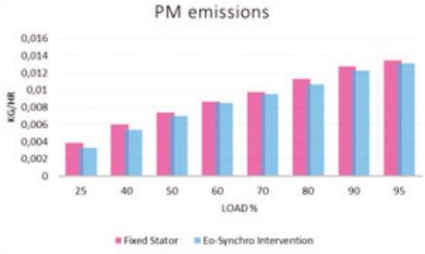

Figure 13 Efficiency of Eo-Synchro on PM emissions

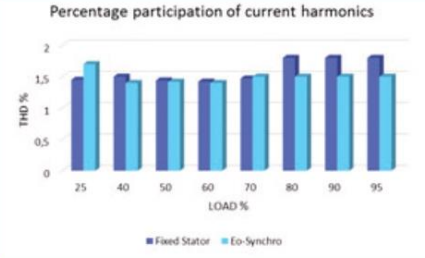

Figure 14 Current harmonics comparison

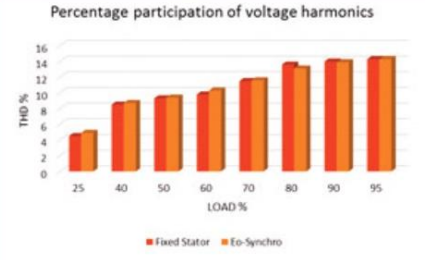

Figure 15 Voltage harmonics comparison

5 Mine Site

In this paper, to evaluate the performance of the proposed technology, a nickel mine in the Canadian North is utilised as case study.

5.1 Configuration

Figure 16 Raglan Mine site location, from Glencore

The Raglan remote nickel mine site located in the Canadian North (figure 16/Northern part of the province of Quebec) is fully dependant on diesel fuel for power generation. The electric grid includes 6 base-load 3,6 MW diesel generator sets of and one 4,4MW genset as well as 5 peak-load 1,8MW gensets [16], as well as various additional gensets of smaller capacities. The electric load is relatively constant through the year with a small reduction during the summer months. Electric load variation for one week is presented in figure 17 while the monthly maximum, average and lows are presented in figure 18.

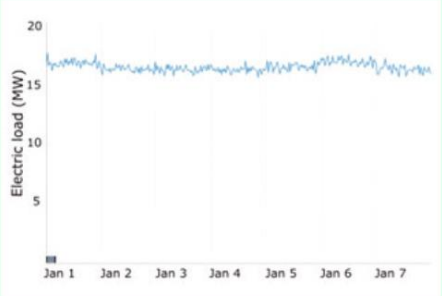

Figure 17 Electric load variation for one week [16]

5.2 Annual diesel fuel consumption and GHG emissions

According to the figures 17 and 18, we fixed the maximum demand in power per day at 17MW for a duration of 10 months per year and 14MW per day for July and August.. The baseload DG units consist of 6 x 3,6MW and 1 x 4,4MW units for a total of 22,4MW of capacity. The peak power DG units consist of 5 x 1,8MW units for a total of 9MW and also include additional smaller DGs. The base load units are operated continuously as the main based load power source where 4 x 3,6MW units and the 4.4MW regularly operate, and 2 x 3,6MW units are available as spare

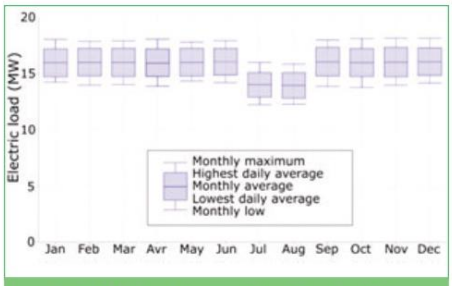

Figure 18 Yearly electric load variation [16]

capacity, one in hot standby, and one typically offline for maintenance. The second group of 5x1.8 MW units and additional smaller units are operated intermittently during peak load periods, and during maintenance works on the 4.4 MW unit. Also, the mine has a 3MW wind turbine generator which operates when sufficient wind conditions are present..

Table 11 illustrates the annual fuel consumption and GHG emissions for both of groups for a nominal load of 85-90%. Fuel cost was established at 1,20$CAD/L and each liter of diesel results in 2,64kg of CO_2 emissions. According to **tables 11 and 12,** the total value of fuel consumption per year is estimated to be approximately at 30 million liters at a cost of 35 million $CAD while the estimated emissions of CO_2 for electricity generation

Group 1: without Eo-Synchro intervention

Genset number	Fuel consumption (L/year)	CO_2 emissions (Tons/Year)	Fuel cost/year (CAD$)
1 X 3,6MW	4,800M	12,672K	5,760M
1 X 3,6MW	4,800M	12,672K	5,760M
1 X 3,6MW	4,800M	12,672K	5,760M
1 X 3,6MW	4,800M	12,672K	5,760M
1 X 3,6MW	0,874M	2,307K	1,048M
1 X 3,6MW	0,874M	2,307K	1,048M
1 X 4,4MW	2,371M	6,259K	2,845M
TOTAL	23,319M	61,561K	27,981M

Group 2: without Eo-Synchro intervention

Genset number	Fuel consumption (L/year)	CO_2 emissions (Tons/Year)	Fuel cost/year (CAD$)
1 X 1,8MW	0,538M	1,420K	0,645M
1 X 1,8MW	0,538M	1,420K	0,645M
1 X 1,8MW	0,538M	1,420K	0,645M
1 X 1,8MW	0,538M	1,420K	0,645M
1 X 1,8MW	0,538M	1,420K	0,645M
TOTAL	2,690M	7,10K	3,225M

Table 11 Economic parameters for the Base Load DGs and the Peak Load DGs

amount to 77 kilotons per year. As the current price for one ton metric of CO_2 is established at 14,35$CAD for the year 2018 [17] , the Raglan mine will be forced to buy 746,000 $CAD in credits based on regulations and the carbon market which target companies in the industrial sectors that emit 25,000 metric tons of CO_2 equivalent or more per year [18].

5.3 Economic performance

According to the demonstrated performance of the Eo-Synchro technology, the project's economic performance for the Raglan remote Nickel mine site is calculated to provide fuel cost savings of 4% based on the fuel savings at 85% load observed during the 500KW unit test work. An economic sensitivity analysis was carried out on the two main economic parameters of the project: fuel cost and carbon credits. Results of the sensitivity analysis are found in figures 19 and 20 while the economic parameters are shows in tables 13 and 14.

Figure 19 further illustrates the effect of the Eo-Synchro technology can have on improving DE fuel consumption while figure 20 illustrates the impact on CO_2 emissions. Based on our results, the fuel savings are projected to be 1,120 000 liters per year which represent 1,300,000 $CAD.

Group 1: with Eo-Synchro intervention

Genset number	Fuel consumption (L/year)	CO_2 emissions (Tons/Year)	Fuel cost/year (CAD$)
1 X 3,6MW	4,608M	12,165K	5,530M
1 X 3,6MW	4,608M	12,165K	5,530M
1 X 3,6MW	4,608M	12,165K	5,530M
1 X 3,6MW	4,608M	12,165K	5,530M
1 X 3,6MW	0,839M	2,214K	1,006M
1 X 3,6MW	0,839M	2,214K	1,006M
1 X 4,4MW	2,280M	6,019K	2,736M
TOTAL	22,390M	59,107K	26,868M

Group 2: with Eo-Synchro intervention

Genset number	Fuel consumption (L/year)	CO_2 emissions (Tons/Year)	Fuel cost/year (CAD$)
1 X 1,8MW	0,516M	1,362K	0,619M
1 X 1,8MW	0,516M	1,362K	0,619M
1 X 1,8MW	0,516M	1,362K	0,619M
1 X 1,8MW	0,516M	1,362K	0,619M
1 X 1,8MW	0,516M	1,362K	0,619M
TOTAL	2,580M	6,810K	3,095M

Table 13 Economic parameters with Eo-Synchro intervention

	Fuel consumption (L/year)	CO_2 emissions (Tons/Year)	Fuel cost/year (CAD$)
Without Eo-Synchro			
Group 1 & 2	26,09M	68,661K	31,206M
With Eo-Synchro			
Group 1 & 2	24,97M	65,917K	29,963M
Difference			
Group 1 & 2	1,120M	2,744K	1,243M

Table 14 Economic parameters comparison

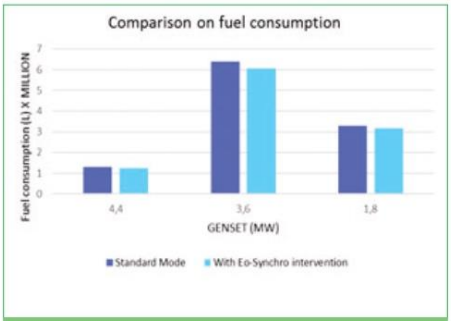

Figure 19 Effect of the Eo-Synchro on fuel consumption applied to the different group of Genset used in Raglan mine

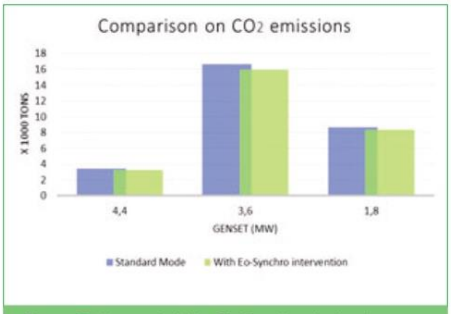

Figure 20 Impact of the Eo-Synchro technology on CO2 emissions

This saving also reduces CO_2 emissions by 4% which allows the mine to save 59,000 $CAD in purchases of carbon credits.

6 Conclusion

This article presented a new technology based on the Eo-Synchro concept improving the performance of a 500KW diesel generator and aims to minimize the cost of electricity production. The experimental results show that significant fuel savings of 15% can be obtained at low power loads which can be considered very attractive for remote areas were DGs frequently run at lower loads (<50%). On the other hand, a significant fuel savings was observed of 5% for high

power loads (80-85%). This allows the Eo-Synchro concept to cover a wide range of industrial applications and to compete with other conventional techniques such as the use of high power electronic variable speed drives. These fuel savings give positive economic returns on investment for different applications as well as CO_2 emissions. At the Raglan mine site, this study concludes that the Eo-Synchro concept can offer reduced fuel consumption. The concept has been demonstrated as a reliable technology for electricity generation at remote mine sites which offers fuel consumption and carbon emissions savings. Lessons learned at the Raglan Mine site are useful for other similar remote grids operating in Northern Canada and other sites. These sites include remote communities and industrial sites where all electricity needs are provided by diesel generators. In our future work, we will evaluate the Eo-Synchro concept on a 1MW DG and present a mathematical model to characterize the generated power and the results on fuel economy savings obtained and CO_2 emissions for a cargo ship vessel powered by 4 DGs. ■

Nomenclature

DE	Diesel Engine
DG	Diesel Generator
GHG	Greenhouse Gas
THD	Total Harmonic Distorsion
PF	Power Factor
MW	MegaWatt
KW	KiloWatt
CAD	Canadian Dollar
O&M	Operation and Maintenance
SFC	Specific Fuel Consumption
AVR	Automatic Voltage Regulator
SA	Synchronous Alternator
Mlpy	Million litre per year
KTpy	KiloTons per year
Mpy	Million per year
CO2	Carbon dioxyde
SOx	Nitrogen Oxyde
PM	Particule Matter
NOx	Nitrogen Oxyde

References

[1] Khvatov, O.S., Controled Generator Complexes Based on Double_Supply Machine, Nizhni Novgorod: Nizhny Novgorod State Technical Univ., 2000

[2] Hussein Ibrahim & Adrian Ilinca, Contribution of the Compressed Air Energy Storage in the Reduction of GHG – Case Study: Application on the Remote Area Power Supply System. 2012 Intech/Chapter 13.

[3] Chemmangot Nayar, High Renewable Energy Penetration – Diesel Generator Systems, - Electrical India Vol. 50, No 6, June 2010.

[4] L. Grzesiak, W. Koczara, M. da Ponte, "Power Quality of the Hygen Autonomous Load – Adaptive Adjustable Speed Generating System", Proc. of Applied Power Electronics Conf. APEC'99. Dallas, USA, March 1999, pp. 398 – 400.

[5] Maciej Kozak, New Concept Of Ship's Power Plant System With varying Rotational Speed Gensets. Maritime University of Szczein, Department of Mechanical Engineering/ 58th ICMD 2017

[6] La stratégie énergétique du Québec 2006-2015. L'énergie pour construire le Québec de demain. https://mern.gouv.qc.ca/publications/energie/strategie/strategie-energetique-2006-2015.pdf

[7] www.dieselserviceandsupply.com/Diesel_Fuel_Consumption.aspx

[8] Diesel Generators : Improving efficiency and emission performance in India. Shakti sustainable energy foundation 2017.

[9] Data derived from the product catalogues of Cummins, Caterpillar, Kirloskar, Powerica, and Ashok Leyland, available on websites. Typically, the catalogue shows information about the specific fuel consumption (SFC), i.e. litre of diesel consumed per hour if operating at 75% of the rated capacity. Using this information and assuming an alternator efficiency of 90%, design value of diesel engine efficiency was estimated.

[10] Zhenying Wu – MSc Thesis : Comparison of Fuel Consumption on A Hybrid Marine Power Plant with Low-Power versus High-Power Engines. NTNU – Norwegian University of Science and Technology – June 2017

[11] Mohamad Issa, Éric Dubé, Jean Fiset, MohammadJavad Mobarra & Adrian Ilinca : Modeling and Optimization of the Energy production Based on Eo-Synchro Concept – IDGTE journal – December 2017, Volume 21 issue 4

[12] L.L.J. Mahon : Diesel Generator Handbook; Chapter 3:AC generators- general; 1st edition (October 1992).

[13] Wood, A. J., & Wollenberg, B. F. (2012). Power generation, operation, and control. John Wiley & Sons.

[14] WILDI, T. SYBILLE, G., Électrotechnique, 4e édition, PUL 2005.

[15] Tajuddin Waris, C.V. Nayar ; Variable Speed Constant Frequency Diesel Power Conversion System using Doubly Fed Induction Generator (DFIG) – Source: IEEE ; Conference: Power Electronics Specialists, 2008. PESC 2008.

[16] S. Simard, K. Fytas, J. Paraszcak, M. Laflame and K. Agbossou ; Wind power opportunities for remote mine sites in the Canadian North. International conference on Renewable Energies and Power Quality (ICREPQ 17) Malaga, Spain, Avril 2017. ISSN 2172-038

[17] http://www.mddelcc.gouv.qc.ca

[18] http://www.mddelcc.gouv.qc.ca/changementsclimatiques/marche-carbone.asp

CHAPITRE VIII

ARTICLE 6

Eco-Friendly Selection of Diesel Generator Based on Genset-Synchro Technology for Off-Grid Remote Area Application in the North of Quebec

Publié dans Journal of Energy and Power Engineering , 2019

Volume 11:232-247 / ISSN : 624- 1947-3818

Résumé

Cet article est une continuité de l'article précédent intitulé «*Optimizing the Performance of a 500kW Diesel Generator : Impact of the Eo-Synchro Concept on Fuel Consumption and Greenhouse Gases*». Il présente les résultats enregistrés pour une génératrice diesel de 600 kW (C-18, Tier III de Caterpillar) testée durant 3000 heures dans un site isolé dans le nord du Québec (Automne 2018 et hiver 2019).

Les résultats ont révélé une baisse dans l'économie du carburant due à la chute de la température ambiante (-15ºC à -30ºC) pour atteindre une économie moyenne de 4,9% pour les faibles charges et moyennes charges au lieu de 8,2%, soit une baisse de 40% approximativement.

Il n'était pas possible de connaitre le taux de la consommation sous une grande charge car la génératrice est surdimensionnée pour le site. D'autre part, la réduction moyenne des

GES enregistrée est évaluée à 4,5% tandis que le taux de distorsion d'harmoniques en tension et en courant restent inchangés.

Le site a réussi quand même à atteindre des économies en carburant d'ordre de 12500 litres durant les 3000 heures enregistrées, équivaut à 18000$CA approximativement par rapport à la même période de l'année 2017-2018.

Energy and Power Engineering, 2019, 11, 232-247
http://www.scirp.org/journal/epe
ISSN Online: 1947-3818
ISSN Print: 1949-243X

Eco-Friendly Selection of Diesel Generator Based on Genset-Synchro Technology for Off-Grid Remote Area Application in the North of Quebec

Mohamad Issa*, Jean Fiset, Hussein Ibrahim, Adrian Ilinca

Department of Mathematics, Informatics and Engineering, Université du Québec à Rimouski, Rimouski, Canada
Email: *missa@imq.qc.ca

How to cite this paper: Issa, M., Fiset, J., Ibrahim, H. and Ilinca, A. (2019) Eco-Friendly Selection of Diesel Generator Based on Genset-Synchro Technology for Off-Grid Remote Area Application in the North of Quebec. *Energy and Power Engineering*, **11**, 232-247.
https://doi.org/10.4236/epe.2019.115015

Received: May 5, 2019
Accepted: May 28, 2019
Published: May 31, 2019

Abstract

For most of their energy requirements, greater part of remote communities and small islands around the world rely on imported fossil fuels. The economical cost of energy is therefore very high not only due to inherent cost of fuel, but also due to transportation and due to maintenance costs. One solution for saving fuel in a diesel generator is to allow the engine to operate directly in relation to the request for electrical load at variable speeds. Genset-Synchro Technology has developed an innovative variable speed generator technology (patent pending) that allows applications where power demand varies widely to benefit from the new technology that maintains constant voltage and frequency while adjusting the generator stator speed to power demand. This paper will present an innovative approach for optimizing the energy production based from the fact that the structure that contains the stator windings of the generator is mounted on roller bearings, which allows its free rotation around the axis of the rotor, consequently stopping the stator structure from being static and aims to minimize the unit cost of electricity. Case study on application in remote area in the north of Quebec is described. A saving of 7% - 9% on fuel consumption and greenhouse gas (GHG) under low winter ambient temperatures has been registered.

Keywords

Diesel Generator, Remote Areas, Fuel Saving, Greenhouse Gas, Electrical Machines, Control of Rotor Speed, Variable Diesel Speed Generator, Total Distortion Harmonics

1. Introduction

Most remote and isolated communities or technical facilities (communication relays, meteorological systems, tourist facilities, farms, etc.) not connected to national electrical grids rely on diesel generators to generate electricity [1]. About 200,000 people in Canada live in more than 300 remote communities (Yukon, Northwest Territories, Nunavut, etc.) that use diesel—generated electricity, which is responsible for the annual emission of 1.2 million tons of greenhouse gases (GHGs) [2]. There are more than 14,000 subscribers scattered in about 40 communities in Quebec that are not connected to the main electrical grid. Each community is an autonomous network using diesel generators to generate electricity [3]. The diesel generating units, while requiring relatively little investment, are generally expensive to operate and maintain, especially when operating at partial load on a regular basis [4]. Under weak operating factors, the use of diesel power generators accelerates wear and increases fuel consumption [5].

Over the past few years, oil prices have reached historic highs, peaking at $ 147/barrel in July 2008, averaging over $ 100/barrel in 2011, averaging over $ 110/barrel by October 2014, then falling to $ 80/barrel. Recently, the oil price is around 69$/barrel. Despite this significant drop, diesel fuel prices in some provinces in Canada are losing just a few cents. According to statistic Canada, in St. John's Newfoundland, the diesel fuel lost only 5.7 ¢/L, and in Whitehorse in Yukon is increased by 3.5 ¢/L and in Yellowknife in Northwest Territories is set to rise up to 9.3 ¢/L in October 2014 compared to 2013. According to Statistics Canada (http://www5.statcan.gc.ca), the decline in crude oil prices is not felt at the pump in this region. However, the pump price gasoline only decreased by 11.8 C/L from a high of $112 per barrel to a low of $35 per barrel in December 2015. Therefore, the decrease in oil prices has not greatly affected the price of diesel fuel, which implies that the electrical energy produced using only oil as energy source will always remain expensive, at any cost of barrel [6]. According to Hydro Quebec, extending the main grid to these isolated areas will cost around (1 M $/ km), which is impossible to do with the actual economic instability. Classic diesel generators are equipped with synchronous generators based on internal combustion engines; therefore, fixed speed operation is necessary. During low load operations, they operate inefficiently, **Figure 1** [7].

In emergency power applications, it is not critical, but very important in continuously operated systems, where fuel consumption is an important economic and logistical aspect. Indeed, remote areas with relatively small communities generally show considerable variation between peak load time and minimum load time [8]. A typical example of a remote community's load profile in northern Quebec is shown in **Figure 2**.

In our project, we investigate another possibility that, when coupled to a DG operating in power unit, **Figure 3**, the Genset-Synchro alternator can operate at variable speeds without the need for costly power electronics components to generate a constant frequency on the terminals of the generator. The system can

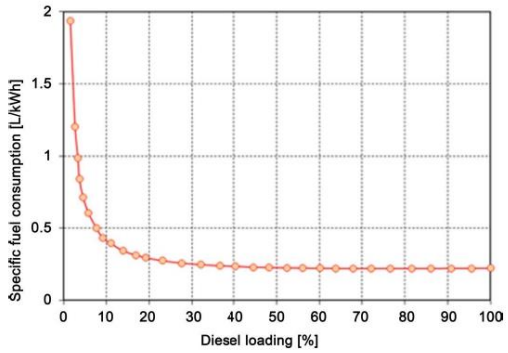

Figure 1. Example of diesel fuel consumption variation Vs loading [7].

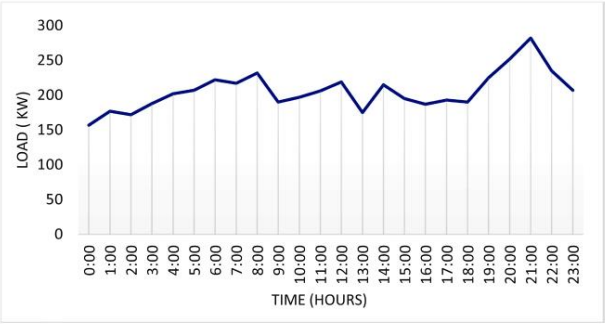

Figure 2. Example of a remote community's load profile at James Bay in the northwestern Quebec.

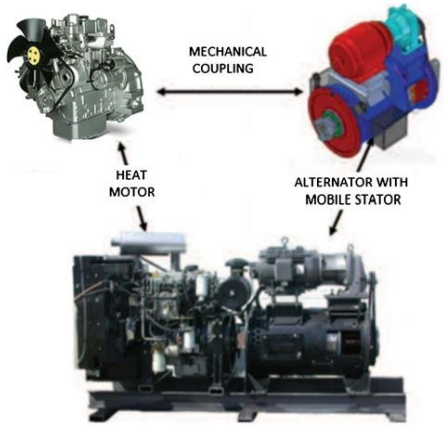

Figure 3. Illustration of the Genset-Synchro concept coupled to the diesel engine (DE).

compensate for a lower or higher heat motor speed without disturbing the wave quality of the generated electricity. The project was developed by Concept Fiset Inc. and was performed by Rimouski University of Quebec's project partners. The Genset-Synchro concept has two international patents, including Canada the US [9] [10].

The objective of this study is to demonstrate that the Genset-Synchro concept can reduce the fuel consumption and the GHGs when applied to a diesel generator (DG). The structure of the present article is as follows. Section 2 presents the design approach of the Genset Synchro and its principal control. In Section 3 we present the bench test and the profile of the remote area in the northwestern Quebec. Section 4 presents the case study and we discuss the results obtained in order to demonstrate the efficiency of the Genset-Synchro technology for DG applications. Finally, in Section 5, we provide a preliminary conclusion and a perspective for the future work.

2. The Design Approach of the Genset-Synchro Alternator

The Genset-Synchro approach is a power unit control system based on new alternator design with a highly original concept to power generation. Changes to the structure holding the stator windings are the guiding principle behind the Genset-Synchro application where this structure now rotates freely in relation to the rotor and frame. An additional motor driven by a dedicated automatic controller assign the speed, desired position or acceleration of the stator structure. The concept ensures regular wave quality irrespective of rotor speed variations. As in conventional technologies, no energy passes through electronic equipment.

A synchronous alternator transforms the mechanical energy from a diesel engine into electrical energy to generate electricity in a power unit [11]. When this alternator integrates the concept of Genset-Synchro, the synchronous speed can remain constant by:

- Control of rotor speed only (existing design).
- Control of stator speed only (new design) [9] [10] [11].
- Control of both speeds simultaneously (new design) [9] [10] [11].

With the Genset-Synchro concept, the synchronous speed of a three-phase alternator can be controlled by controlling the stator's mechanical speed. Furthermore, since the Genset-Synchro is completely independent of the drive mechanism, it can be adapted to any type of rotor speed control and integrated into any type of power generation unit such as wind turbine, hydraulic turbine and gas turbine, etc. **Figure 4** shows a prototype of the Genset-Synchro alternator with the main system components.

The electrical machine (compensating motor) is firmly fixed in an enclosure attached to the top of the synchronous motor enclosure using assembly means consisting of brackets and bolts such that the electrical machine's output shaft is aligned in parallel with the stator shaft. The electrical machine's output shaft and the stator shaft are connected by means of a timing belt and pulleys. The pri-

mary pulley is fitted to the distal end of the stator shaft reaching outside the synchronous alternator enclosure and the top pulley is adapted to the electrical machine's output shaft so that both pulleys are aligned vertically. The timing belt links the two pulleys for one to drive the other. In Figure 5, the controlling unit receives an encoder feedback signal that senses the stator's position or velocity. In this case, the encoder is placed on the rotor to detect the rotor's position, and thus the speed. Additionally, the controlling unit refers to the produced alternating current as a feedback. According to the feedback signal, the controlling unit creates a control signal which is inputted to a variable speed drive in order to control the speed rotation of the electric machine and thereby the speed of the stator.

For example, the controller can be supplied as a programmable logic controller, a computer or any other processing unit. Typically, the variable speed drive is powered by the alternator's electrical current and the frequency regulation consumes part of the power produced. By controlling the rotation of the stator

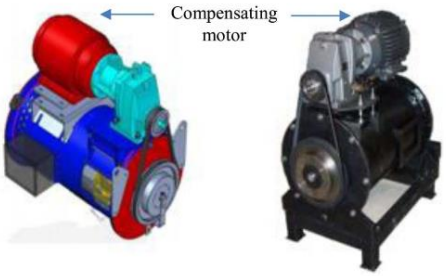

Figure 4. A perspective view of the Genset-Synchro alternator rated at 80 Kw.

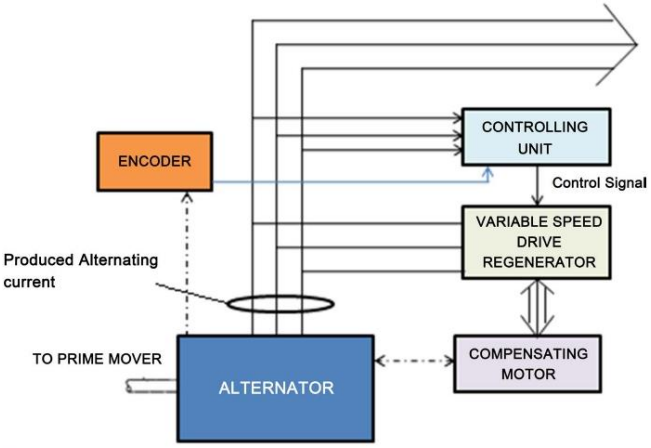

Figure 5. A system for electrical generation with a regulated frequency.

about the rotor, the relative speed, and thereby the frequency of the generated electric current, can be regulated. For instance, a 60 Hz alternating current is generated in a typical wind turbine generator in a four-pole three-phase alternator rotating at 1800 RPM. The speed of the prime mover, *i.e.* the wind turbine, can rotate faster when the wind is strong, for instance at 2000 RPM. Then, the stator is rotated at 200 RPM in the direction of rotation of the rotor to compensate for such a higher rotation speed of the rotor. The relative speed between the rotor and the stator is thus 1800 RPM (2000 RPM - 200 RPM: 1800 RPM). If, for example, the velocity of the rotor decreases due to weak winds, e.g. at 1500 RPM, the stator rotates in the opposite direction to the rotor at 300 RPM.

3. Genset-Synchro Application for Power Units: Description of the Test Bench

Figure 6 shows the schematic of the test bench, while Figure 7 shows the unit employed in the remote communities at James Bay in the northwestern Quebec.

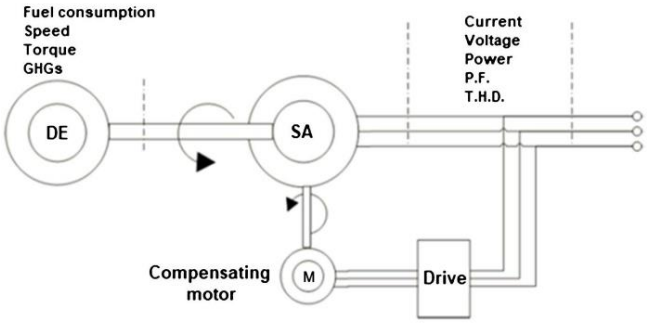

Figure 6. Schematic of the bench test.

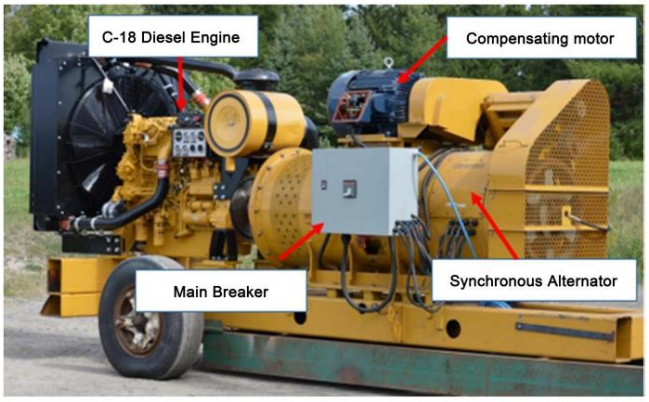

Figure 7. Illustration of the Genset-Synchro GS500X unit with the main components.

It consists of an 800 hp diesel engine (C-18 model Tier III from Caterpillar) as a prime mover coupled to a synchronous alternator of 575 kW (made by the French company Le Roy Somer). A compensating motor (100 hp) provides the necessary rotation speed of the synchronous alternator stator fixed on the top of the alternator and coupled to a three-phase drive. The diesel engine was instrumented by a differential flowmeter with a torque sensor and speed sensor, while the output of the synchronous alternator was instrumented with a power analyzer, Figure 8. Moreover, a combustion flue gas analyzer (Testo 350) was used to evaluate the impact of the Genset-Synchro technology in GHGs emissions.

Description of the Remote Communities

Highway 381 is a rest stop on the James Bay Highway in northwestern Quebec, Figure 9. It includes buildings including a hotel, a cafeteria, garages, a service

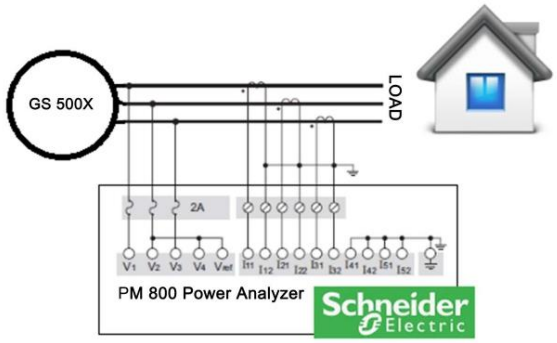

Figure 8. Connection of the power analyzer to the GS-500X output.

Figure 9. (a) Site location for the roadstop km 381; (b) The hotel; (c) Garages and Service Station; (d) The Cafeteria (Source: google map).

station, houses for Hydro-Québec and a visitor's pavilion. The relay is an Off-grid site. Its power comes from diesel generators only.

According to the technical report issued by the Ministry of Energy and Natural Resources in 2015 [12] regarding the roadstop km 381, the diesel fuel consumption for the year 2015 is 362,275 L representing the equivalent of 1011 tonnes of CO_2 emissions.

In order to minimize fuel consumption, GHG emissions and reduce the environmental impact of emissions, it has been proposed to replace diesel generators with electrical equipment (extension of the electricity network). While waiting for the project to be adopted and financed, it has been proposed to ensure the electrification of the site by the GS500X unit from Genset-Synchro Technology which, has demonstrated on a prototype of 500 kW fuel savings by mean of 12% [13].

4. Discussion

Roadstop's km 381 location is characterized by extremely cold winter temperatures that reach −30˚C during the months of January and February. In this section, recorded data are intended to evaluate the performance of the GS500X unit under low registered temperatures with three different stator speed. Attention is given to fuel consumption, GHGs emission and for the total harmonic distortion (THD) at the output of the generator. To do, the standard IEEE-519-2014 is considered as reference [14].

4.1. Fuel Consumption Analysis

Since the Caterpillar C-18 Tier III diesel consumption curve was determined with an ambient temperature of 16˚C (according to the manufacturer manual), it was necessary to redefine this consumption curve in a cold climate to better identify the impact of Genset-synchro technology compared to the standard Genset mode under the same weather conditions. To do this, the generator was employed in standard mode (fixed stator) during the day of February 2019 for 24 hours without interruptions. The recorded data (the longest in terms of operation) are shown in Table 1 including the minimum and maximum recorded ambient temperatures.

According to Table 1, the fuel consumption is higher than that defined by the manufacturer by 9.5%, (according to the manual owner). This can be explained by the fact that low temperatures have an impact on the density of the fuel (for

Table 1. Data recorded for the day of February 1, 2019. The maximum recorded ambient temperature is −18˚C and the minimum is −27.1˚C.

Duration (hr.)	Load (kW)	Load (%)	Engine Speed (RPM)	Fuel consumption (gr./kWh)
6	164	27.3	1800	267
5	189	31.5	1800	254.2
4.75	232	38.6	1800	248.8
3.25	278	46.3	1800	239.6

our tests—fuel density adjusted is 0.80729 kg/liter at 15˚C). Moreover, heat, cold oil and other fluids have a greater effect on fuel economy when the generator is used at less than optimal temperatures. Figure 10 shows a comparison of fuel consumption at +15˚C (according to the Caterpillar fuel consumption curve) and −22˚C for the same DG.

4.2. Effect of the Genset-Synchro Technology on Fuel Consumption

In this section, the results of DG fuel consumption with the mobile stator for February 10, Mars 19 and April 9 are presented. For the day of February 10, the speed of the diesel engine (DE) is set at 1520 rpm and the stator at 280 rpm, while for the day of Mars 19, the speed of the DE is set at 1460 rpm and the stator at 340 rpm and finally, for the day of April 9, the speed of the DE is set at 1385 rpm and the stator at 415 rpm. Tables 2-4 show the recorded data including the minimum and maximum registered temperatures.

In order to clearly distinguish the effect of the Genset-Synchro Technology on fuel consumption, a comparison was made considering the variation of the stator speed. Figure 11 shows the comparison of the fuel consumption for the three different speeds.

According to Figure 11, it can be seen that Genset-Synchro Technology achieve

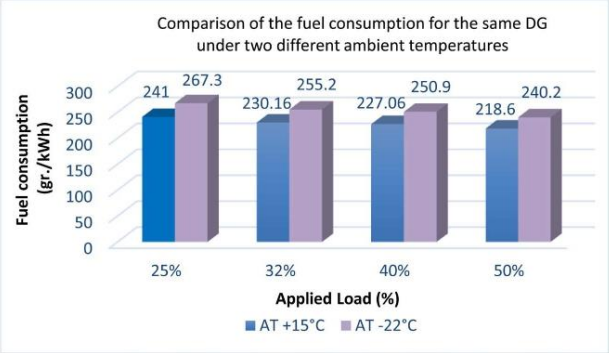

Figure 10. Evaluation and comparison of the C-18 Tier III fuel consumption at +15˚C Vs −22˚C. An increase of 9.5% was recorded.

Table 2. Data recorded for the day of February 10, 2019. The maximum recorded ambient temperature is −20˚C and the minimum is −31˚C.

Duration (hr.)	Load (kW)	Load (%)	Engine Speed (RPM)	Stator Speed (RPM)	Fuel consumption (gr./kWh)
6.5	164	27.3	1520	280	250.1
5	189	31.5	1520	280	242.1
5.5	232	38.6	1520	280	237.2
2.25	278	46.3	1520	280	226.6

Table 3. Data recorded for the day of Mars 18, 2019. The maximum recorded ambient temperature is −10˚C and the minimum is −21˚C.

Duration (hr.)	Load (kW)	Load (%)	Engine Speed (RPM)	Stator Speed (RPM)	Fuel consumption (gr./kWh)
6.3	164	27.3	1460	340	244.6
4.8	189	31.5	1460	340	240.1
4.5	232	38.6	1460	340	231.7
3.25	278	46.3	1460	340	222.4

Table 4. Data recorded for the day of April 9, 2019. The maximum recorded ambient temperature is −7˚C and the minimum is −10˚C.

Duration (hr.)	Load (kW)	Load (%)	Engine Speed (RPM)	Stator Speed (RPM)	Fuel consumption (gr./kWh)
6.3	164	27.3	1385	415	240.2
4.8	189	31.5	1385	415	237.8
4.5	232	38.6	1385	415	228.7
3.25	278	46.3	1385	415	218.1

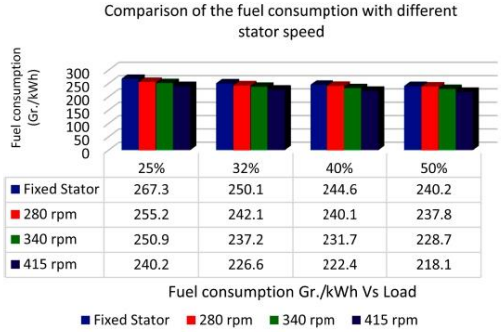

Figure 11. Comparison of the fuel consumption with different stator speed Vs fixed stator under low and medium loads.

the best economy when stator is employed at 415 rpm with an average of 22.2 grams/kWh, while this saving decreases for 18.5 grams/kWh when stator is employed at 340 rpm and to 13.3 grams/kWh when stator is employed at 280 rpm.

4.3. Effect of the Genset-Synchro Technology on Greenhouse Gases (GHGs)

Emissions from diesel engine contribute to divers cardiovascular and respiratory diseases and cancer, in addition to water and soil pollution, visibility reductions and global climates changes [15] [16] [17]. In this context, we evaluate the GHG emissions emitted by the DE with the fixed stator and with the Genset-Synchro concept. To do, combustion analyzer (Testo 350) is used to evaluate the carbon

dioxide (CO_2), sulfur oxide (SO_x), nitrogen oxide (NO_x) and particulate matter (PM). We used number 2 diesel fuel type B-ULS with maximum fuel sulfur of 15 mg/kg. Table 5 shows the emissions rate when the DG is employed in standard mode (fixed stator) while Table 6 shows the emissions rate when DG use the Genset-Synchro concept. Given that the stator speed employed at 415 rpm offers the best economy on fuel, we just take this speed into consideration for comparison purposes.

Based on the data registered on Table 5 and Table 6, it can be concluded that fuel economy achieved with the Genset-Synchro Technology has a positive impact on GHGs reduction. This impact is proportional to the amount of fuel saved. Table 7 shows the overall average of GHGs reduction when the stator is employed at 415 rpm.

4.4. Effect of the Genset-Synchro Technology on the Total Harmonic Distortion (THD)

THD is the measurement of electricity quality. Clean signal is considered good

Table 5. Data recorded concerning the GHG emissions when DG is employed with fixed stator.

Load (kW)	Engine Speed (RPM)	Fuel consumption (l/h.)	CO_2 (Kg)	SO_X (Kg)	NO_X (Kg)	PM (Kg)
164	1800	54.16	148.39	0.230	0.119	0.0054
189	1800	59.56	163.19	0.253	0.131	0.0059
232	1800	71.62	196.23	0.304	0.157	0.0071
278	1800	82.51	226.07	0.351	0.181	0.008

Table 6. Data recorded concerning the GHG emissions when DG is employed with a stator speed of 415 rpm.

Load (kW)	Engine Speed (RPM)	Fuel consumption (l/h.)	CO_2 (Kg)	SO_X (Kg)	NO_X (Kg)	PM (Kg)
164	1385	49.20	134.80	0.209	0.108	0.0049
189	1385	55.67	152.53	0.237	0.122	0.0055
232	1385	65.72	180.07	0.279	0.144	0.0065
278	1385	75.10	205.77	0.319	0.165	0.0075

Table 7. Overall average of GHG's reduction with a stator speed of 415 rpm.

Load (kW)	Difference of the reduction (%)			
	CO_2	SO_X	NO_X	PM
164	10.08%	10.04%	10.18%	10.2%
189	6.98%	6.75%	7.37%	7.27%
232	8.97%	8.96%	9.02%	9.23%
278	9.86%	10.03%	9.69%	6.66%
Average	8.97%	8.94%	9.065%	8.34%

with a THD of less than of 6% and is frequently declared or promoted at 5% or less [18]. Higher heating due to iron and copper losses at the harmonic frequencies is a major effect of harmonic voltages and currents in rotating machines (induction and synchronous). Moreover, according to [19], THD can increase by an amount of 2% due to the effect of vibration. In order to properly evaluate the effect of the Genset-Synchro concept on the signal quality at the output of the alternator, we have referred to the IEEE-519-2014 standard (Recommended practice and requirements for harmonic control in electric power systems). A power analyzer PM800 from Schneider electric is used, **Figure 8**. On the other hand, it was important to know the current and voltage distortion limits for our system. Based on IEEE-519 standard, **Table 8** and **Table 9** show the current and voltage distortion limits for systems rated 120 V through 69 kV.

In order to refer to the right limit, we referred to the manual manufacturer for a C-18 diesel generator defined by Caterpillar for 3 phases, 600 V, 575 kW. Short circuit current is limited to 300%/10sec. which represents a TDD limit of 15% and a voltage distortion limit of 8%.

In this context, we measured the THD limits in current and voltage with the conventional mode (fixed stator) for the purpose of comparing them later with the Genset-Synchro mode. **Table 10** illustrates the THD limits in current and voltage for the conventional mode, while **Table 11** illustrates the THD limits in current and voltage when the stator is employed at 415 rpm.

Based on our results, the Genset-Synchro mode shows an increase in the current and voltage harmonics level versus conventional mode. However, in order to confirms if the speed employed has an impact on the level of vibration and on the THD, we analyzed the recorded measurements when the speed of the stator

Table 8. Current distortion limits for systems rated 120 V - 69 Kv [14].

$\frac{\text{Short-circuit current}}{\text{load current}}$	Total demand distortion (TDD) limit
<20	5%
20 - 50	8%
50 - 100	12%
100 - 1000	15%
>1000	20%

Table 9. Voltage distortion limits [15] and [19].

Bus voltage at PCC*	Individual harmonic (%)	THD limit
$V \leq 1.0$ kV	5.0	8%
1 kV < $V \leq 69$ kV	3.0	5%
69 kV < $V \leq 161$ kV	1.5	2.5%
161 kV< V	1.0	1.5%

PCC: Point of Common Coupling.

used was at 280 rpm. Table 12 shows the recorded results with a stator speed of 280 rpm and a power factor of 0.98.

According to Tables 10-12, the stator speed has a negative impact on the THD level. This can be explained by the fact that as the stator speed increases, the vibration in the generator increases, affecting the THD level [20]. Figure 12

Table 10. Data recorded concerning the THD limits in current and voltage with the conventional mode (fixed stator) and a power factor of 0.98.

Load (kW)	Engine Speed (RPM)	Current THD (%)	Voltage THD (%)
164	1800	2.7	6.0
189	1800	2.5	6.9
232	1800	2.3	8.1
278	1800	2.2	9.2

Table 11. Data recorded concerning the THD limits in current and voltage with a stator speed of 415 rpm and a power factor of 0.98.

Load (kW)	Engine Speed (RPM)	Current THD (%)	Voltage THD (%)
164	1385	3.0	7.6
189	1385	2.7	8.5
232	1385	2.5	9.8
278	1385	2.3	11.4

Table 12. Data recorded concerning the THD limits in current and voltage with a stator speed of 280 rpm and a power factor of 0.98.

Load (kW)	Engine Speed (RPM)	Current THD (%)	Voltage THD (%)
164	1520	2.8	7.0
189	1520	2.7	8.0
232	1520	2.4	9.6
278	1520	2.3	10.8

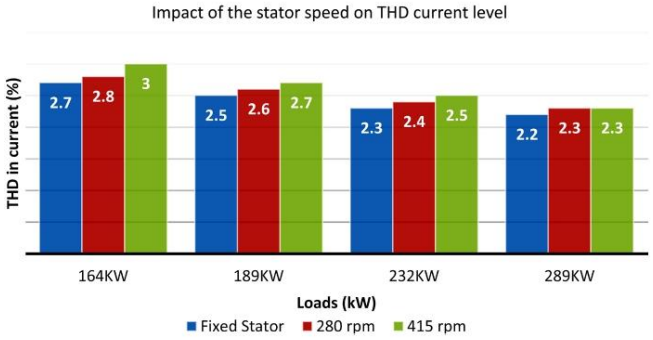

Figure 12. Comparison on the THD current level in relation to the stator speed.

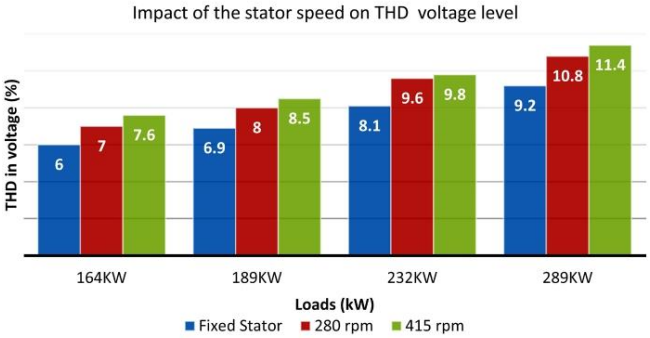

Figure 13. Comparison on the THD voltage level in relation to the stator speed.

and Figure 13 show the difference in the THD rates in relation to the stator speed.

According to the IEEE-519 standard, the Genset-Synchro GS500X respect the current distortion limits, while the voltage distortion limits is higher by 3.4% at 50% of load. However, the generator used is oversized for the site. For this reason, it was not possible to evaluate the THD levels for high applied loads (>70%).

5. Conclusions

This paper presents the innovative feature of the Genset-Synchro Technology which originate from a rotational non-fixed stator design and a fuel savings evaluation for a DG that can be achieved by controlling the rotation of the stator. The experimental results show that significant fuel savings of 7% - 9% can be obtained at low power loads ≤45% which can be very attractive for isolated communities were most of the DGs frequently run under low loads ≤40%. Furthermore, this fuel saving has reduced the level of GHGs by amount of 8% - 9%.

Despites these advantages, the voltage harmonic distortion rate proves to be higher when the Genset-Synchro mode is employed. It has also been found that as the stator speed increases the THD increases due to the vibrations. According to the IEEE-519-2014 standard, it is mandatory to install a filter at the output of the generator to ensure that the voltage distortion rate remains between 6% - 9% for all applied loads. On the other hand, the current distortion rate is lightly higher when Genset-Synchro mode is employed. However, the level remains below 4% limit required by the IEEE-519-2014 standard.

Since the generator used at James Bay is oversized for the site, it was not possible to load more than 48% and to cover all loads range under less optimal temperatures for the operation of the generator. Nonetheless, the Genset-Synchro Technology is interesting (beneficial) to use in isolated sites whose access to the power grid is not possible and where the fuel deliveries are difficult during cold seasons.

Based in our results, the fuel saving is projected to be 8% under low winter temperatures (−7˚C to −30˚C). For equivalent purposes, a 600 kW C-18 DG equipped by a Genset-Synchro alternator can achieve 6.8 l/h of fuel saving for a 50% applied load, which represents an annual fuel saving of 47,600 liters over 7000 hours of annual operation and 130,424 t CO_2.

Conflicts of Interest

The authors declare no conflicts of interest regarding the publication of this paper.

References

[1] Ibrahim, H., Younes, R., Basbous, T., Ilinca, A. and Dimitrova, M. (2011) Optimization of Diesel Engine Performances for a Hybrid Wind-Diesel System with Compressed Air Energy Storage. *Energy*, **36**, 3079-3091. https://doi.org/10.1016/j.energy.2011.02.053

[2] Li, C. and Yu, W. (2016) Techno-Economic Comparative Analysis of Off-Grid Hybrid Photovoltaic/Diesel/Battery and Photovoltaic/Battery Power Systems for a Household in Urumqi, China. *Journal of Cleaner Production*, **124**, 258-265. https://doi.org/10.1016/j.jclepro.2016.03.002

[3] Ibrahim, H., Ilinca, A., Younes, R. and Basbous, T. (2007) Study of a Hybrid Wind-Diesel System with Compressed Air Energy Storage. *Electrical Power Conference* 2007, "*Renewable and Alternative Energy Resources*", Montreal, 25-25 October 2007, 320-325. https://doi.org/10.1109/EPC.2007.4520350

[4] Hunter, R. and Elliot, G. (1994) Wind-Diesel Systems—A Guide to the Technology and Its Implementation. Cambridge University Press, Cambridge. https://doi.org/10.1017/CBO9780511574467

[5] Forcione, A. (2004) Système jumelé éolien-Diesel aux îles-de-la-Madeleine (Cap-aux Meules) Établissement de la VAN optimale. Institut de Recherche, Hydro Québec, Février.

[6] Rezkallah, M. (2016) Design and Control of Standalone and Hybrid Standalone Power Generation Systems. Diss. École de technologie supérieure.

[7] Ibrahim, H. and Ilinca, A. (2012) Contribution of the Compressed Air Energy Storage in the Reduction of GHG—Case Study: Application on the Remote Area Power Supply System. Chapter 13, Intech, London. https://doi.org/10.5772/50131

[8] Pena, R., Cárdenas, R., Proboste, J., Clare, J. and Asher, G. (2008) Wind-Diesel Generation Using Doubly Fed Induction Machines. *IEEE Transactions on Energy Conversion*, **23**, 202-214. https://doi.org/10.1109/TEC.2007.914681

[9] Jean, F. (2007) Canadian Intellectual Property Office—Patent No. 2697420: Mechanical Regulation of Electrical Frequency in an Electrical Generation System.

[10] Jean, F. and Durand, T. (2008) United States Patent & Trademark Office—Patent No. US8258641B2: Mechanical Regulation of Electrical Frequency in an Electrical Generation System.

[11] Tiberiu, T. and Cristian, R. (2010) The Numerical Modeling of Transient Regimes of Diesel Generator Sets. *Acta Polytechnica Hungarica*, **7**, 39-53.

[12] Ministère de l'énergie et des Ressources naturelles (2016) Extension de ligne pour le relais routier du km 381. Doc. No. ECO-20a-15-16-0422-0001, 2016-15-12.

[13] Mohammadjavad, M., Jean, F. and Adrian, I. (2017) Modeling and Optimization of

the Energy Production Based on Eo-Synchro Application. Power Engineer, 3.

[14] 519-2014-IEEE Recommended Practice and Requirements for Harmonic Control in Electric Power Systems. https://ieeexplore.ieee.org/document/6826459

[15] James, M., Paul, C., *et al.* (2007) Respiratory Effects of Exposure to Diesel Traffic in Persons with Asthma. *New England Journal of Medicine*, **357**, 2348-2358. https://doi.org/10.1056/NEJMoa071535

[16] Lloyd, A.C. and Cackette, T.A. (2001) Diesel Engines: Environmental Impact and Control. *Journal of the Air & Waste Management Association*, **51**, 809-847. https://doi.org/10.1080/10473289.2001.10464315

[17] Krivoshto, I.N., Richards, J.R., Albertson, T.E., *et al.* (2008) The Toxicity of Diesel Exhaust: Implications for Primary Care. *Journal of the American Board of Family Medicine*, **21**, 55-62. https://doi.org/10.3122/jabfm.2008.01.070139

[18] Kamenka, A. (2014) Six Tough Topics about Harmonic Distortion and Power Quality Indices in Electric Power Systems. The Schaffner Group, Luterbach.

[19] Fetyan, K. and El Gazzar, D. (2014) Effect of Motor Vibration Problem on the Power Quality of Water Pumping Stations. *Water Science*, **28**, 31-41. https://doi.org/10.1016/j.wsj.2014.05.001

[20] Blooming, T.M. and Carnovale, D.J. (2006) Application of IEEE Std 519-1992 Harmonic Limits. *Conference Record of 2006 Annual Pulp and Paper Industry Technical Conference*, Appleton, 18-23 June 2006, 1-9.

CHAPITRE IX

ARTICLE 7

Integrated a Variable Frequency Drive for a Diesel-Generating Set Using the Genset-Synchro Concept

Publié dans International Journal of Engineering Research & Technology , 2019

Volume 8:232-239 / ISSN : 624- 2278-0181

Résumé

L'objectif principal de l'article est de proposer un système de contrôle automatisé pour le concept Genset-Synchro lorsqu'il est intégré sur une génératrice diesel de 600 kW.

L'article examine la faisabilité de la mise en œuvre d'un variateur de fréquence basé sur un contrôle en temps réel de la vitesse statorique lorsque la charge varie.

L'algorithme du contrôle est conçu à l'aide du logiciel Code composer V8 environnement en code C avec la plateforme TMS320F28335 de Texas instruments.

Les tests pratiques et les simulations théoriques menés sur la génératrice de 600 kW ont démontrés que le concept Genset-Synchro répond aux critères de la classe de performance

de la norme ISO 8528 (partie 5 Groupe 2) concernant le temps de réponse de l'ajustement de la fréquence et de la tension à la sortie du GED.

Un circuit de contrôle a été développé au sein du laboratoire de la recherche en énergie éolienne à l'université du Québec à Rimouski et testé sur un moteur de compensation de 75 kW.

Published by :
http://www.ijert.org

International Journal of Engineering Research & Technology (IJERT)
ISSN: 2278-0181
Vol. 8 Issue 08, August-2019

Integrated A Variable Frequency Drive for a Diesel-Generating Set using the Genset-Synchro Concept

Mohamad Issa[1], Karim Ait-Yahia[1]
[1]Department of Applied Sciences,
Institut Maritime du Québec, Rimouski, G5L 4B4,
Canada

Richard Lepage[2], Hussein Ibrahim[2], Adrian Ilinca[2]
[2]Department of Mathematics,
Informatics and Engineering, Université du Québec à
Rimouski, Rimouski, G5L 3A1, Canada

Mazen Ghandour[3]
[3]Faculty of Engineering,
Lebanese University, Beirut, ULFG1,
Lebanon

***Abstract*— This paper examines the feasibility of implementing a variable frequency drive based on real-time control of the stator speed for a standby diesel generating-set using Genset-Synchro technology. The controller algorithms are designed using the Code Composer Studio version 8.0 software in C code, which can be downloaded to the digital signal controller TMS320F28335 from Texas Instruments in real-time. The paper shows results for the compensator motor that drives the stator speed to maintain the voltage and frequency at the output fixed. The results show the possibility to meet the performance class criteria of ISO 8528 part 5 G2 when diesel generators are equipped with Genset-Synchro technology.**

Keywords*— *Variable Diesel Generator, Genset-Synchro, Eo-Synchro, Real-Time Control, ISO 8528, Variable Frequency Drive.

I. INTRODUCTION

A conventional diesel generator (DG) consists of an engine connected directly to a synchronous alternator to produce electricity. Since the electricity produced must be at fixed frequency, normally 50Hz or 60Hz, the engine must rotate at a constant speed typically 1500rpm for 50Hz or 1800 rpm for 60Hz, no matter what the power demand is. One solution to save fuel in a diesel generator is to enable the engine to operate at variable speeds in direct relation to the electrical load demand [1]. The Genset-Synchro concept is especially, based on a completely different point of view of the known and preconceived ideas of what should be the standard alternator constitution. The innovation of the concept stems from the reality that the structure containing stator windings is mounted on roller bearings enabling its free rotation around the rotor axis, thereby preventing the stator structure from being static [2-4]. In order to ensure the rotation speed of the stator, an electric motor (compensator) installed directly on the alternator drives the rotation of the stator through a belt and pulley, Figure 1 [5].

By allowing the free rotation of the stator, the diesel generator set (DGS) is switched to operate at variable speed [2-5]. The synchronous speed of this alternator can remain constant through three different ways:

- Rotor speed only;
- Stator speed only;
- Both speeds simultaneously.

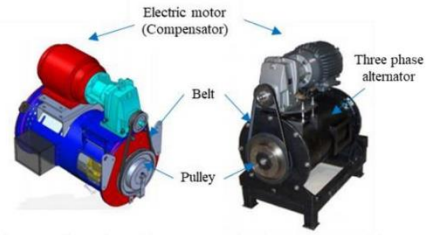

Figure 1. Illustration of the concept and main components of the Genset-Synchro technology

Previous work by the authors [4-8] has shown a potential reduction in fuel and greenhouse gases (up to 15%) when a diesel generator is equipped by a Genset-Synchro alternator with a 300-rpm fixed stator speed. However, in situations where a diesel-generating set is required to operate in standalone mode, the absence of an automated circuit to control the stator speed according to the applied load, can greatly affect the power quality (to maintain constant voltage and frequency with changing load) at the output of the generator.

As the ultimate objective of this work is integrate total control of a diesel-generating set equipped by a rotational stator alternator. This paper examines the development and implementation of a variable frequency drive to govern the stator speed of a 500kW alternator using a 75kW electric compensator motor. The paper shows results for the proposed controller in a basic form. The international standard ISO 8528 Part 5 is considered in order to evaluate the performance class of diesel-generating set using rotational stator in relation to voltage and frequency regulation [9]. This

International Journal of Engineering Research & Technology (IJERT)
ISSN: 2278-0181
Vol. 8 Issue 08, August-2019

standard provides a guide to the performance of an improved automatic control stator speed.

Testing was conducted at Genset-Synchro enterprise in collaboration with the University of Quebec at Rimouski on a 700KVA generating set with a 6-cylinder turbo aspirated electronic engine using resistive load.

II. DIGITAL SIGNAL PROCESSORS (DSP) BASED INDUCTION MOTOR CONTROL

Digital Signal Processors (DSP) provide high speed, high resolution and better induction motor control under different load circumstances.

The DSP-based induction motor drive system is composed of hardware systems such as induction motor, inverter, rectifier, eddy current load configuration, sensing unit DSP board and torque indicator. By comparing the modulated signal and carrier signal as shown in Figure 2, the pulse with modulation (PWM) signal is generated.

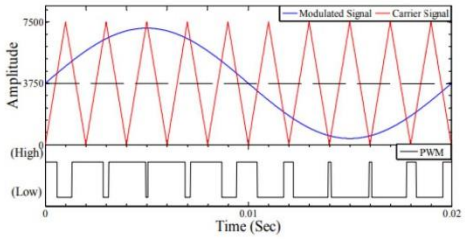

Figure 2. Illustration of the PWM generation by comparison of modulation signal with carrier signal.

For the creation of required SPWM pulse, the sinusoidal signal with frequency 'F_m' and voltage 'V_m' is compared with high frequency triangular carrier with frequency 'F_c' and voltage 'V_c'to operate gate drive for voltage source inverter. The variation in inverter output voltage amplitude and frequency relies entirely on the modulated sinusoidal signal because the carrier triangular signal has fix amplitude and constant frequency. The carrier frequency signal is used to determine the frequency of the PWM switching. The power quality parameter (harmonics, transients, active and reactive power, RMS voltage-current) of output voltage of inverter is depends on switching frequency of PWM signal. In other words, we can say that the modulated signal is used to regulate the speed and torque of the engine while the signal of the carrier is concerned with frequency switching problems and power quality. According to Figure 2, the pulse width is varying according to modulated signal and frequency is varies according to carrier signal. Dead bands were injected into the perfect PWM waveform for realistic security concerns. The dead band is provided by averting conductive overlap to safeguard the IGBTs at the moment of switching. PWM signals are produced according to the algorithm of speed feedback and control. The actual speed of the compensator motor is sensed by quadrature encoder pulse (QEP) speed detector. The voltage/frequency control is used in this suggested scheme, so the compensator motor speed is governed by the stator voltage and frequency in such a way that the air gup flux at the required value is constantly maintained at the steady state.

III. PLATFORM DETAILS

The hardware/software platform employed is the new generation digital signal processor TMS320F28335 with a high sampling rate to make it possible that it achieves good dynamics [10]. The algorithm is designed using MATLAB/SIMULINK and converted into C language using Code Composer Studio Version 8.0 environment. The sine pulse width modulation (SPWM) control algorithm is pro-posed for 3 phase three-leg IGBT voltage source inverter.

A. The PC Software Requirements

The various software packages and toolboxes that are required to build system models and compile real-time executable C code are:

- MathWorks MATLAB R2017B
- MathWorks Simulink R2017B
- Code Composer Studio environnement Version 8.0
- Microsoft Visual Studio 2019

B. The PC Hardware Requirements

Figure 3 is an illustration of the actual test-bed hardware layout. The hardware requirements are as follows:

- Host desktop PC: used to develop the PID controller program using Simulink and then to auto-compile the model into C source code, which can be downloaded to the DSP TMSF320F28335
- DSP TMS320F28335 from Texas Instruments: Implementing the controller to manage the PWM that in turn enables the IGBT gate drivers
- Three full bridge IGBT Gate drivers: to provide total control of the power supply of the compensator motor
- 100 HP electric compensator motor, 208V, 3 phases

IV. KEEPING THE VOLTAGE AND FREQUENCY FIXED

The role of a governor for a diesel-generating set when operated in isolation from the mains utility supply is to maintain the nominal frequency of the alternator terminal voltage. This is achieved by controlling the fuel quantity delivered to the engine combustion chamber. The international standard ISO 8528 Part 5 is used by diesel engine and generating set manufacturers to classify the performance class of a particular generating set in relation to voltage and frequency regulation [11].

International Journal of Engineering Research & Technology (IJERT)
ISSN: 2278-0181
Vol. 8 Issue 08, August-2019

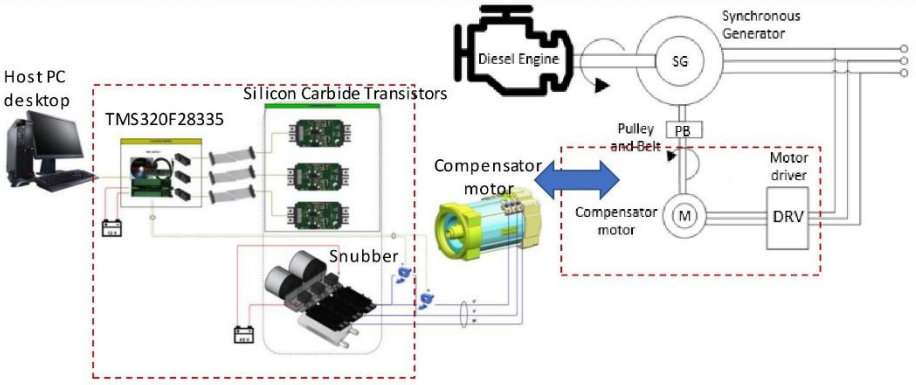

Figure 3. An illustration of the test bed-layout

To achieve a fuel savings, Genset-Synchro technology relies on reducing the diesel engine speed (ranging from 1800 rpm to 1500 rpm) and compensates by the rotation of the stator in the opposite direction of the rotor (300rpm) to keep the frequency (60Hz) and voltage fixed. On a previous work [4-8], the technology has shown significant fuel savings (up to 15%) on different diesel generators (75kW, 500kW and 600kW) under several stable loads. To date, no stator speed control system has been developed and the speed adjustment is done manually at the start-up of the generator. For this, we propose a control system based on the use of a frequency inverter to drive the compensating motor which, in turn, ensures the rotation of the stator. The control algorithm used the engine speed error, change in engine speed error, and the three-phase rectified average terminal voltage value to control the stator speed controlled by the compensator motor. Figure 4 shows a representation of the control strategy used to govern the speed of the compensator motor which, in turn, causes the stator to rotate. The engine information accessible on the engine control module (ECM) such as engine speed, required fuel, etc. are retrieved by the manufacturer and programmed in the DSP controller.

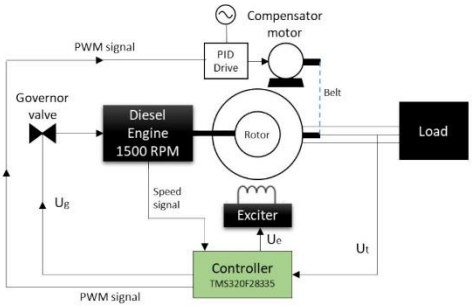

Figure 4. The closed-loop strategy

The engine speed is measured as follows:

- A magnetic pick-up is used to produce a waveform of sinusoidal voltage
- This waveform is converted into a square wave by a buffered Schmitt trigger circuit
- A DSP counter function is integrated to calculate the period of the square wave

The measured engine speed is used to determine the engine speed error and change in engine speed error. The additional input to the DSP controller is a three-phase rectified terminal voltage value which each phase voltage is stepped down to a voltage within the range of the analogue input on the DSP TMSF320F28335 card then sampled by the analogue input. The rectification and averaging of the three-phase voltage are conducted within the DSP con-troller card. The speed error change in speed error, and voltage error values can then be processed by the con-trol algorithm to calculate a new stator speed when the load changes.

A. Why use voltage ?

Voltage was chosen as an additional input to the compensator motor control scheme, as during resistive load disturbances both diesel engine speed and voltage are affected. Speed error- This caused due to real power load disturbances. For example, a resistive load applied to the alternator demands extra electrical energy. However, there will be a shortfall in the Kinetic energy supplied by the diesel engine due to insufficient fuel delivered to the combustion chamber. This causes the engine to decelerate. The inertia of the generating unit determines the deceleration.

Voltage error- this is introduced due to several factors when a complex load is applied to the alternator.

- Armature reaction: this is due to the need for the synchronous alternator to increase the rotor field current (I_f) to meet the increase in demanded main field (F_f). This is shown in Figure 5.

The main field MMF (Ff) depends on several factors. Equation (1) shows the relationship between Ff to the field current (If) and the number of rotor turns Nf.

International Journal of Engineering Research & Technology (IJERT)
ISSN: 2278-0181
Vol. 8 Issue 08, August-2019

$$Ff = Nf\,If\,(AT) \quad (1)$$

The rotor angle δ is regarded as the real power load angle and is the angle between the generated EMF phasor E, which is induced by the main field MMF (F_f), and the terminal voltage phasor V, which is produced due to the resultant MMF F_r. The F_{ar} MMF is termed the armature reaction MMF.

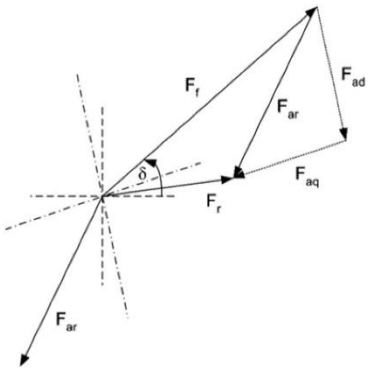

Figure 5. Representation of the space vector diagram of the MMF fields generated by the generated current in the stator in a salient pole alternator.

- Internal voltage drops within the alternator due to the relationship between the output current and the internal synchronous reactance of the alternator. The response time of the engine speed is therefore dependent on the inertia of the engine, flywheel, and alternator rotor combination, while the voltage response is dependent on the electromagnetic characteristics of the alternator.

V. SYSTEM DESIGN AND SIMULATION

The simulation is designed according to hardware specification and control algorithm. The V/F-SPWM model is executed progressively equipment setup utilizing DSP MATLAB interface. The Simulink developed model (Figure 6) consists to simulate the required time for the compensator motor to ensure a stator speed of 300 rpm at the start-up with a 50% resistive load and 350 rpm (passing from 300 rpm to 350 rpm) when applying a load higher than 50%. According to Figure 7, the required time at the start-up for the compensator motor to ensure a stator speed of 300 rpm is 3.6 sec while applying a load higher than 50%, the pulley ratio will change from 1:6 to 1:5.14 and the response time for adjusting the stator speed to 350 rpm is evaluated to 800 ms.

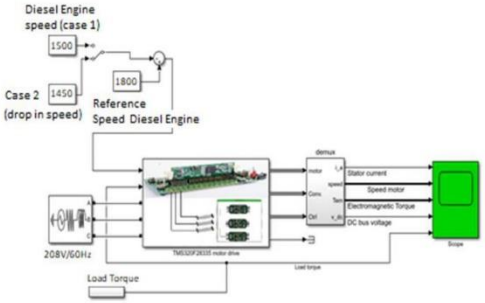

Figure 6. The Simulink developed model

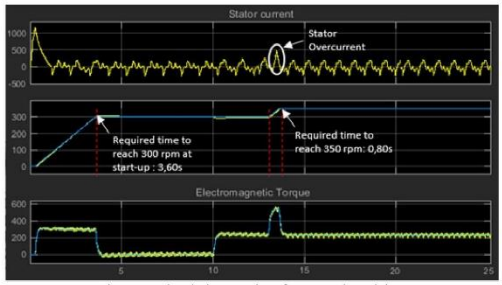

Figure 7. Simulation results of proposed model

The real-time speed of compensator motor is sense by QEP detector which gives pulses of 12.8 kHz at 1800 rpm. The quadrature encoder pulse (QEP) sensor gives two quadrature signals, i.e. QEPA and QEPB. The real time QEP encoder output has been shown in Figure 8. The phase angle between QEPA and QEPB is approximately 90° and signal frequency is approximately 12.02kHz, which indicate 1700 rpm. The frequency of QEPA signal is capture by eCAP module (Actual speed) as capture count. The frequency of QEP sensor and DSP clock must be synchronising for speed measurement. The error between set and actual speed is given to the speed proportional integral (PI) controller. The PI controller is tune by trial and check method. The MATLAB/Simulink model of speed PI controller/regulator is shown in Figure 9.

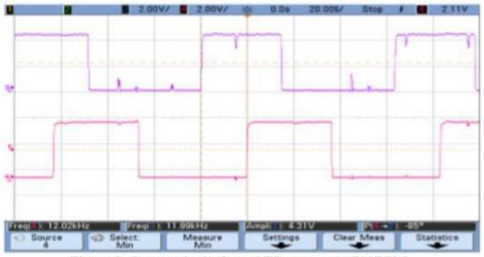

Figure 8. Output obtain from QEP sensor at 1700RPM

International Journal of Engineering Research & Technology (IJERT)
ISSN: 2278-0181
Vol. 8 Issue 08, August-2019

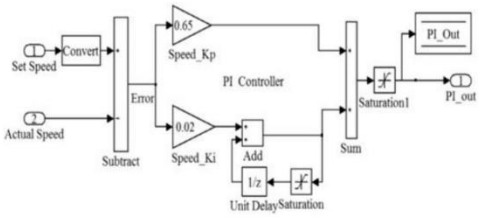

Figure 9. Illustration of the MATLAB/Simulink Model of PI-Controller

The output of PI controller (PI_out) is used to generate desired sinusoidal signal. The control model is design in MATLAB/Simulink for generation of desired modulated sinusoidal signal. The all possible sample of sinusoidal signal is store in memory as look up table. The frequency and amplitude of sinusoidal signal is control by frequency and amplitude modulation index (MI) respectively. The frequency modulation index of sinusoidal signal is derived by given derivation.

Specified frequency of carrier signal (Fc) = 10 KHz

Rated frequency of sinusoidal signal (Fm) = 60 Hz

Required number of sample (n)= F_C/F_m = 10000/60 = 166 (2)

Available sample by DSP = 2^{16} = 65536

Sample step count = Available sample/Required sample = 65536/166 = 395 (3)

Frequency step count = Max. sample set count/Rated speed of motor = 395/1800 = 0.219 (4)

So, frequency Modulation Index (MI_f) = 0.219

The amplitude modulation index of sinusoidal signal is derived by given derivation.

Available maximum amplitude of sinusoidal signal = 3750

Required maximum amplitude of sinusoidal signal = 90% of available maximum amplitude of sinusoidal signal

Required maximum amplitude of sinusoidal signal = 90*3750/100 = 3375

Amplitude step count = Required max. amplitude/rated speed of compensator motor = 3375/1800 = 1.87 (5)

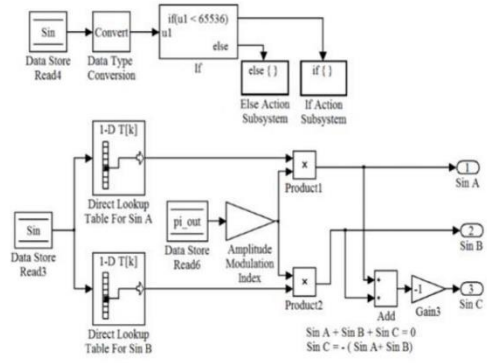

Figure 10. Illustration of the MATLAB/Simulink Model for sinusoidal signal generation

According to above derivation all available (65536) sample of one cycle of sin wave with zero phase and 120° phase are store in lookup table 'A' and lookup table 'B' respectively. The output value of lookup table is depending on predefined sin variable. The sin variable is depending on PI_out and frequency modulation index (MI_f). So according to PI_out value sin variable varies from 0 to 65536 and generates variable frequency sinusoidal signal from lookup table. The desired amplitude of sinusoidal signal is acquired by PI_out and amplitude modulation index. Figure 11 shows that 3 sinusoidal signal each shifted by 120° phase is generated by above model. The signal is used to generate desired PWM Sequence.

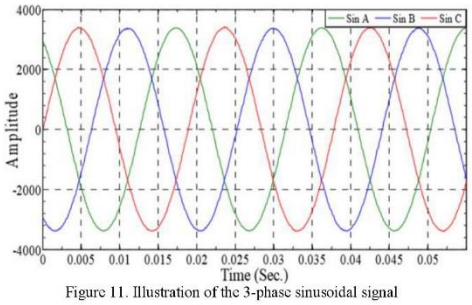

Figure 11. Illustration of the 3-phase sinusoidal signal

The high frequency (10 KHz) triangular carrier signal is generated by ePWM module by up-down count mode. The nature of carrier signal is unidirectional and sinusoidal signal is bidirectional, so they are not intersecting in negative half cycle of sinusoidal signal. The creation of the PWM waveform is accomplished in the practical implementation of the system by comparing the value of a time-base counter (TBCTR) (the carrier signal) with the instantaneous value of the sinusoidal signal. Sinusoidal signal instantaneous value is stored in a counter comparison register (CMPA). When the time-base counter (TBCTR) in up count mode is equal to CMPA, it sets the ePWMA register and the down count mode is clear. To obtain the required PWM frequency, time-base period register (TBPRD) is needed to be determined. PWM frequency (f_{PWM}) can be written as.

$$TBPRD = \tfrac{1}{2} * f_{SYSCLKOUT}/f_{PWM} * CLKDIV * HSPCLKDIV \quad (6)$$

The designated PWM frequency (fPWM) is 10 KHz according to the project design specification and the DSP setup and the clock frequency of system (fSYSCLKOUT) of the DSP F28335 is 150MHz. CLKDIV and HSPCLKDIV are selected to be 1. The value set in the time-base register (TBPRD) can be obtained directly on the basis of equation (6).

$TBPRD = \tfrac{1}{2} * 150*10^6/10*10^3*1*1 = (7500)_{10} = (1D4C)_{16}$

The high frequency complimentary PWM drive signal ePWMA and ePWMB are illustrated in Figure 12.

International Journal of Engineering Research & Technology (IJERT)
ISSN: 2278-0181
Vol. 8 Issue 08, August-2019

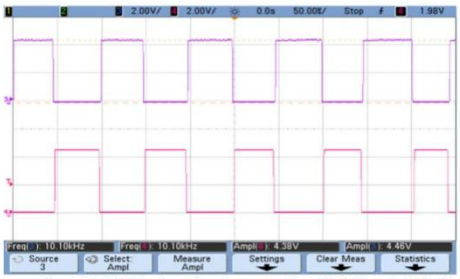

Figure 12. PWM pulses signal generated by ePWMA and ePWMB module.

According to Figure 13, the amplitude of drive signal was found to be 4.45 Volt with a frequency 10 kHz.

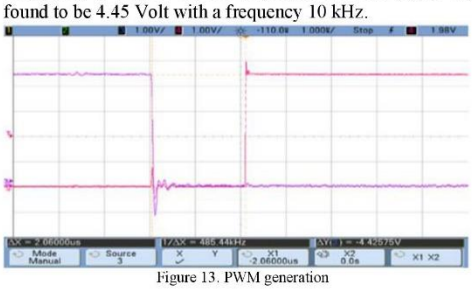

Figure 13. PWM generation

VI. TEST RESULTS

The inverter's DC connection voltage is first set for protection and safety purposes by autotransformer at 300V, and then IGBTs are provided PWM. Table 1 demonstrates the suggested control method's V/F ratio at different speeds of the compensator motor, while Figure 14 illustrates the real-time line parameter measurement of the compensator motor using the power analyzer.

Table 1. Evaluation of V/F and stator speed at various speeds of the compensator motor.

Compensator motor speed (rpm)	Voltage (V)	Frequency (Hz)	V/F ratio	Stator speed (rpm)
500	70.2	18	3.90	83.3
750	105.3	25.0	4.21	125
900	144.2	37.0	3.89	150
1200	170.0	44.9	3.78	200
1500	194.6	50.0	3.89	250
1750	207.9	60	3.46	291.6

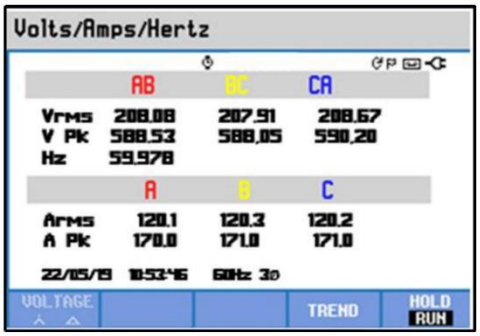

Figure 14. PWM pulses signal generated by ePWMA and ePWMB module.

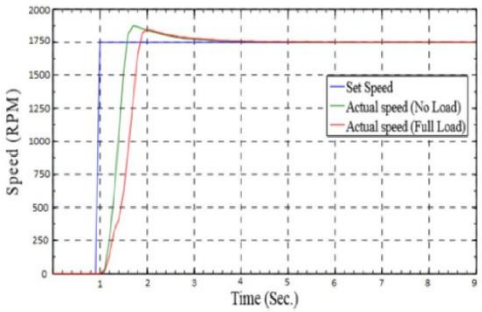

Figure 15. Illustration of the real-time step response (1750RPM of compensator motor)

The real time step and ramp response of motor speed at no load and full load are shown in Figure 15. The Step and ramp set commend is given by GPIO switch on DSP board. The real time current of the compensator motor is sense by hall-effect sensor and measured by DSP (using ADC module). All acquired data of DSP has been transmits to PC (MATLAB) using SCI module. Table 2 performs the time response analysis of the above results. The outcome demonstrates that there is excellent dynamic response to the motor's step response at no load and full load.

Table 2. Illustration of the time response analysis of speed step response (compensator motor)

	Delay Time (sec)	Rise Time (sec)	Peak Time (sec)	Settling Time (sec)	Overshoot (%)
No Load	0.41	0.30	0.7	2.4	7.07
Full Load	0.63	0.47	1.0	2.5	5.57

International Journal of Engineering Research & Technology (IJERT)
ISSN: 2278-0181
Vol. 8 Issue 08, August-2019

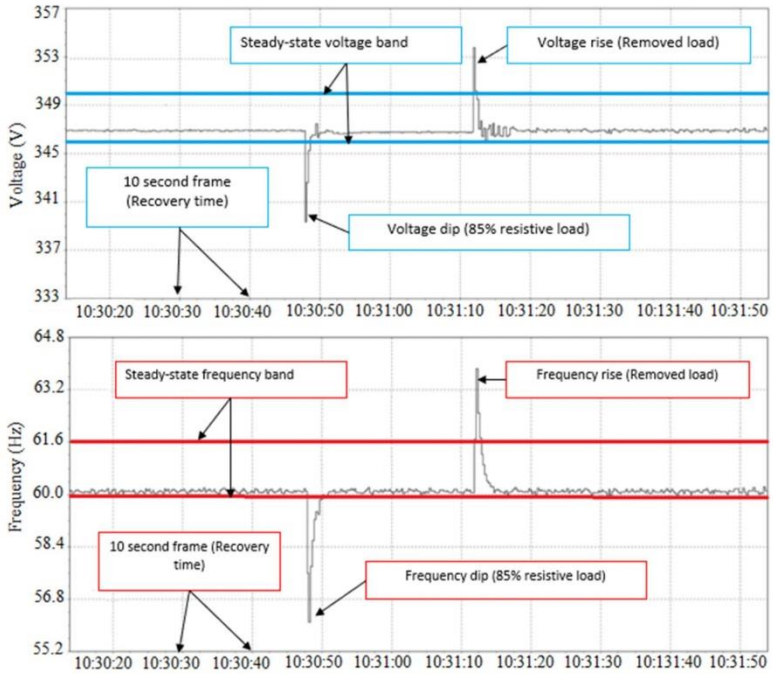

Figure 16. Illustration of the transient time responses of frequency and voltage qualifying the Genset-Synchro alternator to class G2 according to ISO 8528 standard

Finally, in order to evaluate the transient frequency and voltage times at the terminal output of the generator, we referred to ISO 8528-1:2018 standard. According to ISO 8528 standard, the Genset-Synchro set is qualified for class G2. Class G2 assumes that the maximum voltage dip is fixed at -20% while the rise voltage is set at +25% with a voltage retrieval moment of 6 sec. Concerning the frequency, the maximum frequency dip is set at -10%, while the maximum frequency rise is fixed at +12% with a frequency recovery time of 5 sec. Figure 16 illustrates the transient voltage and the transient frequency responses when applying and removing an 85% resistive load.

VII. CONCLUSION

An automatic controller to drives the stator speed for a diesel generator using the Genset-Synchro technology was developed and tested. The work conducted has initially proved successful in minimization the maximum speed deviation during load acceptance and meet the G2 performance classification in ISO 8528 Part 5 standard. The design and execution method of the digital signal processor-based MATLAB/Simulink model for compensator motor speed control has been very obviously described.

The sinusoidal PWM (SPWM) signals are produced using the dead band of the digital signal processor (TMS320F28335) for three phase operation and the signals are provided to the inverter module. In addition, the experimental findings indicate that DSP-based control systems have excellent efficiency, and greater control processor has made the engine velocity control more efficient than other standard methods.

In order to meet G3 performance classification in ISO 8528 part 5, the work must seek an appropriate control input, such as power or power factor, that can determine the actual power element of the complicated load, thus minimizing the influence of proportional voltage during low power factor load applications.

REFERENCES

[1] NAYAR, Chem. Innovative remote micro-grid systems. *International Journal of Environment and Sustainability*, 2012, vol. 1, no 3.

[2] Issa, M. , Fiset, J. , Ibrahim, H. and Ilinca, A. (2019) Eco-Friendly Selection of Diesel Generator Based on Genset-Synchro Technology for Off-Grid Remote Area Application in the North of Quebec. *Energy and Power Engineering*, 11, 232-247. doi: 10.4236/epe.2019.115015.

[3] Issa, M. , Ibrahim, H. , Lepage, R. and Ilinca, A. (2019) A Review and Comparison on Recent Optimization Methodologies for Diesel Engines and Diesel Power Generators. *Journal of Power and Energy Engineering*, 7, 31-56. doi: 10.4236/jpee.2019.76003.

[4] ISSA, Mohamad, FISET, Jean, MOBARRA, Mohammadjavad, *et al.* Optimizing the performance of a 500kW Diesel Generator: Impact

International Journal of Engineering Research & Technology (IJERT)
ISSN: 2278-0181
Vol. 8 Issue 08, August-2019

of the Eo-Synchro concept on fuel consumption and greenhouse gases. *Powr Engineer*, 2018, p. 23.

[5] MOBARRA, Mohammadjavad, FISET, Jean, et ILINCA, Adrian. Modeling and optimization of the energy production based on Eo-Synchro. *Power Engineer*, 2017, p. 3.

[6] Jean Fiset, Tony Durand, United States Patent & Trademark Office - Patent no. US8258641B2:Mechanical Regulation Of Electrical Frequency In An Electrical Generation System

[7] Fiset Jean, Canadian Intellectual Property Office -Patent no.2580360: Energy Transfer Apparatus

[8] Mobarra, M. , Issa, M. , Rezkallah, M. and Ilinca, A. (2019) Performance Optimization of Diesel Generators Using Permanent Magnet Synchronous Generator with Rotating Stator. *Energy and Power Engineering*, **11**, 259-282. doi: 10.4236/epe.2019.117017

[9] ISO 8528. https://www.iso.org/fr/standard/68539.html

[10] DSP. http://www.ti.com/lit/ds/symlink/tms320f28335.pdf

[11] McGowan, D. J., Morrow, D. J., & Fox, B. (2006). Integrated governor control for a diesel-generating set. IEEE Transactions on Energy Conversion, 21(2), 476-483.

CHAPITRE X

ARTICLE 8

Supercharging of Diesel Engine with Compressed Air: Experimental Investigation on Greenhouse Gases and Performance for a Hybrid Wind-Diesel System

Article publié dans Smart Grid and Renewable Energy Journal, le 30 septembre 2019

Volume 10 , No.9 – DOI :10.4236/sgre.2019.109014

Résumé

Dans cet article, un banc d'essai expérimental a été construit au sein de laboratoire de LIMA à l'université du Québec à Chicoutimi pour valider les résultats théoriques de la modélisation du système de suralimentation supplémentaire dans le cadre d'un système hybride éolien-diesel-air comprimé à moyenne échelle.

Les essais réalisés pour cette étude sont classés en 3 grandes catégories :

1- Moteur diesel atmosphérique (sans turbocompresseur et sans suralimentation par l'air comprimé stocké) où l'injection de carburant (idem le régime de rotation) est contrôlée automatiquement par le moteur.
2- Moteur diesel avec turbocompresseur seul et contrôle automatique de l'injection de carburant par le moteur.

3- Moteur diesel avec suralimentation par l'air comprimé stocké où la quantité du carburant injectée dans la chambre à combustion est contrôlée par un système manuel.

Les résultats ont démontré que les gains en consommation du carburant peuvent atteindre jusqu'à 30% lorsque le moteur est suralimenté, et une baisse de 30% pour les GES ont aussi été enregistrés.

Ces tests ont permis de déterminer le meilleur rapport air/fuel correspondant au rendement optimal du moteur. Aussi, ils ont servi à comprendre le comportement d'un moteur qui a subi des modifications pour passer de l'état atmosphérique à l'état suralimenté par air comprimé à pression plus élevée de celle d'un turbocompresseur. De plus, ces tests ont permis de déterminer les performances du moteur modifiés surtout la consommation du carburant et son impact sur les GES, la pression maximale dans le cylindre et le rendement.

Nous avons pu aussi démontrer pour une première fois, que l'excès de la suralimentation dans un bloc moteur (au-delà de ces capacités) a un impact négatif sur son rendement et sur son efficacité, voire sa destruction.

Smart Grid and Renewable Energy, 2019, 10, 213-236
https://www.scirp.org/journal/sgre
ISSN Online: 2151-4844
ISSN Print: 2151-481X

Supercharging of Diesel Engine with Compressed Air: Experimental Investigation on Greenhouse Gases and Performance for a Hybrid Wind-Diesel System

Hussein Ibrahim[1*], Mohamad Issa[2], Richard Lepage[3], Adrian Ilinca[2], Jean Perron[3]

[1]Institut Technologique de Maintenance Industrielle, Sept-Îles, Canada
[2]Department of Engineering, Université du Québec à Rimouski, Rimouski, Canada
[3]Department of Engineering, Université du Québec à Chicoutimi, Chicoutimi, Canada
Email: *Hussein.Ibrahim@itmi.ca, Mohamad_Issa@uqar.ca

How to cite this paper: Ibrahim, H., Issa, M., Lepage, R., Ilinca, A. and Perron, J. (2019) Supercharging of Diesel Engine with Compressed Air: Experimental Investigation on Greenhouse Gases and Performance for a Hybrid Wind-Diesel System. *Smart Grid and Renewable Energy*, **10**, 213-236.
https://doi.org/10.4236/sgre.2019.109014

Received: September 2, 2019
Accepted: September 27, 2019
Published: September 30, 2019

Abstract

Supercharging is the process of supplying air for combustion at a pressure greater than that achieved by natural or atmospheric induction, as applied to internal combustion engines. As a consequence of demonstrated technological, economical and energetic advantages in multiple literature evaluations concerning the large scale wind-compressed air hybrid storage system with gas turbines, the utilization of a hybrid wind-diesel system with compressed air storage (HWDCAS) has been frequently explored. These will mainly have average or small scale application such as the powering of isolated sites. It has been proven in numerous studies that the HWDCAS combined with an additional supercharging of the diesel engines will contribute to the increase of the power and efficiency of the diesel engine, the reduction of both fuel consumption and the emission of greenhouse gases (GHG). This article presents the obtained results from experimental validation of the selected design with an aim to valorize this innovative solution and become trustworthy.

Keywords

Wind Energy, Diesel Generator, Compressed Air Energy Storage, Supercharging, Hybrid Systems, Optimization

1. Introduction

Wind Energy has the largest growth rate among all renewable energies that contribute to electricity generation (more than 30% annually for the last five years

[1]). This is due to a competitive production cost (compared to other traditional sources), for the reduction of GHG emission, the positive impact on employment, the technological development and the creation of wealth. In Quebec, in parallel to an effervescence of wind energy mostly as large wind farms connected to the national grid, the distribution of electricity to isolates sites is still a major technological and financial challenge. Apart from isolated locations, there are countless technical, tourist, agricultural, fish farming and military facilities that are not connected to the provincial or national energy grid. Moreover, power transmission is very difficult due to prohibitive costs of electricity lines. In these remote areas, diesels are used to generate electricity. This electricity production is relatively inefficient, disadvantageous and responsible for the emission of large amounts of GHG. With the growth of fossil fuels and the high cost of transportation, the financial losses are enormous. For example, Hydro-Quebec estimates its losses related to the subsidies responsible for delivering electricity to 14,000 clients scattered in forty communities that are not connected to the main electric grid to be in the order of 133 million Canadian dollars annually [2]. These deficits reflect the gap between the high cost of local electricity production and the consistent price of electrical energy.

Furthermore, it is estimated that 140,000 tons of GHG emissions (Gases that trap heat in the atmosphere such as carbon dioxide, methane and water vapour are called greenhouse gases) result from the use of diesel generators by subscribers of the autonomous grid of Quebec. This is equivalent to the GHG emissions from 35,000 vehicles that run 15,000 km annually [2]. In contrast, most of these communities are situated in regions with high wind energy potential. Wind diesel high-penetration systems (WDS) without storage are those where the production of wind power exceeds the charge for long periods. This enables the diesel engines to stop completely during those periods, leading to a substantial decrease in fuel consumption. The use of wind-diesel hybridization (WDH) at these autonomous grids could consequently, reduce the exploitation deficits by encouraging the use of the wind resource as a local, free "fuel", instead of diesel, which is an imported fuel [3] [4] [5]. In addition, studies have been conducted to analyze the different constraints related to the introduction of wind power in these isolated zones and consequently propose a technological solution, which, on one side, will adapt to the technical and financial challenges, and on the other side, adopted by the major stakeholders—the utilities, the government and the local population. These studies have confirmed the profitability of the WDH will be achieved if the penetration of wind energy is high enough. This can only be achieved if a storage system is implemented [6]. On the other hand, the utilities and the government, concerned about the security of power distribution to isolated sites, consider the WDH as a young and moderately reliable, whereas manufacturers, developers and researches regard it as a mature technology [7]. Hence, we have proposed a solution which replies to these technological and financial requirements while ensuring the reliability of the electricity distribution to these isolate sites—the use of the hybrid wind-diesel with compressed air

energy storage system (HWDCAS) [8]. Before Pneumatic-Diesel hybridization with compressed air storage is commonly exploited, we highlight the different storage techniques exploited in the last decade and the effect of diesel engine boosting.

1.1. Thermal Storage

Thermal storage is used to generate electricity, even when the sun doesn't shine. Solar plants can concentrate heat from the sun and store energy in water, molten salts, or other fluids. Subsequently, this stored energy is used to produce electricity, allowing even after sunset to use solar energy. Plants such as these are presently working or being suggested in California, Arizona and Nevada [9]. For instance, the suggested Rice Solar Energy Project in Blythe, California will use a molten salt storage system with a concentrated solar tower to supply energy to roughly 68,000 households annually [10].

1.2. Hydrogen Storage

Hydrogen can be used for generation as a zero-carbon fuel. Excess electricity can be used to produce hydrogen that can later be stored and used in fuel cells, motors or gas turbines to produce electricity without damaging emissions [9]. The National Renewable Energy Laboratory has researched the ability to create wind hydrogen and store it for electricity generation in the wind turbine towers when the wind does not blow [11].

1.3. Pumped Hydraulic Storage

Pumped hydroelectric storage, by storing surplus electricity for subsequent use, provides a way to store energy at the transmission point of the grid. There are two reservoirs at distinct altitudes in many hydroelectric power plants. These crops store energy when supply exceeds demand by pumping water into the upper reservoir. When demand exceeds supply, by running downhill through turbines to produce electricity, the water is released into the reduced reservoir.

1.4. Fly-Wheels

By storing electricity in the form of a spinning mass, flywheels can provide the grid with a multitude of advantages at either the transmission or distribution stage. The unit is shaped like a cylinder and has inside a vacuum a big rotor. The rotor accelerates to very elevated speeds when the flywheel draws power from the grid, storing the electricity as rotational energy. The rotor switches to generation mode to discharge the stored energy, slows down and operates on inertial energy, bringing electricity back to the grid [12].

1.5. Batteries

Batteries can also be used to store energy on a big scale, such as those in a flashlight or cell phone. Like flywheels, batteries can be situated anywhere so that

they are often seen as distribution storage when a battery plant is situated close customers to provide energy stability; or end-use, like electric vehicle batteries. There are many distinct kinds of batteries that have the ability to store large amounts of energy, including sodium sulfur, metal air, lithium ion, and lead acid batteries. In wind farms, there are several battery facilities; including the Notrees Wind Storage Demonstration Project in Texas, which utilizes a 36 MW battery plant to make the power supply stable even when the wind is not blowing [13] [14].

1.6. Compressed Air

The use of compressed air as a power storage agent is well implemented to both wind and diesel generation. In fact, the compressed air stored in reservoirs during periods of excess production of wind energy (strong winds) is injected in the diesel generators during periods of low wind energy production (light or no wind regimes), the outcome will be energy increase or consumption decrease for the same load [15]. Hence, this hybrid system will react in real time to assure, in an optimized manner, the balance between the generated and consumed power [16] as it is the case for gas turbines which will be discussed in the following paragraph.

1.7. Effects of Diesel Engine Boosting

To achieve a high energy output, the boosting systems are used to raise the intake pressure from these motors. The goal is to improve the volumetric efficiency of an engine by increasing the intake gas density (usually air). The compressor of the turbocharger brings in ambient air and compresses it at enhanced pressure before it enters the intake manifold. This results in a higher mass of air on each intake stroke entering the cylinders. Without raising energy, a turbocharger can also be used to boost fuel efficiency [17]. This is accomplished by diverting fuel waste power from the process of combustion and feeding it back into the "warm" intake side of the turbo that spins the turbine. The cold intake turbine (the other side of the turbo) compresses new intake air and pushes it into the intake of the engine as the warm turbine side is powered by the exhaust energy. By using this otherwise wasted energy to boost air mass, it becomes simpler to guarantee that all fuel is burned before the exhaust phase begins to be vented. The greater pressure temperature provides a greater Carnot efficiency [18].

2. Why to Choose Compressed Air as Energy Storage System for High Penetration in Wind-Diesel System?

Among all the methods for storing intermittent renewable energy, such as pumped hydroelectric storage, batteries, flywheels and CAES (compressed air storage), the latter has an overwhelming benefit given its low price, low effect on the environment and high efficiency [19]. CAES is a technology that has already

been used at large scale, in pilot projects in Germany and few states of USA such as Alabama, Ohio and in a planned project at Texas (3000 MW project) for hybrid wind-natural gas power plants in the order of hundreds to thousands MW (Figure 1). Combining a storage component with a high-penetration WDS makes it possible to store the frequently occurring and otherwise dissipated surplus wind energy and then use it later when necessary. Therefore, the demand for fuel energy is decreased. Figure 2 shows that fuel savings begin when wind speeds exceed 4 m/s. When wind speed reaches 9 m/s, wind power is sufficient to meet the requirement of customers without the contribution of a diesel engine. However, when a 30 percent margin is reached between consumer demand and accessible wind power, the diesel engine is stopped. Excess wind power is lost for wind speeds greater than 9 m/s. According to [15] [16] [19], the annual fuel consumption for a WDS with air storage is estimated at 50% with a 38% decreases in the fluctuation of energy production.

This enables a significant increase in the penetration of wind energy, to about 90% [15]. The additional cost of the CAES, in the order of 0.01 $/KWh is largely compensated by the reduction (around 80%) of natural gas consumption, carbon credits and the credits related to wind energy production [15].

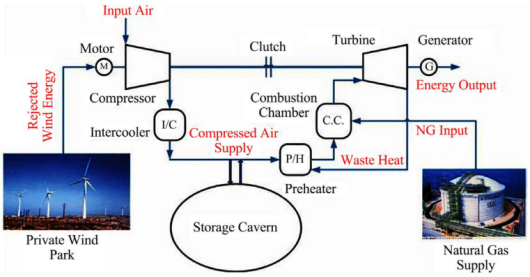

Figure 1. Illustration of the Wind-CAES hybrid system on a large scale.

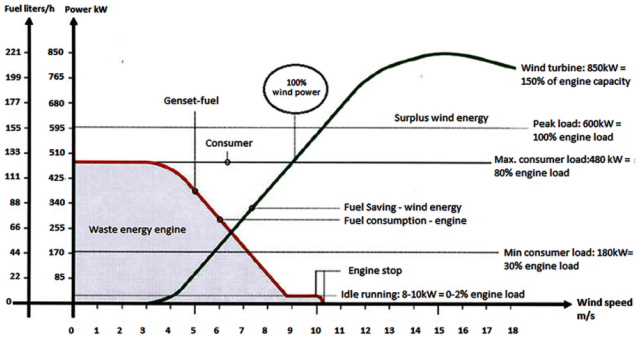

Figure 2. A high-penetration wind-diesel generator's power contribution and fuel consumption [19].

The compressed air storage energy-to-power ratio could be freely selected. The tank size, a standard industrial product, determines the energy content and the size of the engine/generator [15]. Compressed air is generally used to produce electricity by driving a compressed air motor or gas turbine [15]. In our project, we are exploring another option of using the already installed Diesel engine to exploit the stored compressed air. This method is called diesel engine pneumatic hybridization. CAES would make the diesel engine operate at some working points with less fuel consumption or even no fuel injection.

3. Description of the Hybrid Wind-Diesel Compressed Air Energy Storage System (HWDCAS)

The stored compressed air is used in the HWDCAS scheme to overload the diesel engines which consequently increases the wind energy penetration rate (WEPR). Supercharging is a method consisting of a preliminary compression with the aim of increasing motors' air intake density to boost their specific power (energy by swept volume) [15]. Thus, during periods of powerful wind, the wind power surplus (when the wind power penetration rate defined as the quotient between the wind power generated and the charge exceeds 1, WPPR > 1) is used to compress and store the air via a compressor. The compressed air is then used to overload the diesel engine with a double benefit of enhancing its energy and reducing fuel consumption. The diesel generator operates during periods of low wind speed when there is insufficient wind power for the load [15] [16] [19]. **Figure 3** illustrates the principle of such operation.

Pneumatic diesel engine hybridization involves using the stored compressed air to overload the diesel engine. This could be performed using multiple techniques to enhance diesel engine filling through the additional overload associated with the current turbo compressor. Seven systems have been explored among which, at least four demonstrate originality in the design of the diesel engines. These methods are: 1) the use of an air turbine in series with the axis of the turbo compressor (**Figure 4**); 2) the double stage turbocharging; 3) upstream admission in the compressor; 4) the hyperbar supercharging (**Figure 5**); 5) direct injection in the engine via the intake valve; 6) supercharging using the pressurized LENOIR cycle [20] and 7) supercharging with downsizing.

4. Technical Benefits of Diesel Engine Pneumatic Hybridization

Due to their efficiency, reliability, versatility and low price, diesel engines are merely the most economical solution in the range of energy requirements up to 300 MW of the multiple ideas available for power supply in independent grids [15]. To provide a reaction to pollutants and laws on greenhouse emissions, much research is being performed globally to enhance the diesel engine's vigorous efficiency. Over the past decade, the efficiency of the direct injection diesel motor has risen significantly, primarily owing to turbo charging and reduction

techniques [15]. A typical diesel engine's worldwide efficiency is actually around 40% [16].

On the other hand, the majority of diesel generators used in distant regions are already fitted with turbochargers. However, during low regime operation, this sort of scheme loses its benefits because its effectiveness is directly linked to the exhaust gas amount. To understand the advantage of an additional turbocharging of diesel engine and the operation limits of a turbocharger, we present in Figure 6 an example which compares a diesel engine in two functioning modes: atmospheric (without turbocharger) and turbocharged.

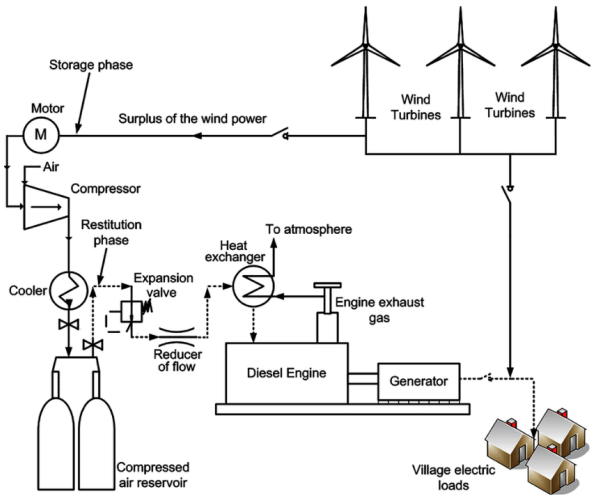

Figure 3. Illustration of the HWDCAS system.

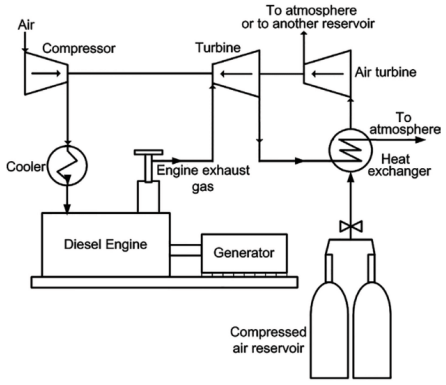

Figure 4. Illustration of the series use of an air turbine with a turbocharger [8].

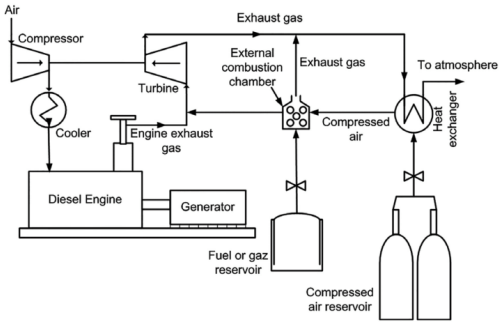

Figure 5. Illustration of the hyperbar supercharger [8].

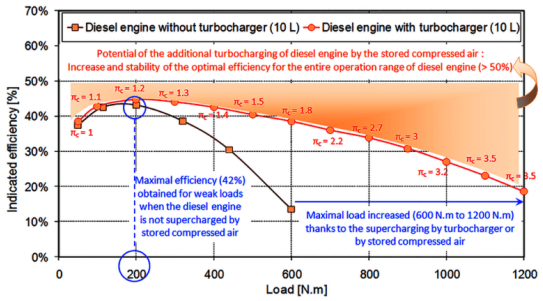

Figure 6. Possibility of extra 300 kW supercharging, 1500 rpm diesel engine by compressed air stored.

Figure 6 shows that as compared to an atmospheric 300 kW, 1500 rpm diesel engine, with a compression ratio of 16.3:1 and capacity of 10 L, supercharging can improve the specified engine efficiency values (maximum efficiency = 45 percent) and extend the high efficiency working variety thanks to the big permissible amount of air in the motor. The supercharged engine's effectiveness is about 38 percent for a load of 600 N.m compared to the atmospheric engine's effectiveness (14 percent), *i.e.* an increase of about 170 percent. Increasing the load applied to the engine, on the other side, causes a degradation of the diesel efficiency owing to the turbocharger's operating boundaries and increased heat loss through the cylinder walls. However, this does not exclude the fact that the effectiveness of elevated loads is greater than the effectiveness achieved with the atmospheric engine by supercharging (a rise of about 64 percent for a load of 1200 N.m).

Figure 6 also shows that the compression ratio reaches its maximal value only for the highest loads (this corresponds to high flow and pressure of exhaust gas). This delay in achieving the maximum compressed air pressure at engine intake will delay the accomplishment of the turbocharged engine's maximum energy.

The objective of the additional supercharging via the stored compressed air is, then, to maximize the overall efficiency of the diesel engine (Figure 6), by Improving meaning, Reducing-meaning and Incrasing-meaning:

- Improving the effectiveness of combustion by always running the motor with an optimum air/fuel ratio that does not enable the turbocharger to function alone.
- Reducing pumping losses for the low-pressure loop of the diesel engine thermodynamic cycle to increase the work supplied for the same burned fuel quantity.
- Increasing the specific power (power per swept volume unit) of the diesel engine and its performance.
- Increase the intake pressure at the point allowing a reduction in the injected fuel amount while keeping the same maximum pressure in the motor cylinder. This enables mechanical and thermal limitations to be reduced owing to the overload.

5. Experimental Validation

Numerical modeling and simulations demonstrated the possibility of fuel economy by 30% - 50% as a function of the wind potential, size of the engine and the used forced induction system [8] [15] [20] [21]. In order to valorize the design and make it more convincing and enable validation with obtained theoretical results, an experimental validation was necessary. For this reason, a test bench has been set up at the Université du Québec à Chicoutimi (UQAC). This bench includes a prototype of an atmospheric diesel engine (non-forced induced) with a 5 kW rating. This engine has been modified: a turbo compressor, as well as a forced induction system directly connected to the collector of the engine admission (using the compressed air circuit of UQAC), was installed. Several tests have been performed for different loads. The obtained results have proven the energetic, economic and ecologic potential of the new design. The new supercharging system has enabled the engine to operate with an efficiency of around 56% with the least possible fossil fuel so as to save around 35% of consumed fuel while perfectly ensuring the electrical demand without disturbing the quality of the electrical current (constant frequency and voltage). The losses are 9% under low load and 17% under a high load.

5.1. Global Description of the Test Bench

Recommendations from preliminary studies lead to the acquisition of a generator driven by an atmospheric non-forced induced diesel engine. This has enabled us to use a number of resistive loads connected to the generator as an applied load on the diesel engine and avoid the application of an external mechanical load (such as hydraulic brakes) on the shaft of the engine. The chosen diesel generator, a KCG-5000DES model from King Canada that has a power rating of 5.0 kW and a 7.35 kW thermal rating with an electrical starting system with a no load speed of 3600 rpm.

Initially, the engine is not equipped with a turbo compressor. For this, a test bench has been set up to tolerate the conditions of the anticipated experience protocol while determining the size and type of the turbocharger which could be adapted for the admission and exhaust of the engine. An advantage of this option is its possibility to perform different trials: operate the engine as 1) an atmospheric engine; 2) a turbocharged engine via a turbo compressor; 3) or as a forced supercharged engine with pre-stored compressed air (supplementary supercharging). This test bench (Figure 7) includes an engine connected to a generator, a turbo compressor installed on the engine, engine monitoring sensors and a rapid data acquisition system. For logistics and financial reasons, the test bench did not include sensors to monitor pollutants. The installation is equipped with instrumentation ensuring: the secured operation of a test bench, the measurements in stationary and transitory regimes.

The engine is experimented in a cell which ensures the following functions: exhaust, cooling, fuel alimentation to the engine in fuel and security of the bench. The engine is completely instrumented and the entire signals are recorded on a calculator by the means of an acquisition card. The details of the sensors and measurements are presented later.

The used sensors, as well as the measured parameters are represented in the synoptic illustration of the test bench in Figure 8, while Figure 9 embodies the test bench (sensors, regulator, compressed air circuits, etc.).

On the other hand, we used an industrial combustion analyzer (Testo 350 with ±5% of accuracy) in order to analyze the Nitrogen Oxide (NOx), Sulfur dioxide (SO_2) and Carbon dioxide (CO_2) effect of supercharging. Figure 10 shows the combustion analyzer connected to the exhaust engine.

5.2. Classification of Tests

The performance trials are grouped into three categories:

1) Diesel engine without turbocharger with no additional supercharging (atmospheric mode), where fuel injection is automatically controlled by the engine.

2) Turbocharged engine with automatic control of the fuel injection.

3) Supercharged diesel engine only with the compressed air network of UQAC, where the amount of injected fuel in the combustion chamber is controlled by a manual system. The compressed air is injected straight into the intake manifold and transferred through the poppet valve (Figure 4) into the cylinder.

In each category, several tests have been performed by varying the applied load on the generator. It is important to mention that the regime of the turbocharger, the torque of the engine and the temperature of the cylinder have not been installed due to logistical, technical and budgetary constraints. However, the ambient temperature has been measured with the help of a numerical thermometer (the frequency of air temperature variation is not significant in a small time period). The atmospheric pressure is assumed constant and equal to 1 bar.

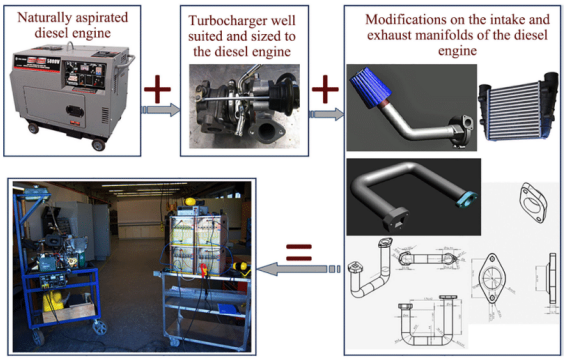

Figure 7. Different components of the test bench.

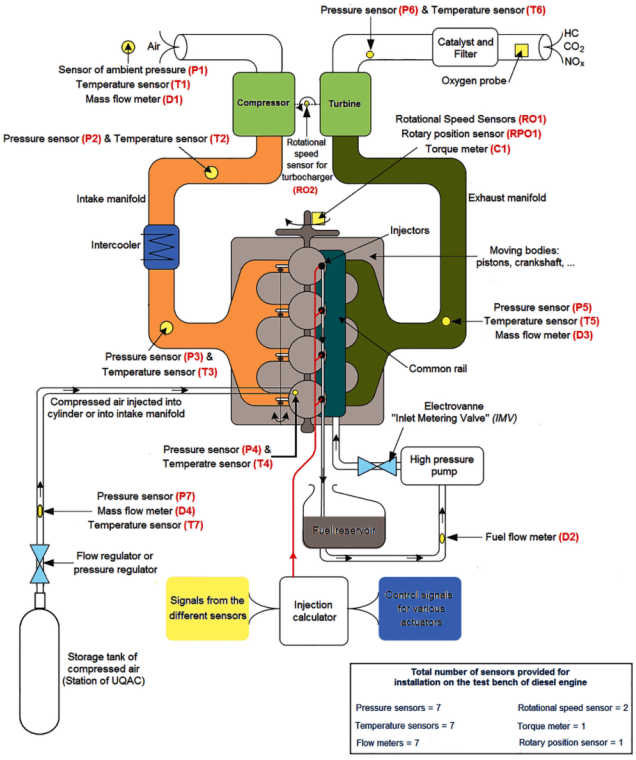

Figure 8. Synoptic illustration of the test bench. Pressure sensor accuracy: ±2%; Temperature sensor accuracy: ±1%; Flow meter accuracy: ±1%; Rotational speed sensor accuracy: ±1%; Torque meter accuracy: ±0.5%.

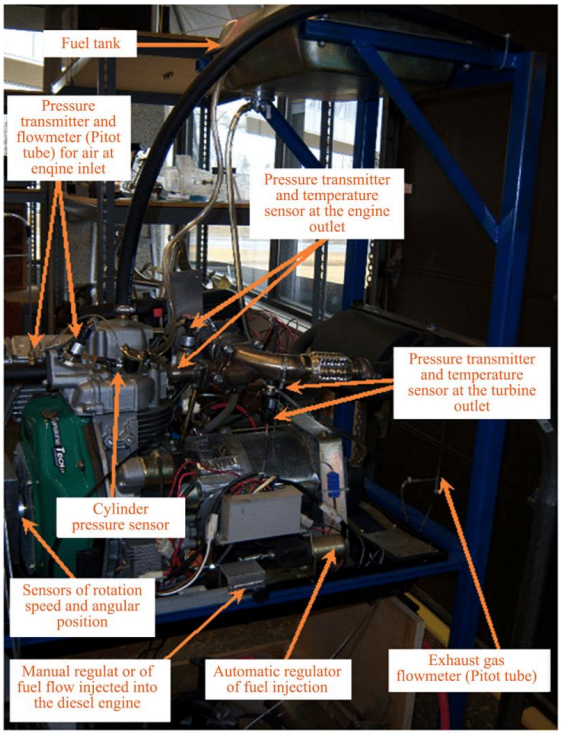

Figure 9. Different sensors and manual injection regulators installed on the engine.

Figure 10. Illustration of the Testo 350 with the probe connected to the exhasut DE.

6. Results and Discussions

The results obtained from the tests performed on the diesel engine in atmospheric mode, with turbocharging and with additional supercharging are represented in **Figures 11-19**.

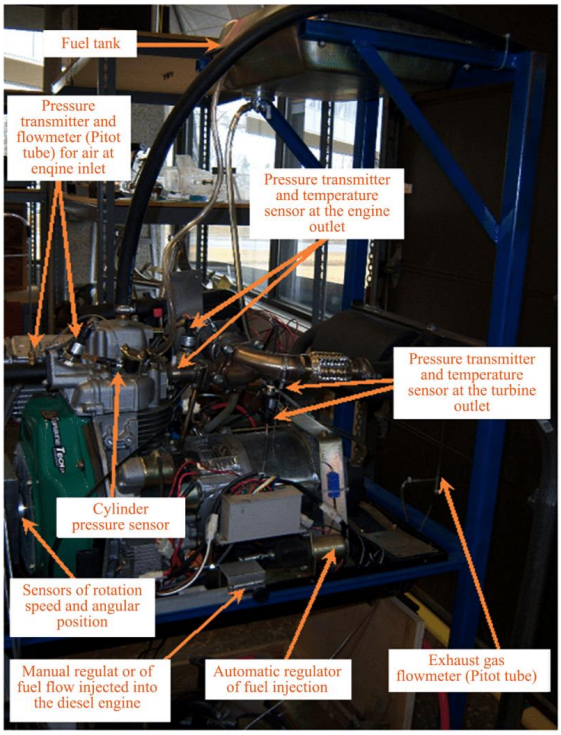

Figure 9. Different sensors and manual injection regulators installed on the engine.

Figure 10. Illustration of the Testo 350 with the probe connected to the exhasut DE.

6. Results and Discussions

The results obtained from the tests performed on the diesel engine in atmospheric mode, with turbocharging and with additional supercharging are represented in **Figures 11-19**.

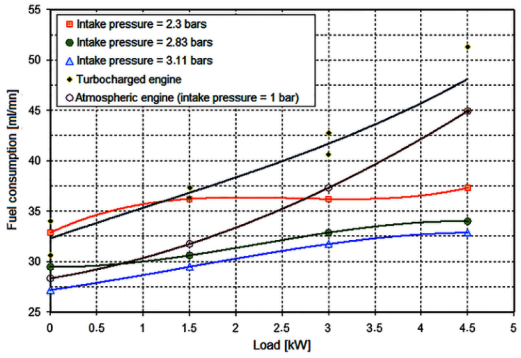

Figure 11. Consumption variation of diesel engine.

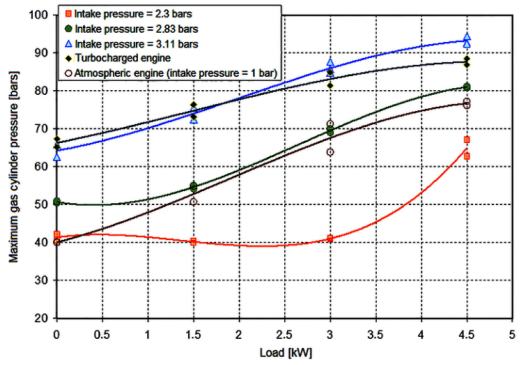

Figure 12. Maximum pressure variation in the cylinder.

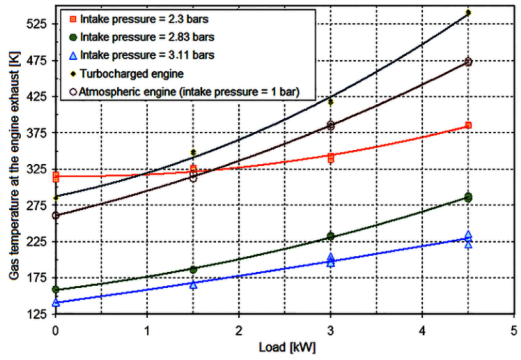

Figure 13. Variation of the exhaust gases.

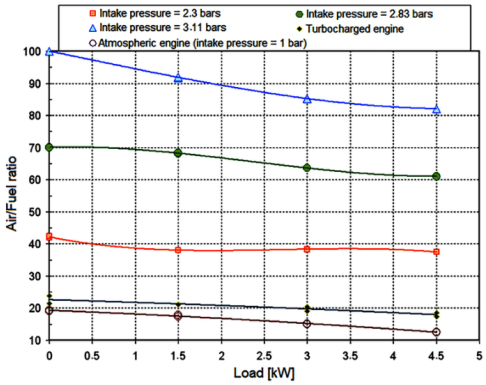

Figure 14. Air/Fuel ratio variation.

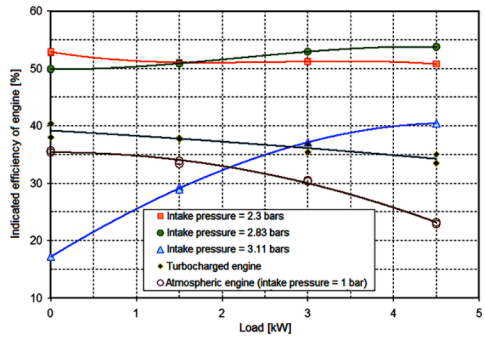

Figure 15. Variation of the indicated effciency function of load.

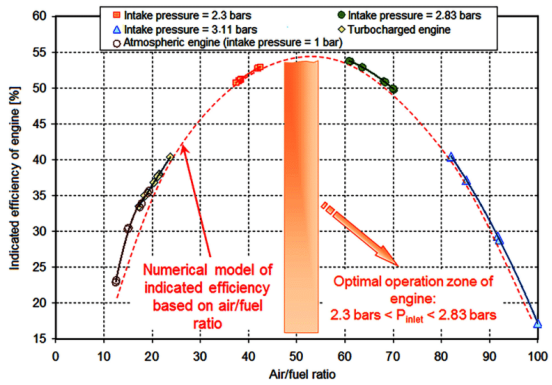

Figure 16. Variation of the effciency in function of air/fuel ratio.

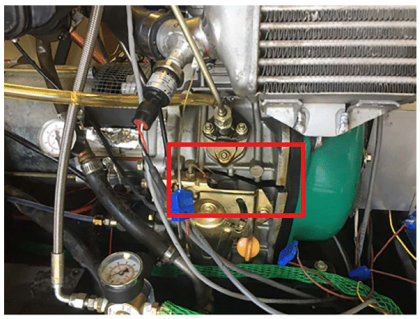

Figure 17. Illustration of the damage (engine is melted) due to the high pressure (3.11 bars > 2.83 bars) applied in supercharging.

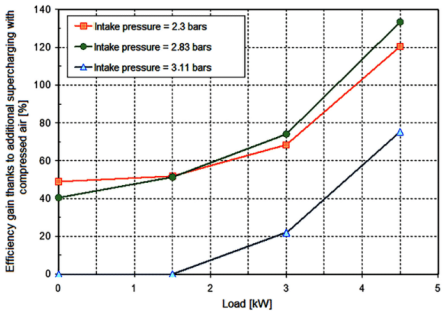

Figure 18. Efficiency gain due to hybrid forced induction in comparison to atmospheric mode operation.

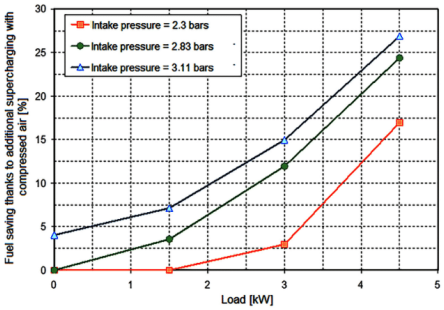

Figure 19. Fuel saving due to hybrid forced induction in comparison to atmospheric mode operation.

6.1. Comparison According to Fuel Consumption

Figure 11, which characterizes the fuel consumption, shows that regardless the

operating mode of the engine (atmospheric, turbocharged by the turbo compressor alone or with the compressed air alone), the consumption of fuel increases with the increase of the load for the same pressure of admission in the engine. It is easy to see that for the whole operating range of the engine (0 kW to 4.5 kW), the turbocharging of the engine by the turbo compressor triggers an increase of fuel consumption by about 11% compared to the quantity consumed by the engine in atmospheric mode. This is due to the fact that the turbo compressor increases the admitted air flow by the engine while forcing the latter to operate with a constant air/fuel ratio close to the stoichiometry.

Furthermore, the engine supercharged by compressed air from the network of UQAC consumes less fuel as the forced induced pressure increases. The rate of such decrease quenches with the growth of the admitted pressure as it is limited by constraints linked to the stability and homogeneity of the combustion. Moreover, this rate is virtually fixed, between two pressure levels, on the whole, operation range of the engine. By supercharging the engine with compressed air at 2.83 bars as admission pressure instead of 2.3 bars, the engine consumes, on average, 10% less fuel. However, if the additional supercharging is done at 3.11 bars, the engine consumes only 3.7% less fuel than it would, had it been alimented at 2.83 bars pressure. In a conclusion, 12% saving on fuel is made by forced inducing the engine at 3.11 bars instead of 2.3 bars.

6.2. Comparison According to the Pressure in the Cylinder

The variation of the maximum gas pressure in the cylinder is represented in Figure 14. First of all, we can easily see that as the power demand to the engine increases, the pressure in the cylinder increases more for all modes of operation. As an effect of the increased fuel consumption in turbo mode, it is clear that the pressure at the end of the combustion during this operation mode will be superior to that obtained for the atmospheric mode. An average increase of 30% can be seen in Figure 12.

However, the maximum pressure in the cylinder remains nearly constant (41 bars on average) in the working range between 0 kW and 3 kW for an induced pressure of 2.3 bars. However, an approximate increase of around 58% occurs for the maximum pressure when the engine operates between 3 kW and 4.5 kW. This can be explained due to the fuel combustion performance which was better under 60% of load (3 kW), while under a weak load (30%), the compressed air injected into the engine compensated for the lack of fuel (weak ratio A/F) allowing for a close pressure between low load and medium load. When the engine is supercharged with compressed air at 2.83 and 3.11 bars pressure, the curves show an increase with respect to the load. By varying the pressure of admitted air in the engine between 2.3 bars 2.83 bars and 3.11 bars, respectively, the average increase in the maximum pressure in the cylinder due to forced induction at 2.83 bars is around 22% as compared to 2.3 bars. The same percentage is obtained when the supercharging is done at 3.11 bars instead of 2.83 bars.

It is easily noted, according to Figure 12, that even with a high forced induction at 3.11 bars, a pressure twice as that produced by the turbocharger, the maximum pressure in the cylinder always remains in the acceptable limits of the engine even in the critical zone of operation of the engine (important loads). However, by operating without any load, the maximum pressure in the cylinder due to a forced induction at 3.11 bars is the same as that obtained for a forced induction via the turbo compressor but always remains superior to that obtained with the atmospheric engine. This enables us to conclude that the mechanical and thermal constraints that could limit the operation of the engine or even damage it have no more importance due to the fact that the choice of the turbocharger has accounted for all the constraints and that the supplementary forced induction has not exceeded the operation limits of the engine with a turbocharger.

In fact, the maximum pressure obtained for high loads is around 90 bars for both cases whereas the temperature of the exhaust gases is very much lower when the engine is forced-induced at 3.11 bars (225˚C) instead of using a turbocharger (550˚C) (Figure 13). The thermal and mechanical constraints can then be neglected given that the maximum pressure in the cylinder is still far from the limit of the acceptable value of the engine (120 bars).

6.3. Comparison According to the Air-Fuel Ratio

Figure 14 represents the variations of the air/fuel ratio for a diesel engine, operating at different modes with respect to the charge. This Figure illustrates that the air/fuel ratio decreases with an increase in the load. However, this decrease becomes more and more significant with a secondary forced induction via the compressed air from the network of UQAC but the ratio always remains superior to that obtained with an atmospheric engine or that of a forced induced by a turbo compressor irrespective of the applied load.

It is important to notice that by forced induction the engine at 2.3 bars pressure, the air/fuel ratio decreases from 42 to 41 in a range situated between 0 and 1.5 kW and stabilizes at 41 for the rest of the operating range (from 1.5 to 4.5 kW) whereas, in the case where the forced induction is done at 2.83 bars, the air/fuel ratio remains nearly constant around 70 when the load varies between 0 and 1.5 kW and it diminishes afterwards to reach a value of 61 when the engine drives a 4.5 kW load, an average drop of 11%. However, by adopting 3.11 bars as pressure at the engine admission, the air/fuel ratio is subjected to a continuous drop with respect to the load where it passes through a value of 100 when the engine operates without load and reaches 82 for maximum operating load, a drop of around 18%.

6.4. Comparison According to Indicated Efficiency

Figure 15 and Figure 16 illustrate for different operating modes, the variations of the indicated efficiency of the diesel engine with respect to the applied charge

and the air/fuel ratio respectively. It is interesting to note that the efficiency diminishes with an increase of the load when the engine operates in atmospheric or turbo mode. However, by supercharging the engine by compressed air from the network of UQAC, the indicated efficiency of the diesel increases with increasing load and is much better and more stable for lower pressures at admission but superior to those produced by the turbo compressor.

Figure 15 shows that by forced induction of the engine with compressed air at 2.3 bars of pressure, the obtained efficiency is around 50% but increases to 54% if the admission pressure becomes 2.83 bars for both cases and for the whole range of engine operation. However, if the admission pressure increases further to reach a 3.11 bars pressure level, the efficiency increases with the load but does not exceed 40%. Moreover, at this pressure level, the efficiency is too low, around 17%, and when the engine is in free operation the efficiency is 28% with a connected load of 1.5 kW. This can be explained by the unstable combustion process in a cylinder given that a large mass of air is admitted (air/fuel ratio being around 80 to 100), which has as consequence the degradation of the combustion and engine efficiency.

To conclude, it can be noticed that, according to Figure 15 and Figure 16, despite the advantages related to efficiency obtained by forced induction at high pressures, this method can lead to a poor operating mode of the engine and in consequence a degradation of the indicated efficiency. For these reasons, this type of forced induction is limited by:

- A maximum pressure level at admission should not exceed 2.83 bars in the case of an engine using this test bench. If this condition is not respected, the engine becomes inefficient mostly for average and small loads and/or damaged. It should be noted here that the engine was damaged when a pressure of 3.11 bars was applied to 4.5 kW (90%) of the load after 5 minutes of testing. This happened because the pressure in the cylinder exceeds the recommended limit for which the cylinder is designed for. Figure 17 shows the damage to the diesel engine.
- An air/fuel ratio ranging from 50 to 60. If this ratio is smaller than this interval, the engine approaches stoichiometric operation and its efficiency will not exceed 35%. If the air/fuel ratio is greater than this range, the engine will then operate in the combustion instability zone with an efficiency which does not exceed 40% even at full load.

6.5. Efficiency Gain

Figure 18 illustrates the obtained gain in efficiency as a consequence of compressed air at high pressure admitted in the cylinder as compared to atmospheric mode operation.

It is easy to notice that the forced induction engine at a pressure varying between 2.3 and 2.93 bars offers greater efficiency improvement for the whole range of operation and mostly for significant loads, thus, confirming the numerical demonstration. In this pressure interval, the engine efficiency can increase

by about 50% if it is in free run operation as compared to atmospheric operating mode. This gain becomes remarkable at full load where it reaches a 130% level. This level has never been achieved in the past. However, the forced induction at 3.11 bars pressure, brings no gain in efficiency when the engine works with small loads (0 to 1.5 kW), whereas the gain for significant loads (4.5 kW) does not exceed the 78% as compared to an atmospheric engine.

6.6. Fuel Saving

The evolution of fuel saving due to hybrid forced induction as compared to an atmospheric mode operating engine is illustrates in Figure 19.

It is clear that as the load increases, the fuel economy becomes more significant. Similarly, as the admission pressure increases, fuel saving increases. For a load of 4.5 kW and a 2.3 bars admission pressure, the engine saves 17% of fuel, around 24% for a 2.83 bars admission pressure and 27% economy for a 3.11 bars admitted pressure.

Furthermore, it can be noticed that the fuel economy decreases as the admitted air pressure increases. This is explained by the fact that the engine will operate in a zone where the efficiency of the combustion process will undergo degradation, thereby, making fuel economy difficult due to the quality and homogeneity of the combustion. Figure 20 illustrates another point: during free running mode, only forced induction at 3.11 bars enables a fuel economy of around 4%. Moreover, the economic advantage of a forced induced engine at 2.3 bars as compared to an atmospheric mode operating engine appears only for loads of 1.5 kW power rating and higher.

7. Impact of the Supercharging on Greenhouse Gases

Emissions from diesel generators (DGs) such as PM, CO_2, NO_x, SO_2 and CO contribute to diver's cardiovascular and respiratory diseases and cancer, in addition to water and soil pollution, visibility reductions and global climates changes [5] [16] [17] [18] [19] [22] [23] [24] [25].

In this context, we have evaluated and compared the emission of exhaust gases emitted by the DG before and after the supercharging mode using number 2 diesel fuel type B-ULS with maximum fuel sulfur of 15 mg/kg. An industrial gas combustion analyzer (Testo 350) is used to evaluate carbon dioxide (CO_2), nitrogen oxide (NO_x), sulfur dioxide (SO_2) and carbon monoxide (CO) levels. Figure 20 illustrates the carbon dioxide level, while Figures 21-23 illustrate the nitrogen oxide, sulfur dioxide and carbon monoxide levels.

According to Figure 20, it is clear to notice that the forced induction of compressed air at a 2.25 bars pressure offers the best reduction of carbon dioxide by an amount of 41% approximately and this for the different levels of applied loads. This can be explained by the homogeneous charge compression ignition and fuel saving due to the supercharging resulting in high peak pressure but relatively lower peak temperature at 2.25 bars.

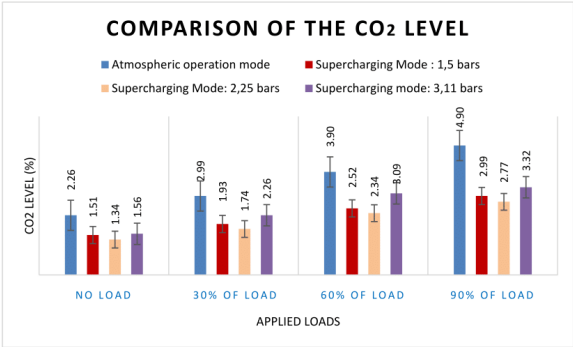

Figure 20. Carbon dioxide reduction due to hybrid forced induction in comparison to atmospheric mode operation.

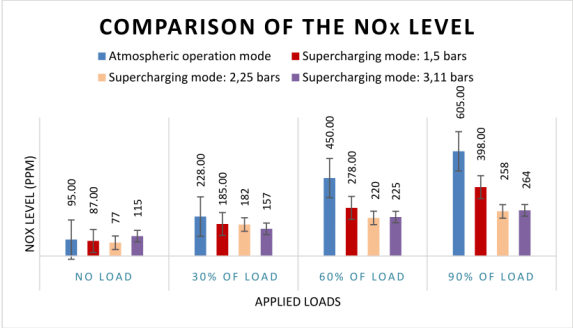

Figure 21. Nitrogen Oxyde reduction due to hybrid forced induction in comparison to atmospheric mode operation.

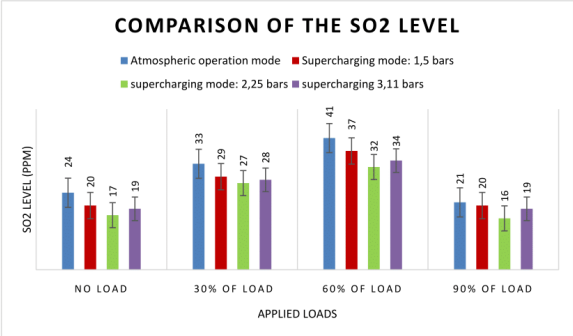

Figure 22. Illustration of the sulfur dioxide reduction due to hybrid forced induction in comparison to atmospheric mode operation.

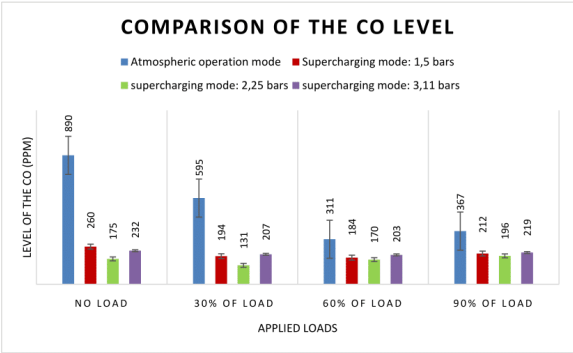

Figure 23. Illustration of the carbon monoxide reduction due to hybrid forced induction in comparison to atmospheric mode operation.

Figure 21 illustrates the evolution of the nitrogen oxide due to hybrid forced induction as compared to an atmospheric mode operating engine. It has been found that the NOx rate has decreased by an amount of 20% under low loads (≤30%) and continue to drop further to reach 50% - 55% approximately under 60% and 90% of applied loads due to the increase in combustion temperature associated with higher engine load. In addition, like carbon dioxide, the best NOx drop was observed at a 2.25 bars pressure and this for the different applied loads.

The characteristics of SO_2 emission are shown in Figure 22. There is a decrease of sulfur dioxide emission on increase in the engine load. As shown in Figure 22, the SO_2 decrease by 18% approximately under low loads (≤30%) at 2.25 bars before to decrease further under medium (60%) and high loads (90%) by an amount of 22% - 24%. The higher combustion temperature at higher engine load combined with the reduction in fuel consumption due to the supercharging mode contributes the general decreasing trend. It can also be seen that the lowest recorded gas emission is below 2.3 bars due to the best ratio of Air/Fuel, efficiency of the system and combustion temperature. The increasing of the emission under high loads can be related to the efficiency of the system on the one hand, and to the quantity of fuel injected on the other hand.

It has been noted that losses increase as the load increases, while the efficiency diminishes with an increase of the load. Finally, Figure 23 shows the variation of carbon monoxide emission with engine load due to hybrid forced induction in comparison to atmospheric mode operation. It has been found that the CO emission during the atmospheric mode operation is highest at low loads (≤30%) due to incomplete combustion of air-fuel mixture. On the other hand, supercharging with compressed air at 2.25 bars pressure reduces CO emissions by an amount of 45% under a medium and high load (60% - 90%) and up to 65% under low loads (0% - 30%). According to [20] and [21], it is possible that the

excess oxygen contained in the fuel due to the supercharging enhances complete combustion in the cylinder and reduces further the CO emission.

8. Conclusions

The hybrid wind-diesel-compressed air system represents an innovative, ecological and very promising concept. The technical, economical and commercial potential of this system is very important for isolated regions in Quebec and elsewhere in the world as it is designed to eliminate most constraints that wind energy development encounters [7].

The test bench at UQAC has enabled us to experimentally validate the gain in power, efficiency, fuel economy and greenhouse gases emissions that a supplementary forced induction can offer to a 7.5 kW thermal power/4.5kW electrical power diesel engine. The obtained results have shown that in an interval between 2.25 and 2.83 bars, the efficiency of the engine can increase to approximately 50% if it is in free run mode as compared to an atmospheric engine. This gain becomes significant at full load where it reaches a 130% level. Furthermore, application of supercharging of diesel engine with compressed air energy has shown a positive impact on GHGs reduction for CO_2, NO_x, SO_2, and CO by an average of 40%, 35%, 21% and 50% respectively. This has never been achieved before. In our future work, we will carry out extra tests by maintaining comparable lambda circumstances and further researching PM emissions.

Conflicts of Interest

The authors declare no conflicts of interest regarding the publication of this paper.

References

[1] World Wind Energy Association (2008) World Wind Energy Report 2008. http://educypedia.karadimov.info/library/worldwindenergyreport2008_s.pdf

[2] Gouvernement du Québec (2005) Énergie et Ressources naturelles Québec. https://mern.gouv.qc.ca/energie/energie-eolienne/

[3] Pinard, J.P. and Weis, T.M. (2003) Pre-Feasibility Analysis of Wind-Energy for Inuvialuit Region in the Northwest Territories. Aurora Research Institute, Report. https://nwtresearch.com/sites/default/files/inuvialuit-region-wind-energy-pre-feasibility-study.pdf

[4] Issa, M., Ibrahim, H., Lepage, R. and Ilinca, A. (2019) A Review and Comparison on Recent Optimization Methodologies for Diesel Engines and Diesel Power Generators. *Journal of Power and Energy Engineering*, **7**, 31-56. https://doi.org/10.4236/jpee.2019.76003

[5] Issa, M., Fiset, J., Ibrahim, H. and Ilinca, A. (2019) Eco-Friendly Selection of Diesel Generator Based on Genset-Synchro Technology for Off-Grid Remote Area Application in the North of Quebec. *Energy and Power Engineering*, **11**, 232-247. https://doi.org/10.4236/epe.2019.115015

[6] Weis, T.M. and Ilinca, A. (2008) The Utility of Energy Storage to Improve the Economics of Wind-Diesel Power Plants in Canada. *Renewable Energy*, **33**, 1544-1557.

https://doi.org/10.1016/j.renene.2007.07.018

[7] Weis, T.M., Ilinca, A. and Pinard, J.P. (2008) Stakeholders' Perspectives on Barriers to Remote Wind-Diesel Power Plants in Canada. *Energy Policy*, **36**, 1611-1621. https://doi.org/10.1016/j.enpol.2008.01.004

[8] Ibrahim, H., Ilinca, A., Younès, R., Perron, J. and Basbous, T. (2007) Study of a Hybrid Wind-Diesel System with Compressed Air Energy Storage. 2007 *IEEE Canada Electrical Power Conference*, Montreal, 25-26 October 2007, 320-325. https://doi.org/10.1109/EPC.2007.4520350

[9] Union of Concerned Scientists (2013) Ramping up Renewables: Energy You Can Count on. https://www.ucsusa.org/resources/ramping-renewables

[10] Solar Reserve (2010) Rice. http://www.solarreserve.com/what-we-do/csp-projects/rice-army-airfield/

[11] Kottenstette, R., and Cottrell, J. (2003) Hydrogen Storage in Wind Turbine Towers. NREL/TP-500-34656. National Renewable Energy Laboratory, Golden, CO. http://www.nrel.gov/docs/fy03osti/34656.pdf

[12] Beacon Power (2013) Islands and Isolated Grids. http://www.beaconpower.com/

[13] Imre, G. (2013) Smoothing Renewable Wind Energy in Texas. Department of Energy. http://energy.gov/articles/smoothing-renewable-wind-energy-texas

[14] Electricity Storage Association (2013) Technologies of Energy Storage. http://www.electricitystorage.org/

[15] Ibrahim, H., Ilinca, A. and Perron, J. (2007) Comparison and Analysis of Different Energy Storage Techniques Based on Their Performance Index. 2007 *IEEE Canada Electrical Power Conference*, Montreal, 25-26 October 2007, 393-398. https://doi.org/10.1109/EPC.2007.4520364

[16] Ibrahim, H., Ilinca, A. and Perron, J. (2008) Energy Storage Systems—Characteristics and Comparisons. *Renewable and Sustainable Energy Reviews*, **12**, 1221-1250. https://doi.org/10.1016/j.rser.2007.01.023

[17] HowStuffWorks (2000) What Is the Difference between a Turbocharger and a Supercharger on a Car's Engine?

[18] Feneley, A.J., Pesiridis, A. and Andwari, A.M. (2017) Variable Geometry Turbocharger Technologies for Exhaust Energy Recovery and Boosting—A Review. *Renewable and Sustainable Energy Reviews*, **71**, 959-975. https://doi.org/10.1016/j.rser.2016.12.125

[19] Basbous, T. (2013) Hybridation pneumatique d'un moteur diesel en vue de son utilisation dans un système hybride éolien-diesel avec stockage d'énergie sous forme d'air comprimé. Université du Québec à Chicoutimi, Québec. https://doi.org/10.1522/030565288

[20] Ibrahim, H., Younès, R., Ilinca, A., Dimitrova, M. and Perron, J. (2010) Study and Design of a Hybrid Wind-Diesel-Compressed Air Energy Storage System for Remote Areas. *Applied Energy*, **87**, 1749-1762. https://doi.org/10.1016/j.apenergy.2009.10.017

[21] Ibrahim, H., Younès, R. and Ilinca, A. (2007) Optimal Conception of a Hybrid Generator of Electricity. CANCAM02007 ETS-39, Toronto, Canada, 358-359.

[22] Issa, M., Ibrahim, H., Ilinca, A. and Hayyani, M. (2019) A Review and Economic Analysis of Different Emission Reduction Techniques for Marine Diesel Engines. *Open Journal of Marine Science*, **9**, 148-171. https://doi.org/10.4236/ojms.2019.93012

[23] Issa, M., Ait-Yahia, K., Lepage, R., Ibrahim, H., Ilinca, A. and Ghandour, M. (2019) Integrated A Variable Frequency Drive for a Diesel-Generating Set Using the Genset-Synchro Concept. *International Journal of Engineering Research & Technology*, **8**, 232-239.

[24] Issa, M., Beaulac, P., Ibrahim, H. and Ilinca, A. (2019) Marinization of a Two-Stage Mixed Structured Packing Scrubber for Sox Abatement and CO_2 Capture. *International Journal of Advanced Research*, **7**, 73-82. https://doi.org/10.21474/IJAR01/8793

[25] Mobarra, M., Fiset, J. and Ilinca, A. (2017) Modeling and Optimization of the Energy Production Based on Eo-Synchro. *Power Engineer*, **3**, 3-9.

CHAPITRE XI

CONCLUSIONS ET PERSPECTIVES

XI.1 CONCLUSIONS

L'objectif de ce travail a été d'explorer les différentes techniques permettant l'optimisation de l'efficacité énergétique, opérationnelle et écologique des GED dans les communautés isolées canadiennes d'une part, et pour l'industrie de transport maritime d'autre part.

La revue de littérature réalisée dans la première partie de la thèse nous a permis de poser les fondements théoriques pour la proposition et la conception des nouveaux concepts. Trois axes ont été particulièrement abordés dans notre recherche. Le premier vise à optimiser l'efficacité des GED existant dans des centrales autonomes. Le deuxième axe s'est articulé autour de la question du profit des épurateurs à gaz de postcombustion pour réduire l'empreinte écologique dans l'industrie du transport maritime. Enfin le troisième axe met en œuvre les possibilités de réduire la consommation de carburant et les GES dans les communautés isolées par la proposition et la conception d'un nouvel alternateur avec le stator tournant d'un part, et par la validation expérimentale d'un système hybride éolien-diesel avec stockage d'énergie sous forme d'air comprimé.

Dans la première partie, afin d'atteindre notre but, un banc d'essai en collaboration avec le centre de recherche d'innovation maritime nous a permis d'élaborer une étude approfondie sur la détection des indices de fonctionnement d'un GED en sous-performance. Or, la plupart des travaux de recherches portant sur la surveillance d'état de santé des GED dans les centrales électriques sont basés sur des techniques de maintenance conditionnelle pour

la détection des défauts, généralement associées à des composants spécifiques du moteur diesel, alors que le contrôle de la performance énergétique globale des GED n'a jamais été développé.

Ayant choisi de développer une stratégie de maintenance préventive pour l'optimisation énergétique globale et d'aborder le problème de détection et de correction de fonctionnement en sous-performance, il a été nécessaire de passer par une première étape d'analyse des phénomènes à l'origine des dégradations des performances du GED afin d'être en mesure de proposer la solution adéquate.

Il a été démontré dans cette première partie que la concentration de SO_2 et le pourcentage de soufre (S) apparaissent comme les meilleurs indices pour prévenir un fonctionnement en sous-performance avec la température des gaz d'échappement. De plus, la consommation du carburant d'un GED par rapport à la charge appliquée peut indiquer que le GED est soumis à une faible charge. L'originalité de cette première partie réside dans la possibilité d'élaborer un algorithme de détection et de correction de sous-performance capable de lire et prévenir un fonctionnement en sous-performance et d'agir par la suite sur une charge secondaire pour forcer le GED à fonctionner dans un niveau de puissance efficace.

Dans la deuxième partie, il a été démontré par les tests menés au sein d'Innovation maritime et de l'entreprise Genset-Synchro que l'utilisation d'un épurateur à gaz de postcombustion en boucle fermée et /ou en boucle ouverte, élimine de 98% le taux du SO_x et de 50% le taux du CO_2 émis par les gaz d'échappement des moteurs diesel. De plus, il a été démontré que l'utilisation des épurateurs à gaz est le seul moyen jusqu'au moment de la rédaction de cette thèse, capable de rencontrer les exigences adoptées par l'OMI pour réduire l'empreinte écologique des navires avec la possibilité de continuer à utiliser le mazout lourd comme carburant principal. Cette technique s'avère intéressante aussi pour des centrales thermiques au bord de la mer, dont l'utilisation de l'eau salée permettra de réagir avec l'oxyde de soufre des gaz d'échappement pour former de l'acide sulfurique sans l'obligation d'utiliser la soude caustique, tel que c'est le cas dans des épurateurs en boucle fermée. Cependant, il a été démontré aussi que le cycle de vie des installations de désulfuration des gaz de combustion dépend principalement des matériaux utilisés et de

leur résistance à la corrosion. En utilisant des alliages inoxydables ou alliages inadaptés, la composition des gaz d'échappement provoque de la corrosion ce qui peut ainsi rapidement occasionner des dommages ou une panne de toute l'installation.

Pour conclure, cette deuxième partie, l'étude techno-économique pour les différentes technologies qui a été menée durant cette thèse, a démontré que l'utilisation de la nouvelle génération des GED fonctionnant en bicarburant (diesel/Methanol) coûtent le moins cher, alors que les systèmes de lavage de gaz sont les plus chers à exploiter et à maintenir. Il a été démontré aussi que l'utilisation d'un catalyseur pour réduire les émissions du NO_x par 95% , vient en deuxième position au niveau des prix à exploiter (après les laveurs de gaz) alors que l'utilisation des gaz naturels liquéfiés ou le méthanol offrent une très bonne réduction des GES et une réduction de coût de 31% annuellement par rapport à l'utilisation du fioul lourd. Toutefois, ils sont confrontés à des problèmes techniques au niveau du stockage et de l'exploitation due à la grosseur de leurs réservoirs de stockage (4 fois plus grands). Il a été démontré aussi que le jumelage de plusieurs techniques peut s'avérer intéressante pour optimiser les moteurs diesel de propulsion et des GED existant à bord des navires marchands afin de rencontrer la norme MARPOL-Annexe VI.

Dans la dernière partie de notre travail, le banc d'essais réalisé à l'Université du Québec à Chicoutimi (UQAC) a permis de valider expérimentalement le gain en termes de puissance, de rendement et d'économie de carburant qu'une suralimentation supplémentaire pourrait apporter à un moteur diesel de 7.5 kW de puissance thermique et 4.5 kW de puissance électrique. Les résultats obtenus pour les différents tests ont montré que, dans un intervalle de pression variant entre 2.3 et 2.83 bars, le rendement du moteur peut augmenter d'environ 50% s'il tourne à vide comparé à un moteur atmosphérique. Ce gain devient remarquable à pleine charge où il atteint le seuil de 130%. En revanche, la suralimentation du moteur à 3.11 bars apporte un gain d'environ 78% à fortes charges (4.5 kW) comparé à un moteur atmosphérique. Dans la même catégorie de comparaison et pour une charge maximale de 4.5 kW, le moteur économise près de 17% du carburant s'il est suralimenté à 2.3 bars de pression, d'environ 24% s'il est suralimenté à 2.83 bars et 27% si la pression à l'admission devient 3.11 bars.

Comparée à un moteur suralimenté par turbocompresseur, la suralimentation avec 2.83 bars de pression apporte un gain maximal du rendement d'environ 47% comparé à celui réalisé à 2.3 bars comme pression de suralimentation et qui ne dépasse pas le 38% en moyenne. Cependant, le fait d'injecter de l'air comprimé à 3.11 bars de pression à l'admission du moteur diesel apporte un gain trop faible (10%) pour la plage du fonctionnement (de 1.5 à 4.5 kW). Dans la même catégorie de comparaison, les résultats obtenus du banc d'essais montrent que plus la pression à l'admission augmente, meilleure est l'économie de fuel réalisée. En effet, pour une charge de 4.5 kW de puissance, le moteur économise près de 22% du carburant s'il est suralimenté à 2.3 bars, d'environ 29% s'il est suralimenté à 2.83 bars et 33% si la pression à l'admission devient 3.11 bars. Aussi, les tests expérimentaux ont révélé que l'économie en carburant réalisée avec une suralimentation externe appliquée sur un moteur turbocompressé reste toujours supérieure et avantageuse à celle obtenue si la suralimentation externe est appliquée sur un moteur atmosphérique et ceci sur toute la plage des charges. De plus, la suralimentation a démontré un impact positif sur les émissions des gaz d'échappement. Il a été constaté une baisse de 25-35% des GES ce qui fait de la suralimentation une solution très intéressante et favorable pour les communautés isolées à haute pénétration éolienne.

Pour conclure, les trois bancs d'essais réalisés avec l'entreprise Genset-Synchro concernant l'utilisation d'un nouvel alternateur avec un stator tournant, ont démontrés qu'il est possible grâce à cette nouvelle technologie, de convertir les GED fonctionnant à vitesse fixe vers des GED à vitesse variable permettant ainsi au moteur diesel de fonctionner directement en relation avec la demande de la charge électrique. Des économies en carburant et en GES allant jusqu'à 15% ont été enregistrée sous une température ambiante de 23ºC avec les deux premiers prototypes, soit le 75kW et le 500kW, alors que le troisième prototype (600kW) a été testé durant 3000 heures dans le nord du Québec sous des températures hivernales atteignant le -31ºC.

Malgré des températures hivernales trop froides, le concept de Genset-Synchro a pu réaliser des économies en carburant et en GES allant jusqu'à 5%, une économie évaluée à 18500$ pour la communauté isolée pour la même période d'électrification de l'an passé.

Due à l'absence d'un système automatisé pour assurer l'ajustement de la vitesse statorique, nous avons pu développer et démontrer par des essais expérimentaux la fonctionnalité d'un nouveau système automatisé permettant d'ajuster la vitesse statorique de l'alternateur en fonction de la charge appliquée. Nous avons démontré qu'il est possible de minimiser l'écart de la vitesse maximale lors de la réception de la charge sur une génératrice de 500kW et de satisfaire à la classification de performance G2 de la norme ISO 8528-partie 5.

Force de conclure que ce système n'a pas besoin de ramener des modifications sur l'architecture du moteur diesel d'une part, et peut fonctionner avec le stator fixe dans le cas où le moteur de compensation entrainant le stator subi une panne (ex. courroie coupée, bearing défectueux, etc.) d'autre part. La continuité du service de l'électrification demeure non coupée.

XI.2 PERSPECTIVES

Cette thèse constitue une base théorique complète sur les différentes technologies permettant l'optimisation de l'efficacité énergétique, écologique et opérationnelle des moteurs et des GED. Bien que plusieurs validations expérimentales aient été menées durant cette thèse, plusieurs développements ultérieurs s'avèrent nécessaires au travers des exigences des systèmes de contrôle et de sécurité.

Les quelques propositions qui suivent constituent des extensions possibles de notre travail qu'il est nécessaire de mener à bien pour compléter les différentes démarches.

Concernant la détection des sous-performances d'un GED et pour la poursuite de ce travail, plusieurs pistes peuvent être envisagées et peuvent faire, par conséquent, l'objet d'un futur projet de recherche. Il pourrait s'agir par exemple de :

1) Valider si les indicateurs de sous-performances liés au soufre demeurent pertinents, même en faisant varier la concentration du soufre dans le carburant ;
2) Évaluer la pression des gaz d'échappement en fonction des charges appliquées ;
3) Évaluer le temps nécessaire pour stabiliser la température des gaz d'échappement ;
4) Prendre des nouvelles données en considérant la température de l'engin et la température de l'huile ;
5) Jumeler la partie de détection de sous-performances et la partie de correction ;

6) Valider par plusieurs essais dans différentes conditions environnementales et opérationnelles avec divers types et profils de charges les indices de détection ;
7) Créer une carte de détection intelligente à base de réseau de neurones artificiel (RNA)

À propos de l'épurateur à gaz de postcombustion, il sera intéressant de mener une étude théorique approfondie sur les coûts d'installation en fonction de la puissance des moteurs et des GED utilisés d'une part, et d'explorer d'autres types de garnissage afin d'étudier l'impact de la chute de pression dans la colonne en fonction des types de garnissage et de la puissance appliquée.

Concernant l'alternateur de Genset-Synchro, il est fortement recommandé de faire une analyse détaillée sur les coûts de modifications à apporter sur un GED existant en fonction de sa puissance d'une part, et sur la limite de son application (voire la puissance maximale des alternateurs qui peuvent subir des modifications à leurs stators).

Finalement, pour ce qui est du système SHEDAC, il sera intéressant de :

1) Valider sur un GED de plus grande taille (voir 50kW et plus) si les données enregistrées sur le banc d'essai de l'UQAC tiennent toujours ;
2) Développer une stratégie de contrôle pour le système dans sa globalité. Cette stratégie devrait permettre au moteur diesel de régler la quantité du carburant à injecter en fonction de la pression et du débit massique d'air comprimé. Il faut que la carte de contrôle ou la stratégie proposée régisse le fonctionnement du gouverneur de la vitesse de rotation du GED en intégrant deux nouvelles entrées dans le calculateur électronique, soit le débit et la pression d'air à l'admission du moteur.

RÉFÉRENCES (HORS ARTICLES)

[1] Ibrahim, H. (2010). Étude et conception d'un générateur hybride d'électricité de type éolien-diesel avec élément de stockage d'air comprimé. Université du Québec à Chicoutimi.

[2] Saad, Y. (2018). Gestion optimale des systèmes hybrides pour la production de l'énergie dans les sites isolés (Doctoral dissertation). Université de Technologie Belfort - Montbéliard, 2018.

[3] Basbous, T. (2013). Hybridation pneumatique d'un moteur diesel en vue de son utilisation dans un système hybride éolien-diesel avec stockage d'énergie sous forme d'air comprimé. Université du Québec à Chicoutimi.

[4] Azzara, A., Rutherford, D., & Wang, H. (2014). Feasibility of imo annex vi tier iii implementation using selective catalytic reduction. The International Council on Clean Transportation, Paper, 4.

[5] Schinas, O., & Stefanakos, C. N. (2014). Selecting technologies towards compliance with MARPOL Annex VI: The perspective of operators. Transportation Research Part D: Transport and Environment, 28, 28-40.

[6] N. Barris, "Stratégie de commande optimale de la production électrique dans un site isolé," École polytechnique de Montréal, 2015.

[7] Y. Saad, R. Younes, S. Abboudi, A. Ilinca, and C. Nohra, "Progress in Energy Generation For Canadian Remote Sites," 2016.

[8] Y. Rafic, B. Tammam, and I. Adrian, "Optimal Design of an Hybrid Wind-Diesel System with Compressed Air Energy Storage for Canadian Remote Areas," INTECH, 2012.

[9] M. Arriaga, C. A. Cañizares, and M. Kazerani, “Renewable Energy Alternatives for Remote Communities in Northern Ontario, Canada,” IEEE Trans. Sustain. Energy, vol. 4, no. 3, pp. 661–670, Jul. 2013

[10] M. Arriaga, E. Nasr, and H. Rutherford, “Renewable Energy Microgrids in Northern Remote Communities,” IEEE Potentials, vol. 36, no. 5, pp. 22–29, Sep. 2017

[11] N. Günter and A. Marinopoulos, “Energy storage for grid services and applications: Classification, market review, metrics, and methodology for evaluation of deployment cases,” J. Energy Storage, vol. 8, no. Supplement C, pp. 226–234, 2016.

[12] VI, Revised Marpol Annex. "Regulations for the Prevention of Air Pollution from Ships. Resolution MEPC. 176 (58)." International Maritime Organization (2008).

[13] Becker, R. (1997). MARPOL 73/78: An Overview in International Environmental Enforcement. Geo. Int'l Envtl. L. Rev., 10, 625.

[14] CLEARSEAS - https://clearseas.org/fr/pollution-atmospherique/

[15] Lee, D.S. (2017), Update of Maritime Greenhouse Gas Emission Projections, rapport de CE Delft Report, p. 3-4. [En anglais seulement]

[16] E. D. Tufte, "Impacts of Low Load Operation of Modern Four-Stroke Diesel Engines in Generator Configuration," 2014

[17] J. Wilson and J. Calow, "Cylinder bore polishing in automotive diesel engines-A progress report on a European study," SAE Technical Paper 0148-7191, 1976.

[18] Elsebaay, A., Ramadan, M., & Adma, M. A. A. (2017). Studying the Effect of Non-Linear Loads Harmonics on Electric Generator Power Rating Selection. European Scientific Journal, 13(18), 1857-7881.

[19] RAU, Bernd. Versuche zur Thermodynamik und Gemischbildung beim Kaltstart eines direkteinspritzenden Viertakt-Dieselmotors. 1975. Thèse de doctorat. Verlag nicht ermittelbar.

[20] D.-I. H. Houben and D.-I. B. M. Rottner, "Influence of modern diesel cold start systems on the cold start, warm-up and emissions of diesel engines," 2008.

[21] F. Schäfer, Handbuch Verbrennungsmotor: Grundlagen, Komponenten, Systeme, Perspektiven: Springer-Verlag, 2005.

[22] Randimbisoa, M. T. (2011). Formation de gels et d'émulsions dans le circuit de blow-by des moteurs à combustion interne (Doctoral dissertation, Université Pierre et Marie Curie-Paris VI).

[23] NAHIM, Hassan Moussa. Contribution à la modélisation et à la prédiction de défaillances sur les moteurs Diesel marins. 2016. Thèse de doctorat.

[24] Sayin, C. (2010). Engine performance and exhaust gas emissions of methanol and ethanol–diesel blends. Fuel, 89(11), 3410-3415.

[25] Brynolf, S., Fridell, E., & Andersson, K. (2014). Environmental assessment of marine fuels: liquefied natural gas, liquefied biogas, methanol and bio-methanol. Journal of cleaner production, 74, 86-95.

[26] ELLIS, Joanne et TANNEBERGER, Kim. Study on the use of ethyl and methyl alcohol as alternative fuels in shipping. Eur. Marit. Saf. Agency, 2015.

[27] López-Aparicio, S., & Tønnesen, D. A. (2015). Pollutant emissions from LNG fuelled ships. Assessment and recommendations.

[28] Authority, D. M., Bech, M. S., AB, Å. I., & AB, S. S. (2012). North European LNG Infrastructure Project. A feasibility study for an LNG filling station infrastructure and test of recommendations, Copenhagen.

[29] Alahmer, A., Yamin, J., Sakhrieh, A., & Hamdan, M. A. (2010). Engine performance using emulsified diesel fuel. Energy Conversion and Management, 51(8), 1708-1713.

[30] Alahmer, A. (2013). Influence of using emulsified diesel fuel on the performance and pollutants emitted from diesel engine. Energy Conversion and Management, 73, 361-369.

[31] Li, T., Gao, Y., Wang, J., & Chen, Z. (2014). The Miller cycle effects on improvement of fuel economy in a highly boosted, high compression ratio, direct-injection gasoline engine: EIVC vs. LIVC. Energy conversion and management, 79, 59-65.

[32] Ge, Y., Chen, L., Sun, F., & Wu, C. (2005). Effects of heat transfer and friction on the performance of an irreversible air-standard Miller cycle. International Communications in Heat and Mass Transfer, 32(8), 1045-1056.

[33] Bedford, F., Rutland, C., Dittrich, P., Raab, A., & Wirbeleit, F. (2000). Effects of direct water injection on DI diesel engine combustion (No. 2000-01-2938). SAE Technical Paper.

[34] Maiboom, A., Tauzia, X., & Hétet, J. F. (2008). Experimental study of various effects of exhaust gas recirculation (EGR) on combustion and emissions of an automotive direct injection diesel engine. Energy, 33(1), 22-34.

[35] Benajes, J., Reyes, E., & Lujan, J. M. (1996). Modelling study of the scavenging process in a turbocharged diesel engine with modified valve operation. Proceedings of the Institution of Mechanical Engineers, Part C: Journal of Mechanical Engineering Science, 210(4), 383-393.

[36] Gonca, G., & Sahin, B. (2016). The influences of the engine design and operating parameters on the performance of a turbocharged and steam injected diesel engine running with the Miller cycle. *Applied Mathematical Modelling*, *40*(5-6), 3764-3782.

[37] Kamo, R., Mavinahally, N. S., Kamo, L., Bryzik, W., & Reid, M. (1998). Emissions comparisons of an insulated turbocharged multi-cylinder miller cycle diesel engine (No. 980888). SAE Technical Paper.

[38] Fukuzawa, Y., Shimoda, H., Kakuhama, Y., Endo, H., & Tanaka, K. (2001). Development of high efficiency Miller cycle gas engine. Stroke, 2000, 180.

[39] Holmer, E. (1989). U.S. Patent No. 4,815,423. Washington, DC: U.S. Patent and Trademark Office.

[40] Thitakamol, B., Veawab, A., & Aroonwilas, A. (2007). Environmental impacts of absorption-based CO2 capture unit for post-combustion treatment of flue gas from coal-fired power plant. International Journal of Greenhouse Gas Control, 1(3), 318-342.

[41] Brynolf, S., Magnusson, M., Fridell, E., & Andersson, K. (2014). Compliance possibilities for the future ECA regulations through the use of abatement technologies or change of fuels. Transportation Research Part D: Transport and Environment, 28, 6-18.

[42] Turner, D. R., Hassellöv, I. M., Ytreberg, E., & Rutgersson, A. (2017). Shipping and the environment: smokestack emissions, scrubbers and unregulated oceanic consequences. Elementa-Science of the Antropocene, 5.

[43] Van Setten, B. A., Makkee, M., & Moulijn, J. A. (2001). Science and technology of catalytic diesel particulate filters. Catalysis Reviews, 43(4), 489-564.

[44] Konstandopoulos, A. G., Kostoglou, M., Skaperdas, E., Papaioannou, E., Zarvalis, D., & Kladopoulou, E. (2000). Fundamental studies of diesel particulate filters: transient loading, regeneration and aging. SAE transactions, 683-705.

[45] Clausen, N. B. (2009). Marine diesel engines: How efficient can a two-stroke engine be. In STG ship efficiency conference.

[46] DNV, G., SAFER, S., & GREENER, D. (2018). Global Sulphur Cap 2020. Compliance options and implications for shipping–focus on scrubbers, Extended and Updated in.

[47] Neeft, J. P., Makkee, M., & Moulijn, J. A. (1996). Diesel particulate emission control. Fuel processing technology, 47(1), 1-69.

[48] Nichols, J. M., Pohl, B. P., Dawe, D. J., Armstrong, O. J., Lohr, C. B., McDaniel, L. T., ... & Stewart, T. L. (2011). U.S. Patent No. 7,959,533. Washington, DC: U.S. Patent and Trademark Office.

[49] CVT CORP : https://www.cvtcorp.com/

[50] Chen, T. F., & Sung, C. K. (2000). Design considerations for improving transmission efficiency of the rubber V-belt CVT. International Journal of Vehicle Design, 24(4), 320-333.

[51] Chen, T. F., Lee, D. W., & Sung, C. K. (1998). An experimental study on transmission efficiency of a rubber V-belt CVT. Mechanism and machine theory, 33(4), 351-363.

[52] Zinner, K. A. (2012). Supercharging of internal combustion engines: additional. Springer Science & Business Media.

[53] Roy, M. M., Tomita, E., Kawahara, N., Harada, Y., & Sakane, A. (2010). An experimental investigation on engine performance and emissions of a supercharged H2-diesel dual-fuel engine. International Journal of Hydrogen Energy, 35(2), 844-853.

[54] Basbous, T., Younes, R., Ilinca, A., & Perron, J. (2012). Pneumatic hybridization of a diesel engine using compressed air storage for wind-diesel energy generation. Energy, 38(1), 264-275.

[55] Wang, X., Tsao, T. C., Tai, C., Kang, H., & Blumberg, P. N. (2009). Modeling of compressed air hybrid operation for a heavy-duty diesel engine. Journal of Engineering for Gas Turbines and Power, 131(5), 052802.

[56] Mayr, M. (2013). U.S. Patent No. 8,549,855. Washington, DC: U.S. Patent and Trademark Office.

[57] Ibrahim, H., Younès, R., Ilinca, A., Dimitrova, M., & Perron, J. (2010). Study and design of a hybrid wind–diesel-compressed air energy storage system for remote areas. Applied Energy, 87(5), 1749-1762.

[58] Kim, Y. M., & Favrat, D. (2010). Energy and exergy analysis of a micro-compressed air energy storage and air cycle heating and cooling system. Energy, 35(1), 213-220.

[59] Trajkovic, S., Tunestål, P., & Johansson, B. (2009). Simulation of a pneumatic hybrid powertrain with VVT in GT-Power and comparison with experimental data (No. 2009-01-1323). SAE Technical Paper.

[60] Trajkovic, S., Tunestal, P., & Johansson, B. (2013). A study on compression braking as a means for brake energy recovery for pneumatic hybrid powertrains. International Journal of Powertrain, 2(1), 26-51.

[61] BBA: https://www.canadianconsultingengineer.com

[62] Walker, S. (2015). Mine Power Options. Engineering and Mining Journal, 216(7), 34.

[63] Lindstad, H. E., & Eskeland, G. S. (2016). Environmental regulations in shipping: Policies leaning towards globalization of scrubbers deserve scrutiny. Transportation Research Part D: Transport and Environment, 47, 67-76.

[64] Fridell, E., & Salo, K. (2016). Measurements of abatement of particles and exhaust gases in a marine gas scrubber. Proceedings of the Institution of Mechanical Engineers, Part M: Journal of Engineering for the Maritime Environment, 230(1), 154-162.

[65] Alonso, D. F., Goncalves, J. A. S., Azzopardi, B. J., & Coury, J. R. (2001). Drop size measurements in Venturi scrubbers. Chemical Engineering Science, 56(16), 4901-4911.

[66] Viswanathan, S. (1997). Modeling of Venturi scrubber performance. Industrial & engineering chemistry research, 36(10), 4308-4317.

[67] Yung, S. C., Barbarika, H. F., & Calvert, S. (1977). Pressure loss in venturi scrubbers. Journal of the Air Pollution Control Association, 27(4), 348-351.

[68] Iliuta, I., & Larachi, F. (2019). Modeling and Simulations of NOx and SO2 Seawater Scrubbing in Packed-bed Columns for Marine Applications. Catalysts, 9(6), 489.

[69] ISSA, M., FISET, J., MOBARRA, M., IBRAHIM, H., & ILINCA, A. (2018). Optimizing the Performance of a 500kW Diesel Generator: Impact of the Eo-Synchro Concept on Fuel Consumption and Greenhouse Gases. Power Engineer, 23, 22-31.

[70] MOBARRA, M., FISET, J., & ILINCA, A. (2017). Modeling and optimization of the energy production based on Eo-Synchro. Power Engineer, 3.

[71] Issa, M., Fiset, J., Ibrahim, H., & Ilinca, A. (2019). Eco-Friendly Selection of Diesel Generator Based on Genset-Synchro Technology for Off-Grid Remote Area Application in the North of Quebec.

[72] Mobarra, M., Issa, M., Rezkallah, M., & Ilinca, A. (2019). Performance Optimization of Diesel Generators Using Permanent Magnet Synchronous Generator with Rotating Stator. Energy and Power Engineering, 11(07), 259.

[73] Jain, A. K., VT, R., Kumar, V. K., & Guruswamy, G. (2010). Diesel engine driven stand-alone variable speed constant frequency slip ring induction generator-theory and experimental results.

[74] Nayar, C. (2012). Innovative remote micro-grid systems. International Journal of Environment and Sustainability, 1(3).

[75] Nikolic, D., Negnevitsky, M., & de Groot, M. (2015, September). Effect of the diesel engine delay on stability of isolated power systems with high levels of renewable energy penetration. In 2015 international symposium on smart electric distribution systems and technologies (EDST) (pp. 70-73). IEEE.

[76] Nayar, C. V. (2010). High renewable energy penetration diesel generator systems. INTECH Open Access Publisher.

[77] Boldea, I. (2015). Synchronous generators. CRC Press.

[78] Gratadour, M. (1991). Application de la suralimentation aux moteurs. Ed. Techniques Ingénieur.

[79] Ibrahim, H., Ilinca, A., Rousse, D., Dutil, Y., & Perron, J. (2012). Analyse des systèmes de génération d'électricité pour les sites isolés basés sur l'utilisation du stockage d'air comprimé en hybridation avec un jumelage éolien-diesel.

[80] Ibrahim, H., Dimitrova, M. H., Ilinca, A., & Perron, J. (2010). Optimisation de l'efficacité du moteur diesel pour un système hybride éolien-diesel: Validation expérimentale.

[81] Ibrahim, H., Ilinca, A., Younes, R., Perron, J., & Basbous, T. (2007, October). Study of a hybrid wind-diesel system with compressed air energy storage. In 2007 IEEE Canada Electrical Power Conference (pp. 320-325). IEEE.

[82] Saad, Y., Nohra, C., Younes, R., Abboudi, S., Ilinca, A., Ibrahim, H., & Feger, Z. (2017, October). Study of an optimized wind-diesel hybrid system for canadian remote sites. In 2017 IEEE Electrical Power and Energy Conference (EPEC) (pp. 1-6). IEEE.

[83] Basbous, Tammam. Étude de faisabilité d'un jumelage éolien-diesel avec stockage d'énergie sous forme d'air comprimé. Diss. Université du Québec à Rimouski, 2009.

ANNEXE I

CIRCUIT DE CONTRÔLE –VARIATEUR DE FRÉQUENCE

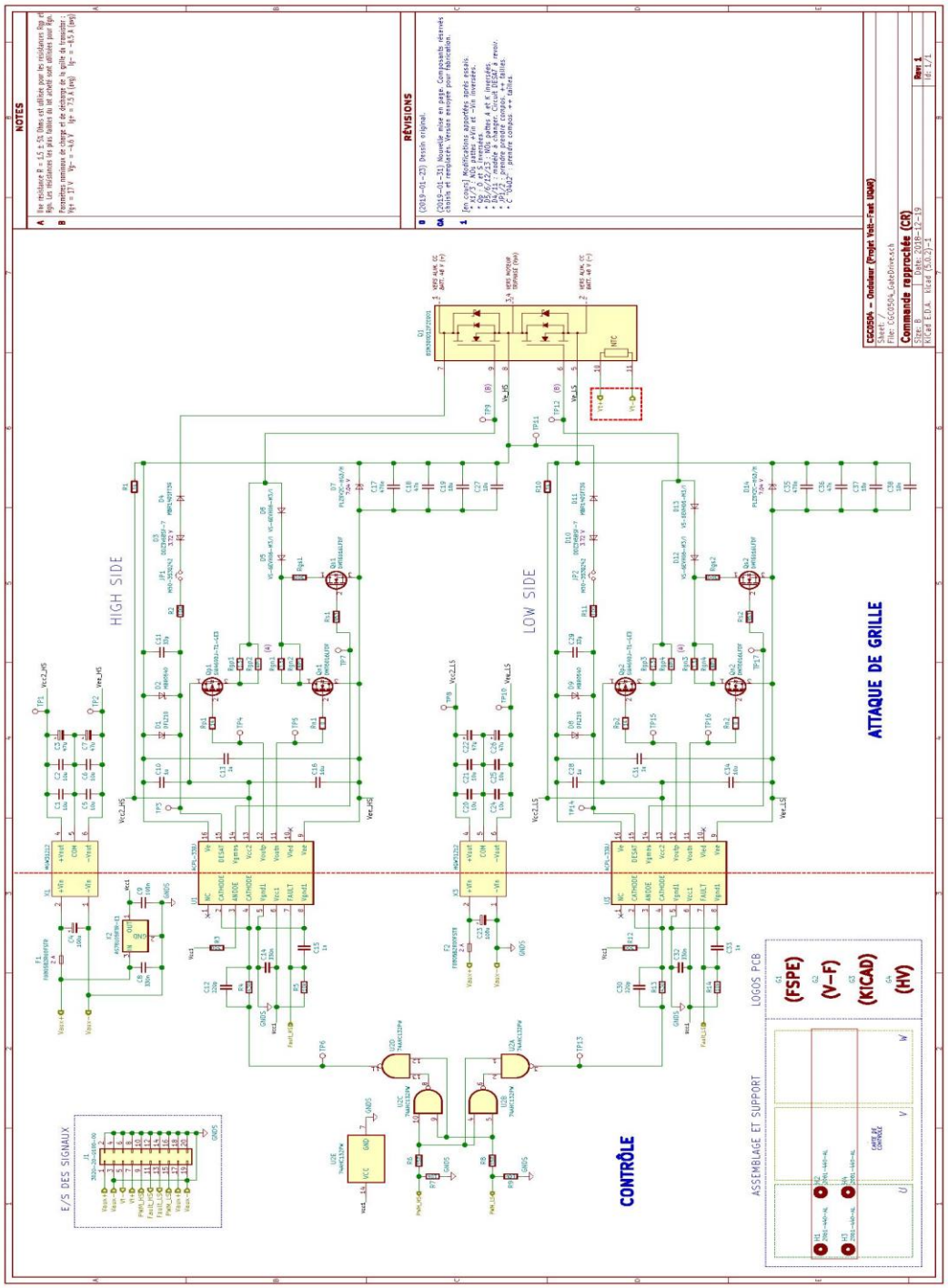

ANNEXE II

Code de programmation –main C

main.c

```
//###########################################################################
//                          Generation of six sines waves
//###########################################################################

#include "DSP2833x_Device.h"
#include "IQmathLib.h"
#pragma DATA_SECTION(sine_table,"IQmathTables");
_iq30 sine_table[512];
float freq;
int ifreq;
float amp1;
float iamp1;
float iamp2;
float iamp3;

// external function prototypes
extern void InitSysCtrl(void);
extern void InitPieCtrl(void);
extern void InitPieVectTable(void);

// Prototype statements for functions found within this file.
void Gpio_select(void);
void Setup_ePWM(void);
interrupt void ePWM_compare_isr(void);


//###########################################################################
//                      main code
//###########################################################################
void main(void)
{
    InitSysCtrl();  // Basic Core Init from DSP2833x_SysCtrl.c

    EALLOW;
    SysCtrlRegs.WDCR= 0x00AF;   // Re-enable the watchdog
    EDIS;           // 0x00AF  to NOT disable the Watchdog, Prescaler = 64

    DINT;               // Disable all interrupts

    Gpio_select();      // GPIO9, GPIO11, GPIO34 and GPIO49 as output
                        // to 4 LEDs at Peripheral Explorer Board

    Setup_ePWM();      // init of ePWM

    InitPieCtrl();      // basic setup of PIE table; from DSP2833x_PieCtrl.c

    InitPieVectTable(); // default ISR's in PIE


    EALLOW;
    PieVectTable.EPWM1_INT = &ePWM_compare_isr;
    EDIS;

    // Enable EPWM INT in the PIE: Group 3 interrupt 1
    PieCtrlRegs.PIEIER3.bit.INTx1 = 1;
    IER |=M_INT3;            // enable INT3 for ePWM 1@6

```

Page 1

```
58    EINT;
59    ERTM;
60
61    while(1)
62    {
63
64        EALLOW;
65        SysCtrlRegs.WDKEY = 0x55;   // service WD #1
66        EDIS;
67
68    }
69}
70
71void Gpio_select(void)
72{
73    EALLOW;
74    GpioCtrlRegs.GPAMUX1.all = 0;       // GPIO15 ... GPIO0 = General Puropse I/O
75    GpioCtrlRegs.GPAMUX1.bit.GPIO0 = 1; // ePWM1A active
76    GpioCtrlRegs.GPAMUX1.bit.GPIO1 = 1; // ePWM1B active
77    GpioCtrlRegs.GPAMUX1.bit.GPIO2 = 1; // ePWM2A active
78    GpioCtrlRegs.GPAMUX1.bit.GPIO3 = 1; // ePWM2B active
79    GpioCtrlRegs.GPAMUX1.bit.GPIO4 = 1; // ePWM3A active
80    GpioCtrlRegs.GPAMUX1.bit.GPIO5 = 1; // ePWM3B active
81    GpioCtrlRegs.GPAMUX1.bit.GPIO6 = 1; // ePWM4A active
82    GpioCtrlRegs.GPAMUX1.bit.GPIO7 = 1; // ePWM4B active
83    GpioCtrlRegs.GPAMUX1.bit.GPIO8 = 1; // ePWM5A active
84    GpioCtrlRegs.GPAMUX1.bit.GPIO9 = 1; // ePWM5B active
85    GpioCtrlRegs.GPAMUX1.bit.GPIO10 = 1; // ePWM6A active
86    GpioCtrlRegs.GPAMUX1.bit.GPIO11 = 1; // ePWM6B active
87
88    GpioCtrlRegs.GPAMUX2.all = 0;       // GPIO31 ... GPIO16 = General Purpose I/O
89    GpioCtrlRegs.GPBMUX1.all = 0;       // GPIO47 ... GPIO32 = General Purpose I/O
90    GpioCtrlRegs.GPBMUX2.all = 0;       // GPIO63 ... GPIO48 = General Purpose I/O
91    GpioCtrlRegs.GPCMUX1.all = 0;       // GPIO79 ... GPIO64 = General Purpose I/O
92    GpioCtrlRegs.GPCMUX2.all = 0;       // GPIO87 ... GPIO80 = General Purpose I/O
93
94    GpioCtrlRegs.GPADIR.all = 0;
95    GpioCtrlRegs.GPADIR.bit.GPIO9 = 1;  // peripheral explorer: LED LD1 at GPIO9
96    GpioCtrlRegs.GPADIR.bit.GPIO11 = 1; // peripheral explorer: LED LD2 at GPIO11
97
98
99    GpioCtrlRegs.GPBDIR.all = 0;        // GPIO63-32 as inputs
100   GpioCtrlRegs.GPBDIR.bit.GPIO34 = 1; // peripheral explorer: LED LD3 at GPIO34
101   GpioCtrlRegs.GPBDIR.bit.GPIO49 = 1; // peripheral explorer: LED LD4 at GPIO49
102   GpioCtrlRegs.GPCDIR.all = 0;        // GPIO87-64 as inputs
103   EDIS;
104}
105
106void Setup_ePWM(void)
107{
108   // Sine PWM1
109   EPwm1Regs.TBCTL.bit.CLKDIV =  0;    // CLKDIV = 0
110   EPwm1Regs.TBCTL.bit.HSPCLKDIV = 0;  // HSPCLKDIV = 0
111   EPwm1Regs.TBCTL.bit.CTRMODE = 2;    // up - down mode
112
113   EPwm1Regs.AQCTLA.all = 0x0060;      // set ePWM1A on CMPA up
114
```

```
225     EPwm5Regs.DBFED = 0;              // for rising and falling edge
226     EPwm5Regs.DBCTL.bit.OUT_MODE = 11;   // S1=1 S0=1
227     EPwm5Regs.DBCTL.bit.POLSEL = 01;     // S3=0 S2=1  inverted signal at ePWM5B FOR (ALC)
    deadband
228     EPwm5Regs.DBCTL.bit.IN_MODE = 00;    //  S5=0 S4=0  ePWM5A = source for RED & FED
229
230     // Sine PWM6
231      EPwm6Regs.TBCTL.bit.CLKDIV =  0;    // CLKDIV = 0
232      EPwm6Regs.TBCTL.bit.HSPCLKDIV = 0;  // HSPCLKDIV = 0
233      EPwm6Regs.TBCTL.bit.CTRMODE = 2;    // up - down mode
234
235      EPwm6Regs.AQCTLA.all = 0x0060;      // set ePWM6A on CMPA up
236
237      EPwm6Regs.TBPRD = 3750;              // timer period for 20 KHz
238                                              // TBPRD = 1/2 ( 150 MHz / 20 kHz)
239
240      EPwm6Regs.ETSEL.all = 0;
241      EPwm6Regs.ETSEL.bit.INTEN = 1;      // interrupt enable for ePWM1
242      EPwm6Regs.ETSEL.bit.INTSEL = 5;     // interrupt on CMPA down match
243      EPwm6Regs.ETPS.bit.INTPRD = 1;      // interrupt on first event
244      EPwm6Regs.CMPA.half.CMPA =  EPwm1Regs.TBPRD/2;
245
246      EPwm6Regs.TBCTL.bit.PHSEN = 1;      // enable phase shift for ePWM3
247      EPwm6Regs.TBPHS.half.TBPHS = 3750; // 1/2 phase shift
248
249      //Add dead time
250      EPwm6Regs.DBRED = 75;              // 1 microseconds delay
251      EPwm6Regs.DBFED = 0;              // for rising and falling edge
252      EPwm6Regs.DBCTL.bit.OUT_MODE = 11;   // S1=1 S0=1
253      EPwm6Regs.DBCTL.bit.POLSEL = 01;     // S3=0 S2=1  inverted signal at ePWM6B FOR (ALC)
    deadband
254      EPwm6Regs.DBCTL.bit.IN_MODE = 00;    //  S5=0 S4=0  ePWM6A = source for RED & FED
255
256 }
257
258 interrupt void ePWM_compare_isr(void)
259 // ISR runs every 10 us (PWM-frequency = 100 KHz)
260 // and is triggered by ePWM1 compare event
261 // run - time of ISR is 630 ns
262 {
263     static unsigned int index1_100 = 0;
264     static unsigned int index1 = 0;    //Phase 0
265     static unsigned int index3_100 = 34100;
266     static unsigned int index3 = 341;  //Phase 120
267     static unsigned int index5_100 =17000;
268     static unsigned int index5 = 170;  //Phase 240
269     static unsigned int index2_100 = 25600;
270     static unsigned int index2 = 256;    //Phase 0
271     static unsigned int index4_100 = 8500;
272     static unsigned int index4 = 85;  //Phase 120
273     static unsigned int index6_100 =42600;
274     static unsigned int index6 = 426;  //Phase 240
275     ifreq = (freq*100)/39.06;
276
277     /*if (freq < 89){
278         amp1 = (freq/89)*100;
279     }
```

```
115     EPwm1Regs.TBPRD = 3750;              // timer period for 20 KHz
116                                          // TBPRD = 1/2 ( 150 MHz / 20 kHz)
117
118     EPwm1Regs.ETSEL.all = 0;
119     EPwm1Regs.ETSEL.bit.INTEN = 1;       // interrupt enable for ePWM1
120     EPwm1Regs.ETSEL.bit.INTSEL = 5;      // interrupt on CMPA down match
121     EPwm1Regs.ETPS.bit.INTPRD = 1;       // interrupt on first event
122     EPwm1Regs.CMPA.half.CMPA =  EPwm1Regs.TBPRD/2;
123
124     EPwm1Regs.TBCTL.bit.SYNCOSEL = 1;    // generate a syncout if CTR = 0
125
126     //Add dead time
127     EPwm1Regs.DBRED = 75;               // 1 microseconds delay
128     EPwm1Regs.DBFED = 0;               // for rising and falling edge
129     EPwm1Regs.DBCTL.bit.OUT_MODE = 11;   // S1=1 S0=1
130     EPwm1Regs.DBCTL.bit.POLSEL = 01;     // S3=0 S2=1  inverted signal at ePWM1B FOR (ALC)
    deadband
131     EPwm1Regs.DBCTL.bit.IN_MODE = 00;    //  S5=0 S4=0  ePWM1A = source for RED & FED
132
133     //Sine PWM2
134     EPwm2Regs.TBCTL.bit.CLKDIV =  0;     // CLKDIV = 0
135     EPwm2Regs.TBCTL.bit.HSPCLKDIV = 0;  // HSPCLKDIV = 0
136     EPwm2Regs.TBCTL.bit.CTRMODE = 2;     // up - down mode
137
138     EPwm2Regs.AQCTLA.all = 0x0060;       // set ePWM2A on CMPA up
139                                          // clear ePWM1A on CMPA down
140     EPwm2Regs.TBPRD = 3750;              // timer period for 20 KHz
141                                          // TBPRD = 1/2 ( 150 MHz / 20 kHz)
142     EPwm2Regs.CMPA.half.CMPA =  EPwm2Regs.TBPRD/2;
143     EPwm2Regs.ETSEL.all = 0;
144     EPwm2Regs.ETSEL.bit.INTEN = 1;       // interrupt enable for ePWM1
145     EPwm2Regs.ETSEL.bit.INTSEL = 5;      // interrupt on CMPA down match
146     EPwm2Regs.ETPS.bit.INTPRD = 1;       // interrupt on first event
147     EPwm2Regs.TBPHS.half.TBPHS = 3750; // 1/2 phase shift
148
149     //Add dead time
150     EPwm2Regs.DBRED = 75;               // 1 microseconds delay
151     EPwm2Regs.DBFED = 0;               // for rising and falling edge
152     EPwm2Regs.DBCTL.bit.OUT_MODE = 11;   // ePWM2A = RED
153     EPwm2Regs.DBCTL.bit.POLSEL = 01;     // S3=0 S2=1 S1=1 S0=1 inverted signal at ePWM2B FOR
    (ALC) deadband
154     EPwm2Regs.DBCTL.bit.IN_MODE = 00;    // ePWM2A = source for RED & FED
155
156     //Sine PWM3
157     EPwm3Regs.TBCTL.bit.CLKDIV =  0;     // CLKDIV = 0
158     EPwm3Regs.TBCTL.bit.HSPCLKDIV = 0;  // HSPCLKDIV = 0
159     EPwm3Regs.TBCTL.bit.CTRMODE = 2;     // up - down mode
160
161     EPwm3Regs.AQCTLA.all = 0x0060;       // set ePWM3A on CMPA up
162                                          // clear ePWM3A on CMPA down
163     EPwm3Regs.TBPRD = 3750;              // timer period for 20 KHz
164                                          // TBPRD = 1/2 ( 150 MHz / 20 kHz)
165     EPwm3Regs.CMPA.half.CMPA =  EPwm3Regs.TBPRD/2;
166     EPwm3Regs.ETSEL.all = 0;
167     EPwm3Regs.ETSEL.bit.INTEN = 1;       // interrupt enable for ePWM3
168     EPwm3Regs.ETSEL.bit.INTSEL = 5;      // interrupt on CMPA down match
169     EPwm3Regs.ETPS.bit.INTPRD = 1;       // interrupt on first event
```

```
170
171     //Add dead time
172     EPwm3Regs.DBRED = 75;              // 1 microseconds delay
173     EPwm3Regs.DBFED = 0;              // for rising and falling edge
174     EPwm3Regs.DBCTL.bit.OUT_MODE = 11;    // ePWM3A = RED
175     EPwm3Regs.DBCTL.bit.POLSEL = 01;      // S3=0 S2=1 S1=1 S0=1 inverted signal at ePWM3B FOR
    (ALC) deadband
176     EPwm3Regs.DBCTL.bit.IN_MODE = 00;     // ePWM3A = source for RED & FED
177
178     // Sine PWM4
179     EPwm4Regs.TBCTL.bit.CLKDIV =  0;     // CLKDIV = 0
180     EPwm4Regs.TBCTL.bit.HSPCLKDIV = 0;  // HSPCLKDIV = 0
181     EPwm4Regs.TBCTL.bit.CTRMODE = 2;     // up - down mode
182
183     EPwm4Regs.AQCTLA.all = 0x0060;       // set ePWM1A on CMPA up
184
185     EPwm4Regs.TBPRD = 3750;               // timer period for 20 KHz
186                                              // TBPRD = 1/2 ( 150 MHz / 20 kHz)
187
188     EPwm4Regs.ETSEL.all = 0;
189     EPwm4Regs.ETSEL.bit.INTEN = 1;       // interrupt enable for ePWM1
190     EPwm4Regs.ETSEL.bit.INTSEL = 5;      // interrupt on CMPA down match
191     EPwm4Regs.ETPS.bit.INTPRD = 1;       // interrupt on first event
192     EPwm4Regs.CMPA.half.CMPA =  EPwm1Regs.TBPRD/2;
193
194     EPwm4Regs.TBCTL.bit.PHSEN = 1;       // enable phase shift for ePWM4
195     EPwm4Regs.TBPHS.half.TBPHS = 3750; // 1/2 phase shift
196
197     //Add dead time
198     EPwm4Regs.DBRED = 75;              // 1 microseconds delay
199     EPwm4Regs.DBFED = 0;              // for rising and falling edge
200     EPwm4Regs.DBCTL.bit.OUT_MODE = 11;    // S1=1 S0=1
201     EPwm4Regs.DBCTL.bit.POLSEL = 01;      // S3=0 S2=1  inverted signal at ePWM4B FOR (ALC)
    deadband
202     EPwm4Regs.DBCTL.bit.IN_MODE = 00;     //  S5=0 S4=0  ePWM4A = source for RED & FED
203
204     // Sine PWM5
205     EPwm5Regs.TBCTL.bit.CLKDIV =  0;     // CLKDIV = 0
206     EPwm5Regs.TBCTL.bit.HSPCLKDIV = 0;  // HSPCLKDIV = 0
207     EPwm5Regs.TBCTL.bit.CTRMODE = 2;     // up - down mode
208
209     EPwm5Regs.AQCTLA.all = 0x0060;       // set ePWM5A on CMPA up
210
211     EPwm5Regs.TBPRD = 3750;               // timer period for 20 KHz
212                                              // TBPRD = 1/2 ( 150 MHz / 20 kHz)
213
214     EPwm5Regs.ETSEL.all = 0;
215     EPwm5Regs.ETSEL.bit.INTEN = 1;       // interrupt enable for ePWM1
216     EPwm5Regs.ETSEL.bit.INTSEL = 5;      // interrupt on CMPA down match
217     EPwm5Regs.ETPS.bit.INTPRD = 1;       // interrupt on first event
218     EPwm5Regs.CMPA.half.CMPA =  EPwm1Regs.TBPRD/2;
219
220     EPwm5Regs.TBCTL.bit.PHSEN = 1;       // enable phase shift for ePWM5
221
222
223      //Add dead time
224     EPwm5Regs.DBRED = 75;              // 1 microseconds delay
```

```
280     else if (freq >= 89){
281         amp1 = 100;
282     }*/
283     iamp1 = 1;//100/amp1;
284     iamp2 = EPwm1Regs.TBPRD/iamp1;
285     iamp3 = EPwm1Regs.TBPRD/iamp1;
286
287     // Service watchdog every interrupt
288     EALLOW;
289     SysCtrlRegs.WDKEY = 0xAA;       // Service watchdog #2
290     EDIS;
291
292     EPwm1Regs.CMPA.half.CMPA =  (EPwm1Regs.TBPRD -
    _IQsat(_IQ30mpy((sine_table[index1]+_IQ30(0.9999))/2,iamp2),EPwm1Regs.TBPRD,0));
293     EPwm2Regs.CMPA.half.CMPA =  EPwm2Regs.TBPRD -
    _IQsat(_IQ30mpy((sine_table[index2]+_IQ30(0.9999))/2,iamp2),EPwm2Regs.TBPRD,0);
294     EPwm3Regs.CMPA.half.CMPA =  EPwm3Regs.TBPRD -
    _IQsat(_IQ30mpy((sine_table[index3]+_IQ30(0.9999))/2,iamp2),EPwm3Regs.TBPRD,0);
295     EPwm4Regs.CMPA.half.CMPA =  EPwm4Regs.TBPRD -
    _IQsat(_IQ30mpy((sine_table[index4]+_IQ30(0.9999))/2,iamp2),EPwm4Regs.TBPRD,0);
296     EPwm5Regs.CMPA.half.CMPA =  EPwm5Regs.TBPRD -
    _IQsat(_IQ30mpy((sine_table[index5]+_IQ30(0.9999))/2,iamp2),EPwm5Regs.TBPRD,0);
297     EPwm6Regs.CMPA.half.CMPA =  EPwm6Regs.TBPRD -
    _IQsat(_IQ30mpy((sine_table[index6]+_IQ30(0.9999))/2,iamp2),EPwm6Regs.TBPRD,0);
298
299     index1_100 += ifreq; //ifreq
300     if (index1_100 > 51199)
301         index1_100 -= 51200;
302     index1 = index1_100/100;
303
304     index2_100 += ifreq; //ifreq
305     if (index2_100 > 51199)
306         index2_100 -= 51200;
307     index2 = index2_100/100;
308
309     index3_100 += ifreq; //ifreq
310     if (index3_100 > 51199)
311         index3_100 -= 51200;
312     index3 = index3_100/100;
313
314     index4_100 += ifreq; //ifreq
315     if (index4_100 > 51199)
316         index4_100 -= 51200;
317     index4 = index4_100/100;
318
319     index5_100 += ifreq; //ifreq
320     if (index5_100 > 51199)
321         index5_100 -= 51200;
322     index5 = index5_100/100;
323
324     index6_100 += ifreq; //ifreq
325     if (index6_100 > 51199)
326         index6_100 -= 51200;
327     index6 = index6_100/100;
328
329     EPwm1Regs.ETCLR.bit.INT = 1;        // Clear ePWM1 Interrupt flag
330     EPwm2Regs.ETCLR.bit.INT = 1;        // Clear ePWM2 Interrupt flag
```

ANNEXE III

ANALYSEUR DE POST COMBUSTION- TESTO 350 V.2

Coffret d'analyse

Grandeur	Précision	Temps de réponse
O_2	±0,2Vol.%	< 20s (t95)
CO, comp. H_2	±10ppm (0…199ppm) ±5% de la valeur moyenne (200…2 000ppm) ±10% de la valeur moyenne (plage restante)	< 40s (t90)
CO_{low}, comp. H_2	±2ppm (0…39,9ppm CO) ±5% de la valeur moyenne (plage restante)	< 40s (t90)
NO	±5ppm (0…99ppm) ±5% de la valeur moyenne (100…1 999.9ppm) ±10% de la valeur moyenne (plage restante)	< 30s (t90)
NO_{low}	±2ppm (0…39,9ppm) ±5% de la valeur moyenne (plage restante)	< 30s (t90)
NO_2	±5ppm (0…99,9ppm) ±5% de la valeur moyenne (plage restante)	< 40s (t90)
SO_2	±5ppm (0…99ppm) ±5% de la valeur moyenne (100…1 999ppm) ±10% de la valeur moyenne (plage restante)	< 30s (t90)
H_2S	±2ppm (0…39,9ppm) ±5% de la valeur moyenne (plage restante)	< 35s (t90)
CO_2-(IR)	±0,3Vol.% ±1% de la valeur moyenne (0…25Vol.%) ±0,5Vol.% ±1,5% de la valeur moyenne (plage restante)	< 10s (t90) Temps de préchauffage : < 15min.

ANNEXE IV

CARACTÉRISTIQUES DES GARNISSAGES STRUCTURÉES ET SOLUTIONS MEA-NaOH

Mellapak 250.Y/X

A highly versatile packing type

0602 2510

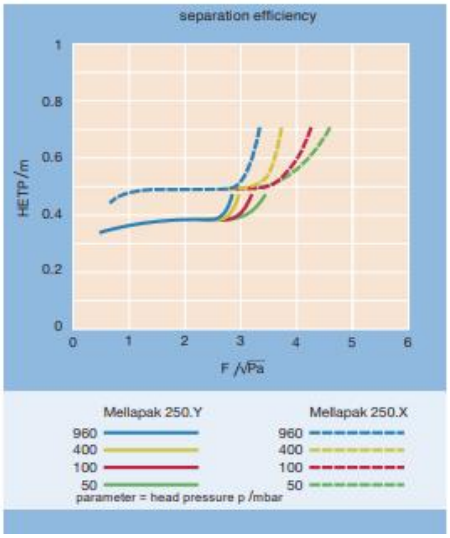

Mellapak is the most widely used structured packing worldwide. It has proven excellent performance in columns with diameters up to 15 m. It is supplied in sheet metal thicknesses from 0.1 mm up.

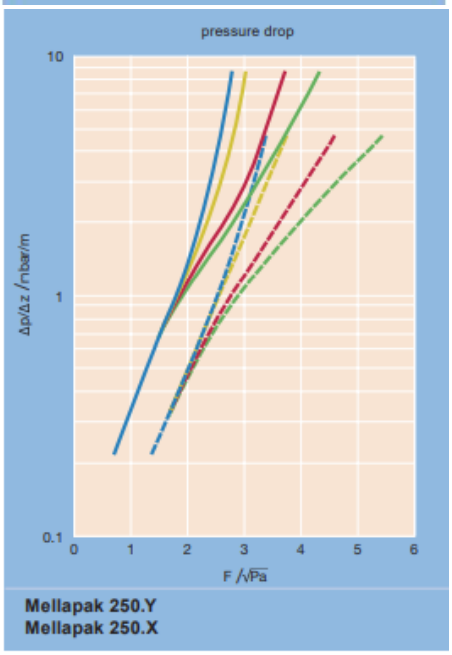

Special features

- Pressure drop per theoretical stage 0.3-1.0 mbar
- Pressure drop at 70-80% flooding about 2 mbar/m
- Minimum liquid load approx. 0.2 m^3/m^2h
- Maximum liquid load up to more than 200 m^3/m^2h (typically in desorption columns)

Preferred applications

- Vacuum to moderate pressure
- High pressure in selected applications
- Increasing capacity of existing tray and packed columns

Typical applications

- Chemical industry: Ethylbenzene/styrene, tall oil, cyclohexonone/-ol, air separation
- Petrochemical industry: Quench columns, C_3- and C_4- splitters, xylene splitters
- Refineries: Vacuum and atmospheric columns
- Absorption: Natural gas drying, CO_2- and H_2S-absorbers and strippers, ethyleneoxide absorbers and strippers, acrylonitrile absorbers

MEA: Aqueous solutions of monoethanolamine (MEA, C_2H_7NO, 30 wt. %) were prepared in a feed reservoir with fresh MEA mixed with deionized water resulted in C_{MEA} = 5 gmol/lit:

Molecular Weight (MW) of MEA= 61.08 g/gmol
Density (ρ) of MEA = 1.012 g/cm^3
One Liter aqueous solution contains 0.3 liter MEA:

$$5\frac{gmol}{lit} \times 61.08\frac{g}{gmol} \times \frac{1\ cm^3}{1.012\ g} = \frac{301.81\ cm^3\ MEA}{liter\ solution}$$

To prepare 20-liter solution as an example, we need 6 Liters MEA.

NaOH: Similar calculations can be carried out for aqueous solutions of caustic soda (NaOH), for example C_{NaOH} = 1 gmol/lit:

Molecular Weight (MW) of NaOH= 40 g/gmol
One Liter aqueous solution contains 40 g NaOH:

$$1\frac{gmol}{lit} \times 40\frac{g}{gmol} = \frac{40\ g\ NaOH}{liter\ solution}$$

To sum up: I think ordering of *two 4-Liter MEA* and *2.5 KG NaOH* would be enough for IMAR experiments. Please find attached files including prices.

ANNEXE V

Caractéristiques du banc d'essai de la suralimentation à l'UQAC

1. Caractéristiques complètes de la génératrice KCG-5000DES

- Puissant moteur "silencieux" au diesel de 10 CV, 4 temps à refroidissement à air.
- Alternateur sans balai et ignition électronique
- Interrupteur de niveau d'huile avec lumière indicatrice arrête et protège le moteur lorsque le niveau d'huile est trop bas
- Prise double: CA de sortie 120V/35 ampères
- Prise verrouillage: CA de sortie 240V/17.5 ampères
- Terminaux: CC de sortie 12V, 8.3 ampères
- Élément de réchauffement pour démarrages au froid
- Démarrage électrique à clé
- Voltmètre, sélecteur de voltage et terminal pour la mise à la terre
- Disjoncteur CA et fusible CC pour une opération en sécurité
- Cabinet isolé avec du matériel d'insonorisation, construction réduit les vibrations, tige d'équilibre et un grand silencieux pour une opération silencieuse.
- Montée sur 4 roues pour faciliter le transport.

ANNEXE VI

Formules utilisées

Dimensionnement du système SHEDAC

- Coefficient de puissance : $C_{p\_WT} = \frac{P_{WT(V_W)}}{PWT_{\_a}(V_W)}$; elle dépend de la vitesse du vent en amont v_w, du nombre des pales, de leur rayon, de leur angle de calage β_{WT} et de leur vitesse de rotation.

- Dimensionnement du compresseur : $P_{C-1} = \frac{n_c}{n_c - 1} m_c r T_a \left[\left(\frac{P_{ou\_C}}{P_a} \right)^{\frac{n_c - 1}{nc}} - 1 \right] \frac{1}{\eta_{p\_c}}$; avec η_{p_c} qui est le rendement polytropique du compresseur; n_c est le nombre d'étages du compresseur; m_c est le débit massique du compresseur.

- Puissance éolienne excédentaire : $P_{EX\_WT} = P_{WT} - P_{CH}$

- Calcul du travail développé par le moteur : Le travail du cycle moteur pneumatique est la somme des travaux pendant les 5 étapes suivantes :

$$W_{CAE} = W_{1-2} + W_{2-3} + W_{3-4} + W_{4-5} + W_{5-1}$$

- Densité d'énergie stockée dans les réservoirs : pour 1m^3 de volume, la densité énergétique du stockage peut être exprimée par l'équation suivante : $w_{st} = k \frac{n_E N_{E\_CAE} P_{st\_r}}{n_E - 1} \left[1 - \left(\frac{P_a}{P_{st\_r}} \right)^{\frac{n_E - 1}{n_E N_{E\_CAE}}} \right]$ avec $k = 2.7778x10^{-6}$ est la constante de conversion de l'énergie en kWh, $N_{E\_CAE\_}$ est le nombre d'étages de détente du MAC, p_a est la pression atmosphérique et p_{st_r} est la pression de stockage.

ANNEXE VII

Les réactions chimiques (SCRUBBER)

Épurateur à gaz de postcombustion : Les réactions chimiques

C1.1 Wet open loop SO_X scrubber (including hybrid system operating in open loop mode)

SO_X scrubbing media is seawater. Sulphur dioxide (SO_2) is dissolved and ionised to bisulphite and sulphite, which is then readily oxidised to sulphate in seawater containing oxygen. Similarly sulphuric acid, formed from SO_3, and hydrogen sulphate dissociate completely to sulphate.

For SO_2:

- $SO_2 + H_2O \Rightarrow$ 'H_2SO_3' (sulphurous acid) $\Rightarrow H^+ + HSO_3^-$ (bisulphite)
- HSO_3^- (bisulphite) $\Rightarrow H^+ + SO_3^{2-}$ (sulphite)
- SO_3^{2-} (sulphite) + ½ $O_2 \Rightarrow SO_4^{2-}$ (sulphate)

For SO_3:

- $SO_3 + H_2O \Rightarrow H_2SO_4$ (sulphuric acid)
- $H_2SO_4 + H_2O \Rightarrow HSO_4^-$ (hydrogen sulphate)$+ H_3O^+$ [i]
- HSO_4^- (hydrogen sulphate) $+ H_2O \Rightarrow SO_4^{2-}$ (sulphate) $+ H_3O^+$

C1.2 Wet closed loop SO_X scrubber (including hybrid system operating in closed loop mode)

SO_X scrubbing media is fresh water dosed with sodium hydroxide (NaOH). Sulphur oxides are dissolved and react to form sodium bisulphite, sulphite and sulphate. The proportion of each is dependent on the pH and available oxygen.

For SO_2:

- $Na^+ + OH^- + SO_2 \Rightarrow NaHSO_3$ (aq sodium bisulphite)
- $2Na^+ + 2OH^- + SO_2 \Rightarrow Na_2SO_3$ (aq sodium sulphite) $+ H_2O$
- $2Na^+ + 2OH^- + SO_2 +$ ½ O2 $\Rightarrow Na_2SO_4$ (aq sodium sulphate) $+ H_2O$

For SO_3:

- $SO_3 + H_2O \Rightarrow H_2SO_4$ (sulphuric acid)
- $2NaOH + H_2SO_4 \Rightarrow Na_2SO_4$ (aq sodium sulphate) $+ 2H_2O$